Sea Grant Program on Marine Corrosion
FINAL REPORT

Volume Four — Supporting Data
Localized Corrosion, Stainless Alloys

Edited by
S. C. Dexter
and
W. H. Hartt

Submitted to
THE OFFICE OF SEA GRANT PROGRAMS
NATIONAL OCEANIC AND ATMOSPHERIC ADMINISTRATION
UNITED STATES DEPARTMENT OF COMMERCE

MAY 1985

UNIVERSITY OF DELAWARE
Sea Grant College Program
LEWES, DELAWARE 19958

SEA GRANT PROGRAM ON MARINE CORROSION
FINAL REPORT

VOLUME FOUR - SUPPORTING DATA
LOCALIZED CORROSION, STAINLESS ALLOYS

Submitted to
The Office of Sea Grant Programs
National Oceanic and Atmospheric Administration
United States Department of Commerce

Marine Corrosion Program Principal Investigators:

Thad S. Lee, LaQue Center for Corrosion Technology

Robert M. Kain, LaQue Center for Corrosion Technology

Michael A. Streicher, University of Delaware

and

Stephen C. Dexter, University of Delaware
Overall Program Leader and
Localized Corrosion Project Leader

May 1985
University of Delaware
Sea Grant College Program
Lewes, Delaware 19958
DEL-SG-06-85

PREFACE

The Sea Grant Program on Marine Corrosion began in the fall of 1980 as a cooperative research project involving eight principal investigators from both academia and industry. An important component of the Program was the establishment of an Industrial Advisory Panel, whose primary functions were to keep the investigators aware of developing industrial problems in the area of marine corrosion, and to assist the investigators in technology transfer.

The Program was to last for three years, and was viewed by both the National Sea Grant Office and by the investigators themselves as an experiment in forging closer ties between a substantial academic research effort and its ultimate beneficiaries in industry.

This report, in four volumes, will serve, not only to document the technical results from three years of work by the eight principal investigators with their associates and students, but also to evaluate the success of that experiment, and to recommend whether the structure of the Program should be continued, and perhaps used as a model in other fields of research.

Volume One of the report is a stand-alone document, summarizing and evaluating the results of the entire program, while Volumes Two through Four present the technical details for each of the major segments of the program. Volume One is intended to be readable for the general educated public, whereas Volumes Two, Three and Four are intended to be reference volumes for those interested in specific areas of marine corrosion research and engineering.

Stephen C. Dexter
Overall Program Leader

Sea Grant Program on
Marine Corrosion

FINAL REPORT

Table of Contents

1. EXPERIMENTAL PROCEDURES.

EXPERIMENTAL

The following sections describe the basic experimental procedures used in both immersion crevice corrosion tests and mathematical modelling. Additional discussions on the methods described are included in the References listed at the end of this section.

I.A. Crevice Corrosion Tests

1. Multiple Crevice Assembly

This device was originally developed for the purpose of providing a convenient and economical means of screening relative alloy performance in natural seawater. It consists of two serated washers each with a series of plateaus such that 20 separate crevice sites are created beneath each washer (Figure A1). Two such washers when attached with a nut and bolt to a test specimen, create 40 individual crevice sites. Figure A2 shows a drawing of a multiple crevice assembly (MCA) washer.

Surface finish effects were assessed by testing materials in the as-received (usually acid pickled) condition as well as by wet surfacing grinding (120 SiC) the area where the MCA washer was affixed. Effects of crevice tightness were studied by controlling the initial torque applied to the titanium nut and bolt assembly used to hold the crevice washers in place. Initial tightening torques of 2.8 or 8.5 Nm were used. It should be noted that these torque values do not have any specific engineering design value. Rather they provide a convenient means of expressing a convenient and referenceable initial application of the MCA washers.

Initially, a probability concept was employed to describe crevice corrosion initiation and propagation behavior since the phenomena appeared random in their occurrence. The data were thus presented as a probability that a given material would be susceptible. However, the development of a model of crevice corrosion helped to identify a number of factors which would affect the occurrence of crevice corrosion. The modelling showed

that experimental factors such as reproducibility of the crevice geometry could be as important as metallurgical variables in accounting for the observed crevice corrosion behavior of a given stainless steel. As such, the probability concept was abandoned since it implied a material property, when in reality it more likely represented the probability that a given crevice site was sufficiently severe to initiate crevice corrosion.

Because the crevice corrosion process can be clearly separated into an initiation and propagation phase, test data were analyzed to determine relative alloy resistance to each of these stages of the process. The parameter chosen to define alloy resistance to crevice corrosion initiation was the number of individual crevice sites on each MCA washer where corrosion occurred. The maximum depth of attack incurred at any of the 20 possible sites under each washer was selected as the parameter defining the relative extent of crevice corrosion propagation.

2. Remote Crevice Assembly

The schematic in Figure A3 shows the difference between a conventional crevice test specimen and the remote crevice assembly (RCA). By separating the crevice area from the larger boldly exposed surface, the RCA method enables measurement (through a zero resistance ammeter) of any current between the larger, boldy exposed cathode member and the smaller, shielded anode (crevice member). This offers the advantages of electrochemical data collection without the uncertainties of electrochemical stimulation employed by various applied current test methods. The potential of the coupled members as well as other corrosion data can also be monitored and determined.

The primary advantage of the RCA method over some other crevice corrosion test method is its ability to more clearly identify crevice corrosion initiation and describe the extent of any subsequent crevice corrosion propagation. The current measurements at any time provide an indication of the instantaneous rate of crevice corrosion propagation.

Since previous work has shown good correlations between the corrosion rates determined from the total current and mass loss, these instantaneous measurements are accurate reflectors of ongoing propagation rates. Furthermore, changes in the rate of crevice corrosion for already initiated sites can be detected as a function of changes in environmental parameters, e.g., temperature.

The continued use of the remote crevice assembly concept has evolved variations in the method of forming and controlling the geometry of the crevice. One fixture (Figure A4) has been used extensively in the past few years to study alloy behavior in a variety of natural and synthetic environments. In this case, the crevice member was positioned between two acrylic blocks to which plastic tape has been applied. The tape provides a deformable cushion to help enhance crevice tightness. A torque wrench was used when tightening the constraining bolt to provide some degree of consistency from one assembly to another. All of the RCA tests described in the present work utilized an assembly torque of 2.8 Nm (25 in-lbs). Assembly of the components was performed without any pre-wetting of the specimen. For the most part, a nominal crevice area of 4.5 cm^2 (cathode:anode area ratio ~37:1) was used. Surfaces of the anode members were either wet ground with 120 grit SiC paper, acid pickled or left with a mill finish prior to cleaning (pumice scrub, water rinse, acetone degrease) and weighing. Depending on test objectives, cathode members were either ground or left in their respective mill finish. Drilled holes in the stem of both anode and cathode members allowed electrical connections to be made above the waterline.

Waterline attack may be a problem for some alloy/environment combinations. The use of coatings, except for above waterline application, is not recommended as this may create additional sites for crevice corrosion. Periodic cleaning of the waterline area by simple swabbing with the bulk environment has been moderately successful. Additional

improvement in this regard is necessary, particularly for tests involving less resistant materials.

To further study the influence of crevice geometry control, i.e., tightness, additional experimental designs have been investigated. Figure A5, for example, shows one of several air operated crevice loading devices which have been constructed. In this case, regulated air pressure is used to replace the load screw shown previously. Tests described herein utilized the same type of cathode and anode members. Loading was applied at a level of 69000 Pa (~10 psi) to wetted anode members.

3. Compartmentalized Cell Test

Compartmentalized cell methodologies have been previously used to investigate general and localized corrosion. The present cell design, as shown in Figure A6, has been used to study the effects of differences in cathode and anode electrolyte compositions on propagation and cessation of crevice corrosion. The technique is similar to the RCA tests in that the respective members are again physically separated but electrically connected. The anode and cathode compartments are separated by an agar gel prepared with the crevice solution and held in place between two fritted glass discs.

The anode member is exposed without a crevice former in a predetermined crevice solution. Selection of the crevice solution concentrations is based on mathematical modelling predictions for specific inputs of alloy composition, bulk environment and known, but frequently uncontrollable, crevice geometries. One of the primary advantages of this method is that the time factor for development of a critical crevice solution (CCS) is eliminated. Secondly, it allows for characterization of the polarization behavior of cathode and anode member under purely spontaneous conditions, i.e., without the application of external current.

Specimen configuration and preparation were typical of those described for RCA tests. However, the exposed area ($\sim$10 cm^2) for anode members, which include wetted portions of the stem as well as edges, were larger. The exposed surface area of the cathodes was $\sim$170 cm^2. Each cell contained two specimens of the respective size. After a one hour exposure under freely corroding conditions in the bulk environment and simulated crevice solution, one set of cathode and anode members were coupled through a zero resistance ammeter. The remaining uncoupled "cathode" and "anode" members served as freely corroding control specimens. Potential data were also collected via reference electrode connections in both environments. Potentials measured for the coupled "cathode" member in the bulk environment are analogous to potentials measured for the remote crevice assembly or any other crevice bearing sample.

Materials

Table A1 provides the chemical composition of a number of stainless alloys for which crevice data are presented.

Environments

Results are presented for tests conducted in a variety of natural and synthetic solutions. In addition to natural and synthetic seawater, other chloride containing environments which have been used are given in Table A2. All crevice tests described in the present work were conducted at a controlled temperature as indicated and at controlled velocity conditions. This was generally <0.01 m/s. Execpt for the natural seawater tests which were continuously refreshed, all other tests were closed loop.

I.B. Mathematical Modelling

The first step in modelling crevice corrosion was to identify and organize those factors that have either been proven, or would be expected, to influence the occurrence of crevice corrosion. Figure A7 summarizes these factors. They can be categorized as environmental, electrochemical, metallurgical and geometric factors.

The second step involved the defining of a sequential mechanism by which stainless steels undergo crevice corrosion in seawater. The initiation process involves oxygen depletion within the crevice (Stage I), followed by increasing acidity and chloride content due to hydrolysis of metal ions within the crevice (Stage II), then breakdown of the passive film and the onset of corrosion (Stage III), and finally, propagation of crevice corrosion (Stage IV).

This generally accepted mechansim provides the basis of a mathematical model which allows a systematic examination of the various factors which influence crevice corrosion.

1. Initiation Model

The initiation model utilizes several inputs to define the times required to progress through the first three stages of crevice corrosion and to define the nature of reactions occurring within the crevice environment. The inputs include:

- the oxygen content of the bulk solution which is either known or measurable
- the crevice gap (width or spacing between the metal surface and the crevice former) and crevice depth (distance from the mouth to the base of the crevice)
- the passive current density which is experimentally determined by potentiostatic polarization of specimens at -100 mV (SCE) for one hour in the bulk environment (typically 0.1 $\mu A/cm^2$ or less in seawater)

- the bulk solution chloride level and pH which are known or measurable
- the chemical equilibria which describe the relevant hydrolysis reactions for the metal ions considered by the model (i.e., iron, chromium, and nickel)
- the alloy composition (i.e., iron, chromium, nickel and molybdenum)
- the critical crevice solution in which the passive film breaks down. This is defined as the pH and chloride level at which a 10 $\mu A/cm^2$ active peak height is obtained on the polarization curve. This is determined experimentally from a series of potentiodynamic polarization curves in acid-chloride solutions.

The first output of the model yields the time required to deplete oxygen (t_d) within the crevice. Using this calculated time, the distance which oxygen can diffuse into the crevice is determined from the relationship $\delta_d = (Dt_d)^{1/2}$ where D is the diffusion coefficient for oxygen. This parameter defines the crevice depth for a given crevice gap, which must be exceeded in order for oxygen depletion to occur and for Stage II of the crevice corrosion process to begin.

The second stage of the model is the most complex. The key component in this stage is the calculation of the time required to decrease the pH from its bulk solution value to the critical value at which the passive film breaks down. This pH reduction is calculated from the rate of production of the various metal ions. It is dominated by the rate of chromium ion production since it is the chromium hydrolysis reaction that controls the pH within the crevice.

The rate at which metal ions are produced within the crevice can be calculated by first determining the portion of the passive current (I_p) that corresponds to the production of ions of component metal "i". These variables are related by the equation:

$$\frac{I(i)}{I_p} = \frac{A(i)\ B(i)}{\sum_{j=1}^{n} A(j)\ B(j)}$$

where A represents the molar fraction of metal "i" in the alloy and B represents the charge of the metal ion.

Using this current, the rate of production of metal ions, R, in a crevice gap, x, can be calculated from the relationship:

$$R(i) = \frac{I(i)\ \ 1000}{F\ \ B(i)\ x}$$

Calculating the total amount of chromium required to decrease pH and knowing the rate of chromium production allows a calculation of the time required for the pH to fall by an increment ΔpH. This process is then repeated for each ΔpH increment and the basic relationship between pH in the crevice and time is determined.

There are three adjustments to this pH-time relationship. Two adjustments to the time to reduce pH are made to take account of mass transport in and out of the crevice and a third adjustment is made to correct the pH in the crevice to account for the chloride present.

Two additional adjustments to the time to reduce pH are made to take account of mass transport in and out of the crevice. The migration adjustment takes into account the movement of cations out of the crevice and anions into the crevice as a result of current flow. The diffusion adjustment accommodates the movement of metal ions and chloride ions out of the crevice as a result of the concentration gradients which develop between the crevice solution and the bulk solution.

The net effect of these two factors is that the crevice solution will increase in acidity and chloride content until the chloride flux out of the crevice due to diffusion equals the chloride flux into the crevice due to migration. At this point, a steady state

(i.e., limiting pH) is achieved. If the passive film will break down in this solution, then crevice corrosion is possible for the particular crevice geometry considered.

With this basic model, a number of calculations can be performed to allow examination of the relative effects of various factors on crevice corrosion initiation.

2. Propagation Model Concept

Since the development of the initiation model of crevice corrosion, a plan was outlined for the development of an extended model to encompass the propagation stage of crevice corrosion.

Crevice corrosion propagation can be conveiently considered in terms of an electrochemical corrosion cell with an anode, the actively dissolving alloy within the crevice, and a cathode, usually sustaining oxygen reduction outside the crevice and/or hydrogen evolution within the crevice. The rate of reaction is determined by the cell voltage, the electrolyte resistance, the cell geometry and the relevant polarization relationships for the anodic and cathodic reactions.

The active area within the crevice, generated by the breakdown of the passive fim, constitutes the anode. The anode parameters of interest are:

- the nature of the initial active area within the crevice and its location, i.e., the nucleation kinetics
- the kinetics of growth of the corroding area, both lateral and in depth
- the relationship between the anode potential and the anode current as a function of electrolyte composition, pH and temperature

In marine environments, for example, in the majority of situations the cathodic reaction associated with crevice corrosion propagation is oxygen reduction and/or hydrogen evolution. Oxygen reduction occurs on areas external to the crevice while

hydrogen evolution occurs within the crevice. Factors to be considered for these two reactions include:

Oxygen Reduction -

- the relationship between current and potential as a function of solution flow, temperature and oxygen concentration
- the area external to the crevice and the shape of this area

Hydrogen Evolution -

- the relationship between current and potential as a function of electrolyte composition, pH and temperature
- the area within the crevice available for this reaction
- the influence of this reaction on preventing the pH from falling within the crevice by effectively removing hydrogen ions from within the crevice

The overall corrosion cell geometry during propagation includes consideration of a number of factors including:

- the crevice gap and depth
- the exterior to interior crevice area ratio
- the number of crevice sites
- the location of the anode with respect to the mouth of the crevice
- the available cell voltage
- the electrolyte resistance and pH within the crevice
- the electrolyte volume within the crevice
- the electrolyte resistance outside the crevice
- the extent of oxygen reduction on the external crevice area

- the degree of hydrogen evolution possible within the crevice

In constructing a model of crevice corrosion propagation, the concept of a corrosion cell is linked with the crevice corrosion initiation model. Four separate models are being considered in this process, including a time dependence model. While work is progressing on developing these models, a preliminary model for determining propagation rates has already been established.

Propagation Rate Calculations

Prior to breakdown of passivity and the onset of crevice corrosion, it is assumed that the passive current flows over the entire crevice area with an equal oxygen reduction current external to the crevice. Since this current is small, it is unlikely to be restricted by IR drop considerations down the crevice. On breakdown of passivity, both of these assumptions change. First, breakdown occurs over a discrete area within the crevice and secondly, the current increases by orders of magnitude. Thus, it becomes necessary to consider the IR drop down the crevice.

There is no simple way to predict the area where accelerated corrosion will first occur within a crevice. In practice, it will start in a small area and increase by some two or three dimensional growth mechanism. In the present model, it is assumed that the breakdown will occur in the last 1 mm of the crevice, furthest from the crevice mouth. With this definition of the active area and its relative position within the crevice, it is then possible to calculate the resistance from the mouth of the crevice to the active area.

Figure A8 shows a schematic illustration of the change in current within the crevice as a function of crevice solution pH. The current is assumed to increase instantaneously from the pasive value of typically 0.1 $\mu A/cm^2$ to an active value of 10 $\mu A/cm^2$. It then increases according to a linear relationship between the log peak current and pH as

determined from polarization data. The pH of the crevice solution eventually becomes limited by mass transfer considerations. This can occur either before or after the current is limited by the IR drop down the crevice. The maximum value of this IR limited current is determined from the resistance down the crevice and the corrosion cell voltage by simply applying Ohm's law.

By definition in the model, the corrosion cell voltage is represented by the potential difference between the freely-corroding passive potential of stainless steel and the potential of the anodic current peak on the polarization curves in deaerated acid-chloride solutions. For austenitic stainless steels in aerated seawater, this value is typically 275 mV, representing the difference between the active peak potential of -250 to -300 mV_{SCE} in the crevice environment and the passive potential of around 0 mV_{SCE} in aerated seawater.

This approach to handling the propagation stage requires two additional input parameters to the model for each alloy considered. These are the slope of the log peak current versus pH curve and the corrosion cell voltage. This information, coupled with the value of resistance down the crevice and the previous inputs from the initiation model, allow calculations of anticipated initial propagation rates within defined crevice conditions. It is recognized that as propagation proceeds, several parameters such as the cell voltage, crevice resistance and crevice geometry will change in some interrelated fashion.

REFERENCES

I.C.

Oldfield, J. W., Lee, T. S. and Kain, R. M., "Mathematical Modelling of Crevice Corrosion of Stainless Steels," Corrosion and Corrosion Protection, Proceedings, Vol. 81-8, The Electrochemical Society, 1981, p. 213.

Lee, T. S., "A Method for Quantifying the Initiation and Propagation Stages of Crevice Corrosion," Electrochemical Corrosion Testing ASTM STP 727, 1981, p. 43.

Oldfield, J. W., Lee, T. S. and Kain, R. M., "A Mathematical Model of Crevice Corrosion Propagation of Stainless Steel," CORROSION/81 - Research in Progress Symposium, Toronto, Canada, April 1981.

Kain, R. M., "Crevice Corrosion and Metal Ion Concentration Cell Corrosion Resistance of Candidate Materials for OTEC Heat Exchangers, Parts I and II," ANL/OTEC-BCM-022, May 1981.

Kain, R. M., "Crevice Corrosion Resistance of Several Iron Base and Nickel Base Cast Stainless Alloys in Seawater," Paper No. 66, CORROSION/82, Houston, Texas, March 1982.

Lee, T. S., Oldfield, J. W., Kain, R. M. and O'Dell, C. S., "Assessing Crevice Corrosion Behavior of Stainless Steels in Natural Waters Via Mathematical Modelling," CORROSION/82 - Research in Progress Symposium, Houston, Texas, April 1982.

Lee, T. S., Oldfield, J. W. and Kain, R. M., "The Role of Oxygen Reduction in Crevice Corrosion of Stainless Steels," Presented at 162nd Electrochemical Society Meeting, Detroit, Michigan, October 17-22, 1982.

Kain, R. M. and Lee, T. S., "Polarization Characteristics of Stainless Steel Cathode and Anode Areas Involved in Crevice Corrosion," Presented at 162nd Meeting of Electrochemical Society Meeting, Detroit, Michigan, October 17-22, 1982.

ASTM Designation G78-82 - 1983 Annual Book of ASTM Standards, Vol. 03.02 - Metal Corrosion, Erosion and Wear, p. 463.

Lee, T. S. and Kain, R. M., "Factors Influencing the Crevice Corrosion Behavior of Stainless Steels in Seawater," Paper No. 69, CORROSION/83, Anaheim, California, April 1983.

Lee, T. S., Oldfield, J. W. and Kain, R. M., "The Influence of Environmental Variables on Crevice Corrosion of Stainless Steels," Presented at CORROSION/83 - Research Symposium, Anaheim, California, April 18-22, 1983.

Kain, R. M., "Electrochemical Measurement of the Crevice Propagation Resistance of Stainless Steels: Effect of Environmental Variables and Alloy Content," Paper No. 203, CORROSION/83, Anaheim, California, April 1983.

Kain, R. M. and Lee, T. S., "Recent Developments in Test Methods for Investigating Crevice Corrosion," International Symposium on Laboratory Corrosion Tests and Standards, ASTM, BAI Harbour, Florida, November 14-17, 1983.

Kain, R. M. and Lee, T. S., "The Effect of Crevice Solution pH on Corrosion Behavior of Stainless Alloys," Paper No. 27, To be presented CORROSION/84, New Orleans, Louisiana, April 2-6, 1984.

Kain, R. M., Lee, T. S. and Scully, J. R., "Crevice Corrosion Resistance of Type 316 Stainless Steel in Marine Environments," To be presented at 9th International Congress on Metallic Corrosion, Toronto, Canada, June 3-4, 1984.

TABLE A1

Compositions of Alloys Evaluated in Crevice Corrosion Tests

Alloy	Nominal Percent Composition (wt.)				
	Cr	Ni	Mo	Cu	Other
Type 430	16	1	--	--	--
Type 304	18	8	--	--	--
Type 316	18	10	2.5	--	--
18Cr-2Mo	18	--	2	--	0.1 Ti, 0.4 Nb
Type 317	19	15	3.5	--	--
317 Plus	19	16	4.5	--	--
alloy 904L	20	25	4.5	1.5	--
alloy G	22	45	6.0	1.8	2 Nb+Ta, 0.3 W
26Cr-1Mo	26	0.1	1	--	0.1 Nb
28Cr-4Ni-2Mo	28	4	2	--	0.3 Nb
alloy 254SMO	20	18	6	0.8	0.2 N

TABLE A2

Summary of Environments Utilized in Multiple
Crevice Assembly, Remote Crevice Assembly, and Compartmentalized Cell Tests

Non-Marine

- 1,000 mg/L Cl^- at pH=3 and pH=6
- 10,000 mg/L Cl^- at pH=3 and pH=6
- 15,000 mg/L Cl^- at pH=3
  - (above prepared with NaCl and HCl)
- 3.5% NaCl (neutral)

Marine

- Natural (filtered) seawater
  - 19,000 mg/L Cl^-
  - 35,000 mg/L TDS (salinity)
  - pH=8, dissolved oxygen
    - 80% saturation
- Synthetic Seawater

Simulated Crevice Solutions

- Synthetic Seawater
  - (0.5 M Cl^-) + 3.5 M Cl^-
  - (0.5 M Cl^-) + 4.0 M Cl^-
  - (0.5 M Cl^-) + 4.5 M Cl^-
  - (0.5 M Cl^-) + 5.5 M Cl^-
    - (above prepared with NaCl and HCl)

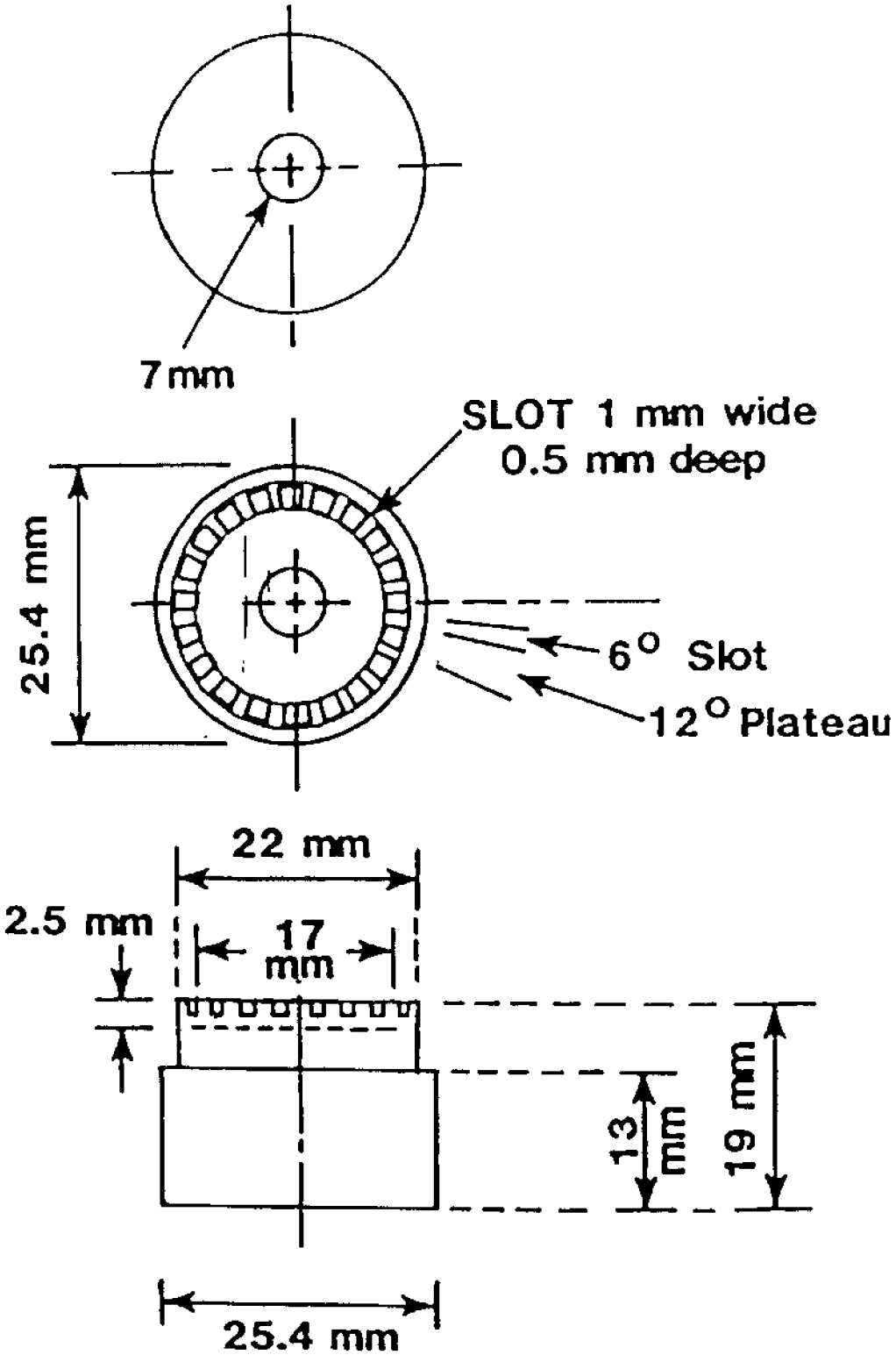

Figure 1 Drawing of multiple crevice assembly washer (not to scale). Two washers are held in place with an insulated, corrosion resistant fastener.

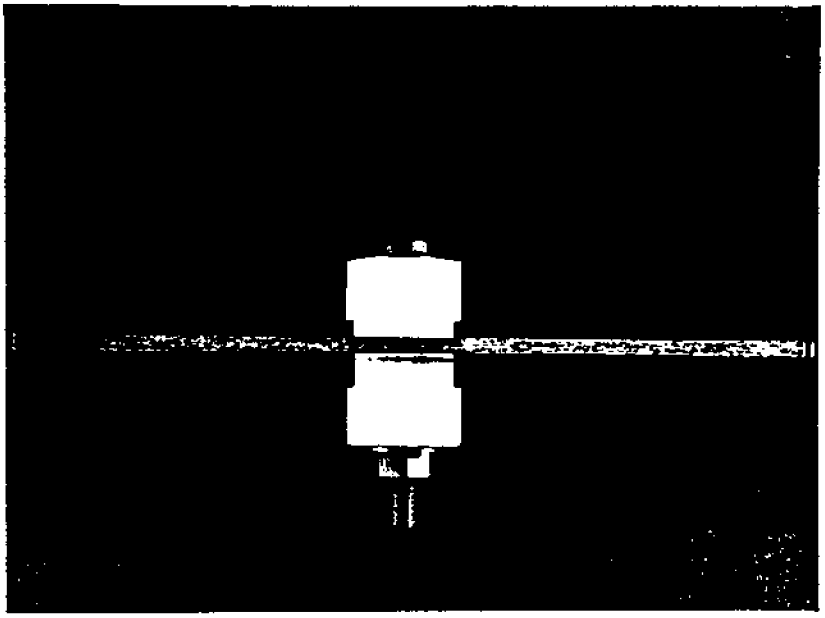

Figure 2 Completed multiple crevice assembly.

Figure 3 Schematic showing differences between conventional crevice test specimen and remote crevice assembly test specimen which enables measurement of corrosion currents.

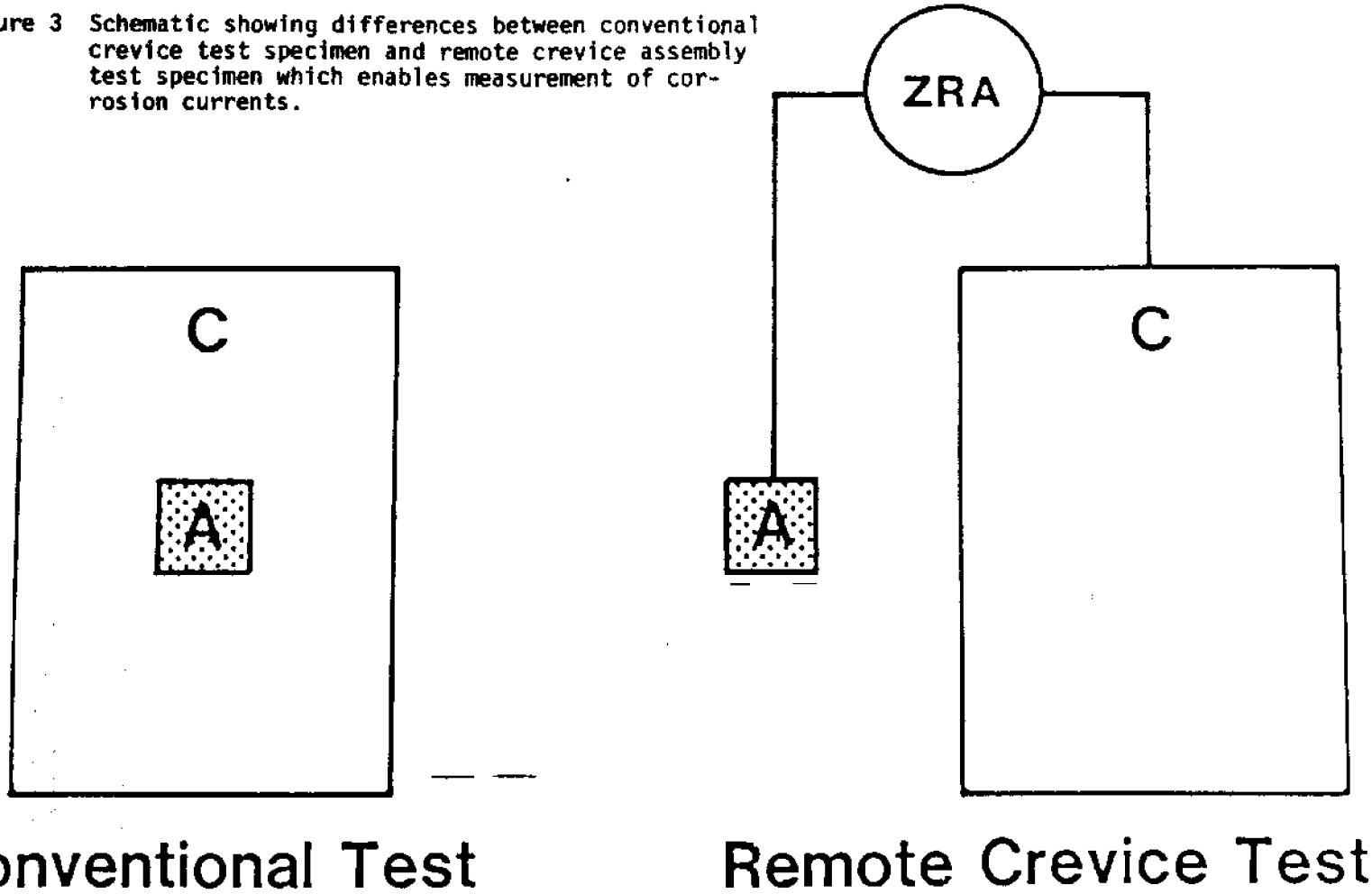

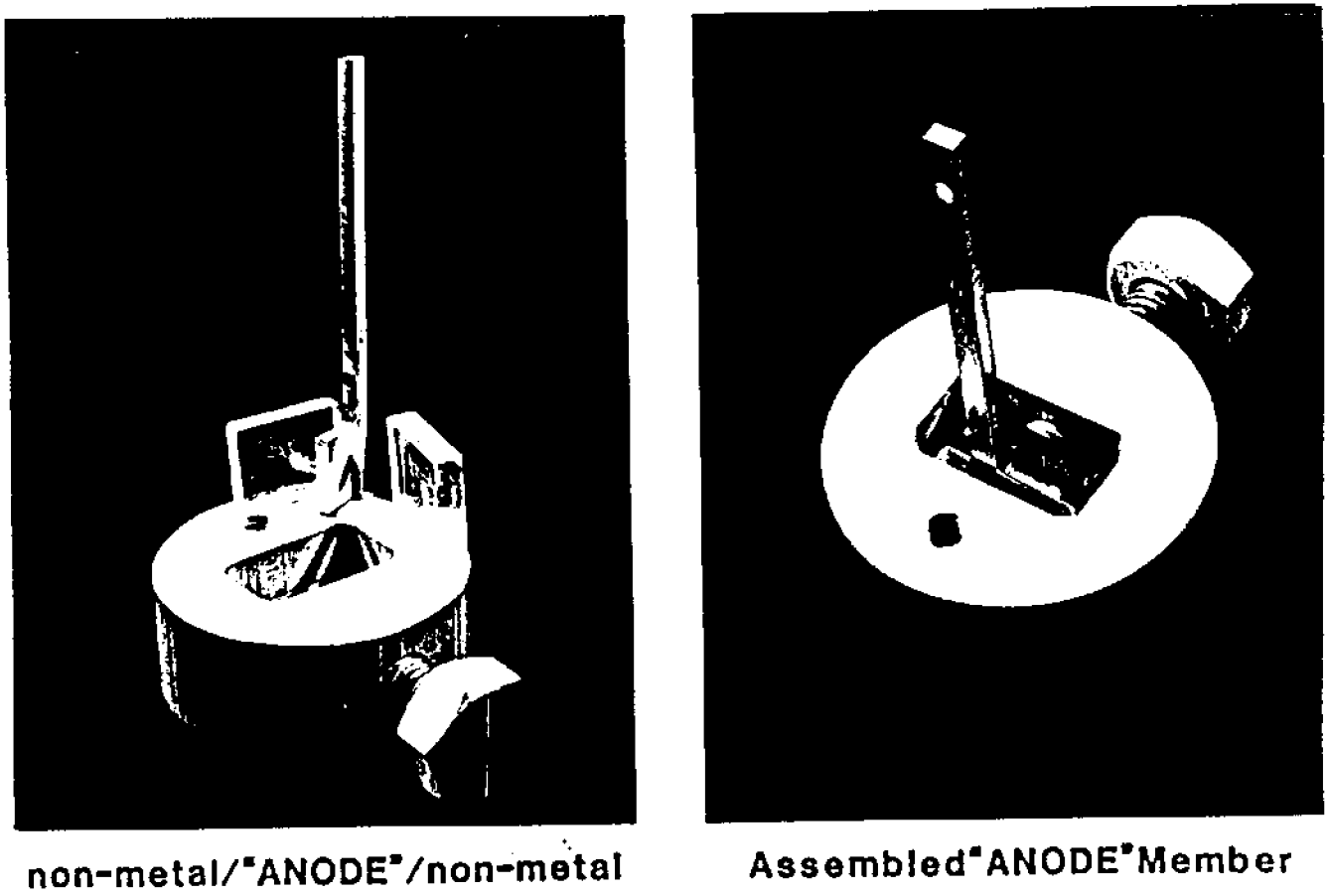

Figure 4 Open and assembled views of bolt loading device used to form non-metal to metal crevice sites on anode member of remote crevice assembly.

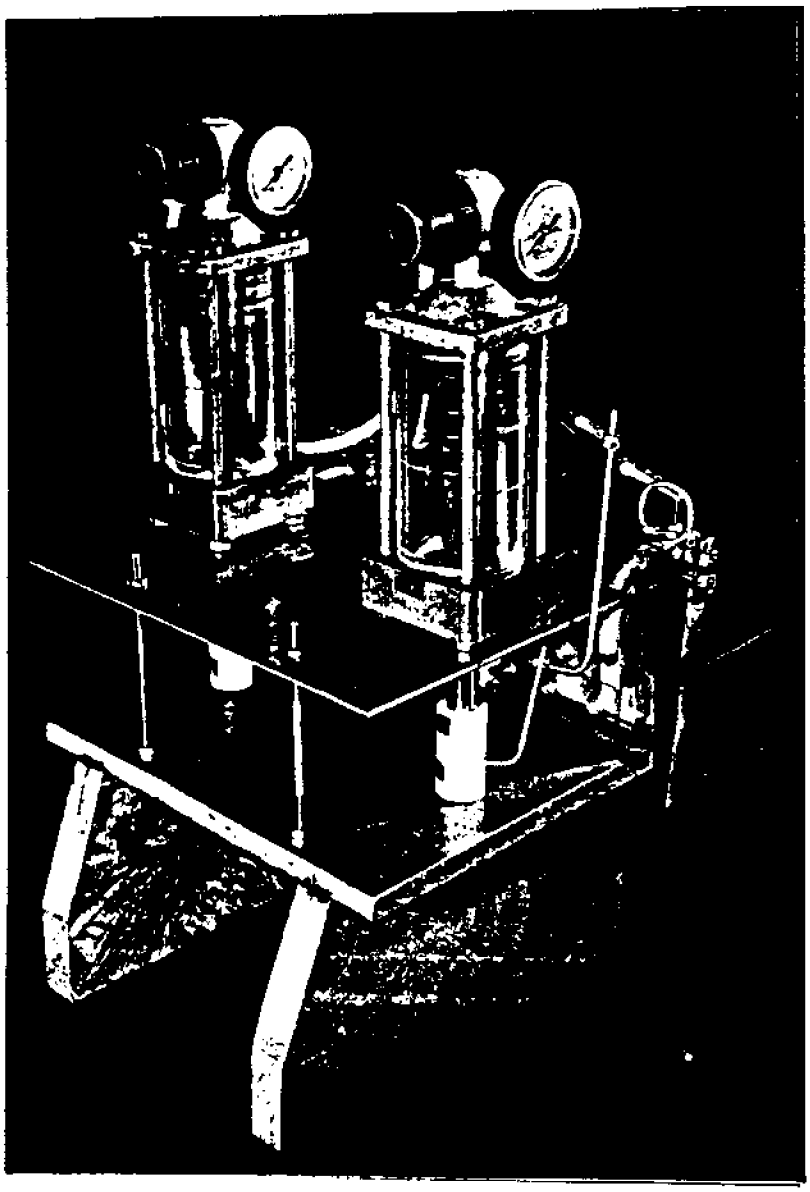

Figure 5 Photograph of experimental, air-operated crevice loading device used in conjunction with remote crevice assembly test method.

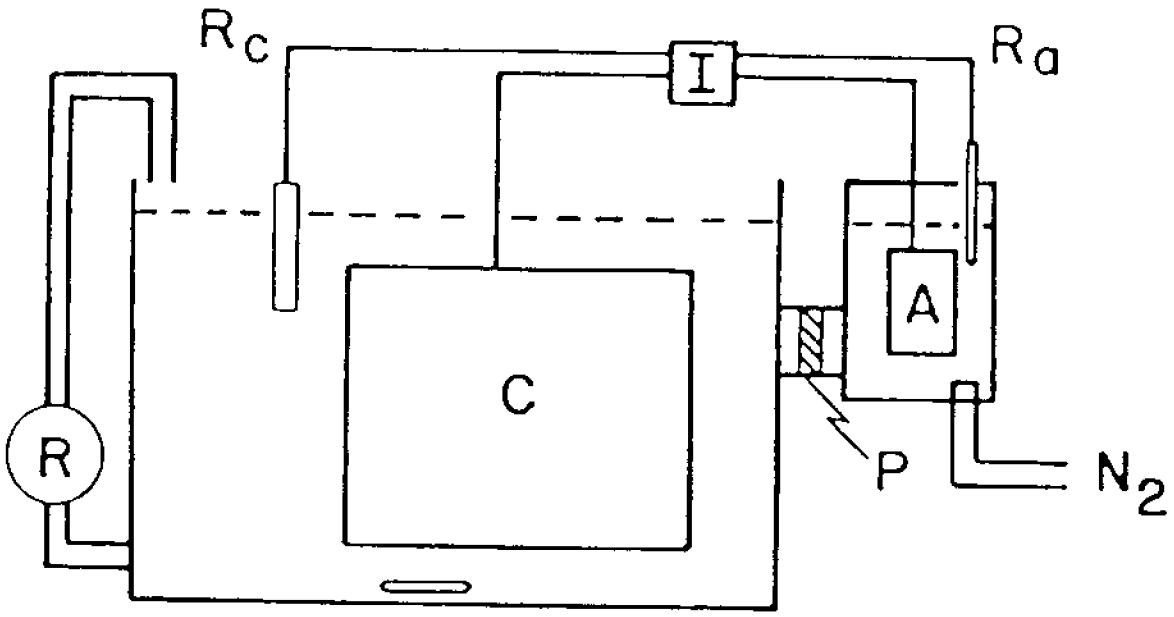

COMPARTMENTALIZED CELL

A = Anode Cell
C = Cathode Cell
R_a, R_c = Reference Electrodes
P = Cell Partition
I = Instrumentation
R = Recirculation Pump/Reservoir

Figure 6 Schematic identifying various components of the compartmentalized cell.

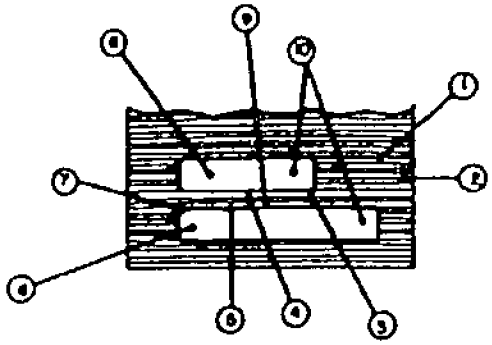

1) BULK SOLUTION COMPOSITION
   - Cl^- content
   - O_2 content
   - pH
2) BULK SOLUTION ENVIRONMENT
   - temperature
   - agitation
3) MASS TRANSPORT IN AND OUT OF CREVICE
   - migration
   - diffusion
   - convection
4) CREVICE SOLUTION
   - hydrolysis equilibria
5) ELECTROCHEMICAL REACTIONS
   - metal dissolution
   - O_2 reduction
   - H_2 evolution
6) ALLOY COMPOSITION
   - major constituents
   - minor additions
   - impurities
7) PASSIVE FILM CHARACTERISTICS
   - passive current
   - film stability
8) CREVICE TYPE
   - metal/metal
   - metal/non-metal
   - metal/marine growth
9) CREVICE GEOMETRY
   - gap
   - depth
10) TOTAL GEOMETRY
   - exterior to interior crevice area ratio
   - number of crevices

Figure 7 FACTORS AFFECTING CREVICE CORROSION

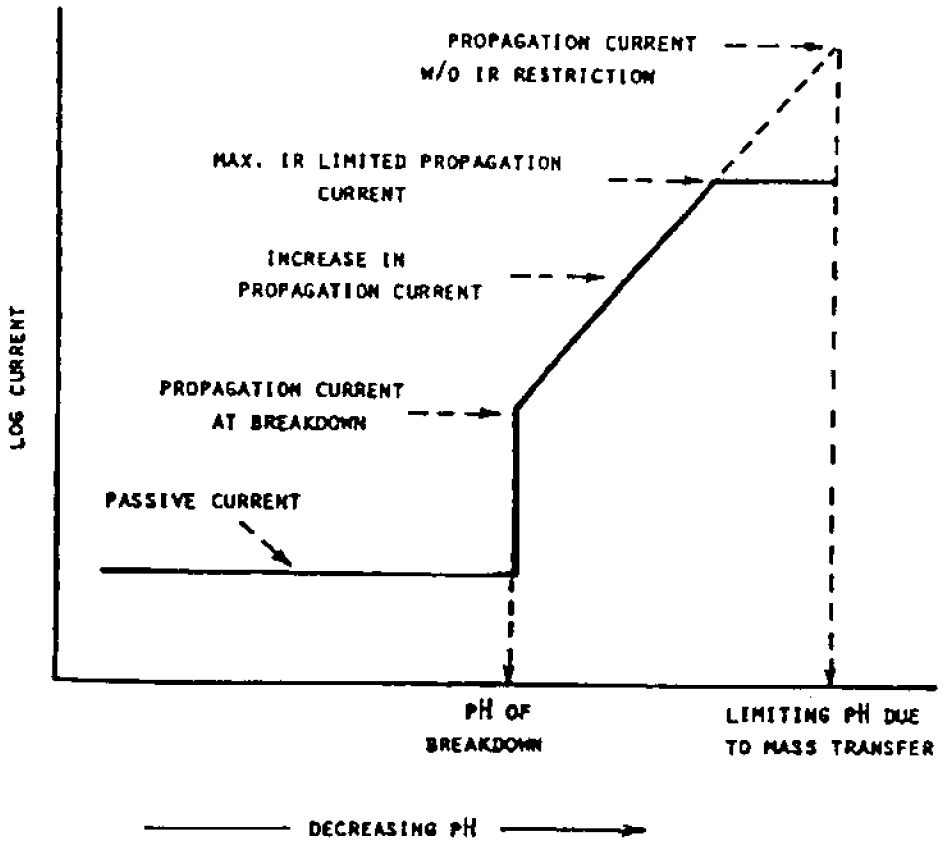

Figure 8 Change in current within the crevice as a function of crevice solution pH.

II. ANALYSIS OF OTEC AND NAVY/LCCT MULTIPLE CREVICE ASSEMBLY DATA

II.A.

FACTORS INFLUENCING THE CREVICE CORROSION BEHAVIOR OF STAINLESS STEELS IN SEAWATER

By

T. S. Lee
R. M. Kain

Presented at
CORROSION/83, Paper No. 69
Anaheim, California, April 1983

LaQUE CENTER FOR CORROSION TECHNOLOGY, INC.
Post Office Box 656
Wrightsville Beach, North Carolina 28480
(919) 256-2271

PAPER NUMBER
69

CORROSION 83

The International Corrosion Forum Sponsored by the National Association of Corrosion Engineers
Anaheim Convention Center, Anaheim, California
April 18-22, 1983

FACTORS INFLUENCING THE CREVICE CORROSION BEHAVIOR OF STAINLESS STEELS IN SEAWATER

T. S. Lee and R. M. Kain
LaQue Center for Corrosion Technology, Inc.
Post Office Box 656
Wrightsville Beach, North Carolina 28480

ABSTRACT

Crevice corrosion has often been regarded as a highly unpredictable occurrence. Recent research has begun to identify the relative influence of several factors which impact crevice corrosion resistance of stainless steels in natural seawater. Results utilizing several experimental methods will be presented to describe the effects of metallurgical and geometric factors.

INTRODUCTION

A wide variety of stainless steels exist from which an engineer may select for a given application. A number of factors will influence this selection including availability, cost, mechanical and physical properties and corrosion resistance of the stainless steel. In seawater applications, resistance to crevice corrosion is of primary concern since it is this form of corrosion which will generally limit the range of application of a given stainless steel.

Considerable research has been conducted in recent years to investigate the factors which can affect the crevice corrosion process. A significant aspect of this research has been the development of a model of crevice corrosion[1,2] which organized the critical factors as environmental, metallurgical, electrochemical and geometrical in nature. For stainless steels in seawater, several of the more critical factors include the salinity, temperature, dissolved oxygen level and velocity of the seawater, the chromium and molybdenum content of the stainless steel, the electrochemical behavior of the passive film and the crevice geometry.

Given the number of factors and the possible interactions between factors, it becomes apparent that reliably defining the expected behavior of a given stainless steel is indeed difficult. Identification of proper experimental methods and critical tests to

assess crevice corrosion behavior in the laboratory is important to enable credible selection of stainless steels which will yield satisfactory field service performance.

Recent research at the LaQue Center for Corrosion Technology, Inc. has been organized to both enhance the understanding of the crevice corrosion process itself as well as characterize relative alloy behavior. This activity includes exposures in natural seawater using a variety of crevice formers and use of a computer-based mathematical model. The present paper summarizes the status of this on-going research.

NATURAL EXPOSURE TESTS IN SEAWATER

Crevice corrosion tests in natural seawater have primarily utilized two types of crevice assemblies, the multiple crevice assembly[3] and the remote crevice assembly[4] (Figure 1). The multiple crevice assembly is a washer with a series of plateaus such that two washers fastened to a test specimen will result in 40 individual crevice sites. The remote crevice assembly utilizes a physically separated, but electrically connected, pair of specimens with the smaller of the two specimens "sandwiched" between two non-metallic plates which create the crevice. The measurement of current between this creviced anode and the larger uncreviced cathode provides an indication of time to initiation and rate of propagation of corrosion in the crevice.

Multiple Crevice Assembly

Two sizeable data bases have been previously generated on a series of stainless steels with the multiple crevice assembly test technique.[5,6] While each data set was analyzed and conclusions about relative alloy performance were stated by the respective authors, the apparent scatter in the data precluded a definitive alloy ranking based on either crevice initiation or propagation resistance.

Since the multiple crevice assembly technique offers a convenient, economical means of conducting crevice corrosion tests in the natural environment and a large data base exists in the literature, there is some motivation to develop an acceptable means of data analysis and presentation. This analysis and presentation should be as simple as possible to facilitate practical use, theoretically credible, consistent between data bases and consistent with known field experience for comparable conditions.

The identification of such a data reduction method has been the object of recent activity. The data base includes a portion of the previously reported tests[5,6] as well as additional tests conducted to complement the earlier multiple crevice assembly tests. The experimental procedures utilized in the conduct of the addtional tests were identical to those reported previously.[5,6] The combined results allow an assessment of relative alloy performance (see Table I for nominal alloy compositions) and an identification of the effects of crevice test parameters such as test duration, torque utilized in attachment of the multiple crevice assembly and alloy surface condition.

Because the crevice corrosion process can be clearly separated into an initiation and a propagation phase, the test data were analyzed to determine relative resistance to each stage of the process. This involved an assessment of the number of individual crevice sites of each multiple crevice assembly washer where corrosion occurred as the parameter defining initiation resistance. The maximum depth of attack incurred under each multiple

crevice assembly washer was selected as the parameter defining the relative extent of crevice corrosion propagation. The data presented in Figures 2-7 represent the mean values (plus and minus one standard deviation) of these two parameters from replicate tests.

To examine the effect of surface finish on crevice corrosion behavior, results of tests on alloys common to both earlier studies[5,6] can be compared. Figures 2 and 3 show initiation and penetration data for 11 alloys exposed for 30 days with crevice assemblies affixed with a torque of 8.5 Nm. The specific ranking or sequence of alloys in Figures 2 and 3 is based on an increasing number of sites initiated or increasing depth of attack measured in the tests on as-received material (open bars). For comparison, the results on 120 SiC surface ground material (surface ground in the area of the crevice assembly only) are shown by the solid bars.

A review of the initiation data (Figure 2) clearly reveals that the ranking of alloys based on initiation resistance is affected by the surface grinding. In all cases where crevice corrosion occurred except alloy SC-1, surface grinding increased the incidence of crevice corrosion. The magnitude of the increase varied from quite significant for Nitronic 50 to a very slight increase for Ferralium. These differences can likely be attributed to variations in surface layer chemistry relative to the bulk alloy chemistry. These variations could include relative enrichment or depletion of critical elements such as chromium and molybdenum as well as removal of surface inclusions such as manganese sulfides from acid pickling of the as-received surfaces. Surface grinding could also serve to enhance contact with the crevice former thus creating more severe conditions.

In the case of crevice corrosion propagation behavior (Figure 3), the alloy ranking is much more consistent when comparing the two surface finishes. As with the initiation data, some increase in depth of attack is noted with the 120 SiC surface ground material when compared to as-received material. This increase can be attributed to some degree to the earlier observed times to initiation documented[6] for the surface ground materials and hence the longer times possible for crevice corrosion propagation.

A comparison of the relative alloy rankings shown in Figure 2 versus those in Figure 3 reveals differences when using the data from either type of surface finish. This confirms the importance of treating the two phases of the crevice corrosion process separately when ranking alloy resistance as well as when considering the effect of a variable such as surface finish.

Another variable which would be expected to affect crevice corrosion is the duration of the exposure. Figures 4 and 5 summarize the number of sites and depth of attack, respectively, for 16 alloys which were surface ground with 120 SiC paper and exposed for 30 days in 30°C seawater. The relative alloy ranking shown in each Figure is based on these 30 day data. For comparison, data from 60 day tests are shown for 6 of the alloys and data from 82 day tests are shown for 4 alloys which were resistant to crevice corrosion in the present tests. As can be seen in Figure 4, an increase in exposure time did not increase the number of initiated sites for SC-1 or Ferralium but did result in a slight increase in number for alloys G, 20 mod and 6X. Anomalous behavior was exhibited by 254SMO with the panels exposed for 60 days exhibiting fewer sites initiated than on companion panels exposed for 30 days. Except for this 254SMO behavior, the relative alloy ranking of initiation resistance can be seen to be unaffected by the test duration.

Increased exposure time consistently increased the maximum depths of attack for all 6 of the susceptible alloys tested for the two time periods as shown in Figure 5. As with the initiation data, the relative alloy ranking of resistance to crevice propagation is not altered except for a slight repositioning of alloy G. Again, the ranking of the alloys based on initiation criteria is different from that based on propagation criteria (Figure 4 versus Figure 5).

Finally, the effect of relative crevice tightness can be examined from the data in Figures 6 and 7. The crevice tightness is varied by using different levels of torque to affix the multiple crevice assembly. A torque level of 2.8 Nm was used in one series of 60 day tests which established the relative alloy ranking. For comparison, data are also shown for 6 alloys which were exposed with an assembly torque level of 8.5 Nm. As can be seen, the relative alloy rankings are not changed if these latter data are the base.

The initiation data in Figure 6 show an increase in number of sites initiated for all 6 alloys with the tighter crevices created at the higher torque level. As will be discussed in a later section, this is consistent with the theoretical predictions of the mathematical model. In the case of propagation resistance, an increase in assembly torque resulted in an increase in depth of attack for the 3 alloys that were susceptible to corrosion in tests at both torque levels.

Remote Crevice Assembly

Using the remote crevice assembly test method, a data base is being developed to evaluate the relative effects of factors such as crevice geometry, material surface finish, anode/cathode area ratio, seawater temperature and seawater velocity the rate of crevice corrosion propagation. These data will estabish a baseline for defining optimum conditions to minimize the extent of crevice corrosion likely to be incurred by a given alloy in field service applications. It will also provide critical feedback in the verification and refinement of the mathematical modelling.

The data derived from a remote crevice assembly test are quite extensive and can be analyzed in a variety of ways. Figure 8 graphically depicts the typical current and corrosion potential data obtained with this test technique. The data are from tests on Type 316 stainless steel in 30°C seawater at a constant crevice geometry (torque used to affix crevice formers was 2.8 Nm) and anode/cathode area ratio (1/35). In these tests, the effect of surface finish was examined by the use of 120 SiC surface ground, nitric acid pickled and electropolished surfaces. The experimental procedures are described in more detail elsewhere.[7]

The rapid increase in current evidenced in Figure 8 after approximately two days of test is indicative of the onset of crevice corrosion and can be confirmed by visual observation of staining of the crevice specimen. A slight enobling of the corrosion potential followed by a shift to more active potential coincident with this increase in current is also seen in Figure 8. This is consistent with the expected effect of an active anode in the acid-chloride environment of the crevice controlling the potential of the specimen assembly.

The magnitude of current after initiation provides a measure of the relative rate of propagation of crevice corrosion at any time. An analysis of these current data and post-test physical measurements of mass loss and depth of attack on the crevice anode

specimen provide the basis for comparing and assessing the effects of factors such as surface finish as shown in Table II. All of the data related to propagation of crevice corrosion, i.e., maximum current, total charge, weight loss and maximum attack depth, consistently show the lowest propagation rates for the electropolished surface and the highest propagation rates for the nitric acid pickled surface.

These results appear, at first glance, to contradict the earlier conclusions about surface grinding based on the multiple crevice assembly data. However, the remote crevice assembly tests were performed with both anode and cathode surfaces prepared in the given surface conditions. This is contrasted to the multiple crevice assembly tests where surface grinding was performed only in a 50 mm diameter area of the crevice assembly and the remaining cathode surface was in the as-received condition. That the nature or kinetics of the reactions occurring on the uncreviced, cathode areas clearly influence the rate of propagation can be deduced by comparing the two sets of data.

MATHEMATICAL MODEL ANALYSES

The second major focus of recent crevice corrosion research involves use of a mathematical model of crevice corrosion.[1,2] The computer-based model is based on the commonly accepted mechanism of crevice corrosion of passive materials involving

1. deaeration within the crevice
2. decrease in pH and increase in chloride concentration of the crevice environment
3. breakdown of the passive film on the metal surface in the crevice area
4. propagation of corrosion

The model separates the first three steps into the initiation phase of crevice corrosion with the fourth step as the propagation phase. This systematic method provides an organized approach to investigating the predicted effects of the multitude of factors which can influence crevice corrosion. This modelling serves to provide guidance in the design of crevice experiments as well as providing a predictive tool for relative alloy performance.

In the case of experimental design, the model can focus attention on the critical variables which will influence the crevice corrosion process and thereby influence the test results. It is this approach that has defined the criticality of crevice tightness in assessing the observed initiation behavior of a given stainless steel. This is demonstrated by the data in Figure 9 which rank a series of alloys based on the range of crevice gaps where crevice initiation could be expected. This modelling exercise was performed assuming a fixed crevice depth of 0.1 cm which is nominally the width of one plateau on a multiple crevice assembly. It can be seen that Type 430 stainless steel would be prone to crevice corrosion initiation at crevice gaps that range two orders of magnitude larger (up to 0.5 μm) than the gaps necessary for crevice corrosion initiation of alloy 625 (<0.005 μm).

The data also demonstrate that if a range of crevice gaps exist with a given crevice former then a range in relative alloy performance would be evident.[8] For example, at a gap of 0.005 μm (metal to non-metal gap), the differentiation in initiation times for Type 430 and for alloy 6X would be minimal. However, at a metal to non-metal gap of 0.01 μm,

a much greater time to initiation of crevice corrosion would be expected for alloy 6X. Similarly, the variation in crevice gaps over a very small range, which would be expected in any real-life situation, would yield a range in performance for a given alloy. For example, variations in gap between the individual plateaus of a single multiple crevice assembly could be expected to result in some sites initiating quickly while some individual sites may take longer to initiate or never initiate. This concept helps to explain the often observed large variability in initiation behavior for seemingly replicate test conditions yet, in the case of the multiple crevice assembly, provides the basis for its utility as an effective screening tool.

Characterization of the actual crevice gaps observed on crevice test assemblies then becomes a key component of the feedback circuit necessary to correlate and verify the model predictions with observed natural exposure data. To this end, analysis of typical crevice gaps present on the remote crevice assembly and multiple crevice asembly have been carried out as shown in Figure 10. A range of crevice gaps in the specific area photographed is evident with both crevice formers. This range is typically from 0.1 μm to as great as 2-3 μm. Numerous such measurements have been made and the data base provides valuable input into the mathematical model. The magnitude of gaps observed and the impact of this parameter as shown by the model help to explain the variability as well as the difficulty in practically achieving a uniformly reproducible crevice gap.

A second manner in which the model can be utilized incorporates variations in both crevice gap and crevice depth. As shown in Figure 11, a range of depths which are greater than the value used in Figure 9 and a range of crevice gaps have been modelled to depict the relative performance of several alloys. In this situation, the limiting combinations of crevice depth and gap have been plotted to delineate the boundaries between geometries which would be expected to result in initiation of crevice corrosion (below and to the right of the curves) as contrasted to those geometries where crevice initiation would not be expected (above and to the left of the curves).

This approach allows one to establish a relative order of expected performance based on the percentage of geometries where crevice corrosion might occur. Table III summarizes such a limited ranking based on the modelling results shown in Figure 11. As can be seen, alloy 625 is predicted to be resistant to crevice corrosion in most instances as is consistent with the observed experimental results presented earlier in which no crevice corrosion occurred. The subsequent ranking of the other alloys is generally consistent with the observed experimental data shown earlier. Refinements to the assumptions made in the modelling process and the logic sequence of the model itself can be made to enable a closer correlation with the natural exposure data and enhance the credibility of the model as a predictive tool.

The second phase of the model assesses propagation resistance of alloys. The preliminary model can again be used[9] to define the relative influence of crevice geometry on predicted alloy performance as shown schematically in Figures 12 and 13. Figure 12 represents behavior of an alloy which demonstrates relatively "poor" resistance to propagation of crevice corrosion as evidenced by the rapid increase in propagation current as the pH in the crevice decreases. The horizontal lines reflect limiting propagation rates which would result from IR restrictions. Limiting rates for three different assumed crevice gaps are shown.

The data show that the propagation rate in this IR limited condition increases with increasing crevice gap. This is opposite to the effect of crevice geometry on crevice

initiation where a tighter crevice is more severe. In this particular case, however, the large gap results in a large volume of electrolyte in the crevice and hence a lower resistance. This lower resistance results in a higher allowable maximum current for propagation.

This particular effect of increasing gap allowing a higher propagation rate is often counteracted, however, by the effects of mass transport on the crevice solution composition. As the effective crevice gap is increased, either in original design or as a result of on-going crevice corrosion, an increase in propagation rate can be expected only to the point where diffusion of chloride and hydrogen ions from the crevice confines is enhanced. At that point, the pH within the crevice may increase with the net result of a decrease in overall propagation current. This can be seen in Figure 12 where an order of magnitude decrease in propagation rate is observed with an increase in crevice solution pH of less than one unit.

An opposite effect of crevice gap is shown in Figure 13 which demonstrates the same type of data for a stainless steel with the same initiation resistance as before but with a more shallow log propagation current peak versus pH slope (by definition, a greater resistance to propagation than in the previous case). With this alloy, the IR limited conditions are not reached for the gaps considered and the limiting crevice solution pH is reached as a result of mass transfer restrictions. In this situation, the tighter crevices result in the development of a lower pH crevice solution and a resultant higher propagation rate. Referring back to the experimental data shown in Figure 7, it can be seen that the maximum depth of attack was decreased for alloys G, 6X and 20 mod when the less tight crevice gaps created by the lower assembly torque of 2.8 Nm were used. For all 3 alloys, propagation resistance behavior as depicted in Figure 13 has been measured.

SUMMARY

Accurately assessing the relative crevice corrosion resistance of iron and nickel base stainless alloys requires a recognition of many factors. It has been shown that in seawater, metallurgical, environmental and design factors are important. With an understanding of the operative mechanism of crevice corrosion, a combination of theoretical treatments and natural seawater exposures can be utilized to define the influence of many variables.

ACKNOWLEDGEMENT

This work has been sponsored by the National Sea Grant Office of NOAA and the LaQue Center for Corrosion Technology, Inc.

REFERENCES

1. Oldfield, J. W. and Sutton, W. H., "Crevice Corrosion of Stainless Steels. I. A Mathematical Model," British Corrosion Journal, Vol. 83, p. 13, 1978.

2. Oldfield, J. W. and Sutton, W. H., "Crevice Corrosion of Stainless Steels. II. Experimental Studies," British Corrosion Journal, Vol. 13, p. 104, 1978.

3. Anderson, D. B., "Statistical Aspects of Crevice Corrosion in Seawater," Galvanic and Pitting Corrosion, ASTM STP 576, p. 261.

4. T. S. Lee, "A Method for Quantifying the Initiation and Propagation Stages of Crevice Corrosion," presented at Electrochemical Corrosion Testing, ASTM STP 727, p. 43.

5. Kain, R. M., "Crevice Corrosion and Metal Ion Concentration Cell Corrosion Resistance of Candidate Materials for OTEC Heat Exchangers, Parts I and II," ANL/OTEC-BCM-022, May 1981.

6. Hack, H.P., "Crevice Corrosion Behavior of 45 Molybdenum-Containing Stainless Steels," CORROSION/82, Houston, Texas, March 1982, Paper No. 65.

7. Kain, R. M., "Electrochemical Measurement of the Crevice Corrosion Propagation Resistance of Stainless Steels: Effect of Environmental Variables and Alloy Content," Paper No. 203, CORROSION/83, Anaheim, California, April 18-22, 1983.

8. Kain, R. M., "Crevice Corrosion Resistance of Stainless Steels in Seawater and Related Environments," CORROSION/81, Toronto, Canada, April 1981, Paper No. 200.

9. Oldfield, J. W., Lee, T. S. and Kain, R. M., "Mathematical Modelling of Crevice Corrosion of Stainless Steels," Corrosion and Corrosion Protection, Proceedings, Vol. 81-8, The Electrochemical Society, 1981.

TABLE I

Nominal Alloy Compositions for Several Iron Base and Nickel Base Stainless Alloys

Alloy	Cr	Ni	Mo	Cu	Other
29-4C	29	0.8	4		0.6 Ti
alloy 625	22	61	9		3.5 Cb + Ta
alloy C-276	15.5	55	15.5		4 W, 2 Co
MONIT	25	4	4		
SC-1	25	2	3		0.5 Ti
Ferralium	26	5.5	3	1.8	0.2 N
alloy G	22	47	6	1.8	2 Cb, 0.3 W, 1 Co
alloy 20 mod	22	25	5		
alloy 6X	20	25	6		
254SMO	20	18	6	0.8	0.2 N
Type 316	18	10	2.5		
alloy 825	22	44	3	1.5	0.7 Ti
alloy 904L	20	25	4.5	1.5	
alloy 700	20	25	4.5		
alloy 777	20	25	4.5	2	
Nitronic 50	21	14	2		4 Mn

TABLE II

The Effect of Surface Finish on Remote Crevice Assembly Test Results on Type 316 Stainless Steel in 30°C Seawater

Surface Finish	Time to Initiation (Days)	Maximum Current ($\mu A/cm^2$)	Total Charge ($Coul/cm^2$)	Weight Loss (mg/cm^2)	Maximum Attack Depth (mm)	Area Attacked (%)
Electropolished	2.0	180	145	24	1.30	13
120SiC	1.5	440	663	162	1.68	78
HNO_3	2.0	710	988	240	2.00	90

TABLE III

Mathematical Model Prediction of
Relative Alloy Resistance to Crevice Corrosion Initiation

Alloy	Percent of Geometric Conditions* for Crevice Initiation
alloy 625	16
254SMO	24
alloy 6X	29
alloy 904L	34
Type 316	54
Type 304	90

* Geometries include:
0.2 μm < metal-to-metal crevice gap < 10 μm
0.3 cm < crevice depth < 6.5 cm

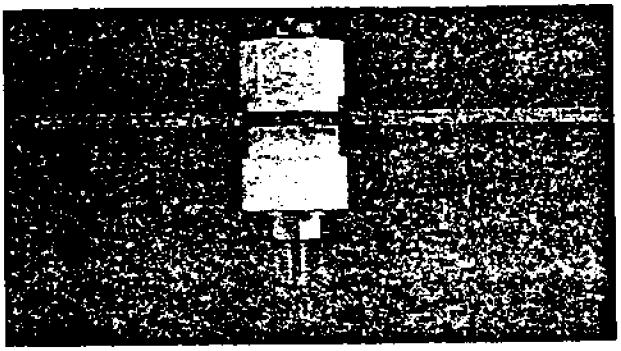

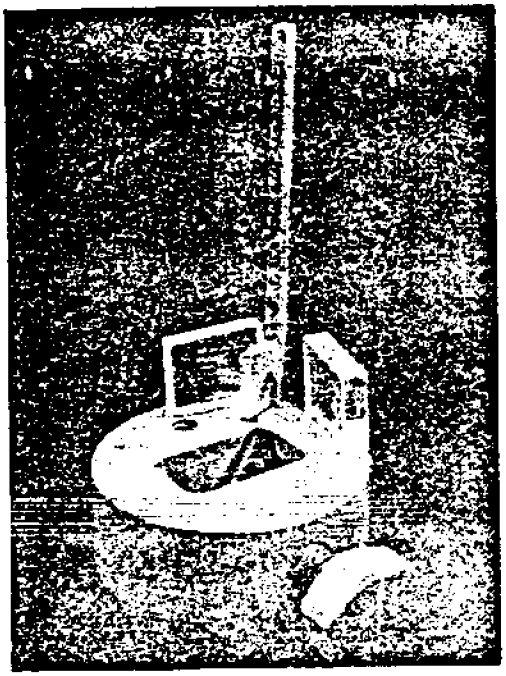

1. Multiple crevice assembly (top) and remote crevice assembly anode (bottom) utilized in natural seawater crevice corrosion tests at LCCT.

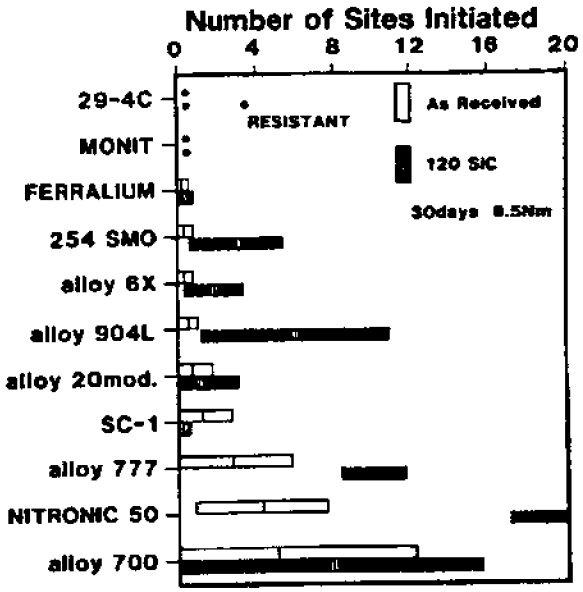

2. Summary of number of initiated crevice sites beneath a multiple crevice assembly washer for a series of alloys tested in natural seawater. Bar graphs represent the mean values (plus and minus one standard deviation) for replicate tests conducted for 30 days on as-received surfaces and 120 SiC surface ground material using an assembly torque of 8.5 Nm.

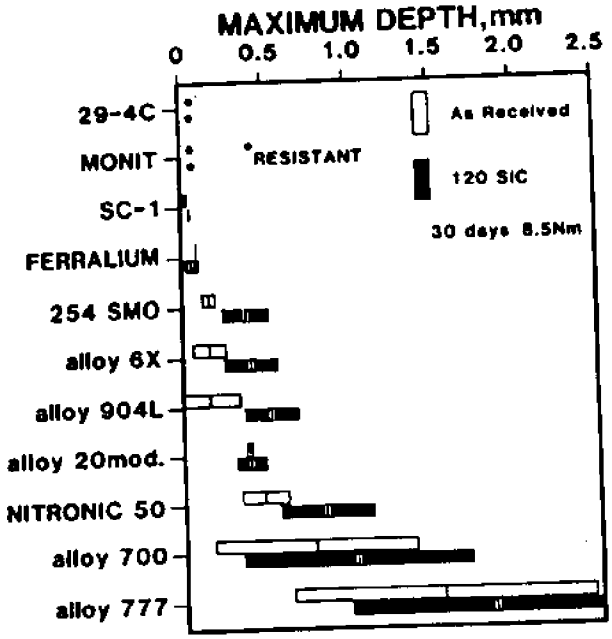

3. Summary of maximum depth of attack beneath a multiple crevice assembly washer for a series of alloys tested in natural seawater. Bar graphs represent the mean values (plus and minus one standard deviation) for replicate tests conducted for 30 days on as-received surfaces and 120 SiC surface ground material using an assembly torque of 8.5 Nm.

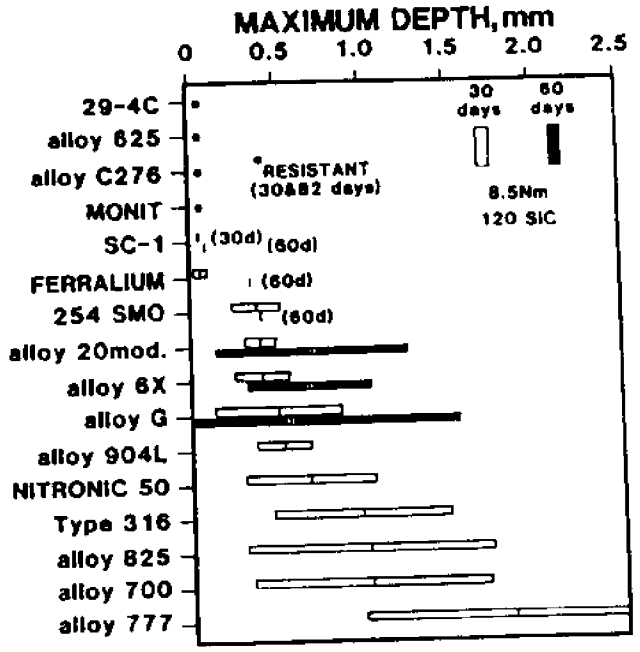

5. Summary of maximum depth of attack beneath a multiple crevice assembly washer for a series of alloys tested in natural seawater. Bar graphs represent the mean values (plus and minum one standard deviation) for replicate tests conducted for 30 days (16 alloys) or 60 or 82 days (10 alloys) using an assembly torque of 8.5 Nm.

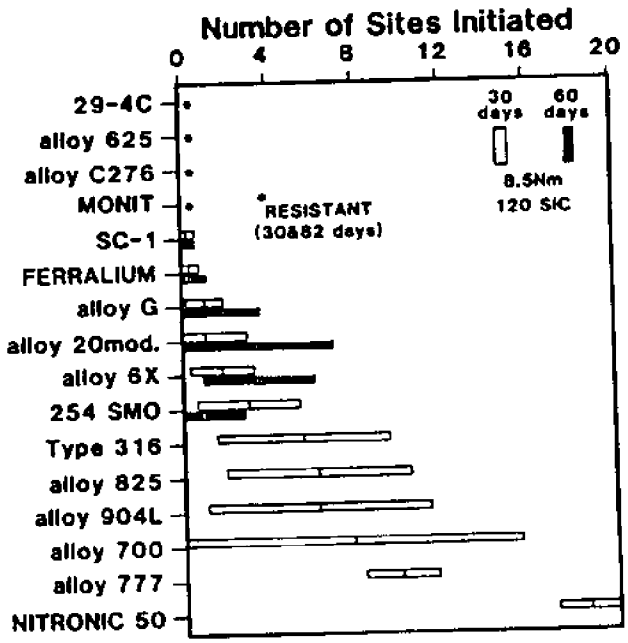

4. Summary of number of initiated crevice sites beneath a multiple crevice assembly washer for a series of alloys tested in natural seawater. Bar graphs represent the mean values (plus and minus one standard deviation) for replicate tests conducted for 30 days (16 alloys) or 60 or 82 days (10 alloys) using an assembly torque of 8.5 Nm.

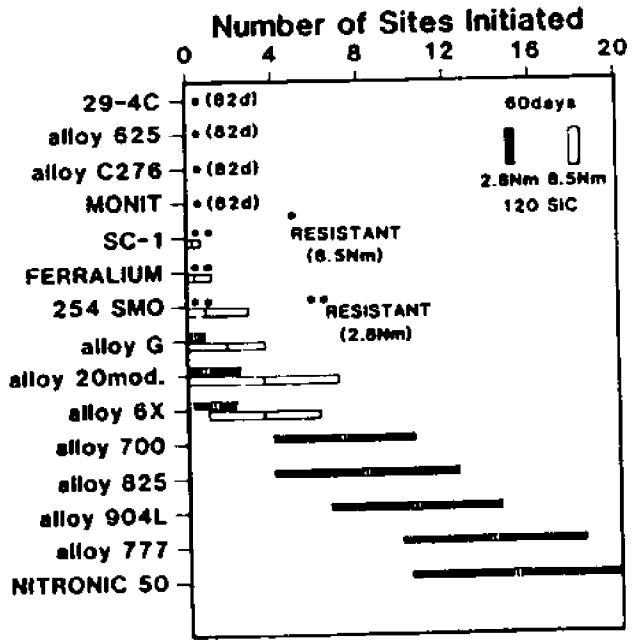

6. Summary of number of initiated crevice sites beneath a multiple crevice assembly washer for a series of alloys tested in natural seawater. Bar graphs represent the mean values (plus and minus one standard deviation) for replicate tests conducted for 60 days using an assembly torque or either 2.8 Nm (11 alloys) or 8.5 Nm (10 alloys).

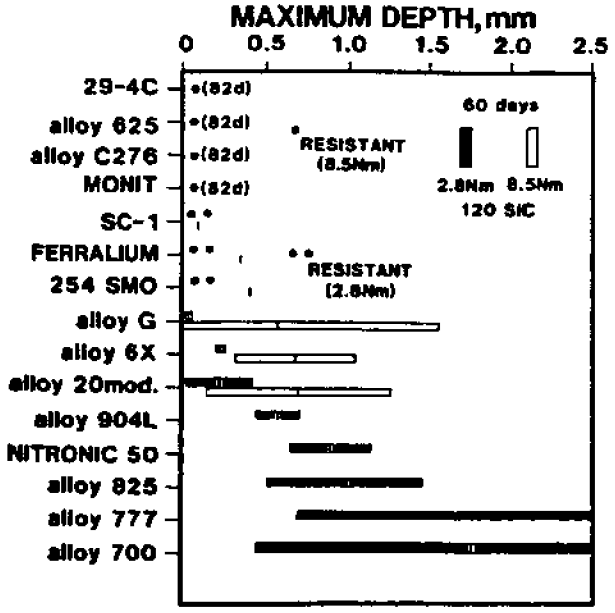

7. Summary of maximum depth of attack beneath a multiple crevice assembly washer for a series of alloys tested in natural seawater. Bar graphs represent the mean values (plus and minus one standard deviation) for replicate tests conducted for 60 days using an assembly torque of either 2.8 Nm (11 alloys) or 8.5 Nm (10 alloys).

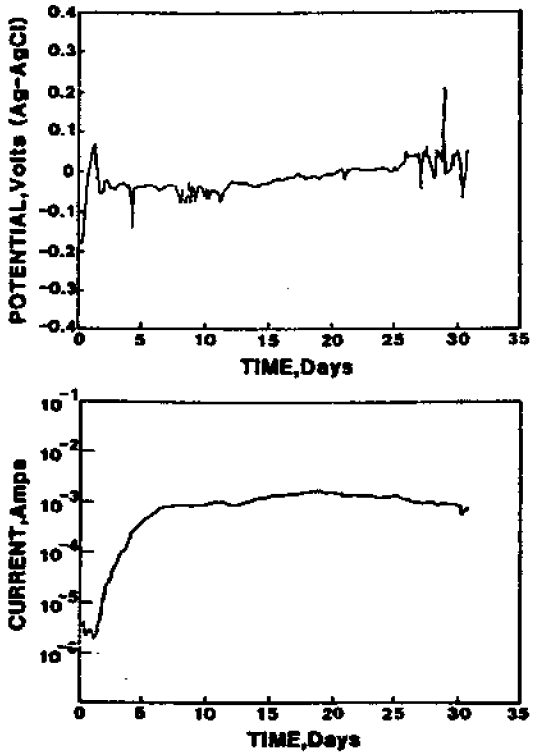

8. Corrosion potential (top) and current (bottom) from remote crevice assembly test on Type 316 stainless steel in 30°C seawater. Specimen surfaces were 120 SiC surface ground.

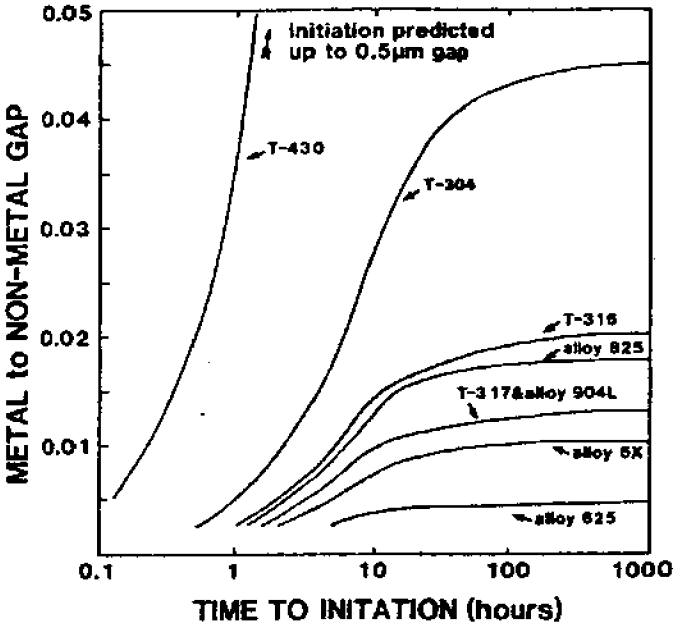

9. Typical mathematical model prediction of effect of crevice gap (constant crevice depth of 0.1 cm) on time to crevice corrosion initiation for several alloys in seawater.

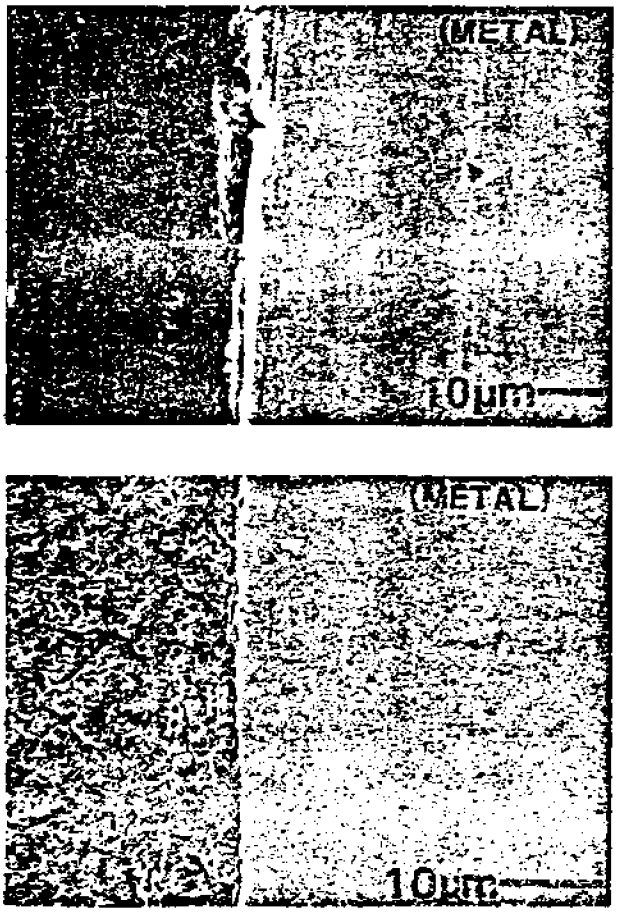

10. Cross section of remote crevice assembly (top) and multiple crevice assembly (bottom) showing typical range of crevice gaps which can exist.

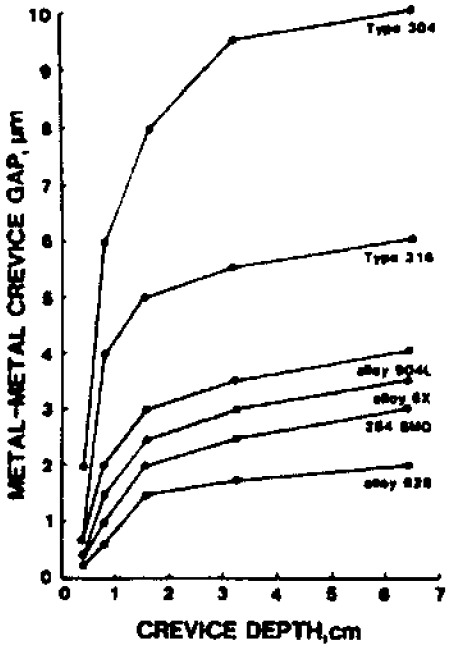

11. Effect of crevice gap and depth on initiation of crevice corrosion. The gaps and depths below and to the right of the curve for each alloy define geometries where crevice initiation is predicted.

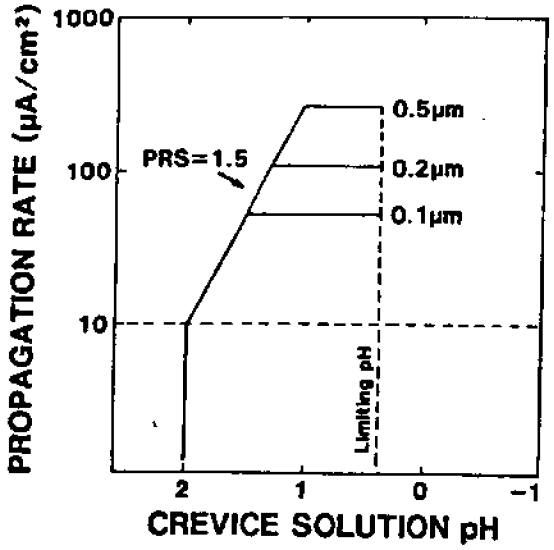

12. Predicted crevice corrosion propagation rate as a function of crevice solution pH for a stainless steel showing initiation of crevice corrosion at pH 2 and with a propagation rate slope (PRS) of 1.5.

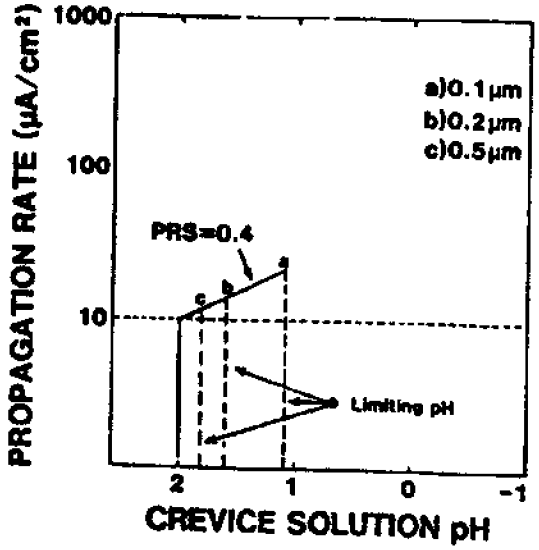

13. Predicted crevice corrosion propagation rate as a function of crevice solution pH for a stainless steel showing initiation of crevice corrosion at pH 2 and with a propagation rate slope (PRS) of 0.4.

II.B. ANALYSIS OF CREVICE CORROSION DATA FROM TWO RECENT SEAWATER EXPOSURE TESTS ON STAINLESS ALLOYS

By

Michael A. Streicher

Presented at
CORROSION/83, Paper No. 70
Anaheim, California, April 1983

Department of Chemical Engineering
University of Delaware
Newark, Delaware 19716

PER NUMBER
70

CORROSION 83

The International Corrosion Forum Sponsored by the National Association of Corrosion Engineers
Anaheim Convention Center, Anaheim, California
April 18-22, 1983

ANALYSIS OF CREVICE CORROSION DATA FROM TWO RECENT SEAWATER EXPOSURE TESTS ON STAINLESS ALLOYS

Michael A. Streicher
Department of Chemical Engineering
University of Delaware
Newark, Delaware 19711

Abstract

Publications on two concurrent series of crevice corrosion tests on a total of 46 stainless alloys have recently become available. These tests were made at the Francis L. LaQue Center for Corrosion Technology, Wrightsville Beach, NC, using filtered, essentially quiescent seawater heated to 30°C. The same 46 alloys are being used for a laboratory investigation of crevice corrosion. In order to compare the results of the laboratory tests with those obtained in natural seawater, a detailed analysis of the data from both series of seawater tests has been undertaken.

For the analysis, a Crevice Corrosion Index (CCI) consisting of the product of the number of panel sides showing any attack (S) and the maximum depth of attack in mm (D) was calculated for all of the alloys. With this Index the 46 alloys were ranked in order of increasing values. The resulting tables were then used to derive information on the effect of testing time, torque on the crevices, surface finish and alloy composition. In addition to the major effect of chromium and molybdenum, copper, manganese, nitrogen and niobium were found to have a significant effect on crevice corrosion of stainless alloys in seawater. The results have been used to derive improved testing procedures for crevice corrosion tests, as well as suggestions for new test series. Applications and limitations of rankings based on the Index are discussed.

INTRODUCTION

Testing Conditions

The completion in 1980 of two series of crevice corrosion tests in natural seawater has provided us with comparable data for a large range of stainless alloys. Both tests were carried out at the LaQue Center for Corrosion Technology, Inc., Wrightsville Beach, NC, under the supervision of R. M. Kain. For both series of tests, three panels, 10 x 15 cm, were exposed for each test condition with Delrin™* crevice devices on the front and back of each panel, Fig. 1. Each Delrin device (1) had 20 "teeth" or plateaus ground to a 600-grit finish (SiC). The ratio of unshielded to creviced area was 150:1. Both tests were made in filtered seawater heated to 30°C. Filtration eliminates the growth of marine organisms on the test panels. The normal velocity through the test section in the 400-liter troughs was less than 0.1 m/sec. There were 6 to 7 complete changes of water daily. Some details of the properties of the test solution are given in Table I. It is shown below that these test conditions are severe and have provided a wide range of crevice corrosion on a total of 46 alloy compositions.

Data on the two series of tests have been reported in detail by R. M. Kain (2) and H. P. Hack (3). The report by R. M. Kain contains a separate page of data for each alloy tested. One such page is given in Table II. For each side of every test panel the following data have been provided: a) time to initiation of corrosion as detected by discoloration from corrosion products near the crevice devices, b) number of sites ("teeth" or plateaus) on each side at which there was attack, and c) range of depth of crevice attack for each crevice device. The publications by H. P. Hack (3) do not contain such tables of data. However, he has made the tables, provided on the Navy tests by R. M. Kain, available to the author for this analysis, Table III.

Even though the two series of tests were carried out simultaneously and under almost identical conditions, the objectives of each program were different. The tests reported by R. M. Kain were made to obtain data to aid in the selection of materials for heat exchangers for the Ocean Thermal Energy Conversion (OTEC) program. This series included 12 commercially available alloys and one experimental alloy (Carpenter Exp. 58), with various mill finishes, Table IV. Microscopic examination of these surfaces showed clear evidence of pickling on all alloys except on Monit, which had a mechanically ground finish. The tests were run for 30, 60, and some even 90, days, Table II.

The 12 commercially available alloys from the OTEC series were also included in the Navy series reported by H. P. Hack (3)

---

*Delrin™ - Trademark, E. I. du Pont de Nemours & Co., Inc. Wilmington, DE.

along with 33 other commercially available alloys. All the Navy tests were for only 30 days. Also, all specimens in the Navy series were given a 120-grit finish on that part of the surface to which the crevices were applied (Fig. 2). An overview of these testing parameters is given in Table III. The objective of the Navy tests was to provide comparable marine corrosion data on a wide range of molybdenum-bearing alloys which have greater resistance to crevice corrosion than Type 316 stainless steel, but which cost less than certain nickel-base alloys, such as Inconel alloy 625™†.

Despite these differences in objectives and testing conditions, there are enough similarities in the two test series to make it possible to use data from both for an analysis of such factors as surface finish, testing time, torque on the crevice devices, and, to some extent, alloy composition.

Alloys Tested

Chemical analyses for the 13 alloys in the OTEC series are given in Table IV. The chromium contents are in the range of 20 to 29%, with nickel from 0.5 to 26% and molybdenum from 1.4 to 6.5%. Other alloying elements include copper, manganese, titanium and nitrogen. Of the 13 alloys, three are completely ferritic (29-4C, Monit and SC-1), two have a duplex, austenite-ferrite structure (Ferralium and Type 329) and the remainder are completely austenitic. The 29-4C™* alloy, produced by the Allegheny Ludlum Steel Corp., is a titanium stabilized argon-oxygen decarburized (AOD) modification of the high purity, vacuum-induction melted Fe-29%Cr - 4%Mo alloy (4,5,6,7). Because of the higher nitrogen contents of the 29-4C AOD melts, titanium is added to prevent precipitation of chromium nitrides during welding. Such precipitates would make the alloy subject to intergranular attack in acids and also impair the resistance to attack by chlorides. Both the interstitial impurities, C and N, and the stabilizing element, Ti, reduce the toughness of this alloy as compared with the high-purity vacuum-induction melted 29-4 version. For this reason the thickness of 29-4C welded (condenser) tubes is limited to 0.028 in (0.75 mm). This is the thickness of the panels tested in both the OTEC and the Navy series.

Analyses for the alloys in the Navy series are given in Tables V and VI. The alloy contents of the 36 wrought and 9 cast materials in this series covered even wider ranges than the OTEC series. Chromium varied from 12 to 29.6%, nickel from a "residual" 0.07% to 63.7%, and molybdenum from "residual" to 17.6%. Other alloying additions included copper, manganese, nitrogen and stabilizers (Ti and Nb). The groupings in Table V follow those given by H. P. Hack (3).

---

† Inconel alloy 625, Trademark, The International Nickel Co., Huntington, WV.

* Trademark, Allegheny Ludlum Steel Corp.

Prior Evaluations

R. M. Kain (2) has not used the test results to "rank" the alloys or to discuss the role of alloying elements. He summarized his conclusions as follows:

> "Except for stainless alloy 29-4C which was found to be resistant to initiation under these test conditions, the remaining 12 materials exhibited some degree of susceptibility. For these, attack ranged from only a few shallow penetrations to numerous sites which in some cases resulted in perforation of the specimens."
>
> "While several alloys responded favorably to changes in the level of applied torque, others were apparently unaffected. In general, extending the test duration from 30 to 60 days had no pronounced effect on initiation and penetration behavior."

H. P. Hack (3) has concluded that, because of the large variability of the data, a detailed ranking of the alloys is not possible. However, he has divided the 45 alloys into four groups on the basis of the number of sites per side. He has described these four groups as: "No attack (0 sites/side), minimal attack (0 to 7 sites/side), variable attack (0 to 20 sites/side), and heavy attack (at least 12 sites/side). H. P. Hack has added:

> "It is recognized that in some applications the depth of attack may be the more important consideration, and this would affect the grouping. This grouping is not meant to suggest that all materials within a group will behave similarly in service, only that their behavior could not be separated with any confidence in this study."

H. P. Hack (3) has also drawn some conclusions on the effect of alloying elements, "The austenitic alloys studied required 8%Mo to prevent crevice corrosion in these exposures, while the ferritic alloys required 25%Cr and about 3.5%Mo to prevent localized attack. The effect of other alloying elements on localized corrosion in this study was insignificant compared to the data scatter."

DEVELOPMENT OF A CREVICE CORROSION INDEX

Several recent investigations in which laboratory studies (4,5,6,8) on crevice corrosion were combined with tests in marine environments have indicated that there may be some correlation between the temperature at which crevice corrosion occurs in 10% ferric chloride solution and the performance of the same alloys in natural seawater under crevices. This finding has led to an

extensive laboratory investigation (9) aimed at the development of accelerated laboratory crevice corrosion tests for correlation with performance in natural seawater. Both the ferric chloride solution and an electrochemical test in synthetic seawater are being used in this investigation to determine "critical" crevice corrosion temperatures, CCCT, i.e., the temperature at which crevice corrosion is initiated. For this effort, the data from the OTEC and Navy programs are now available, as well as material from the same heats of alloys which were used in the OTEC and Navy programs.

In preparation for the comparison of the laboratory results with the data from the OTEC and Navy programs, an attempt has been made to provide additional analysis of the extensive data from these two test series. The objectives of this effort were to find a means for ranking the alloys which would make it possible to derive conclusions on the effect of torque, testing time, surface finish and alloying elements. If successful, the results were to be used to guide the research on accelerated laboratory tests. In combination, the findings from the field and laboratory tests are intended to assist in the assessment of alloys for use in marine environments, the improvement of alloy compositions, specifications for new tests in natural seawater, improved procedures for standard (ASTM) tests in natural seawater and for a better understanding of crevice corrosion.

The current dilemma for persons attempting to rank the results of crevice corrosion tests in chloride environments is illustrated by the following precautions provided in connection with procedures (10) for a crevice corrosion test in seawater and other chloride-containing environments: "Alloys should not be ranked by the specific number of specimens or sites showing crevice corrosion," and "-maximum depth of corrosion may be an important parameter to consider. However, caution must be exercised in ranking alloys solely on the basis of maximum penetration measurements."

Definition of an Index

As in the case of chloride pitting attack (11), crevice corrosion can be divided into two components, initiation and growth. Thus, of the measurements made on the test panels in the OTEC and Navy tests, Table II, the time (hr.) to initiation of crevice attack and the number of sites of attack in each multiple crevice assembly (MCA) reflect initiation of corrosion, while the depth of attack is an indication of progress or rate of crevice growth. Thus, there could be many points of break-down with relatively little depth or progress of attack. The other extreme would be just one or only a few points of attack with such rapid progress of crevice growth that the material is perforated. It is also possible that the various factors governing crevice corrosion have different effects on initiation and growth, as has been found to be the case for chloride pitting of stainless steels (11). Nevertheless, as a first approximation, it could

tentatively be assumed that there may be a correspondence between susceptibility to initiation and susceptibility to growth of crevice corrosion.

Initiation

The next step is the selection of a measurement or indicator for both initiation and growth of attack. The time (hours) to the first sign of crevice corrosion could not be used as a primary measure of initiation because this requires the detection of visible corrosion products adjacent to the crevice devices without disturbing or removing the panels from the seawater. Both R. M. Kain (2) and H. P. Hack (3) have reported tests in which no visible corrosion products were detected even though, upon removal of the crevice device at the end of the test, there had been measurable attack. Visual inspection was about 80% effective because of limited accessibility of the specimens and the inspection schedules. Thus, it is necessary to select a measurement of the number of breakdowns of the surface. Some possibilities are the actual number of sites attacked (per crevice device, or the total for all three specimens tested simultaneously) or the total number of sides, or even panels, attacked, regardless of the number of sites per side. Three panels were used for each test condition (torque, time). Thus, the total number of sides available for observation for each test condition was six.

However, both R. M. Kain and H. P. Hack found that the large variations in results limited the conclusions which could be drawn. To minimize the problem of the variations in test results, the data on all nine panels (18 sides) of each of the 13 alloys tested in the OTEC series were grouped together. This procedure could be used because, with only a few exceptions, the test program (length of testing times, torque) was the same for each of the 13 alloys. The only exceptions to the test schedule shown in Table II were 29-4C, Monit and SC-1. These three alloys were tested for 30, 60 and 90 days with a torque of 75 in-lb on all panels. Thus, in place of the 60-day test with a torque of 25 in-lb, these alloys were tested under the more severe conditions of 90 days at 75 in-lb. The 29-4C alloy showed no attack on any specimen. Monit was attacked only on the 90-day panels and SC-1 showed attack on some panels under all three test conditions. Therefore, the impact of these somewhat different test conditions on the comparison of these three alloys with the ten other alloys is negligible. The grouping provided a larger data pool for each alloy.

Minor differences were also minimized by the selection of the number of sides rather than the number of sites as the measure of initiation of crevice corrosion. This choice eliminated or minimized any differences in the number of sites resulting from variations in the sizes or geometries of the 20 individual "teeth" or plateaus, and from any effect which the formation of one point of crevice attack might have in retarding or promoting the initiation

of attack at other "teeth" in the same device. The flatness and surface finishes of both the metal surface and the Delrin crevice may vary. Furthermore, when there is attack under one crevice plateau, its load must be redistributed to other plateaus on which the pressure is increased, thereby increasing the crevice conditions under the remaining plateaus. Attack on one crevice device can also affect the pressure on the device on the reverse side of the panel. It is of interest that even on the least resistant alloy in the OTEC series, Type 329, there was one side out of 18 which was completely free of all attack. Another factor which may increase the variation in test results is the change with time in Delrin during immersion in seawater at 30°C. In laboratory tests in synthetic seawater we have found (9) that the torque decreases from 75 in-lb to 45 in-lb in four hours.

Nevertheless, the available limited information on the length of time to initiation and also the number of sites of attack has been used below to supplement the analyses based on the number of sides as a measure of initiation of crevice corrosion. Because of the larger data-pool available for each of the 13 alloys from the OTEC tests and the greater range in testing conditions (time and torque), the first phase of this analysis was focused on the OTEC data.

Growth

For each crevice device, i.e., side, the range of depth of attack in millimeters was reported, Table II. Thus, this range, or an average value, or the maximum depth of attack or even a rate of attack based on the testing time, could be used as an indication of growth of crevice corrosion. Ideally, a rate measurement would probably be most useful. However, for a meaningful measurement, it would be necessary to know exactly when crevice corrosion was initiated and to know the effect of testing time on the rate of growth. This rate can be assumed to vary with time because the crevice geometry and chemistry change as corrosion progresses. Because a direct, rather than average, measurement was desired, and because frequently a single perforation of a heat exchanger tube or vessel terminates its usefulness, the direct measurement of maximum depth of attack was selected as an indication of growth of crevice attack.

Index

The number of sides out of all 18 test panels, a combination of all of the 30, 60 or 90-day tests at 25 or 75 in-lb of torque, has been plotted in Fig. 3 against the maximum depth of attack observed among these 18 sides. It is apparent that there is some validity to the hypothesis that there is a relationship between initiation and growth of crevice corrosion in most of the 13 alloys of the OTEC series. A large number fall within the shaded band in Fig. 3. Plots of average depth of attack vs. number of

sides, maximum depth of attack vs. number of sites or the average number of sites, result in a greater scatter of data. Only when the maximum depths are plotted against the number of panels attacked is there a similar concentration of data as in Fig. 3 for which the number of sides was used. The use of the number of panels minimizes the potential effect of attack under one device on the tightness of the crevice device on the reverse side of the same panel. If a direct relationship between initiation and growth applied to all alloys, a list of alloys ranked in increasing order of initiation (number of sides attacked) would be identical to a list based on maximum depth of attack. When these two types of lists are made and the alloys in Fig. 3 which fall outside the band are noted, it is apparent that the two ranking criteria do not result in identical rankings. This may lead to attempts to adjust rankings based on initiation by moving alloys with "unusual" growth of crevice attack down in this list. In the case of the rankings based on maximum depth of attack attempts may be made to find places lower down in the list for alloys with attack on an "unusually" large number of sides.

The above considerations led to the use of a Crevice Corrosion Index based on the product of the number of sides attacked, S, and the maximum depth (in mm) of attack, D,: CCI = S x D. This Index is a combination of initiation and growth of crevice corrosion. A given value may, therefore, be a result of several combinations of S and D. However, for a particular test the range of the number of sides, S, is fixed and the range of the maximum depth is limited by the smallest depth measured (0.01 mm in these tests) and the thickness of the test panel. Because there are crevice devices on each side of a panel and because in cases of rapid crevice growth it has been found that there may be perforation resulting from attack on both sides, the largest possible penetration is sometimes 1/2 the thickness of the panels.

The justifications for combining results on all nine panels of the OTEC series and for applying the Crevice Corrosion Index for an analysis of the OTEC and the Navy test series depend on results derived from these procedures. Can the alloys be ranked in a meaningful way by means of this Index? Can conclusions be drawn about the effects of torque, length of time of testing and surface condition? Does the Index provide a tool for detecting the effects of alloying elements? Do the results provide leads for better test procedures and for new research?

The Index is intended to facilitate the analysis of data on crevice corrosion. Comparisons of Indexes can be made only for tests carried out with identical crevice devices, panel numbers and sizes, seawater conditions and test programs (time and torque). Obviously, this Index is not a unique property of the alloy, such as its melting point or density.

It is shown below that the conditions for both the OTEC and Navy tests, Table III, are very severe. In actual use of stainless alloys in marine environments there may be unfiltered, rapidly flowing seawater at temperatures other than 30°C with small (cathodic) areas outside the crevices, and with cathodic protection, perhaps, resulting from contact with carbon steel structural components. Any of these factors may have a strong effect in reducing the severity of attack at crevices (12, 13). Additional uses and limitations of the crevice corrosion Index are discussed below.

ANALYSIS OF OTEC TESTS

The number of sides attacked, S, and the maximum depth of attack, D, are listed for each of the 13 alloys in Table VII, together with the Crevice Corrosion Index, CCI. The alloys have been ranked in ascending order of Index values. Only the 29-4C alloy was completely immune to crevice attack on all 9 panels, i.e., the Index is 0.00. Three of the panels were tested for 90 days to verify the findings from the 60-day test. The Monit alloy was also resistant for 60 days, but during the 90-day test, three sides showed some attack. On the 12 alloys which suffered various degrees of attack, the CCI ranged from 0.03 to 27.54. Note that even on the least resistant alloy (Type 329) there was at least one side out of a total of 18 which was completely immune to attack, i.e., not even one crevice site out of 20 was attacked on that side.

On the basis of the CCI, the 13 alloys can be divided into five groups, Tables VII and VIII: total immunity (I), a group of relatively high CCI values (V), and three intermediate groups. It is shown below that these groupings aid in the analysis of factors such as length of testing time, torque and surface finish. A comparison of the S, D and CCI columns shows that if either the "S" or "D" values had been used for ranking, different sequences would have resulted. The two alloys whose entire thickness was penetrated by crevice attack from the front and back of the panel were left in the ranking order. Both are in the group of most severely attacked alloys and one, Type 329, already has the highest CCI. The total thickness of Nitronic 50 was 1.3 mm and that of Type 329 was 1.8 mm.

The Effect of Length of Testing Time

The effect of length of testing time was investigated in the OTEC series in two ways, a) by testing all 13 alloys for 30 and 60 days, and b) by testing the two most resistant alloys for 90 days. All tests were made with a torque of 75 in-lb. A summary of the data is given in Table VIII. Note that these data are based on only three panels per test or a total of six sides. Nevertheless, to maintain the groupings, the ranking based on all tests (18 sides), as shown in Table VII, was used to list the alloys for the table on the effect of time.

Increasing the testing time increases the number of sides attacked, S, for alloys in Groups III and IV (Table VIII), except for alloys 904L and SC-1. On the latter there actually was an increase in the total number of sites from 7 to 12, even though there was no increase in the number of sides. The 904L alloy contains 1.6%Cu. As might be expected, the effect of time up to 60 days is less important both for the more resistant alloys (Group II) and for the least resistant, Group V. Jessop 777 with attack on only 3 sides is somewhat of an exception in Group V. It too contains copper, 2.0%. Ferralium 255 is another alloy which contains copper, 1.8%. On this alloy too, there is no effect of time. The remaining copper-bearing alloy is 254 SMO, but its copper content of 0.8% is only one-half of that of the alloy whose content is nearest that of 254 SMO. The above observations on the effect of time on crevice corrosion of copper-bearing alloys indicate that copper in excess of about 0.8% imparts superior resistance to attack of alloys with a mill finish.

The effect of time on the maximum depth, D, of attack is similar to the changes in initiation, S. There generally is an increase in D for alloys in Groups III and IV. Alloys in the more resistant Group, II, show that these testing times up to 60 days are too short for meaningful results. Also, on the least resistant alloys, Group V, the attack is so severe that extending the testing time from 30 to 60 days does not increase significantly the maximum depth of attack. For two of these alloys the attack resulted in complete penetration of the thickness of the panels. These results on alloys in Group V suggest that there is a decrease in the rate of crevice growth with time. As the crevice grows because of corrosion, the volume of solution in the crevice increases and there is more opportunity for diffusion and flow from and into the crevice to make the composition in the crevice more like that in the bulk solution. The chloride content is reduced, the pH and the oxygen content are increased from the values which led to breakdown of the passive film in the original, small crevice. The result is a progressively less severe environment for growth of crevice attack.

In general, the time to initiation of crevice corrosion as measured by the appearance of corrosion products decreases with increasing values of the Index of the alloy, Table IX. Two exceptions are 254 SMO which is relatively resistant, but on which corrosion products were visible after only 72 hr, and SC-1 on which either no corrosion products were detected or it took 703 hr to detect them. Attack on this alloy was relatively shallow with a maximum depth of 0.11 mm. Thus, corrosion products may have diffused away before they could be detected. The finding that visible corrosion products are formed on 254 SMO after only 72 hr may indicate that, while more than 0.8% copper (1.6% in 904L and 2% in Jessop 777) may retard break-down of the passive film, the smaller concentrations weaken the resistance of protective films. This finding (Table IX) applies to both the overall OTEC tests

(9 panels) and the 30-day tests on 3 panels in the OTEC and Navy tests.

Results on 29-4C and Monit alloys derived from 90-day tests show that the 60-day test period is not long enough to differentiate between these two alloys. The 29-4C alloy was resistant, but the Monit alloy showed susceptibility to attack in the 90-day panels which was not revealed in 30 and 60-day tests. There was some attack on 3 out of 6 sides.

Table IX also shows that the surface finish affects the time to initiation. This effect is discussed in the section on Surface Finish.

The Effect of Torque

On the basis of observation and theoretical considerations it may be concluded that the severity of a crevice increases as the volume between the two surfaces of the crevice is decreased. Oxygen is more readily depleted in the smaller crevice and the pH will drop more rapidly when there is some corrosion. Thus, it might be expected that crevice attack increases with the magnitude of the torque on the crevice device. Table X shows the effect of increasing torque from 25 to 75 in-lb in 60-day tests. Again, as in the case of the effect of time, an effect of torque is observed only on the alloys in the intermediate groups, III and IV. For obvious reasons there is no effect of torque on completely resistant alloys. In the case of 60-day tests on only 3 panels this includes both Groups I and II.

In Group III (Table X), the increase in torque increases both initiation and growth. On the alloys in Group IV the increase in torque only increases the maximum depth of attack. The data show that the expected effect of torque applies only to crevices for which the maximum depth does not exceed 0.5 mm. Such a limit might be expected because, as soon as there is some crevice attack, the spacing between the Delrin™ device and the metal surface is increased and the severity of the crevice is decreased. This probably explains the lack of a consistent effect of torque on the least resistant alloys in Group V. The only exception is Jessop 777. This alloy has essentially the same composition as Jessop 700 except for the 2%Cu in the 777 alloy. Examination of the analyses of all other alloys in Table VII shows that none of the other copper-bearing (>1%) materials (Ferralium 255, 904L, Jessop 777) suffered any crevice attack in the 60-day tests at a torque of 25 in-lb, Table X. With the exception of SC-1, these were the only alloys which were not attacked. Presumably the 25 in-lb crevices are less severe than the 75 in-lb crevices. This, and the findings above on the effect of time, suggest that copper may retard initiation of crevice attack on alloys with mill finishes.

When some of the "plateaus" in the crevice device no longer are in contact with the metal surface the total load is redistributed among the other "plateaus." It might be expected that they now produce a narrower crevice and, therefore, the severity increases under these "plateaus." Thus, one or more points of attack might promote attack at the remaining crevices, a form of self-acceleration. However, we have found in our investigation (9) that "Delrin™" is affected by exposure to aqueous solutions and by temperature. In some cases, initial torque values of 75 in-lb decrease to 45 to 50 in-lb in 4 hr at 30°C. Thus, there are opposing factors operating on the crevice which make it difficult to maintain constant and reproducible crevice geometries during these tests. The above factors, in addition to the problems of maintaining constant and reproducible flatness in the metal surface and the crevice device, as well as the difficulties involved in producing reproducible surface finishes on the metal and the Delrin™, probably are the major factors which cause the large variations in crevice attack on a given alloy and make it necessary to combine data on 9 panels (18 sides) for analysis of the effects of various test parameters.

The data on the effect of torque support ranking by means of the Crevice Corrosion Index. The less severe crevice at 25 in-lb leaves alloys of rank one through six unattacked. As might be expected, increasing the severity of the crevice to 75 in-lb, reduces the unattacked ranks from one through four (Table X). At 25 in-lb the only exception to this progressive trend to initiation with increasing position in the ranking order is the copper-bearing Jessop 777 which resists attack even though its overall ranking puts it in Group V.

The Effect of Surface Finish

Twelve of the 13 alloys used for the OTEC tests were also included in the Navy program. Only the Carpenter Exp. 58 alloy was not included in the Navy tests. Because the OTEC tests were made on mill finishes and the Navy tests on 120-grit surfaces, it is possible to examine the data for effects produced by this great difference in surfaces, Fig. 4. The data for both series of tests given in Table XI are for 3 panels, for 30 days at 75 in-lb. Note that the ranking sequence used for the OTEC alloys in this table is based on only three panels per test. Therefore, this ranking is different from that in Table VII, which is based on all 9 panels. For 7 of the 12 alloys available for comparison, the material for both series was from the same heat. For the 5 remaining alloys, material from a second heat was used for the Navy tests. These have been identified in Table XI. In each case, the analyses for the two heats were very nearly identical (Tables IV, V and VI).

Alloys that were completely resistant with a mill finish in the 30-day test were also resistant with a 120-grit polish, Table XI. On the other alloys both the maximum depth, D, of attack and

the Index are higher for the 120-grit surfaces than for mill finishes with only two exceptions. One of these is Type 329 on which there was complete penetration in both tests making it impossible to determine the effect of surface finish. The other exception is the ferritic, SC-1 alloy with 2.3%Ni, for which the Index actually was lower for the 120-grit than for the mill finish. The reason for this is not a decrease in D, but a significant decrease in the number of sides attacked from four to one (and from 7 to 1 in the number of sites).

There is a possibility that this singular performance is a result of selective removal of chromium in a thin layer at the surface during mill processing of the hot alloy in oxidizing atmospheres (air). Such a case of chromium-depletion has been described by R. V. Trax and J. C. Holzwarth (14) on Type 430 (Fe-16%Cr) stainless steel sheet. The chromium content at the surface was reduced from 16 to 10% in a layer which was 10 micro-inches (2.54×10^{-4} mm) thick. If a similar chromium-depletion has taken place during processing of the SC-1 alloy (mill finish), then the removal of this depleted layer by polishing to a 120-grit finish might restore the chromium content at the surface to that of the bulk analysis and, of course, provide greater resistance to initiation of crevice corrosion without a significant effect on growth.

Initiation, S, is increased in all the other alloys by the 120-grit finish. In two alloys the number of sides was the same in both tests, but for these alloys (Haynes 20 Mod. and Jessop 700) the number of sites increased, Table XI. The number of sites was particularly large for the alloys in Group IV. The greater maximum depth, D, observed on the series with the 120-grit finish is at least in part related to the more rapid break-down of the crevices in the Navy tests as compared to the tests with the mill finish. Data in Table IX show that the reduction in time is particularly large for the alloys in Groups II and III and that this difference in time essentially vanishes on the least resistant alloys, i.e., Group IV in the 3-panel ranking in Table XI.

As might be expected, the creation of a fresh, new surface by mechanical grinding and polishing to a 120-grit finish removes protective oxide films formed during processing of the alloys at elevated temperatures and, perhaps, in chemical pickling and rinsing procedures and also removes chromium-depleted surface layers. In addition, the mechanical finish creates ridges with sharp edges whose chemical reactivity has been found to lead to greater corrosion rates in acids (15). The polishing operation also introduces a new finish for the cathodic reactions which take place outside the crevices, Fig. 2 on the 50 mm diameter circle. There are then two kinds of cathodically active surfaces, a 120-grit surface nearest the crevices and a surface with a mill finish on the rest of the panel. There is a possibility that cathodic reactions are promoted by the sharp edges of the 120-grit finish.

The result is more rapid crevice attack on the fresh surfaces. The flatter, more reproducible surfaces formed by machining to a 120-grit finish also may result in more narrow crevices and a further intensification of the crevice conditions.

Note that the copper-bearing alloys (Ferralium 255, 904L, 254 SMO and Jessop 777), Table XI, stand out with somewhat higher increases in the number of sides or sites developed by application of the 120-grit finish than the alloys near them in rank. This is especially the case for Jessop 777 which can be compared with its copper-free counterpart, Jessop 700.

The above results on ground surfaces show that the protective effect of copper in retarding crevice corrosion on mill finishes, as described in the sections above on torque and length of testing time, is probably a result of the effect of copper on the protective qualities of the film formed during mill processing. The data in Table VII based on all nine panels with mill finishes support this concept. The number of sides attacked is lower for the copper-bearing Jessop 777 than for the 700 alloy, but the depth of attack is greater for the 777 alloy. This also applies to the number of initiation sites in the 9-panel tests. For the 700 alloy this number was 45 as compared with 22 for the 777 alloy, pg. 73 and 76 in Ref. (2).

The Effect of Composition

It is apparent from the results on the A.L. 29-4C ferritic alloy that complete immunity to crevice corrosion can be obtained in the OTEC tests which were run as long as 90 days on this alloy. Thus, a concentration in iron of 28.5%Cr and 3.8%Mo provides this level of corrosion resistance without any other essential alloying additions. The somewhat lower levels of chromium (25.3%) and molybdenum (3.1%) in the SC-1 alloy made it subject to crevice corrosion. In the case of Ferralium 255 (26.15%Cr, 3.20%Mo) the effect of chromium and molybdenum may be somewhat impaired by its copper and its higher nickel contents as compared with SC-1.

Several alloys had considerably more molybdenum than the 3.8% in 29-4C, but it appears that, at least in the presence of significant amounts of nickel (24.6%), this additional concentration of molybdenum in 254 SMO (6.1%), and A.L. 6X (6.5%) is not sufficient to make up for the lower (20%) chromium content. The low resistance of Nitronic 50 (21%Cr) and Type 329 (26.7%Cr) is largely a result of their very low molybdenum contents, 2.3 and 1.4%, respectively.

Copper

The role of copper can be summarized as follows. In Fig. 3, the copper-bearing version of the Jessop alloy, 777, falls outside the main band. There are two reasons for this. Copper a) reduces initiation, $\underline{S}$, by enhancing the protective properties of oxide films

formed during mill-processing, and b) increases the growth, D, of crevices, probably by galvanic action in the acid chloride environment of the crevices. Support for these conclusions is derived from comparisons with copper-free alloys.

Increasing the testing time on copper-bearing alloys with more than 0.8%Cu from 30 to 60 days did not increase either the initiation or growth, Table VIII. This is contrary to the behavior of alloys of similar ranking. Thus, the oxide film on copper-bearing alloys with more than 0.8%Cu appears to be more resistant than the film on comparable alloys without this copper content.

When a relatively milder crevice (25 in-lb) was applied to any of the copper-bearing alloys with a mill finish (OTEC series), there was no attack within 60 days on any of them (Table X). All of these alloys are attacked when 75 in-lb crevices are applied for 60 or more days, Table VII, and VIII. (Note that on Ferralium 255 there was initiation only on the 30-day and not the 60-day tests. That is why it is not shown as subject to attack in Table X.)

When the oxide film formed during mill-processing is removed by the application of a 120-grit finish, there is a marked increase in initiation and growth. Also, when panels with mill-finishes are cut or sheared, the protective oxide film is ruptured and new surfaces are created. It might, therefore, be expected that copper-bearing alloys might be vulnerable to edge attack and tunneling when the unusually protective oxide film is removed and the growth of the resulting "pit" is promoted by the galvanic action of copper. This has been the case with two of the three copper-bearing (>0.8%) alloys, 904L and Jessop 777. The other alloy with more than 0.8%Cu, Ferralium 255, has 26.2%Cr with 3.2%Mo and is basically more resistant than the other two copper-rich alloys. Data on the performance of cast alloys in the 30-day Navy tests show that three out of the four alloys which had attack away from the crevices contained between 1.6 and 3.2%Cu. The fourth alloy, which had no copper, contained only 12%Cr, 8%Ni and no molybdenum. Among the wrought alloys, Incoloy 825 with 1.7%Cu (44%Ni-22%Cr-2.7%Mo) also had attack outside the crevice areas: gravity assisted tunneling.

Manganese (with Nitrogen)

Another element which is associated with alloys which fall outside the main band in Fig. 3 is manganese. Nitronic 50 contains 4.8% and the Carpenter Experimental Alloy 58 has 5.4%Mn. None of the other OTEC alloys contain more than 1.7%. Because all of these alloys also contain molybdenum, there is a possibility that manganese may reinforce the action of this element in reducing crevice growth. Both alloys have a relatively high rate of initiation. Thus, the main reason that the manganese-rich alloys are located to the right of the band in Fig. 3 is that the maximum depth of attack is reduced by manganese. Without the manganese addition they would, presumably, have been located higher on the graph,

somewhere within the band. It should be noted that all of the high manganese alloys also contain deliberate additions of nitrogen to promote the formation of austenite. Nitrogen (0.2%) has been found to increase resistance to chloride pitting (11,16) and to crevice corrosion (17,18).

Surface Effects

The position of SC-1 so far outside the band in Fig. 3 is most likely the result of chromium-depletion of the surface during mill-processing in a very thin layer (0.00025 mm). Because it is so thin, it is without effect on the maximum depth of attack. This is almost the same for the specimens with the mill finish (0.04 mm) and the 120-grit finish (0.05 mm), Table XI. Removal of the depleted layer greatly reduced the number of sides attacked (4 vs. 1) in the 30-day tests of Table XI. In his report, R. M. Kain (2) states that in addition to the 30-day Navy tests on ground specimens in which one site or side was attacked, another test was run with a 120-grit finish on 3 panels for 60-days and again there was attack on only one site. If we extrapolate and assume that in a third test of 90-days on 3 panels there would again have been attack on only one site, we now have "data" on nine surface ground panels for comparison with data in Fig. 3. There would then be attack on 3 sides out of 18 with a maximum depth of 0.05 mm. Such a point would fall within the band in Fig. 3.

Analysis of Rankings

A comparison of similar pairs of alloys provides some reasons for the positions of alloys in the ranking order of Table VII.

1) The two ferritic alloys, 29-4C and Monit, have the same molybdenum content, but 29-4C has 28.5%Cr as compared with only 25.3% for Monit. This 3% difference in chromium content is probably the reason that Monit is in second place.

2) Even though Ferralium 255 has about 1% more chromium than Monit, it ranks below this alloy because of its somewhat lower molybdenum content (3.2 vs. 3.8%) and its copper content of 1.8%. The Index for Ferralium 255 is high because of its relatively large maximum depth, D, which is probably a result of the copper content. Its S value is actually lower than that of Monit (1 vs. 3). This also appears to be a function of the copper content in Ferralium 255, i.e., its beneficial effect in increasing the resistance of the oxide film in the mill finish.

3) Ferralium 255 and SC-1 have almost identical compositions except for the 1.8%Cu in the 255 alloy, Table IV. The 0.19%N in the 255 alloy can be expected to contribute to resistance (11, 16, 17, 18). Yet the 255 alloy is in the third position and SC-1 in the sixth position. As described above, in the mill-finish condition, SC-1 is probably impaired in its resistance to initiation by depletion of chromium while the protective properties of the

oxide film on Ferralium 255 are improved by its copper content (1.8%). When these two alloys are surface ground to a 120-grit finish, these two factors are essentially eliminated and they are ranked 3 and 4 (Table XI) with the SC-1 alloy actually having the lower Index. (Data from the Navy tests, see below, suggest that the 0.5% titanium in SC-1 and, perhaps, its lower nickel content enhance its resistance to attack.)

4) The drop in chromium from more than 25% to about 20% results in a large enough jump in the Index to define two new groups of alloys, II and III. The only exception is SC-1, which has 25.3%Cr and 3.1%Mo. When this alloy is given a 120-grit finish, which apparently removes a chromium-depleted surface layer, its ranking is increased from position 6 to 3, Table XI. It then even out-ranks Ferralium 255, whose rating in the mill-finished condition may be a result of the protective action in the oxide film by its copper content.

5) Haynes 20 Mod and Jessop 700 have very similar compositions. The lower Index of the Haynes 20 Mod alloy can be attributed to its slightly higher chromium (0.9%) and molybdenum (0.5%) contents.

6) The compositions of Haynes 20 Mod (position 9) and 904L (position 4) are also very similar, except for the 1.6%Cu in 904L. Chromium and molybdenum are actually slightly higher in the alloy which is the less resistant (Haynes 20 Mod, H-20). The reason for the lower Index for 904L is that the copper in the protective oxide film reduced initiation from 8 sides on H-20 to 3 sides on 904L. As expected, the time to initiation on the 904L alloy was much longer, 388 hr, than for H-20, 48 hr, Table IX. When the 904L is given a 120-grit finish the time to initiation is reduced to 51 hr and the maximum depth of attack is greater on 904L (0.74 mm) than on H-20 (0.46 mm), Table XI.

ANALYSIS OF NAVY TESTS

The method developed for the analysis of the results of the OTEC tests has been applied to the 45 alloys in the 30-day, 3-panel Navy tests. All specimens in this series had a 120-grit finish and the applied torque was 75 in-lb (8.5 Nm). From the analysis of the OTEC series it was found that the 30-day period is too short and 3 panels are too few to sort out the more resistant alloys and to identify the alloys having total immunity to attack in the crevice tests in filtered seawater at 30°C. Ninety days or more are needed to differentiate among the most resistant alloys. Also, at least 60 days and 9 or more panels are required to distinguish differences among alloys of intermediate resistance. Only for the least resistant alloys is the 30-day test period long enough to rank the alloys. Nevertheless, the 30-day, 3-panel Navy series can provide helpful supplemental information for the findings derived from the more extensive OTEC series.

It has already been shown above in the section on The Effect of Surface Finish that the removal of the mill finish by polishing to a 120-grit finish can result in several opposing effects. In most cases, there is a reduction in time to initiation, especially in the case of alloys with more than about 0.8%Cu, and on certain alloys there may be an increase when a surface layer, which has been depleted in chromium during high-temperature mill-processing, is removed. In addition, the severity of the crevice may be increased by the greater flatness of the machined, 120-grit finish and the creation of sharp edges, which may have greater chemical reactivity, not only for the anodic reactions in the crevices, but also the cathodic reactions outside the crevices.

Twelve of the 13 alloys from the OTEC series were also tested in the Navy program. A comparison of the results has already been given in Table XI and in the section on the Effect of Surface Finish. Data on the number of sides attacked and the maximum depth of attack are given in Table XII for all wrought and in Table XIII for all cast alloys in the Navy tests, along with the Crevice Corrosion Index. As before, the alloys have been listed in the order of increasing Index values. Note that for these compilations separate listings were made for alloys which were completely perforated and for alloys which had attack outside crevice areas. These groupings represent subdivisions of the least resistant alloys.

First Group - Six alloys were completely resistant in the 30-day Navy tests and have all been ranked "1" in Table XII. This group includes the AOD-melted 29-4C alloy and its two vacuum-induction melted antecedents, 29-4 and 29-4-2. Hastelloy C-276, also known for its very high resistance to crevice corrosion in marine environments (5,12), is also in this highest ranking group in Table XII. Another nickel-base alloy, Inconel 625, with chromium and molybdenum, along with Monit complete this group. However, from the OTEC tests it is known that during a 90-day exposure Monit is attacked even with a mill finish. Thus, available information on long-time performance in this test is in doubt only for Inconel 625, which has been described (12) as "approaches Hastelloy C in total resistance" to marine environments. The two nickel-base castings, Table XIII, whose compositions are similar to Inconel 625 and Hastelloy C, were also completely resistant.

Second Group - The second group in Table XII, ranked from 2 through 5, fall just short of immunity to attack in the 30-day, 3-panel Navy tests. Only one or two sides out of a possible 6 are attacked and the depth does not exceed 0.50 mm. However, the longer tests on 9 panels in the OTEC series show that there are major differences among these four alloys. The relatively low chromium contents in Haynes 20 Mod (21.6%) and in SC-1 (25.6%) made these alloys subject to additional attack during these tests, while Ferralium 255, with 26.2%Cr and 3.2%Mo, retains its position near the top of the list.

The higher position, rank 4, of Hastelloy G-3 (22.8%Cr) as compared with Hastelloy G (22.2%Cr), rank 12, appears to be a result of its higher molybdenum content, 7.0 vs. 5.8%. This is supported by the high Index for Incoloy 825, which has only 2.7%Mo and the same chromium, nickel and copper contents as Hastelloys G and G-3.

Third Group - The third group contains alloys on which 3 or 4 sides are attacked in 30 days. Two have relatively low (1%) concentrations of molybdenum, but have 25% or more chromium, Table V. EB 26-1 is a vacuum-induction melted, low-carbon and low-nitrogen alloy (C+N = 0.0080%), with 0.1%Nb to prevent susceptibility to intergranular attack by even these low concentrations of carbon and nitrogen. The more resistant 26-1S alloy contains almost 1% less chromium, 0.054%C and 0.009%N, but also has 1.06%Ti to tie up these interstitials and is melted by the less costly AOD process. These differences may be related to the presence of the stabilizing elements. It has been reported (19,20) that niobium decreases and titanium increases resistance to chloride attack.

Chromium $\leq$ 20% - When the chromium content is about 20% or less, the effect of the concentration of molybdenum is reduced and appears more variable. This is shown in a number of ways.

- The chromium, nickel and manganese contents of A.L. 4X and 6X are identical, but the additional 2%Mo in 6X has not resulted in less initiation or growth compared with the 4X alloy, even though the 4X alloy contains 1.45%Cu, which, in other cases, has increased both forms of attack on 120-grit surfaces.

- Three Type 317 compositions, some of which are attacked outside the crevices, even though one contains as much as 4.2%Mo, are far down in the list. The relatively low rankings of Jessop 700 and 777 with 4.4%Mo may also be related to their low chromium contents, as well as to the fact that they both contain about 0.25%Nb, which has been found in other tests (19,20) to decrease resistance to chlorides.

Copper in Jessop 777 increases both initiation and growth of crevice corrosion on surfaces with a 120-grit finish. Except for the addition of niobium in the Jessop 777, its composition is very similar to that of 4X, 904L and 254SLX: 20%Cr, 25%Ni, 4.5%Mo, 1.5%Mn with copper. Their rankings are #9, #13 and #16, with attack on 4, 5 and 6 sides and a maximum depth of attack of 0.50, 0.74 and 0.92 mm. Their copper contents are 1.45, 1.57 and 1.67% respectively. Jessop 777 has 2.0%Cu (and 0.25Nb) and ranks #23. These results suggest that crevice corrosion is very sensitive to the concentration of copper between 1.5 and 2.0%.

- Haynes Mod 20 alloy (rank #5) is clearly more resistant than 4X, 904L and 254SLX. It has slightly more chromium (21.6%) and molybdenum (5.0%) and no copper.

• Both 20Mo-6 and Carpenter 20 Cb-3 have essentially the same nickel (33.2%), manganese (0.4%) and copper (3.2%) contents. However, the 20 Mo-6 alloy (rank #7) has 23.9%Cr and 5.6%Mo as compared with 19.4%Cr and 2.2%Mo for Carpenter 20 Cb-3 with a rank of #22.

Note that Type 216 (2.5%Mo), which ranks as #14, is superior to Type 316 and Carpenter 20 Cb-3, which are ranked as #21 and 22, and to 317L and 317L+ which have Indexes of 11.52 and 6.54 respectively and are attacked outside the crevice areas. This again indicates that manganese (8.0% in Type 216 with 0.35%N) reinforces the effect of molybdenum. All of the high manganese alloys, Type 216, Nitronic 50 and Carpenter Exp 58 (in the OTEC series) also contain large additions of nitrogen (0.24 to 0.35%). Such concentrations of nitrogen not only promote the formation of austenite, but have been found to enhance resistance to pitting and crevice corrosion even in the absence of large additions of manganese (11,16,17,18).

Beginning with Type 216, all the alloys show attack on 5 or 6 sides, but the depth of attack increases progressively so that the Index increases from about 4 to 20, Table XII. In general, as the molydenum content decreases, the depth of attack increases. Not even the 29.4%Cr in 254 SFER alloy can off-set its low (2.1%) molybdenum content.

The non-resistant castings, Table XIII, confirm the findings on minimum requirements for chromium and molybdenum. Either one or both of these elements is too low to provide even moderate resistance in these tests. This also applies to the Ferralium casting with 3.2%Cu, whose molybdenum content is lower than that of the wrought alloy. Two of the other casting alloys which had attack outside of the crevice areas also contained copper. The fourth alloy had no molybdenum additions at all and only 12%Cr.

Other Elements - Studies of chloride pitting of austenitic 18Cr-8Ni steels have shown that silicon (2%) and nitrogen (0.2%) in solid solution increase and that carbon in solid solution decreases resistance to pit initiation (4,11,16,17). A number of the 45 alloys in the OTEC and Navy tests contained additions of 0.2%N or more, but it could not be determined directly whether these additions improved the resistance to crevice corrosion by comparison with alloys of the same composition but without nitrogen additions. The silicon contents of all but one alloy were less than 0.7% and, therefore, no analysis of its effect could be made. The only alloy (CN7MS) with a large concentration (3%) of silicon (Table VI) had such low concentrations of chromium and molybdenum that this obscured any beneficial effect that silicon might have had. There is also a possibility that silicon, while increasing resistance to initiation of crevice corrosion, may increase the rate of growth of crevices (11). The carbon contents were generally very low. Only a few alloys had more than 0.04%C.

Many of the alloys contained stabilizing elements (Ti, Nb) to combine with carbon and nitrogen. This also complicates any analysis of the effect of carbon and nitrogen in solid solution.

DISCUSSION AND CONCLUSIONS

1) Initiation and Growth - Using data on 13 stainless alloys derived from recent (OTEC) crevice corrosion tests in quiescent, filtered seawater at 30°C, it was found that there is a general relationship between initiation of crevice corrosion under multiple crevice devices and growth of crevice attack. In most cases when there is an increase in initiation of crevice attack there is also an increase in the depth of attack. This relationship became apparent from a graph in which the total number of sides which showed any attack out of a total of 18 sides (9 panels) was plotted against the maximum depth (mm) developed among all the crevices showing attack, Fig. 3. The few alloys which fell outside the main range for most alloys in this graph provided leads for the effects of alloying elements, such as copper and manganese on initiation and growth of crevice attack, and for the effects of surface composition.

2) Index - These findings led to the definition of a Crevice Corrosion Index, CCI, for ranking alloys and for evaluating the effect of test variables: SxD = CCI, where S is the number of sides on which there is any attack under a multiple crevice device and D is the maximum depth, in mm, of attack produced by any of the individual crevices involved in a given test. Analysis of data from both the OTEC and Navy tests led to conclusions about the effect of testing time, torque on the crevice devices, surface finish and the role of alloying elements. These results provide leads for new seawater test series and improved test procedures.

3) OTEC Series - In the OTEC series, 3 groups of three panels of each alloy were tested. Both the testing time and the torque applied to the crevice devices were varied. Because the same testing program was applied to almost all alloys, results on all nine panels were grouped together to enlarge the pool of data. The CCI was calculated for each of the 13 alloys and was used to rank them in ascending values of the Index from 0.00 for the completely resistant Fe-29Cr-4Mo alloy to 27.54 for Type 329. On the basis of the Index, the 13 alloys could be divided into 5 groups: Completely Resistant, 3 Intermediate Groups, and one Least Resistant Group.

4) Time - A 30-day test period is too short to differentiate performance among the more resistant alloys (Group II, Table VIII) and to identify the alloys having total immunity. Ninety days or more are needed to differentiate among the most resistant alloys. At least 60 days are needed to distinguish differences among alloys

of intermediate resistance (Groups III and IV). Only for the least resistant alloys is the 30-day test period long enough to rank the alloys.

5) Torque - Increasing the torque which was applied to the crevice devices from 25 to 75 in-lb increased crevice attack in 60-day tests only on the alloys in two intermediate groups, III and IV of Table X. With the exception of 904L, on which there was no attack, for all of the alloys in Group III increasing torque increased the number of sides attacked and the maximum depth of attack. In Group IV it only increased the depth of attack.

Because there was no attack on any of the alloys in Group II in the 60-day test, it was not possible to establish the effect of torque on these alloys, which did show some attack in other tests. Of course there was no effect of torque on the alloys in Group I because they resisted attack in all tests. There was no consistent effect on the least resistant materials, Group V, with the exception of Jessop 777 whose position in this group is explained by its copper content.

The expected effect of torque on depth of attack (increasing torque produces more severe crevices and more crevice corrosion) was observed only on crevices for which the maximum depth did not exceed 0.5 mm. Such a limit might be expected because, as soon as there is some crevice attack, the spacing between the Delrin device and the metal surface is increased and the severity of the crevice is decreased. This is also the reason that growth of crevice attack decreases with time.

Crevice geometries are difficult to reproduce and to maintain. One factor is the relaxation of the Delrin. We have found that a torque of 75 in-lb drops to 50 in-lb in 4 hr after immersion of the crevice in synthetic seawater at 30°C.

6) Surface Finish - The effect of the surface finish on crevice corrosion was determined on 12 of the 13 alloys in the OTEC Series. In the OTEC tests they were tested with a mill finish. A 120-grit surface was applied to these same alloys on the area under the crevices in the Navy tests. All tests used for this comparison were for 30 days with a torque of 75 in-lb. The two alloys that were completely resistant with a mill finish in the 30-day OTEC tests were also resistant with the 120-grit finish. With only two exceptions, on all the other alloys, both the maximum depth, D, and the Index were higher for the specimens with a 120-grit finish. One of these exceptions was Type 329 which was penetrated even on the specimen with the mill finish. The other was the SC-1 ferritic alloy on which the Index was actually lower for the 120-grit surface than for the specimen with the mill finish. The reason for this was that surface polishing to 120-grit finish reduced, not the depth of attack,

but the total number of sides attacked from four to one. This singular performance may be a result of the removal during the preparation of the 120-grit finish of a layer of metal and oxide which had been depleted in chromium by selective oxidation during mill processing at high temperatures.

7) Optimum Resistance - On the basis of the limited number of alloys tested in the OTEC series, it can be concluded that 28.5%Cr and 3.8%Mo (29-4C) in iron are required to resist the severe conditions of the tests in filtered seawater at 30°C for 90 days with a torque of 75 in-lb on the crevices. In the 30-day Navy tests, the two related alloys were also resistant as well as Hastelloy C-276 and Inconel 625. Of these, at least Hastelloy C-276 could be expected to equal the 29Cr-4Mo type of alloy.

C. W. Kovach (21) has recently reported that the chromium and molybdenum contents of Sea Cure (SC-1) have been increased to the range of 25 to 28%Cr and 3.0-3.5%Mo. Tests similar to the OTEC series (nine panels, up to 90 days, mill finish, 75 in-lb) have been made at Wrightsville Beach, NC, on four of the new compositions. There was no crevice attack on any of these alloys. Of these four, the alloy with the lowest chromium and molybdenum contents had 26.25%Cr, 3.1%Mo, 1.7%Ni. These results appear to lower somewhat the requirements for chromium and molybdenum needed to provide immunity to crevice corrosion in the (mill finish) OTEC-type test. Tests on panels with a 120-grit finish are yet to be made. It should be noted that SC-1 alloy also contains about 0.5%Ti, which may enhance its resistance to crevice corrosion. The chromium and molybdenum contents of this new SC-1 alloy are similar to those of Ferralium 255 (26.2%Cr, 3.2%Mo, 5.6%Ni and 1.8%Cu). The slight susceptibility to attack on this alloy (1 out of 18 sides in the OTEC series and 2 out of 6 in the Navy series) may reflect a deleterious effect of its higher nickel content, the addition of 1.75% copper and the absence of 0.5%Ti. The effect of copper is indicated by the increase in initiation resulting from surface (120-grit) grinding. There is also a possibility that its duplex structure, a combination of ferrite and austenite, resulting from the 5.6%Ni and 0.19%N additions, may have some influence because the distribution of alloying elements in the two phases may not be identical, i.e., one phase may be lower in chromium and molybdenum than the bulk analysis.

In general, for the iron-base alloys of the OTEC and Navy tests, the further the chromium and molybdenum contents decrease from the minimum requirements for chromium and molybdenum, the greater the value of the Index. Molybdenum decreases the maximum depth of attack. However, when the chromium content drops to 20% or less, the effect of molybdenum is sharply decreased.

8) Copper - Copper, which is present between 1.6 to 3.3% in some of the alloys tested, has a significant effect on crevice corrosion. It appears to increase the resistance to break-down

of the oxide films formed during mill processing. But when this film is removed by polishing to a 120-grit finish or by cutting and shearing at edges, copper promotes initiation and growth of crevice attack. The reason is probably galvanic action by copper in the acid chloride environment of crevices.

9) Manganese and Nitrogen - Manganese, when present in concentrations greater than about 4%, together with about 0.25%N or more, reinforces the effect of molybdenum in retarding the growth of crevices. For example, Type 216 (8%Mn, 2.5%Mo, 6%Ni, 0.35%N) was found to be superior to Types 316 and 317 stainless steels (2.4 to 4.2%Mo).

10) Titanium and Niobium - Titanium, added as a stabilizer for carbon and nitrogen, seems to enhance resistance to crevice corrosion, while niobium has the opposite effect.

11) Correlation with Other Seawater Tests - Exposures up to 90 days in filtered seawater at 30°C with a torque of 75 in-lb on Delrin crevice devices has proven to be a very severe crevice corrosion test environment. Another very severe test consists of long-time (9 months or more) exposure in racks immersed in naturally quiescent, unfiltered seawater, including spring and summer months, the periods of maximum temperature and greatest activity of marine organisms. In such long-time tests limited data show that only Hastelloy C or C-276, titanium and the Fe-29Cr-4Mo and Fe-29Cr-4Mo-2Ni alloys are completely resistant (5,12,13). Recently, C. W. Kovach (21) has reported that the SC-1 alloy, used in the OTEC test, with 25.34%Cr, 3.1%Mo and 2.25%Ni was also immune to crevice attack in quiescent seawater during a 33 month exposure at Wrightsville Beach, NC. The fact that this composition was not immune to attack in either the OTEC or the Navy tests in filtered seawater at 30°C with Delrin crevices (75 in-lb) suggests that the test in filtered seawater at 30°C is more severe than the test in natural (unfiltered, at ambient temperature) seawater.

12) Correlation with Service - There is a need to correlate the results obtained in the crevice tests in quiescent, filtered seawater at 30°C with various types of service exposures in marine environments. One such correlation is available for the old and new Sea Cure alloys. It has been found (21) that the old Sea Cure, which showed a slight degree of susceptibility in both the OTEC and Navy tests, also was attacked ("slight pitting and crevice corrosion") in service in several condensers on power plants using brackish water. Thus, in this case the severe OTEC crevice test did detect a degree of susceptibility which also made this alloy vulnerable in the one kind of service which is of greatest importance for this alloy. In contrast, on the new version of Sea Cure with more than 26.0%Cr and 3.0%Mo there has been no attack in the field (21).

Available data (12,13) suggest that rapidly flowing, unfiltered seawater at temperatures other than 30°C may provide a less severe corrosion environment than that used for the OTEC and Navy tests. Cathodic protection, deliberate or incidental, by contact with carbon steel, can also effectively reduce crevice attack on stainless steels. These factors must be taken into account in the application of data from the ranking lists developed in this analysis.

13) Use of Index - The ranking methods used in this analysis may, nevertheless, be of some use even before more extensive correlations with marine service become available. If a ranking table based on the Crevice Corrosion Index is supplemented with two other columns, the combination can serve as an aid in the selection of materials. These other columns would be lists of available mill forms (tubes, sheet, plate) for each alloy and unit prices for these forms. To select a replacement material for an alloy that has failed in service, this list might then be used to review alloys which have lower Crevice Corrosion Indexes than the alloy that failed and, amongst these, to select the alloy nearest the top of the list whose mill forms have the most favorable price.

14) Test Conditions - The findings of this investigation also provide guidance for improvements in ASTM crevice corrosion test procedures. The recommended conditions for tests of maximum severity are:

- Surface Finish - 120 grit.
- Torque - 75 in-lb on Delrin crevices. (Perhaps with periodic re-application of torque to promote more constant crevice conditions.)
- Time - 30, 60, 90 and 120 days depending on the alloys.
- Number of panels - 12.
- Quiescent conditions.
- Analysis of results by the number of sides or panels attacked, the maximum depth of attack and by application of the Crevice Corrosion Index.
- For comparison of two or more alloys, the testing program must be the same. This includes the number of panels, testing times, torque, surface finish, temperature and seawater conditions.

15) New Test Series - To provide direct experimental support for some of the conclusions derived from the analysis of the two test programs, several new series of crevice corrosion tests are

needed, not only on commercially available alloys, but also on some compositions specifically designed to reveal the effect of alloying elements. The following are subjects for some new crevice corrosion tests in natural, filtered seawater:

a) To promote constant crevice conditions, investigate "relaxation" of Delrin with time and, if necessary, devise a method for periodic re-application of the initial level of torque without removal of the specimen from the water.

b) Using the original and the new method for applying torque on the crevices, determine the number of panels needed to provide reproducible results. Do the more constant levels of torque provide reliable data on the effect of testing time and levels of torque and, therefore, make it possible to reduce the number of panels which must be tested?

c) Select series of alloys to define more precisely:

1. The minimum requirements for chromium and molybdenum in iron;

2. the effect of nickel on the requirements for chromium and molybdenum;

3. the effect of copper on initiation and growth of crevice attack;

4. the effect of titanium and niobium; and

5. crevice growth in Fe-Cr-Mo ferritic stainless steels to determine whether it differs from alloys with 8% or more nickel.

ACKNOWLEDGMENT

The author would like to acknowledge the support of the National Sea Grant Office under Contract Number NA 81 AA-D-00006, Sea Grant Program on Marine Corrosion, R. Kolf, Sea Grant Office Program Monitor, and S. C. Dexter, University of Delaware, Overall Program Director.

R. M. Kain, F. L. LaQue Center for Corrosion Technology (Inco), Wrightsville Beach, NC, H. P. Hack, David W. Taylor Naval Ship Research and Development Center, Bethesda, MD, and Ivan A. Franson, Allegheny Ludlum Steel Corp., Wallingford, CT, have provided data and comments for this analysis. Their contributions are very much appreciated.

REFERENCES

1. D. B. Anderson, "Statistical Aspects of Crevice Corrosion in Seawater," in ASTM STP 576, "Galvanic and Pitting Corrosion - Field and Laboratory Studies," American Society for Testing and Materials, 1976, pp. 231-242.

2. R. M. Kain, "Crevice Corrosion and Metal Ion Concentration Cell Corrosion Resistance of Candidate Materials for OTEC Heat Exchangers, Parts I and II," May, 1981, LaQue Center for Corrosion Technology, Inc. Prepared for the U. S. Department of Energy, Division of Solar Technology under Contract No. 31-109-38-4974. Also issued as OTEC Report ANL/OTEC-BCM-022.

3. Harvey P. Hack, "Crevice Corrosion Behavior of 45 Molybdenum-Containing Stainless Steels in Seawater," Preprint No. 65, Meeting of National Association of Corrosion Engineers, Houston, March 22-26, 1982. Also published as Report DTNSRDC/SME-81/87, Dec., 1981, by the David W. Taylor Naval Ship Research Center, Bethesda, MD.

4. M. A. Streicher, "The Development of Pitting Resistant Fe-Cr-Mo Alloys," Corrosion, 30, 77-91 (1974).

5. M. A. Streicher, "Microstructures and Some Properties of Fe-28%Cr-4%Mo Alloys," Corrosion, 30, 115-124 (1974).

6. J. Maurer, "Development and Application of New High Technology Stainless Alloys for Marine Exposures," in "Advanced Stainless Steels for Seawater Applications," published by Climax Molybdenum Co., 1980, pp. 11-29.

7. M. A. Streicher, "Stainless Steels: Past, Present and Future," in "Stainless '77," published by Climax Molybdenum Co., pp. 1-34, 1978.

8. A. P. Bond, H. J. Dundas, S. Ekerot and M. Semchyshen, "Stainless Steels for Seawater Service," in "Stainless '77," published by Climax Molybdenum Co., ed. R. Q. Barr, 1978, pp. 197-203.

9. N. S. Nagaswami and M. A. Streicher, NACE Preprint No. 71, Corrosion/83, Anaheim, CA.

10. "Standard Guide for Crevice Corrosion Testing of Iron-Base and Nickel-Base Stainless Alloys in Seawater and Other Chloride-Containing Environments," ASTM Committee G-1.09.02.

11. M. A. Streicher, "Pitting Corrosion of 18Cr-8Ni Stainless Steel," J. Electrochemical Soc., 103, 375-390 (1956).

12. F. W. Fink and W. K. Boyd, "The Corrosion of Metals in Marine Environments," Defense Information Center Battelle Memorial Institute, Columbus, OH 43201, DMIC Report 245, 1970, p. 38.

13. F. L. LaQue, "Marine Corrosion, Causes and Prevention," John Wiley and Sons, New York, 1975, pp. 150, 166.

14. R. V. Trax and J. C. Holzwarth, Corrosion, 16, 271t-274t (1960).

15. M. A. Streicher, "General and Intergranular Corrosion of Austenitic Stainless Steels," J. Electrochem. Soc., 106, pp. 161-180 (1959).

16. H. J. Dundas and A. P. Bond, "Effects of Delta Ferrite and Nitrogen Contents on the Resistance of Austenitic Steels to Pitting Corrosion," Preprint No. 159, NACE/75, Toronto.

17. J. J. Eckenrod and C. W. Kovach in "Properties of Austenitic Stainless Steels and Their Weld Metals" STP 679, Brinkman, C. R., Garvin, H. W., ed., American Soc. for Testing and Materials, p. 17, 1979.

18. T. Sakamoto, H. Abo, T. Okazaki, T. Ogawa, H. Ogawa and T. Zaizen, "High Corrosion Resistant Nitrogen-Containing Stainless Steels for Use by the Chemical Industry," in "Alloys for the Eighties" pp. 269-279, publ. by the Climax Molybdenum Co., Greenwich, CT, 1982.

19. L. Troselius, Corrosion Science, 11, 473-84 (1971).

20. E. A. Lizlovs and A. P. Bond, J. Electrochem. Soc., 116, 574 (1969).

21. C. W. Kovach, letter dated August 23, 1982.

TABLE I

Test Solution

Solution:	**Filtered seawater**
Temperature:	**Controlled at 30°±1.4°C**
pH	**7.7 to 8.2**
Salinity (mg/L):	**34.4 to 39.1**
Chloride (mg/L):	**19.2 to 21.7**
Dissolved Oxygen (mg/L):	**5.3 to 6.7**
Velocity:	**<0.1 m/sec.**

Table IV

Analyses of Stainless Alloys Used in OTEC Tests

Alloy	Composition; Percent by Weight									
	Cr	Ni	Mo	Cu	Si	Mn	C	S	P	Other
JESSOP 700	20.70	24.80	4.45	0.29	0.37	1.68	0.025	0.015	0.025	Cb 0.30
JESSOP 777**	21.0	25.0	4.5	2.0	-	-	0.04	-	-	
HAYNES 20 Mod*	21.58	25.52	4.95	<0.05	0.49	0.90	<0.01	-	-	Co 0.49
FERRALIUM 255*	26.15	5.64	3.20	1.75	0.37	0.77	0.02	-	-	N 0.19
A.L. 29-4C	28.54	0.49	3.78	-	0.53	0.23	0.023	0.001	0.021	N 0.035
A.L. 6X*	20.35	24.64	6.45	-	0.41	1.39	0.018	0.001	0.022	-
UDDEHOLM 904L*	20.5	24.7	4.7	1.57	0.46	1.46	0.014	0.005	0.028	-
MONIT (Uddeholm)*	25.3	4.1	3.8	0.37	0.31	0.43	0.012	0.006	0.031	-
Type 329 Stainless Steel	26.68	4.23	1.37	-	0.28	0.32	0.06	-	-	-
CARPENTER Exp. 58	20.41	15.39	5.06	-	0.28	5.36	0.072	0.007	0.021	N 0.24
CRUCIBLE SC-1	25.34	2.25	3.10	-	0.20	0.20	0.010	0.007	0.025	Ti 0.5
NITRONIC 50*	21.08	13.70	2.28	-	0.47	4.81	0.045	0.012	0.025	0.26 N
AVESTA 254SMO*	20.0	17.9	6.10	0.78	0.41	0.49	0.013	0.008	0.023	N 0.203

*Heats common with Navy crevice test program.

**Nominal composition.

R. M. Kain

Table V

Analyses of Stainless Alloys Used in Navy Tests

Alloy	Composition, Percent by Weight									
	Cr	Ni	Mo	Mn	C	Si	S	Other		
Type 316	17.5	10.7	2.4	1.60	0.04	0.52	0.004	0.03 P	-	0.28 Cu
34LN	16.8	13.76	1.21	1.57	0.03	0.52	0.004	-	0.14 N	-
Type 216*	20.	6.	2.5	8.	0.08	1.	-	-	0.35 N	-
Rex 734	21.32	9.44	2.67	3.81	0.04	0.26	0.005	0.30 Nb	0.42 N	0.0025 B
Type 317L	18.92	12.25	3.58	1.71	0.025	0.20	0.009	0.035 P	0.056 N	-
Type 317LM	19.52	14.52	4.08	1.32	0.016	0.40	0.025	0.28 Co	0.056 N	0.16 Cu
Type 317L+	18.30	15.80	4.25	1.49	0.010	0.63	0.006	0.16 Co	-	0.16 Cu
Nitronic 50	21.08	13.70	2.28	4.81	0.045	0.47	0.012	0.025 P	0.26 N	-
904L (Uddeholm)	20.5	24.7	4.7	1.46	0.014	0.46	0.005	0.028 P	-	1.57 Cu
AL 4X	20.15	24.38	4.44	1.45	0.014	0.57	0.001	0.019 P	-	1.5 Cu
Jessop 700	20.70	25.20	4.45	1.65	0.013	0.42	0.008	0.28 Nb	-	0.24 Cu
254 SLX	19.9	25.0	4.67	1.64	0.011	0.45	0.003	-	0.042 N	1.67 Cu
Jessop 777	20.80	25.6	4.48	1.37	0.023	0.48	0.013	0.24 Nb	0.25 Co	2.18 Cu
254 SMO	20.0	17.9	6.1	0.49	0.013	0.41	0.008	0.023 P	0.203 N	0.78 Cu
AL 6X	20.35	24.64	6.45	1.39	0.018	0.41	0.001	0.022 P	-	-
Haynes 20 Mod	21.58	25.52	4.95	0.90	<0.01	0.49	-	-	0.49 Co	<0.05 Cu
Carpenter 20 Cb-3	19.36	33.22	2.15	0.44	0.020	0.36	0.002	0.51 Nb	-	3.19 Cu
20 Mo 6	23.91	33.44	5.65	0.44	0.031	0.35	0.007	-	-	3.27 Cu
254 SFER	29.4	22.2	2.13	1.72	0.016	0.30	0.001	-	0.145 N	0.06 Cu

*Nominal composition.

(Table V cont.)

Alloy	Composition, Percent by Weight										
	Cr	Ni	Mo	Mn	C	Si	S	Other			
Incoloy 825	22.02	44.03	2.74	0.35	0.01	0.07	0.004	0.70 Ti		1.66 Cu	
Hastelloy G	22.22	46.84	5.78	1.52	0.007	0.43	-	0.28 W	2.07 Nb	1.85 Cu	1.27 Co
Hastelloy G-3	22.76	43.69	7.01	0.82	0.006	0.37	-	0.95 W	0.19 Nb	1.85 Cu	3.49 Co
Inconel 625	22.29	61.02	8.48	0.10	0.03	0.24	0.001	0.24 Ti	3.57 Nb+ Ta	-	-
Hastelloy C-276	15.51	54.72	15.49	0.46	0.003	0.04	-	3.82 W	-	0.11 Cu	1.89 Co
Type 329	26.98	4.22	1.39	0.28	0.052	0.39	0.014	-	-	0.09 Cu	-
44LN	25.0	5.9	1.46	1.75	0.028	0.53	0.003	-	0.19 N	0.12 Cu	-
Ferralium 255	26.15	5.64	3.20	0.77	0.02	0.37	-	0.16 Co	0.19 N	1.75 Cu	
Type 439	17.66	0.31	0.03	0.26	0.047	0.70	0.010	1.68 Al	-	0.40 Ti	-
Type 444	18.92	0.07	1.99	0.43	0.020	0.56	0.004	0.020 P	0.012 N	0.13 Ti	0.39 Nb
EB-26-1 A.L.	25.9	0.13	1.00	0.10	0.002	0.29	0.015	0.010 P	0.006 N	-	0.10 Nb
26-1S	25.05	0.15	0.96	0.17	0.054	0.16	0.011	0.015 P	0.009 N	1.06 Ti	-
A.L. 29-4	29.6	0.07	4.00	0.10	0.003	0.04	0.011	0.013 P	0.012 N	-	-
A.L. 29-4C	28.85	0.79	3.81	0.22	0.012	0.19	0.002	-	0.026 N	0.59 Ti	-
A.L. 29-4-2	29.5	2.20	3.95	0.10	0.002	0.10	0.010	0.010 P	0.013 N	-	-
SC-1 (Crucible)	25.56	2.14	2.94	0.20	0.01	0.25	0.004	0.04 Al	0.016 N	0.51 Ti	-
Monit (Uddeholm)	25.3	4.1	3.8	0.43	0.012	0.31	0.006	0.37 Cu	0.031 P	-	-

Table VI

Analyses of Cast Stainless Alloys Used in Navy Tests

Alloy	Composition, Percent by Weight								
	Cr	Ni	Mo	Mn	C	Si	S	Other	
CA6N	12.44	8.0	-	0.18	0.02	0.64	0.013	0.010 P	-
CF8M	19.30	10.05	2.36	0.95	0.04	0.79	0.019	-	-
IN 862	20.92	24.46	5.00	0.47	0.03	0.52	0.009	0.007 P	-
CN7MS	19.37	22.10	2.93	1.00	0.05	3.00	0.010	0.006 P	1.55 Cu
CN7M	20.01	28.18	2.51	0.18	0.04	0.76	0.025	0.007 P	3.12 Cu
625	20.58	63.7	8.53	0.02	0.02	0.01	0.011	0.006 P	3.48 Nb
CW 12M-2	18.10	62.8	17.58	0.54	0.01	0.56	0.007	0.010 P	0.08 Cu
Illium PD	24.55	5.39	1.97	0.86	0.04	0.80	0.016	0.004 P	5.74 Co
Ferralium*	25.2	5.2	2.5	1.	-	1.10	-	-	3.2 Cu

*Nominal composition.

Table VII

OVERALL RANKING OF ALLOYS IN OTEC TESTS FOR CREVICE CORROSION IN FILTERED SEAWATER AT 30°C

(All panels; 30, 60 and 90 days, 25 and 75 in-lb; mill finish)

Rank	Alloy	Composition, % by wt.						Number of Sides (S) Attacked(c)	Maximum Depth (D) (mm)	Index (SxD)
		Cr	Ni	Mo	Mn	Cu	N			
1	A.L. 29-4C	28.5	0.5	3.8	-	-	-	0	0.00	0.00
2	Monit (Uddelholm)	25.3	4.1	3.8	0.4	0.4		3	0.01	0.03
3	Ferralium 255 (Cabot)	26.2	5.6	3.2	0.8	1.8	0.19	1	0.09	0.09
4	904L (Uddeholm)	20.5	24.7	4.7	1.5	1.6	-	3	0.37	1.11(a)
5	254 SMO (Avesta)	20.0	17.9	6.1	0.5	0.8	0.2	6	0.19	1.14
6	Crucible SC-1	25.3	2.3	3.1	0.2	-	(0.5 Ti)	14	0.11	1.54
7	A.L. 6X	20.4	24.6	6.5	1.4	-	-	8	0.34	2.72
8	Carpenter Exp 58	20.4	15.4	5.1	5.4	0.1	0.24	13	0.32	4.16
9	Haynes 20 Mod	21.6	25.5	5.0	0.9	-	-	8	0.80	6.40
10	Jessop 777	21.0	25.0	4.5	(1.4)	2.0	-	6	2.26	13.56(a)
11	Nitronic 50	21.1	13.7	2.3	4.8	-	0.26	17	1.15	19.55(b)
12	Jessop 700	20.7	24.8	4.5	1.7	0.3	-	14	1.75	24.50
13	Type 329	26.7	4.2	1.4	0.3	-	-	1[illegible]	1.62	27.54(b)

(a) Also had tunneling - attack perpendicular to upper edge, or attack at edges.
(b) Perforated by attack from both sides.
(c) Total number of sides was 18.

Table VIII

THE EFFECT OF LENGTH OF TESTING TIME IN OTEC TESTS ON CREVICE CORROSION IN FILTERED SEAWATER AT 30°C

(Mill Finish; Torque = 75 in-lb)

	Rank (Overall)*	Alloy	Number of Sides (S) Attacked**		Maximum Depth (D) of Attack (mm)		Index (SxD)	
			30 Days	60 Days	30 Days	60 Days	30 Days	60 Da
(I)	1	A.L. 29-4C	0	0	0.00	0.00	0.00	0.0
(II)	2	Monit (Uddeholm)***	0	0	0.00	0.00	0.00	0.0
	3	Ferralium 255†	1	0	0.09	0.00	0.09	0.0
(III)	4	904L (Uddeholm)†	3	0	0.37	0.00	1.11	0.0
	5	254 SMO (Avesta)	2	4	0.19	0.18	0.38	0.7
	6	Crucible SC-1	4	4	0.04	0.11	0.16	0.4
	7	A.L. 6X	2	5	0.23	0.34	0.46	1.7
(IV)	8	Carpenter Exp 58	4	5	0.20	0.32	0.80	1.6
	9	Haynes 20 Mod	2	3	0.39	0.80	0.78	2.4
(V)	10	Jessop 777†	3	3	2.18	2.26	6.54	6.7
	11	Nitronic 50	5	6	0.67	0.26	3.35	4.0
	12	Jessop 700	5	5	1.75	0.44	8.75	2.2
	13	Type 329	6	5	1.48	1.62	8.88	8.1

*Based on all tests, including some 90-day tests, see Table VII.
**Results on three panels or 6 sides for each test.
***Crevice corrosion in 90-day test.
†Copper content >1.0%.

Table IX

TIME TO APPEARANCE OF VISIBLE CORROSION PRODUCTS IN OTEC AND NAVY TESTS
Filtered Seawater at 30°C

Rank*	Alloy	Time When Corrosion Products were Observed, Hr. OTEC Tests (Mill Finish) 9 Panels up to 90 days (25 and 75 in-lb)	OTEC Tests (Mill Finish) 3 Panels 30 days (75 in-lb)	Navy Tests (120 grit) 3 Panels 30 days (75 in-lb)
1	29-4C	No attack	No attack	No attack
2	Monit	772	No attack	No attack
3	Ferralium 255	509	509	365
4	904 L	388	388	51
5	254 SMO	72	72	51
6	Crucible SC-1	703	Not detected	Not detected
7	A.L. 6X	388	388	51
8	Carpenter Exp. 58	100	120	Not tested
9	Haynes 20 Mod	48	48	51
10	Jessop 777	72	72	36
11	Nitronic 50	24	24	36
12	Jessop 700	72	72	51
13	Type 329	24	48	51

*Rank based on 9 panels in OTEC tests.

Table X

THE EFFECT OF TORQUE IN OTEC TESTS ON CREVICE CORROSION IN FILTERED SEAWATER AT 30° C

(60-Day Tests, Mill Finish, 3 panels for each test)

	Rank*	Alloy	Number of Sides (S) Attacked 25 in-lb	Number of Sides (S) Attacked 75 in-lb	Maximum Depth (D) of Attack (mm) 25 in-lb	Maximum Depth (D) of Attack (mm) 75 in-lb	Index (SxD) 25 in-lb	Index (SxD) 75 in-lb
(I)	1	A.L. 29-4C	-	0	-	0.00	-	0.00
(II)	2	Monit (Uddeholm)	-	0	-	0.00	-	0.00
	3	Ferralium 255†	0	0	0.00	0.00	0.00	0.00
(III)	4	904L (Uddeholm)†	0	0	0.00	0.00	0.00	0.00 (a)
	5	254 SMO (Avesta)	0	4	0.00	0.18	0.00	0.72
	6	Crucible SC-1	0	4	0.00	0.11	0.00	0.44
	7	A.L. 6X	1	5	0.02	0.34	0.02	1.70
(IV)	8	Carpenter Exp 58	5	5	0.15	0.32	0.75	1.60
	9	Haynes 20 Mod	3	3	0.50	0.80	1.50	2.40
(V)	10	Jessop 777†	0	3	0.00	2.26	0.00	6.78 (a)
	11	Nitronic 50	6	6	1.15 (a)	0.26	6.90	1.56 (b)
	12	Jessop 700	4	5	1.29	0.44	5.16	2.20
	13	Type 329	6	5	1.55 (a)	1.62	9.30	8.10 (b)

* Overall ranking based on 9 panels.
(a) There was tunneling or attack at edges.
(b) Complete penetration of 1.3 mm (N-50) and 1.8 mm (329) panels.
† Copper content >1.0%

Table XI

The Effect of Surface Finish

Comparison of OTEC and Navy Data on Crevice Corrosion in Filtered Seawater at 30°C (30-day tests at torque of 75 in-lb)

Rank 30-day OTEC Tests	Alloy	OTEC - Mill Finish				NAVY - 120 Grit Finish				Rank
		No. of Sites[a]	No. of Sides(S)[b]	Max. Depth(D) (mm)	Index (SxD)	No. of Sites[a]	No. of Sides(S)[b]	Max. Depth(D) (mm)	Index (SxD)	
1	A.L. 29-4C	0	0	0.00	0.00	0	0	0.00	0.00	1*
2	Monit (Uddeholm)	0	0	0.00	0.00	0	0	0.00	0.00	2
3	Ferralium 255†	1	1	0.09	0.09	2	2	0.08	0.16	4
4	Crucible SC-1	7	4	0.04	0.16	1	1	0.05	0.05	3*
5	254 SMO (Avesta)	2	2	0.19	0.38	18	5	0.51	2.55	7
6	A.L. 6X	2	2	0.23	0.46	11	4	0.62	2.48	6
7	Haynes #20 Mod	4	2	0.39	0.78	6	2	0.46	0.92	5
8	Carpenter Exp 58	8	4	0.20	0.80	-	-	-	-	(8)
9	904L (Uddeholm)†	3	3	0.37	1.11	36	5	0.74	3.70	9
10	Nitronic 50	25	5	0.67	3.35	112	6	1.10	6.60	10
11	Jessop 777†	16	3	2.18	6.54	60	6	2.90	17.40	12*
12	Jessop 700	30	5	1.75	8.75	47	5	2.00	10.00	11*
13	Type 329	70	6	1.48**	8.88**	73	6	1.29**	7.74**	13*

[a] Total number of crevices = 120

[b] Total number of sides = 6

* A second heat was used for the Navy tests.

** Perforated

† Copper content >1.0%.

Table XII

RANKING OF ALLOYS IN NAVY TESTS FOR RESISTANCE TO CREVICE CORROSION IN FILTERED SEAWATER AT 30°C

(30-day tests on 3 panels with 120 grit finish and torque of 75 in-lb)

Rank	Alloy	Composition, % by wt.						Number of Sides (S) Attacked	Maximum Depth (D) of Attack mm	Index (SxD)
		Cr	Ni	Mo	Mn	Cu	Other			
1	Hastelloy C-276	15.5	54.7	15.5	0.5	0.1	3.8 W	0	0.00	0.00
	Inconel 625	22.3	61.0	8.5	0.1	-	3.6 Nb	0	0.00	0.00
	29-4 (A.L.)	29.6	0.1	4.0	-	-	-	0	0.00	0.00
	29-4-2 (A.L.)	29.5	2.2	4.0	-	-	-	0	0.00	0.00
	29-4C* (A.L.)	28.8	0.8	3.8	0.2	-	0.6 Ti	0	0.00	0.00
	Monit (Uddeholm)	25.3	4.1	3.8	0.4	0.4	-	0	0.00	0.00
2	Crucible SC-1 (Crucible)	25.6	2.1	2.9	0.2	-	0.5 Ti	1	0.05	0.05
3	Ferralium 255 (Cabot)	26.2	5.6	3.2	0.8	1.8	0.19 N	2	0.08	0.16
4	Hastelloy G-3 (Cabot)	22.8	43.7	7.0	0.8	1.8	3.5 Co	1	0.21	0.21
5	Haynes 20 Mod (Cabot)	21.6	25.5	5.0	0.9	-	0.5 Co	2	0.46	0.92
6	26-1S	25.0	0.2	1.0	0.2	-	1.1 Ti	4	0.30	1.20
7	20Mo-6	23.9	33.4	5.6	0.4	3.3	-	3	0.53	1.59
8	EB 26-1 (A.L.)	25.9	0.1	1.0	-	-	0.1 Nb	4	0.46	1.84
9	A.L. 4X	20.2	24.4	4.4	1.4	1.5	0.019 P	4	0.50	2.00
10	A.L. 6X	20.4	24.6	6.4	1.4	-	-	4	0.62	2.48
11	254 SMO (Avesta)	20.0	17.9	6.1	0.5	0.8	0.2 N	5	0.51	2.55
12	Hastelloy G (Cabot)	22.2	46.8	5.8	1.5	1.8	3.5 Co	4	0.87	3.48
13	904L (Uddeholm)	20.5	24.7	4.7	1.5	1.6	-	5	0.74	3.70
14	Type 216	20.0	6.0	2.5	8.0	-	0.35 N	6	0.64	3.84
15	254SPER (Avesta)	29.4	22.2	2.1	1.7	0.1	0.15 N	5	0.90	4.50
16	254 SLX (Avesta)	19.9	25.0	4.7	1.6	1.7	0.04 N	6	0.92	5.52
17	Rex 734	21.3	9.4	2.7	3.8	-	0.42 N	6	1.00	6.00
18	Type 317 LM	19.5	14.5	4.1	1.3	0.2	0.056 N	6	1.07	6.42
19	Nitronic 50	21.1	13.7	2.3	4.8	-	0.26 N	6	1.10	6.60
20	Jessop 700	20.7	25.2	4.4	1.6	0.2	0.28 Nb	5	2.00	10.00
21	Type 316	17.5	10.7	2.4	1.6	0.3	-	6	1.93	11.58
22	Carpenter 20 Cb-3	19.4	33.2	2.2	0.4	3.2	0.51 Nb	5	3.10	15.50
23	Jessop 777	20.8	25.6	4.5	1.4	2.2	0.24 Nb	6	2.90	17.40
24	44 LN	25.0	5.9	1.5	1.8	0.1	0.2 N	6	3.35	20.10
	Perforated									
	Type 444	18.9	0.1	2.0	0.4	-	0.4 Nb	6	1.21	7.25
	Type 329	27.0	4.2	1.4	0.3	0.1	-	6	1.29	7.74
	34 LN	16.8	13.8	4.2	1.6	-	0.14 N	6	1.04	6.24
	Attack Outside Crevice Areas									
	Type 439	17.7	0.3	-	0.3	-	0.4 Ti	6	0.72	4.32
	Type 317L	18.9	12.2	3.6	1.7	-	0.056 N	6	1.92	11.52
	Type 317L +	18.3	15.8	4.2	1.5	0.2	0.16 Co	6	1.09	6.54
	Incoloy 825	22.0	44.0	2.7	0.4	1.7	0.7 Ti	6	2.42	14.52

*Three additional panels were tested for 82 days with the same results.

Table XIII

CREVICE CORROSION OF CAST ALLOYS
IN FILTERED SEAWATER AT 30°C

(Navy Tests, 120 Grit Finish, 75 in-lb, 30 days, 3 panels)

Rank	Alloy	Composition, % by wt Cr	Ni	Mo	Mn	Cu	Number of Sides (S) Attacked*	Maximum Depth (D) of Attack mm	Index (SxD)
1	Inconel 625	20.6	63.7	8.5	-	-	0	0.00	0.00
	CW 12M-2	18.1	62.8	17.6	0.5	0.1	0	0.00	0.00
2	IN-862	20.9	24.5	5.0	0.5	-	6	1.22	7.32
3	CF-8M	19.3	10.0	2.4	1.0	-	6	3.77	22.62
4	Illium PD	24.6	5.4	2.0	0.9	-	6	4.53	27.18
Attack Outside Crevice Areas									
5	Ferralium	25.2	5.2	2.5	1.0	3.2	4	2.21	8.84
6	CN7M	20.0	28.2	2.5	0.2	3.1	6	2.33	13.98
7	CN7MS	19.4	22.1	2.9	1.0	1.6	6	3.82	22.92
8	CA6N	12.4	8.0	-	0.2	-	6	2.00	12.00

*Total of six sides.

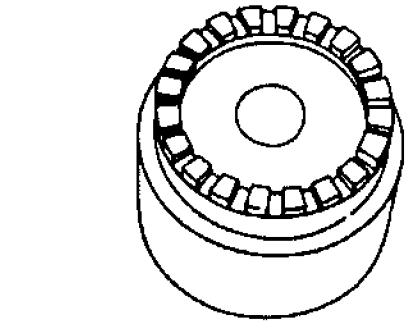

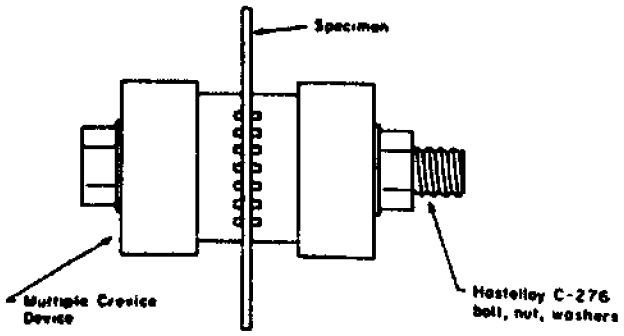

Fig. 1 Crevice Assembly.

20 "plateaus" with grooves 1 mm wide and 0.5 mm deep between them. The external radius of the "plateaus" is 23 mm and the internal radius 20.6 mm.

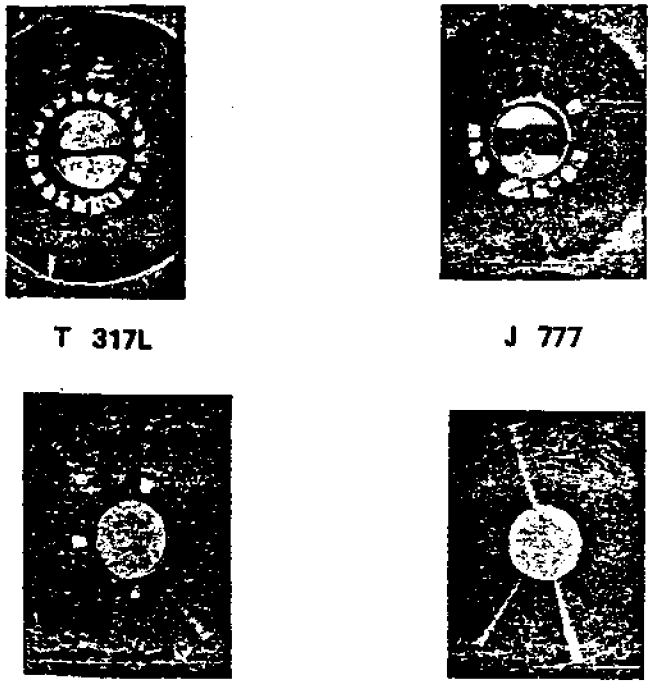

Fig. 2 Crevice Corrosion in Filtered Seawater at 30°C, 30-Day Test.

The four specimens were cut from panels (10 x 15 cm) exposed in the Navy Tests (3). A 120-grit finish was applied in a circle 5 cm in diameter before testing.

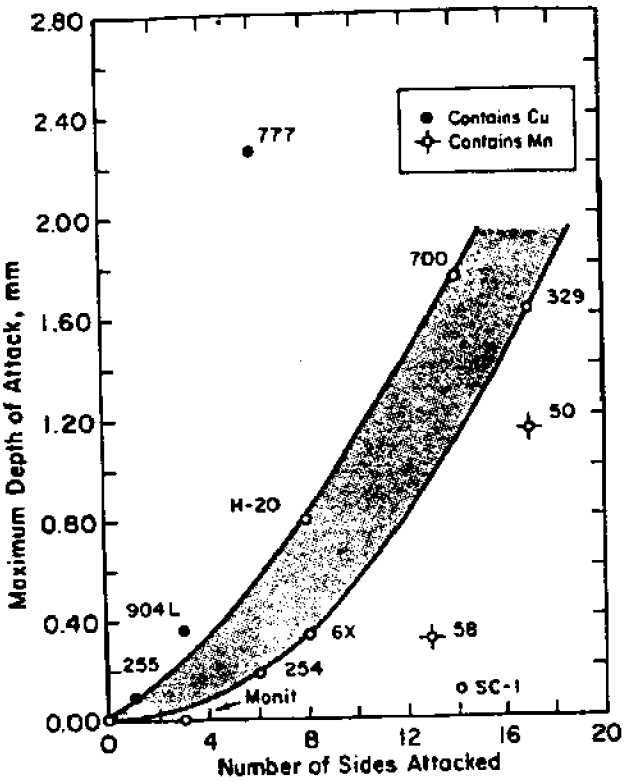

Fig. 3 Crevice Corrosion in Filtered Seawater at 30°C, OTEC Tests on Panels with Mill Finishes.

For this graph, all 9 panels (18 sides) of each alloy in the OTEC tests were treated as a group.

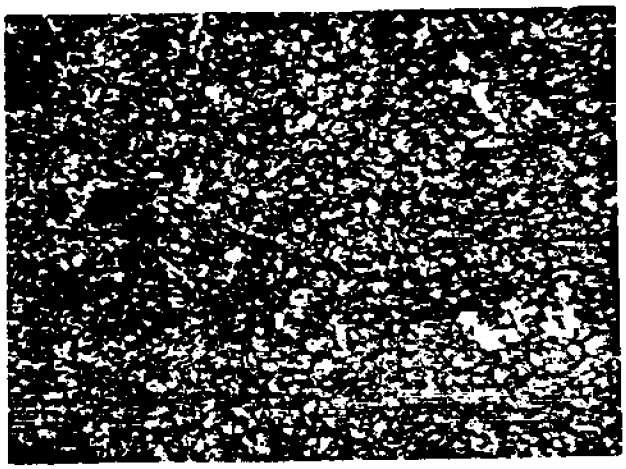

a) Jessop 700 Mill Finish

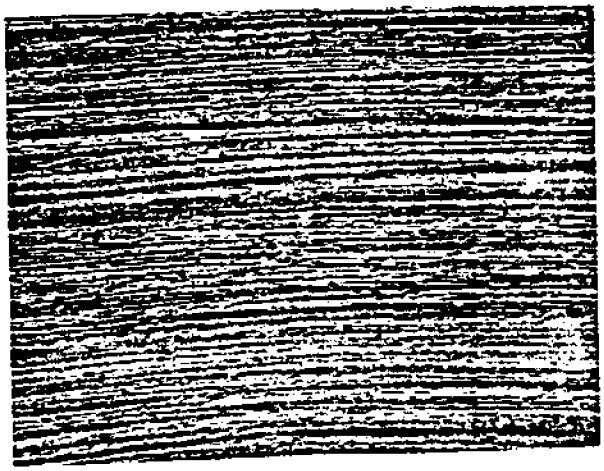

b) Jessop 777 120-grit Finish

Fig. 4 Surface Finish Under Crevice Devices (100X).

III. MATHEMATICAL MODELLING AND MULTIPLE AND REMOTE CREVICE ASSEMBLY DATA

1. Crevice Geometry and Resistance to Initiation

Figure 1 provides a schematic describing factors of crevice depth and crevice gap. These variables are used as inputs for mathematical modelling predictions of resistance to crevice corrosion initiation. Effects of crevice geometry are shown for several stainless steels in Figure 2.

The actual values for crevice gap are difficult to determine. However, through the use of scanning electron microscopy, a range of gaps have been quantified for a variety of assemblies (see Figures 3-20).

Additional examples of mathematical modelling predictions and measurements are found in the attached papers:

1. "Factors Influencing the Crevice Corrosion Behavior of Stainless Steels in Seawater," by T. S. Lee and R. M. Kain (see Section 2.)
2. "Crevice Corrosion Resistance of Several Iron Base and Nickel Base Cast Stainless Alloys in Seawater" by R. M. Kain
3. "Crevice Corrosion Resistance of Type 316 Stainless Steel in Marine Environments," by R. M. Kain, T. S. Lee and J. R. Scully
4. "The Effect of Crevice Solution pH on Corrosion Behavior of Stainless Alloys" by R. M. Kain and T. S. Lee

2. Natural Versus Synthetic Environments

Figures 21 to 29 give the potential (cathode and anode member couples) and corresponding crevice corrosion current for duplicate assemblies of Type 316 stainless steel, alloy 904L (20Cr-25Ni-4.5Mo-1.5Cu) and 18Cr-2Mo stainless steel. While the initiation response for Type 316 was about the same in both the natural and synthetic environments, alloy 18-2 and especially alloy 904L exhibited greater resistance in the synthetic environments. Table 1 gives results which quantify the overall propagation

resistance in terms of total charge for the various alloy/environment combinations. Generally, the results for duplicate assemblies were comparable. Since the test durations varied between 400 and 800 hours, the total charge after 400 hours has been calculated for assemblies exposed in the two synthetic environments. Results from the seawater tests show similar charge values for Type 316 and alloy 904L while those for 18-2 are nearly doubled.

3. **Monitoring the Effects of Environmental Variables**

Figure 30 describes typical current data collected for one of two alloy 904L specimens initially exposed to seawater at 30°C (see also Figure 31). As evidenced by the sharp increase in current, initiation occurred at about the seventh day of exposure. The magnitude of this current is consistent with the total current shown earlier in Figure 2. During the course of testing, the temperature of the seawater was elevated in 5°C increments approximately every 5 days. While some perturbations are noted through the first 40 days (temperature up to 45°C), the magnitude of current remains relatively high. Upon a further increase in temperature to 50°C, the magnitude of total current dramatically decreased by several orders of magnitude. After almost four weeks of corroding at this low rate, the propagation rate was returned to its earlier higher level by allowing the seawater to cool back to 30°C.

Figure 37 shows current data for a companion RCA sample of alloy 904L which was introduced after the above test temperature was established at 50°C. As can be seen, initiation in this case did not occur until the seawater was cooled to 30°. Note that the times at 50°C was more than twice that required for initiation of the material described in Figure 30. Subsequent propagation currents, however, are comparable.

4. **Effect of Seawater Velocity: Remote Crevice Assembly Testing of Alloy 904L in Filtered Seawater at 30°C**

Effects of seawater velocity on crevice corrosion propagation resistance were examined according to the following procedure:

Velocity (1)	Start up to day 12 cathode and anode members at ~0 m/s (slight flow due to refreshment)
Velocity (2)	Day 12 to 19 velocity increased to 0.037 m/s (recirculation pumps on)
Velocity (3)	Day 19 to 28 velocity increased to 0.064 m/s for cathode members (baffle installed), anode members at Velocity (2)
Velocity (4)	Day 28 to 35 velocity increased to 0.147 m/s for cathode members (flow section reduced with baffle), anode members at Velocity (2)
	Day 35 to 44 both cathode and anode members in 0.147 m/s flow channel

Figure 33 gives a plot of the cathode and anode coupled potential and corresponding crevice corrosion currents for duplicate assemblies of alloy 904L. Little effect of velocity at the present levels of flow was detected.

5. **Effect of Bulk Environment O_2 Concentration**

The effect of bulk seawater environment oxygen concentration on the potential of coupled anodes for alloy 904L was examined in a series of compartmentalized cell tests (anode or crevice cell separated from cathode-bulk environment by a porous plug). Figures 34 and 35 show potentials for freely corroding "cathodes." Figures 36 to 50 show corresponding potentials for coupled anode and cathode members in their respective environments. Data for replicate tests are provided. Increasing the oxygen concentration by purgin with various gas mixtures, i.e., 95% N_2-5%O_2, compressed air (80%N_2-20%O_2) and 50%N_2-50%O_2, resulted in an increase in the anode potential to more noble values.

Under these alloy-environment conditions, polarization to the passive state was described by decay in current densities to ~ 1 uA/cm2 or less. Different area ratios and/or more concentrated crevice solutions could account for the results described by other RCA testss where ongoing crevice corrosion was observed at a couple potential around +0.05 V.

Controlled Crevice Loading Device

An air operated loading device (see Experimental) used in concert with the remote crevice assembly concept has been used to further study the effects of crevice tightness. In these tests, the anode members were positioned between acetal resin (Delrin) blocks. Tests were conducted with and without plastic tape inserts between the blocks and both metal surfaces.

Figure 51 shows the remote crevice assembly current and potential data for duplicate assemblies exposed without the inserts. While anodic currents were recorded, the levels were fairly low.

Figures 52 and 53 shows results for tests using the tape inserts in the crevice formers. In both cases, conditions were sufficiently severe to cause initiation within 50 hours. While two additional samples initiated within 5 hours, one of these spontaneously repassivated and re-initiated several times during the 7 day test. The average initiation time (~20 hours) is consistent with the results described earlier for Type 316 in seawater tests using the bolt loading type RCA fixture (with tape inserts).

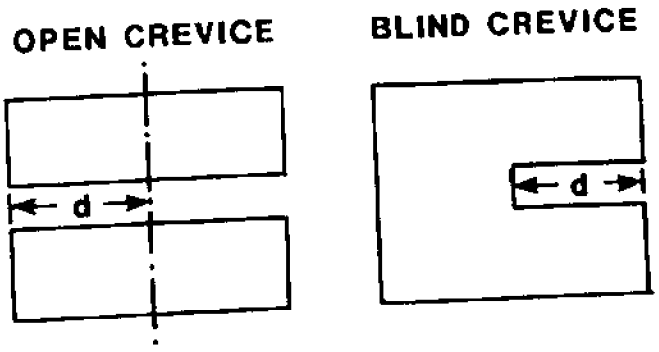

CREVICE DEPTH (d)

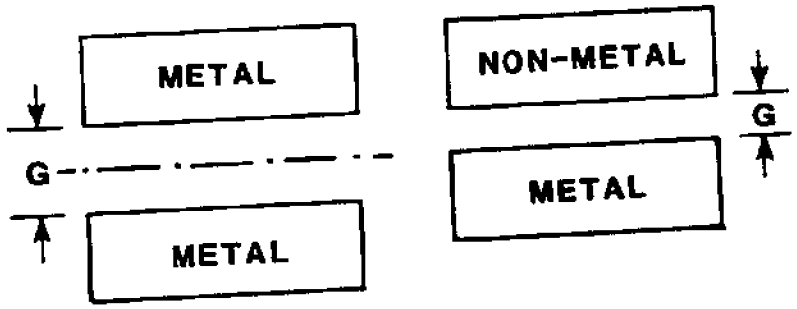

CREVICE GAP (G)

SCHEMATIC of CREVICE GEOMETRY FACTORS

Figure 1.

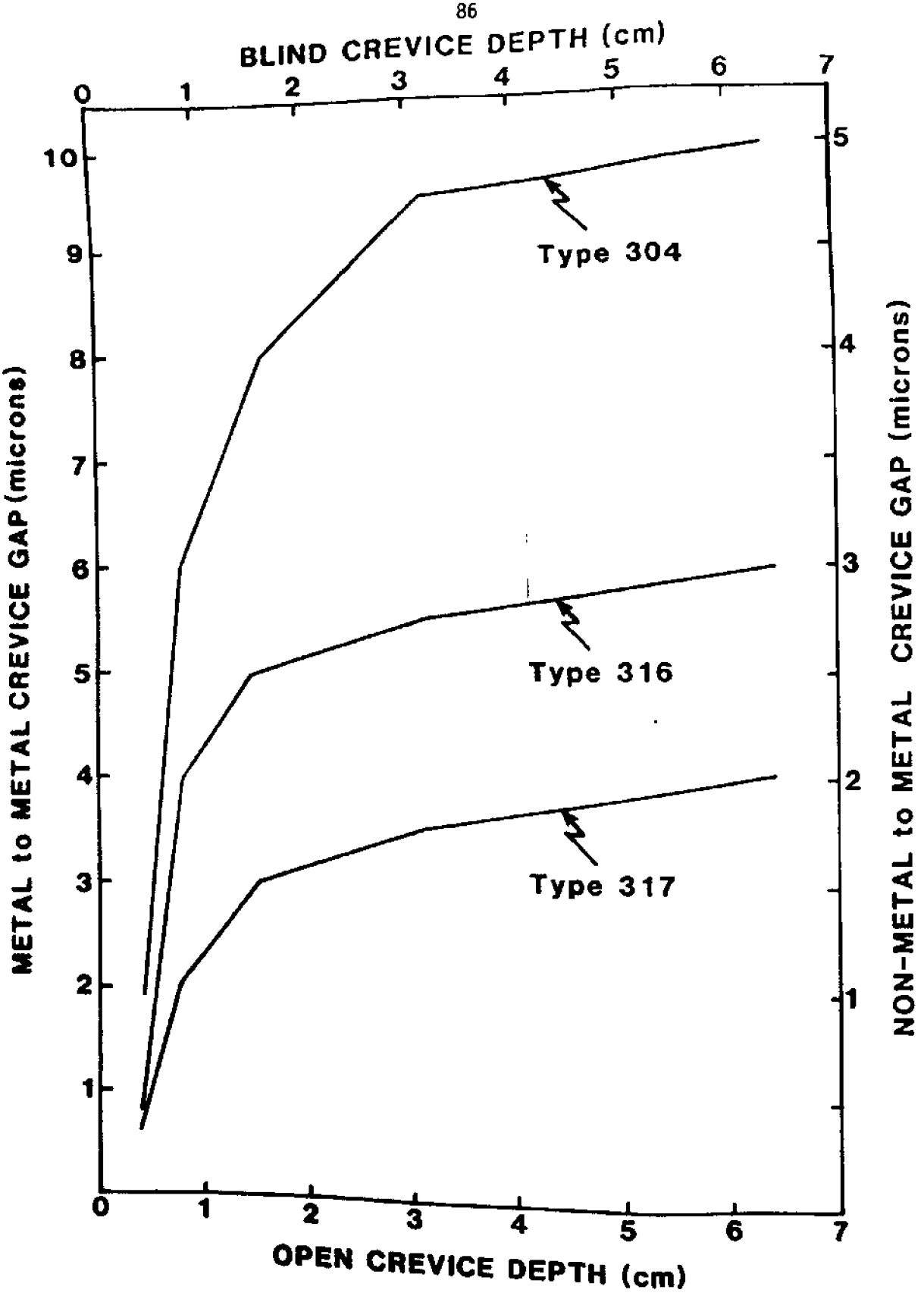

Figure 2.

EFFECT OF CREVICE GEOMETRY ON PREDICTED RESISTANCE TO INITIATION IN SEAWATER

Quantification of Actual Crevices

Index to Figures

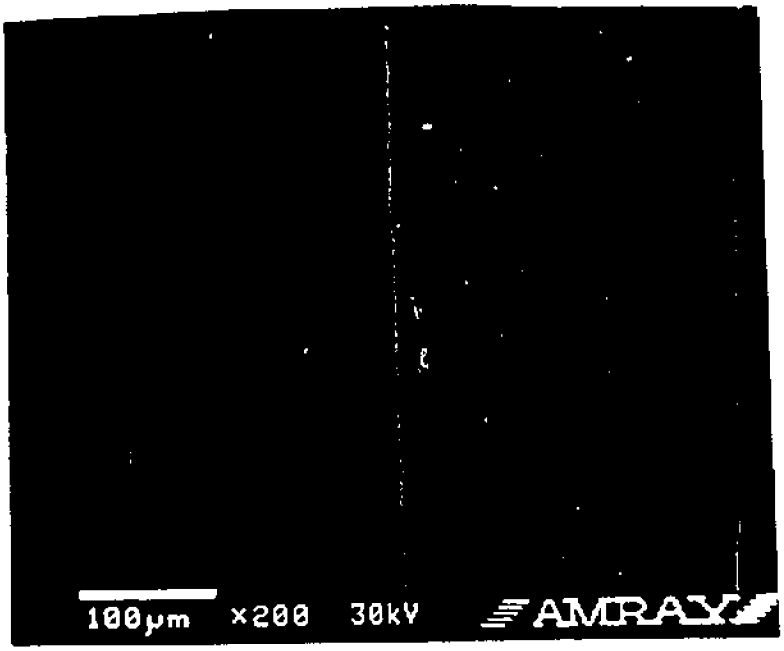

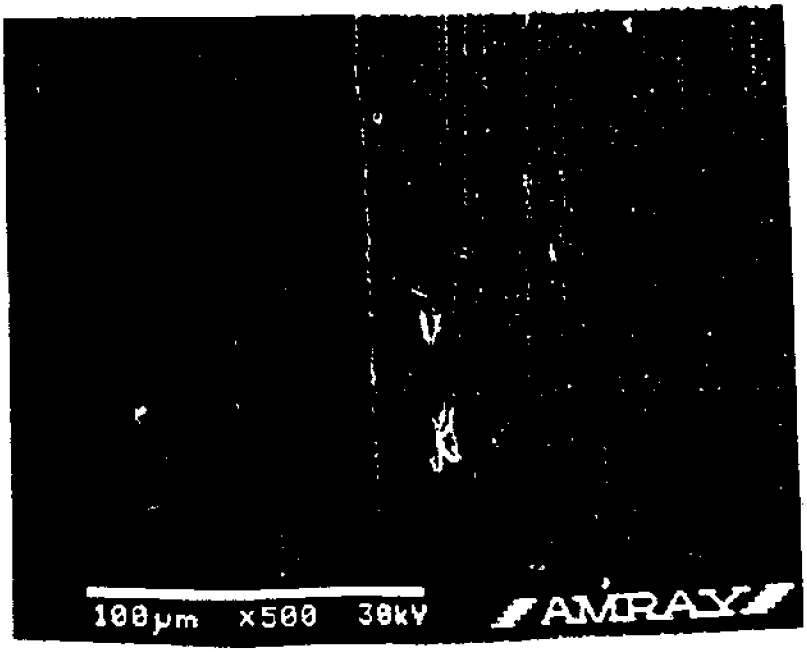

Figure 3.

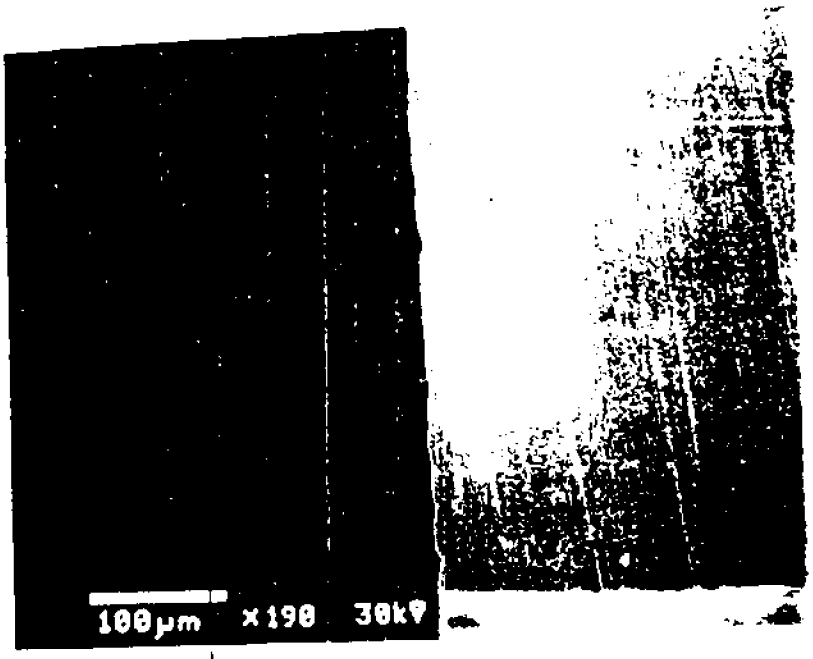

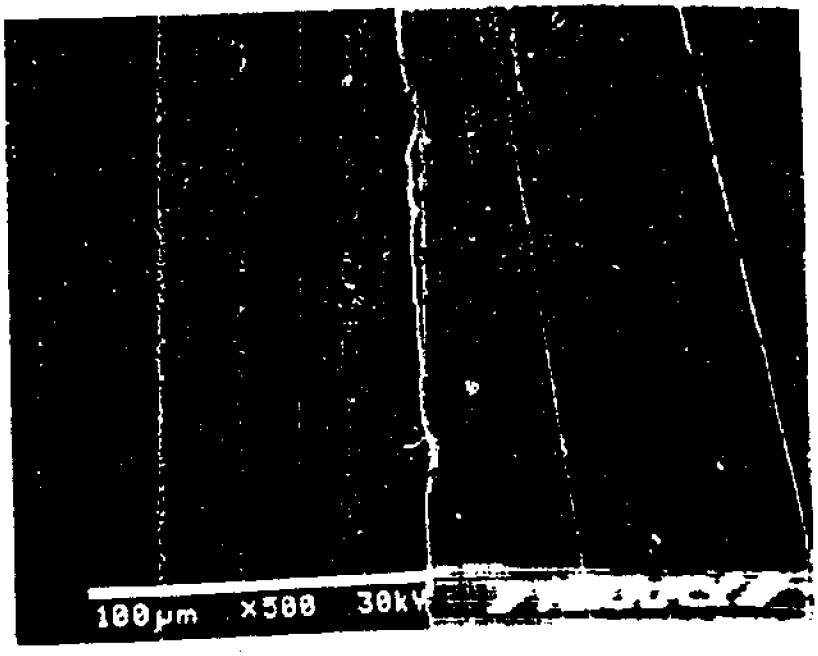

Figure 4.

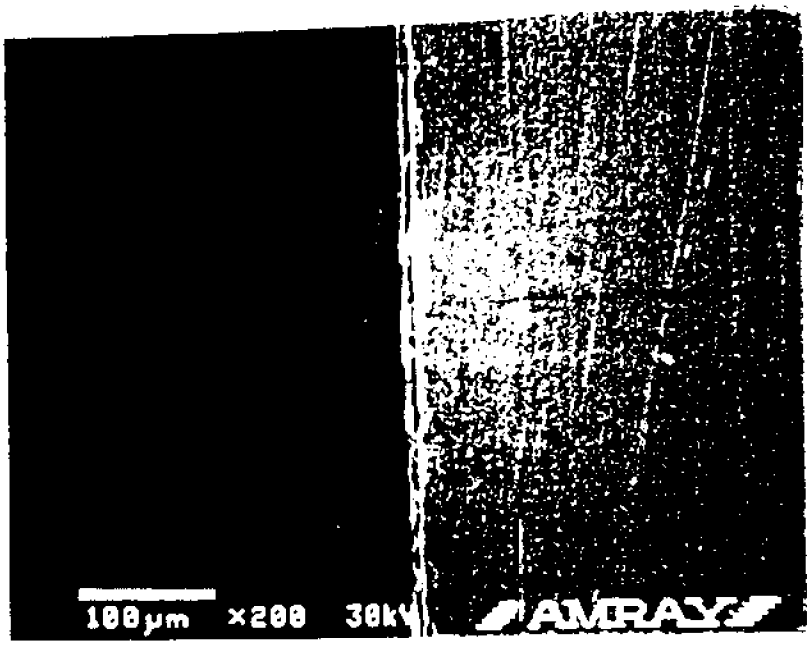

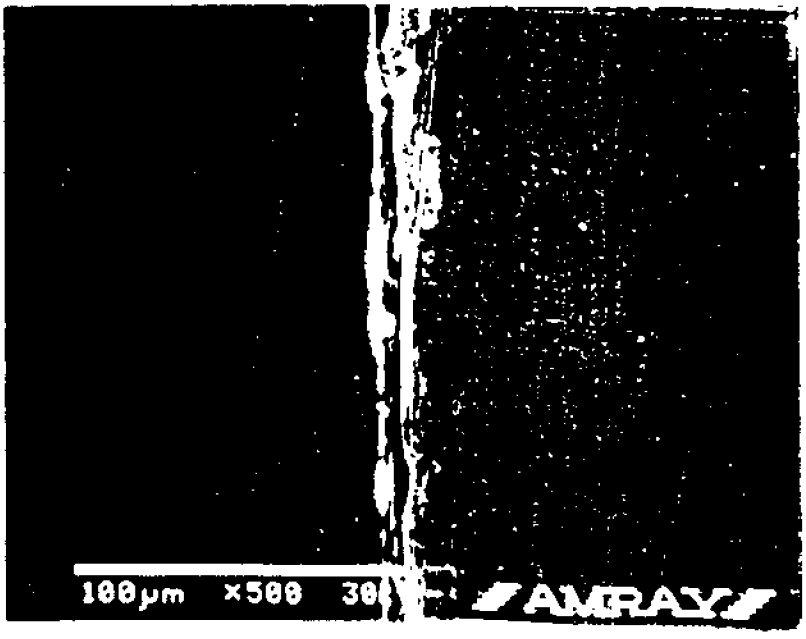

Figure 5.

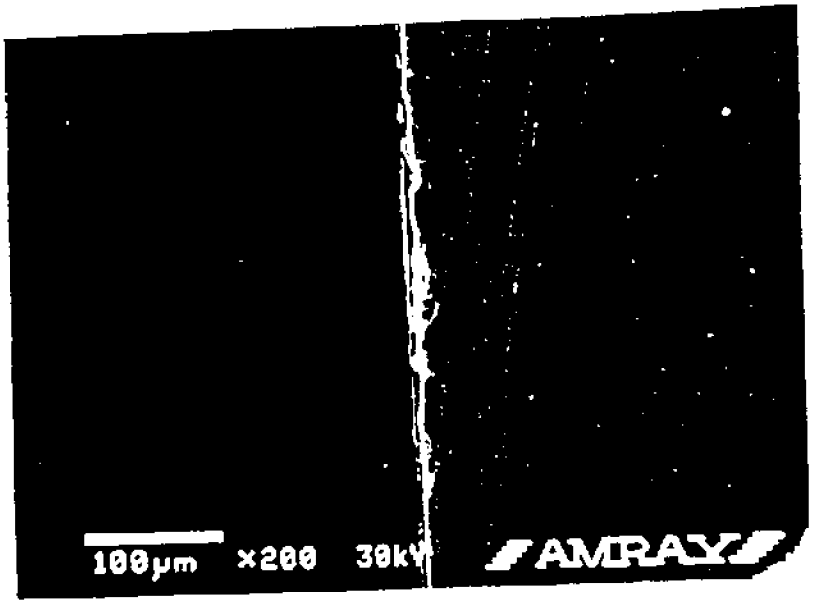

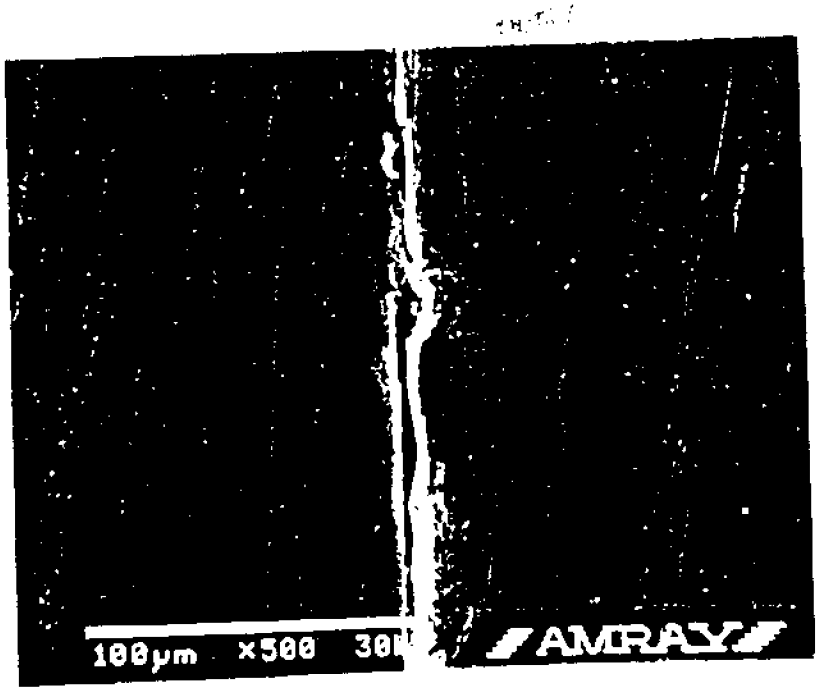

Figure 6.

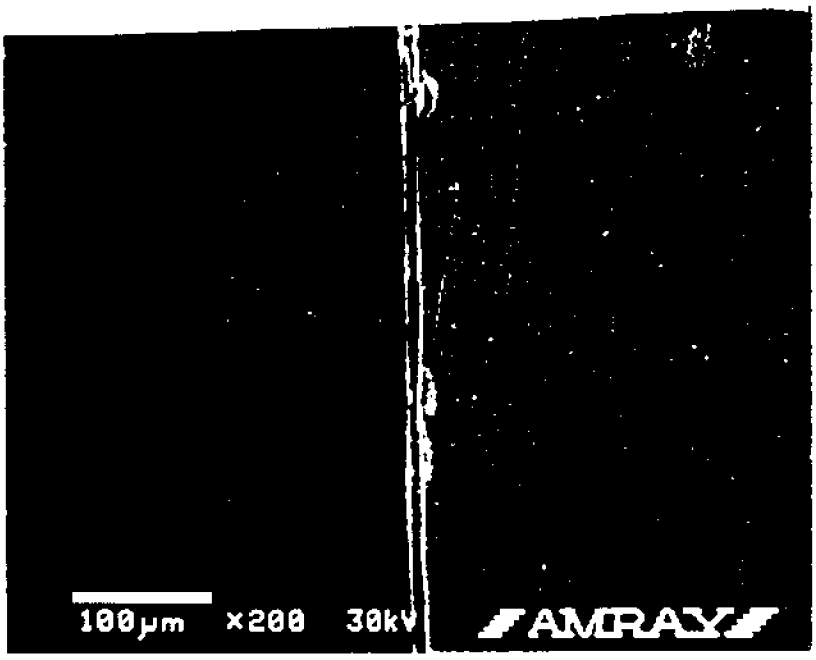

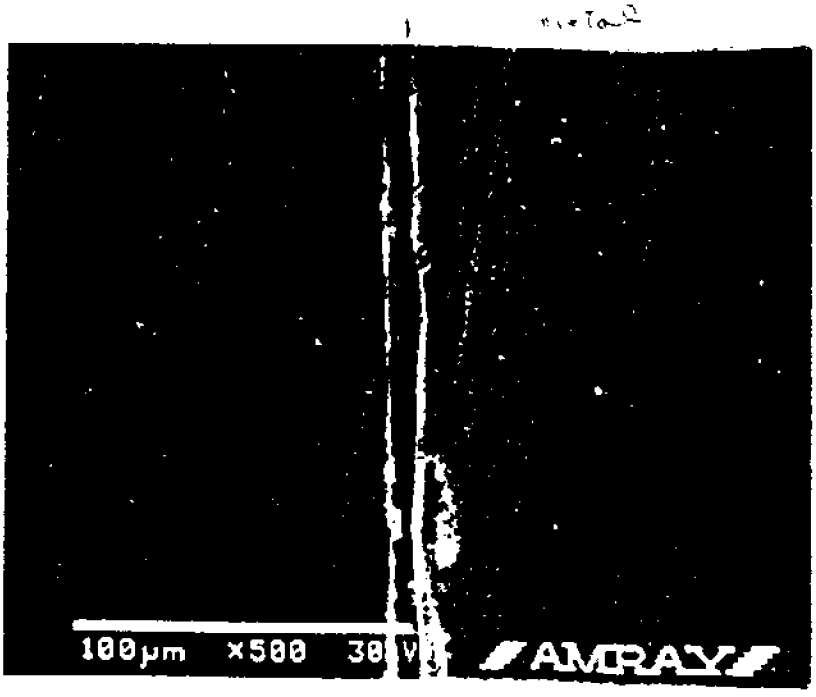

Figure 7.

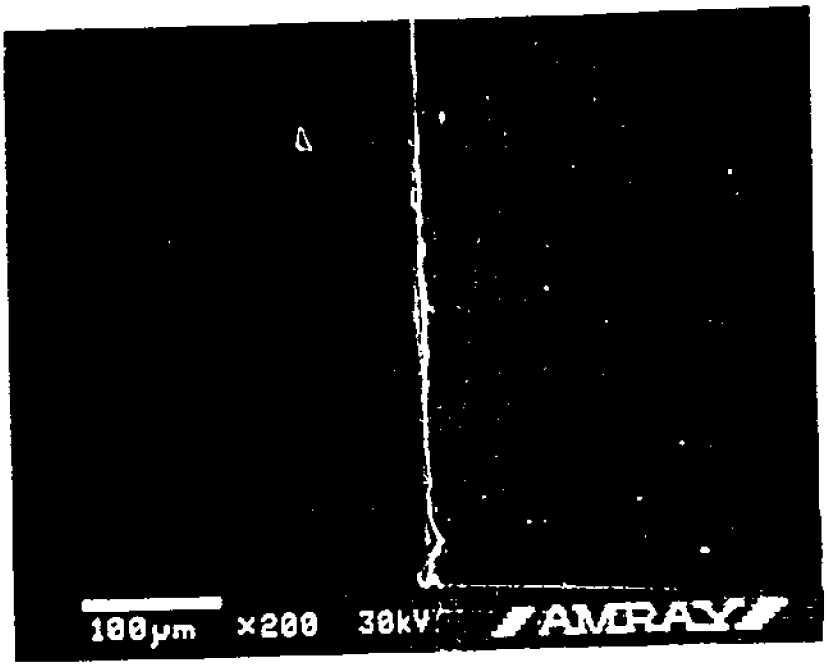

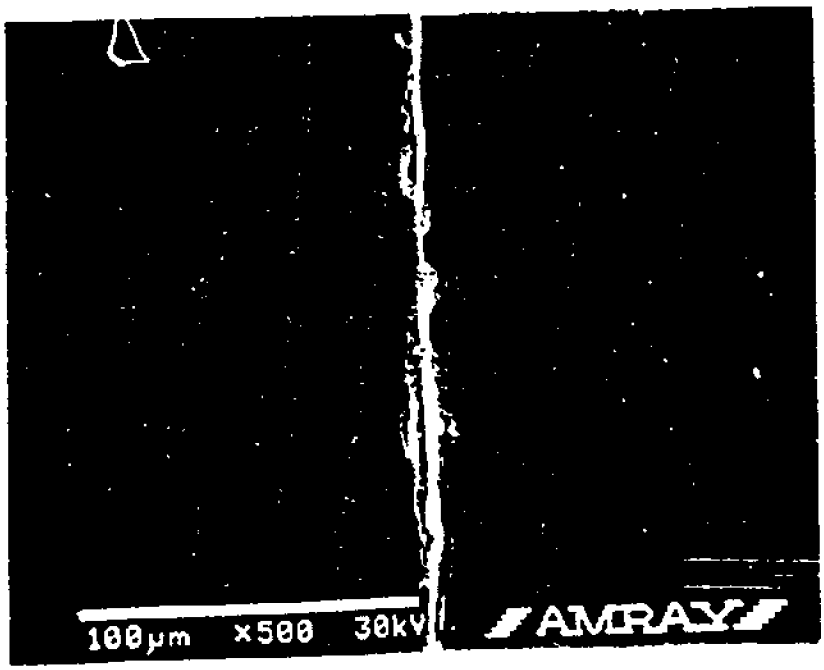

Figure 8.

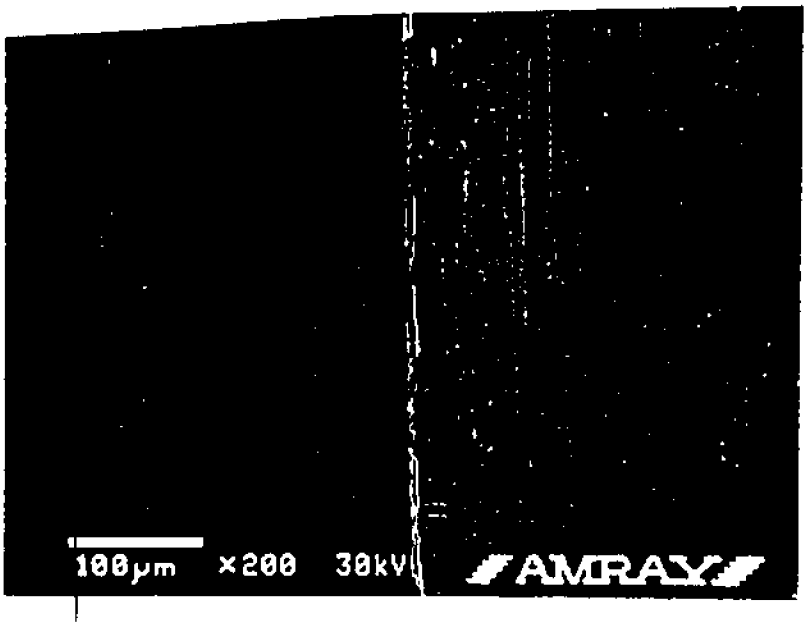

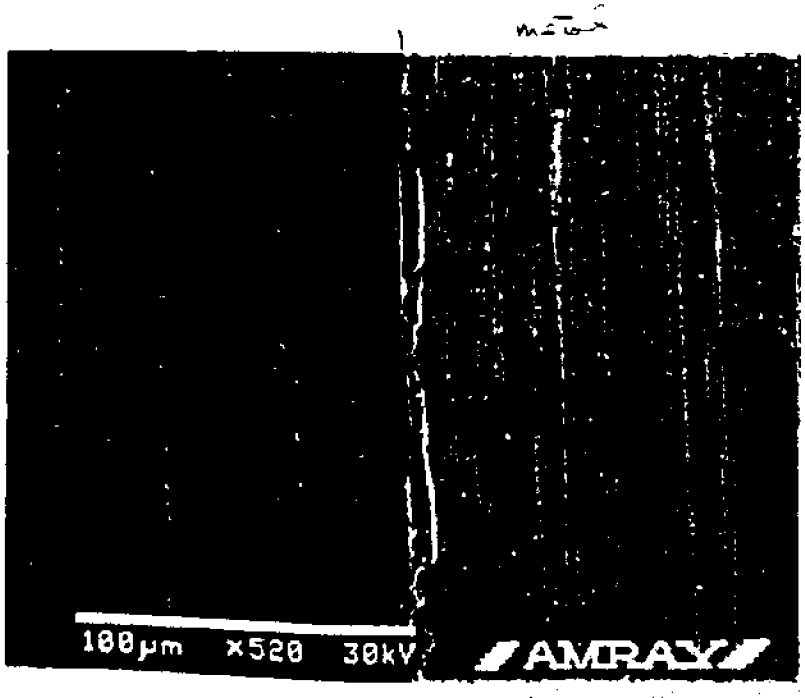

Figure 9.

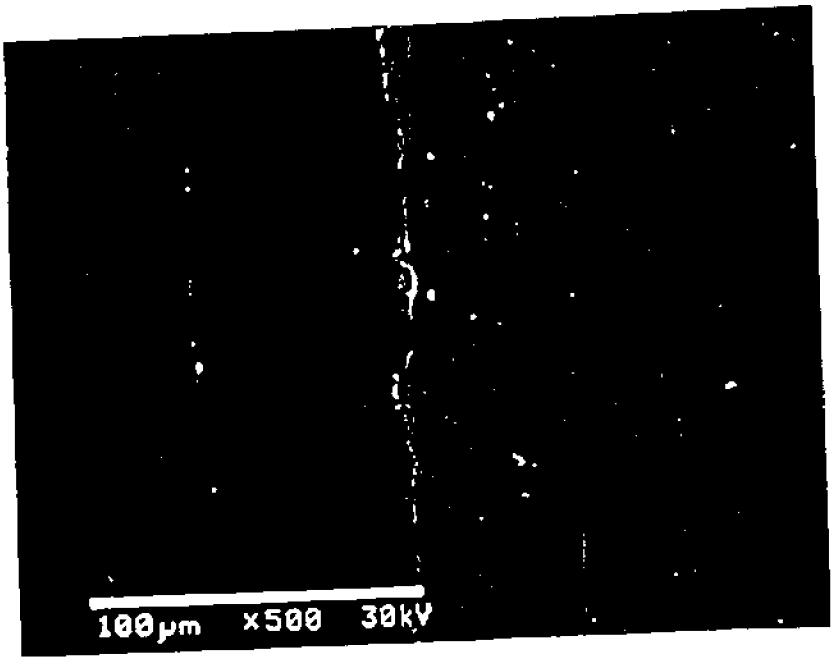

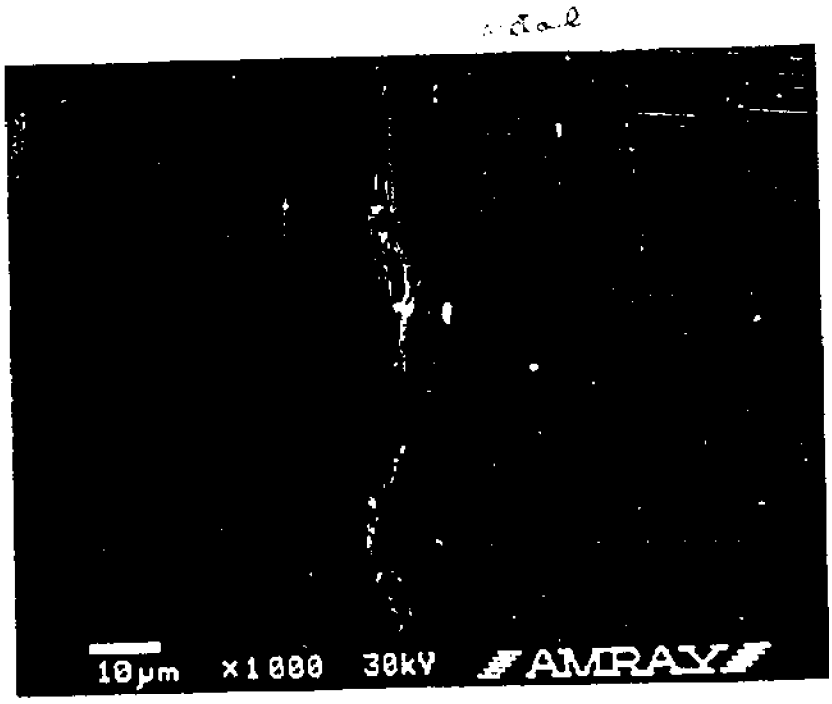

Figure 10.

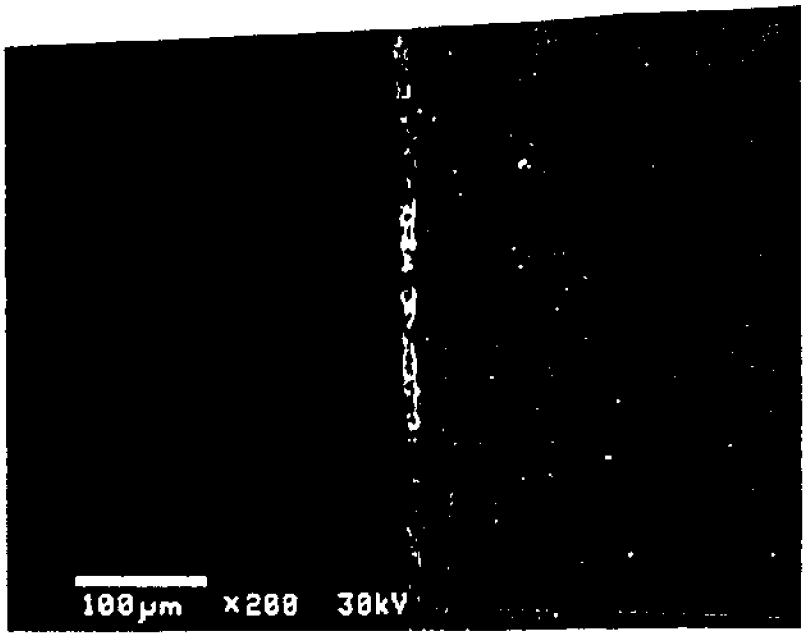

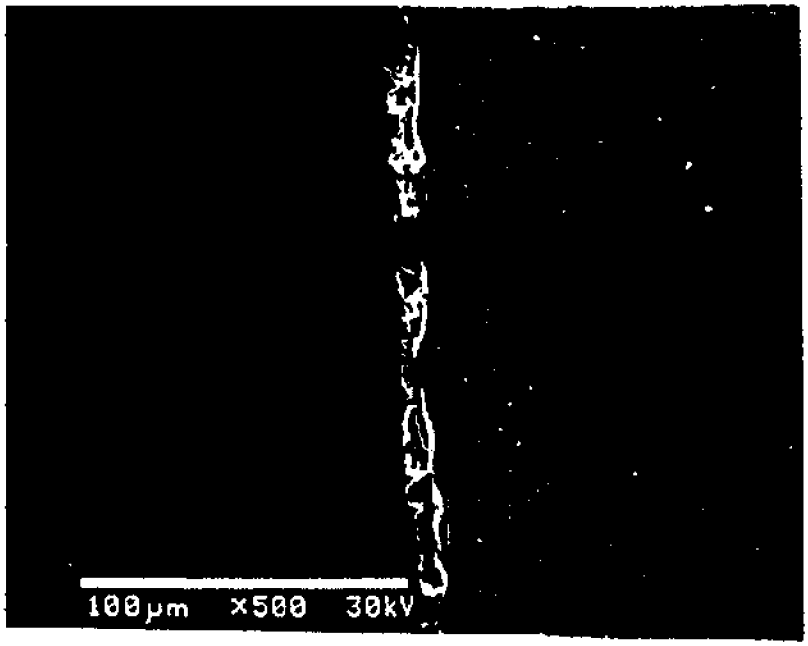

Figure 11.

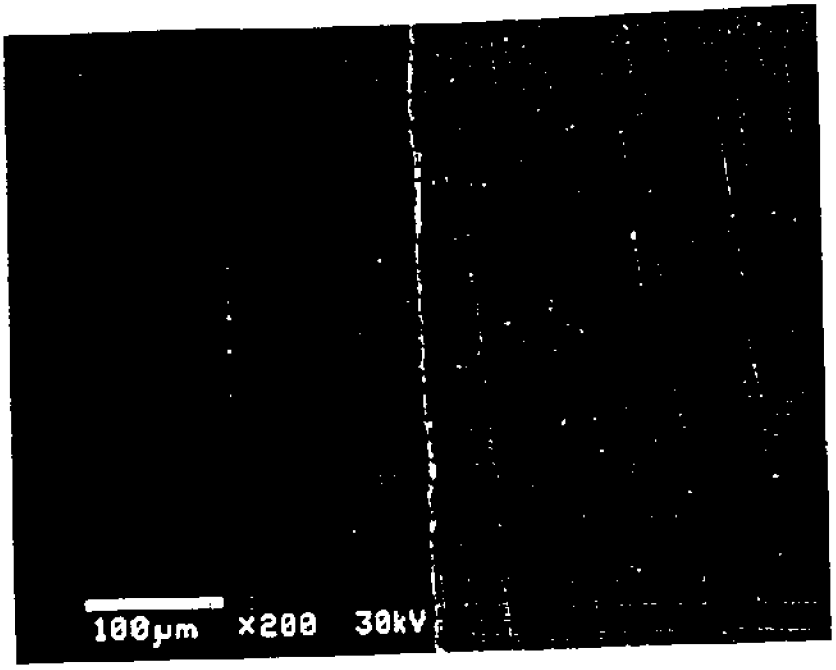

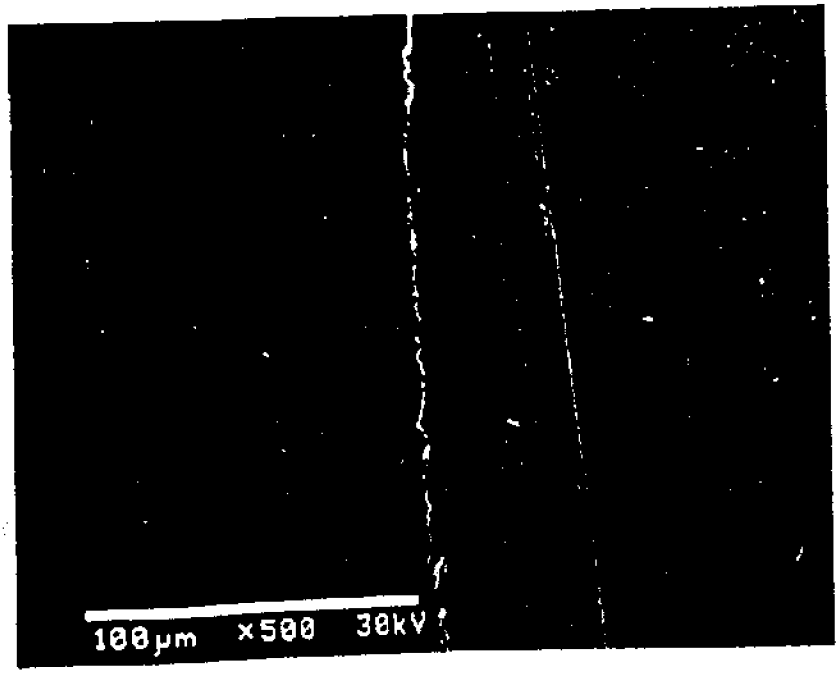

Figure 12.

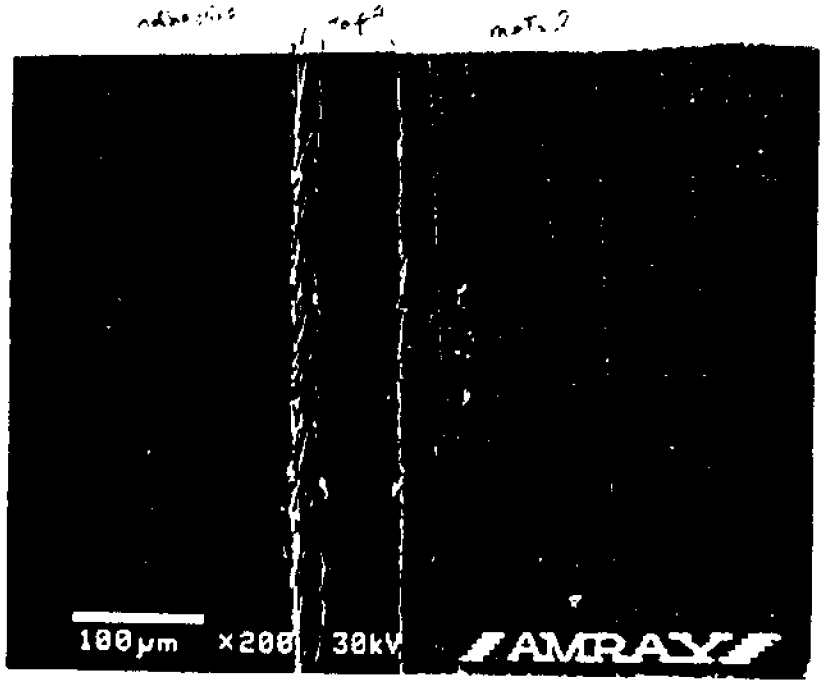

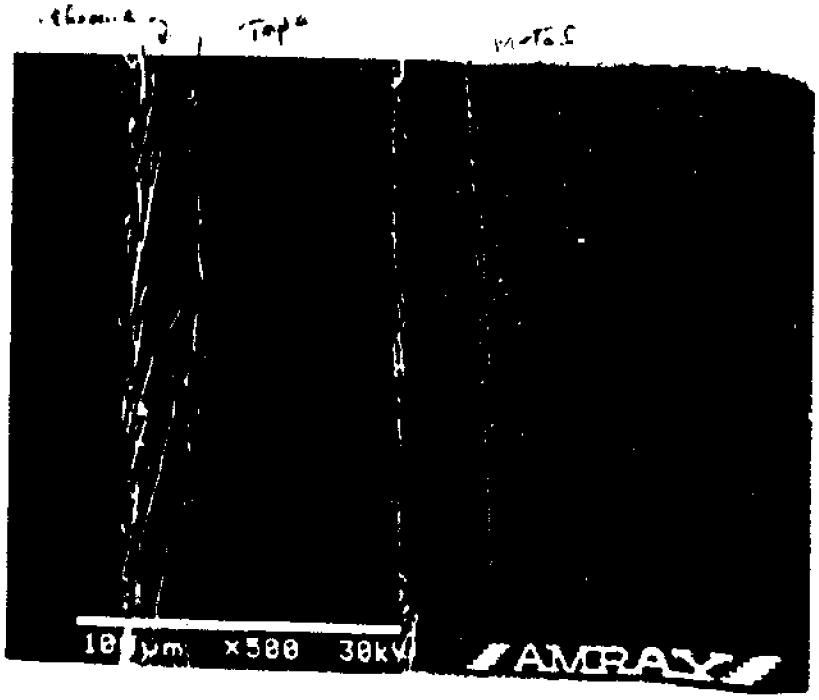

Figure 13.

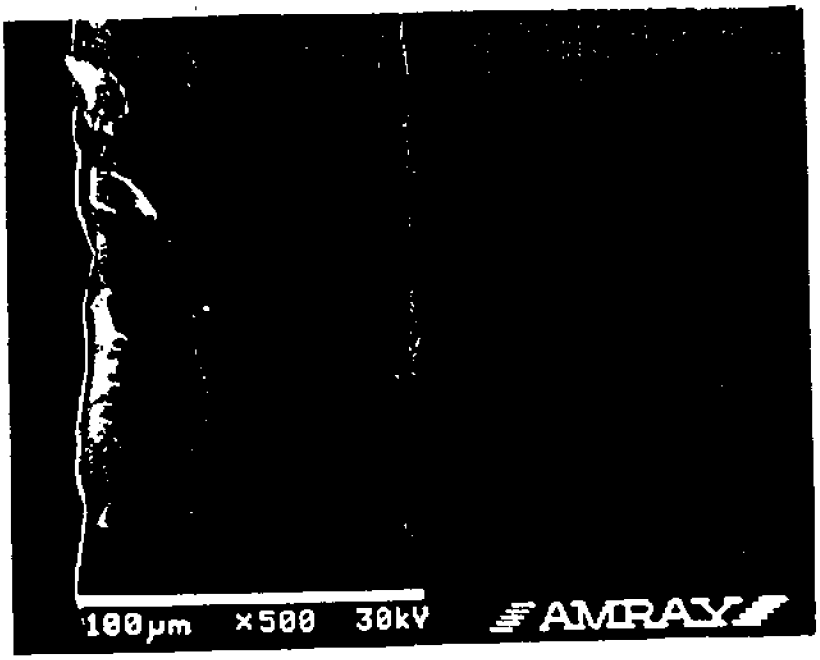

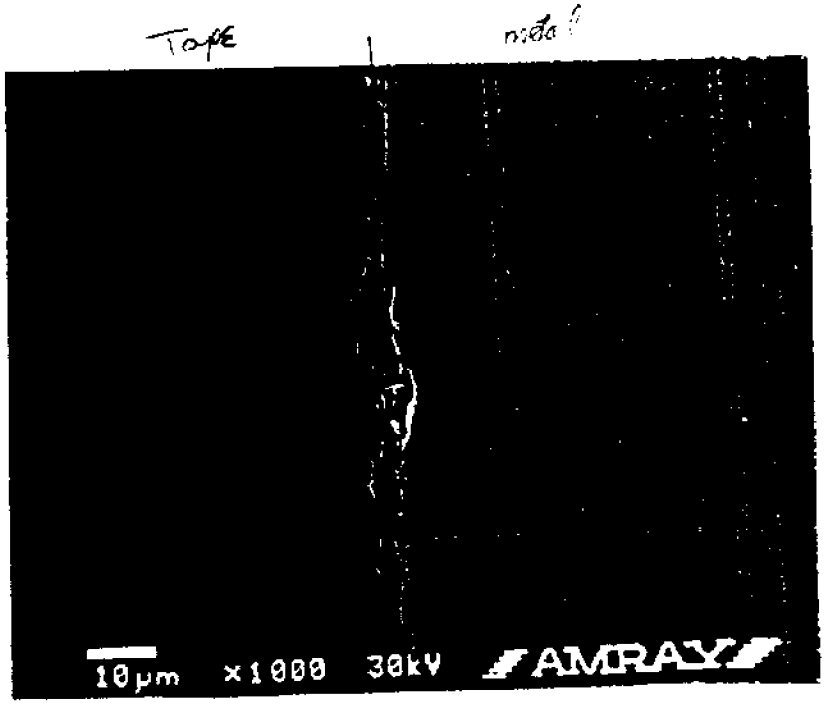

Figure 14.

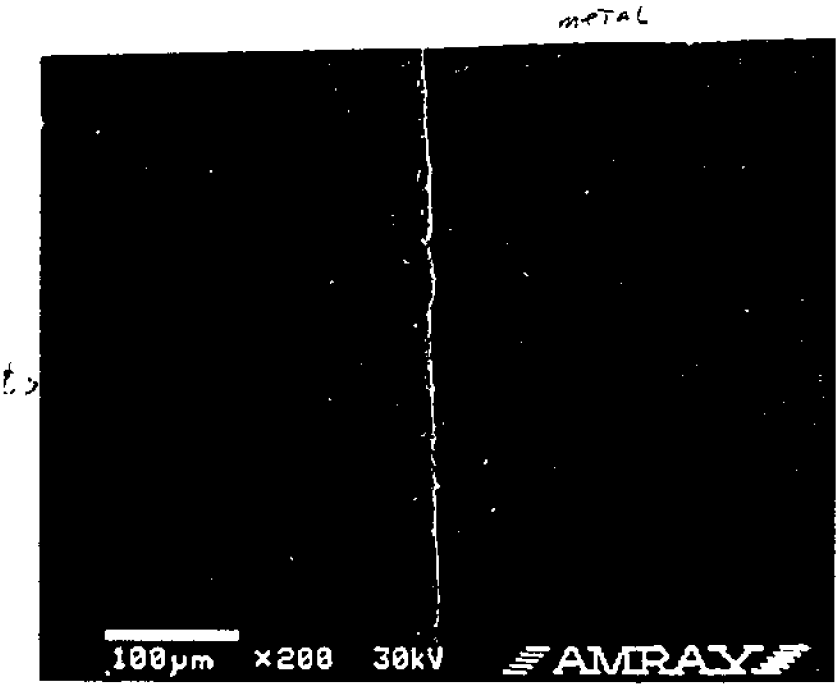

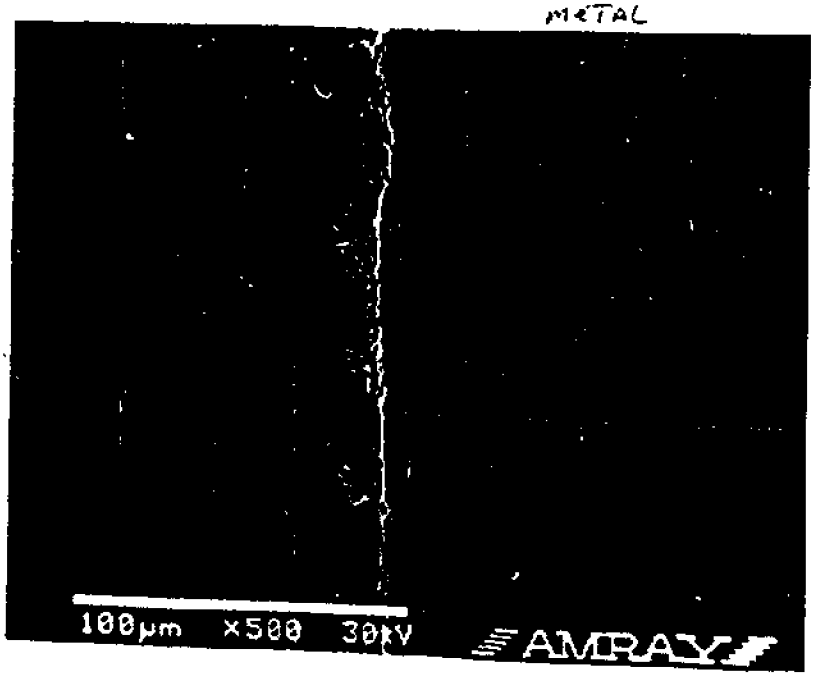

Figure 15.

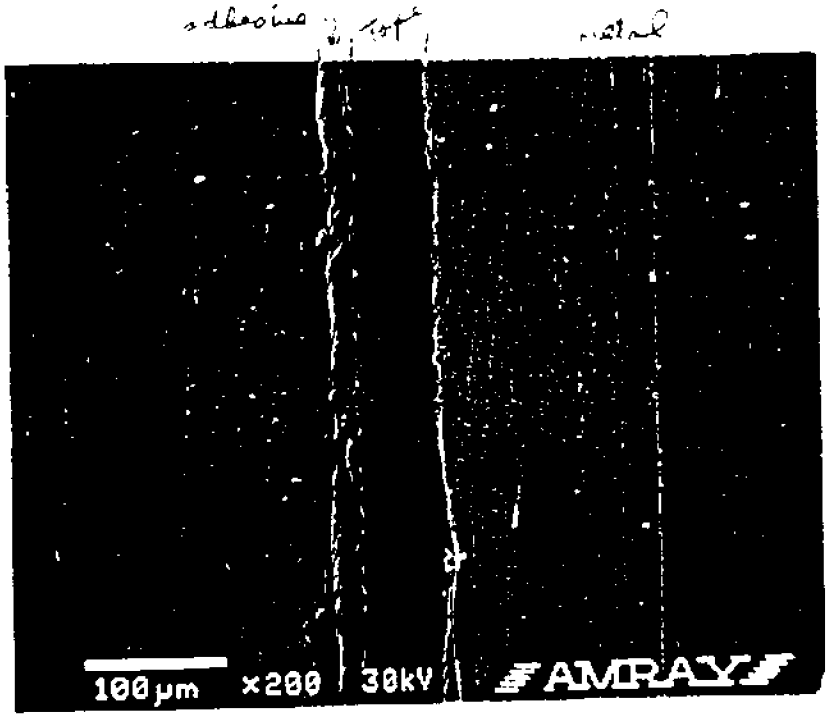

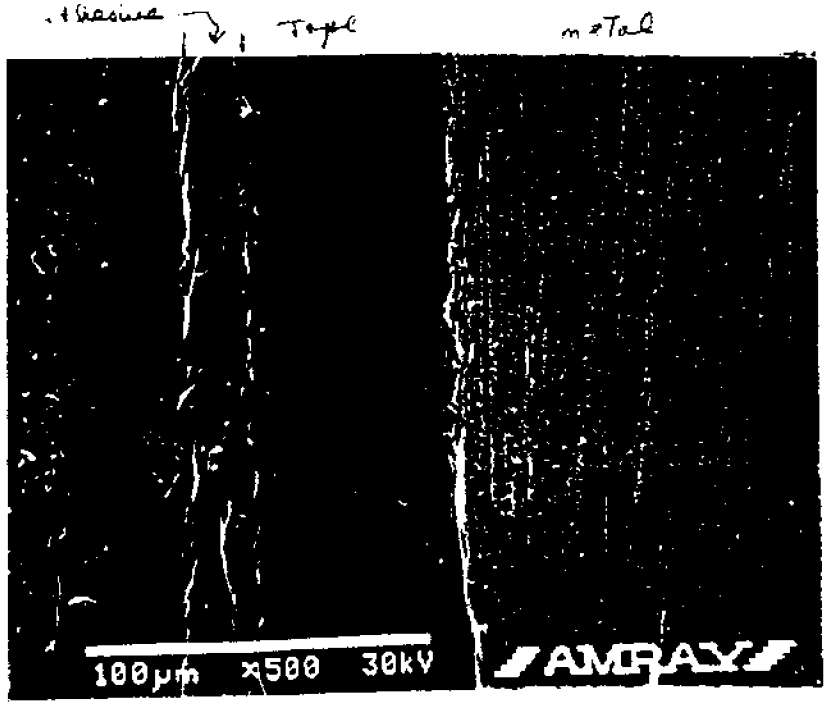

Figure 16.

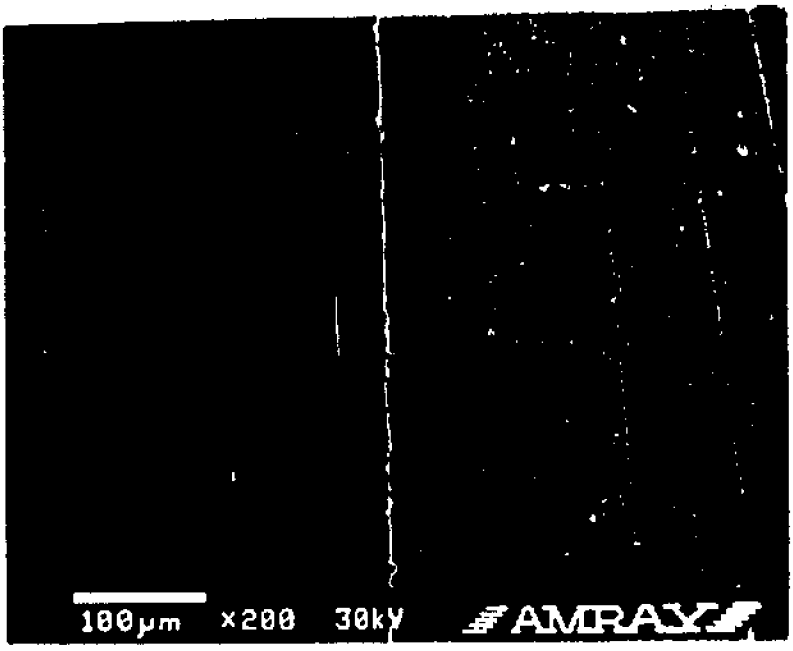

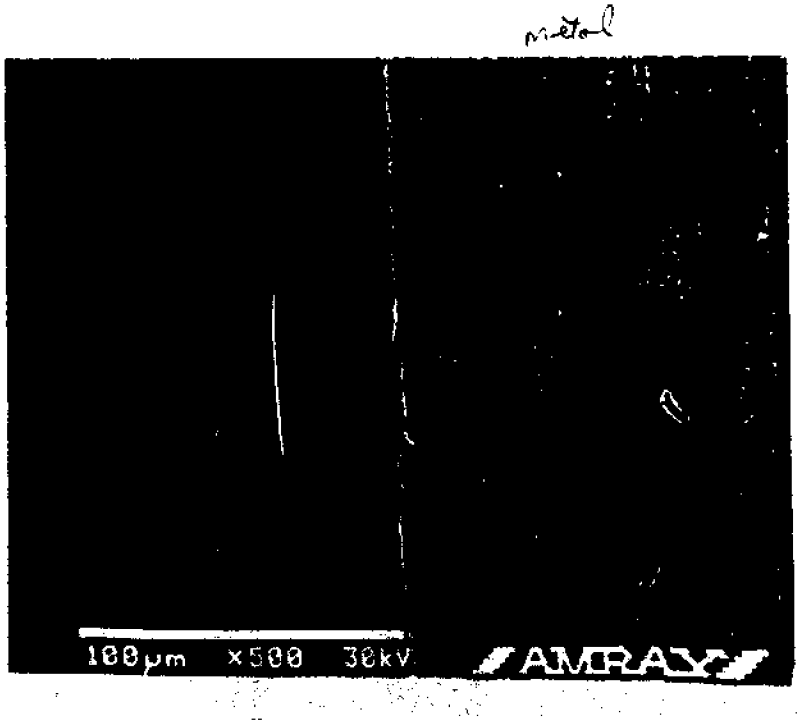

Figure 17.

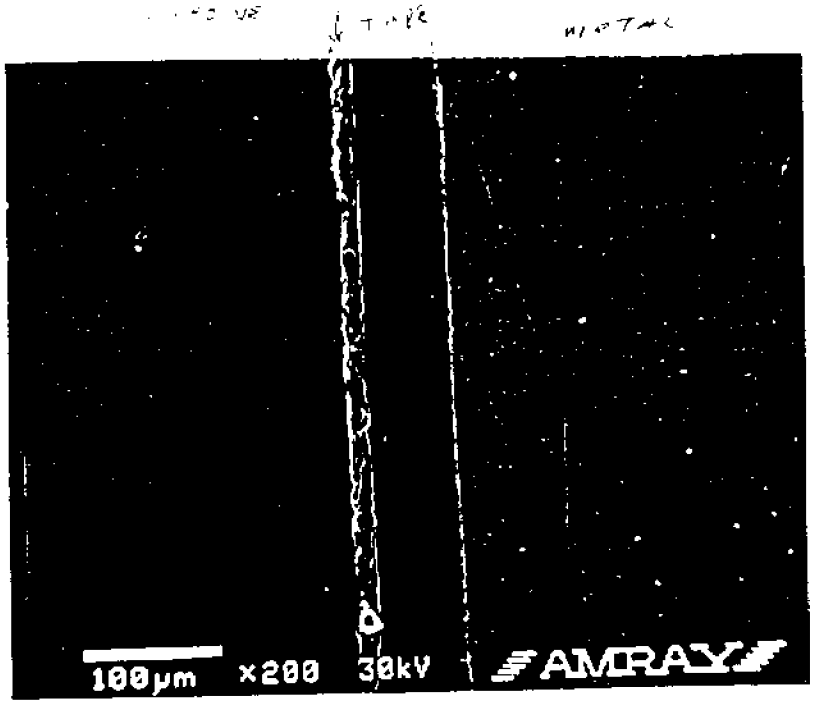

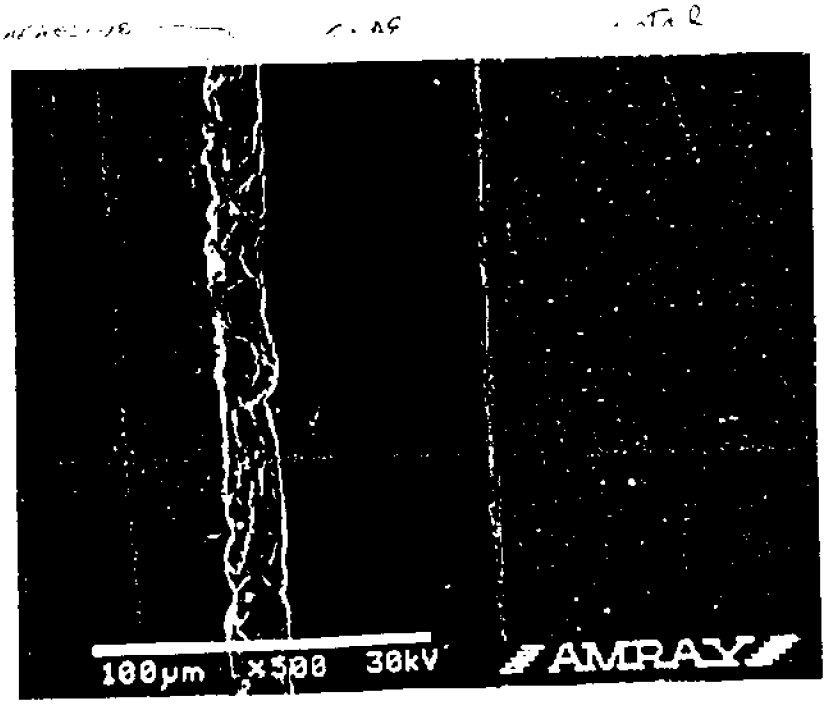

Figure 18.

Location	Gap Dimension (μm)
# 1	30 at mouth/0.2 to 0.3 inward
# 2	0.1 to 1.0
# 3	25 at mouth /0.1 to 0.3 inward
# 4	8 to 10
# 5	100 at mouth / 12 inward
# 6	12 to 16
# 7	10 to 12

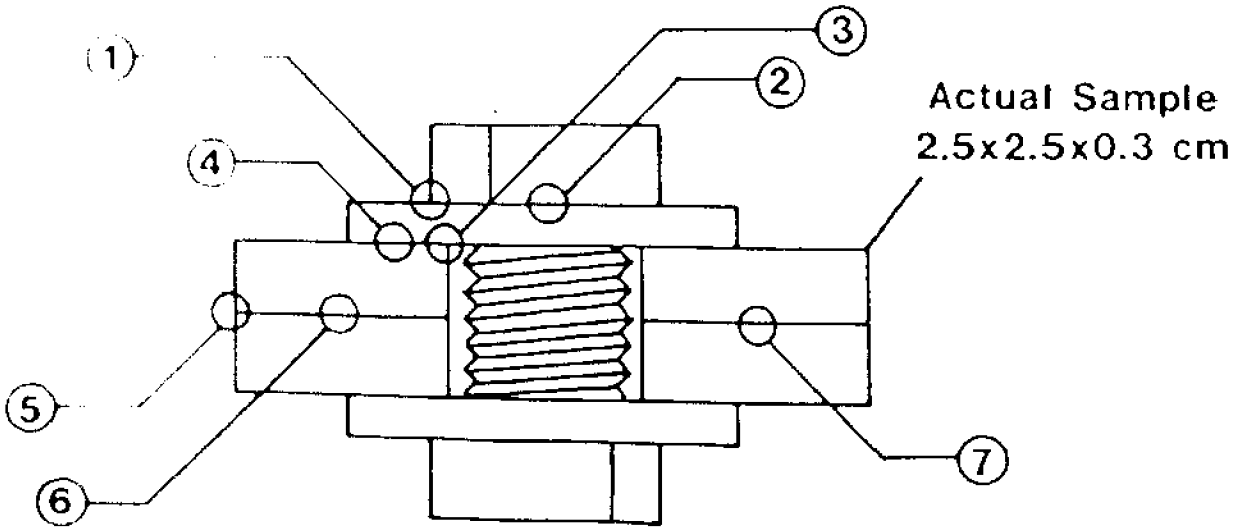

Figure 19.

Measured crevice gaps for bolted metal-to-metal assembly fastened to a torque of 8.5 Nm.

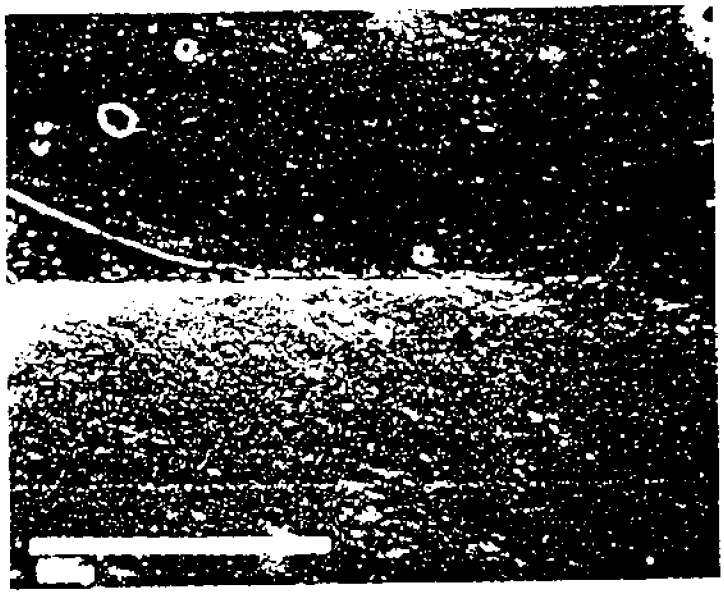

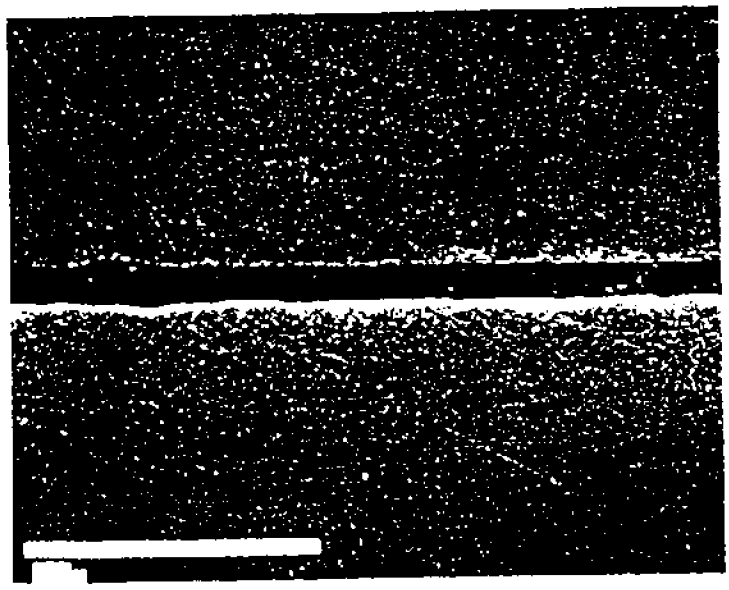

Figure 20.

Scanning electron micrographs showning variations in crevice gaps found in bolted stainless steel assembly. (Original Magnification 400X)

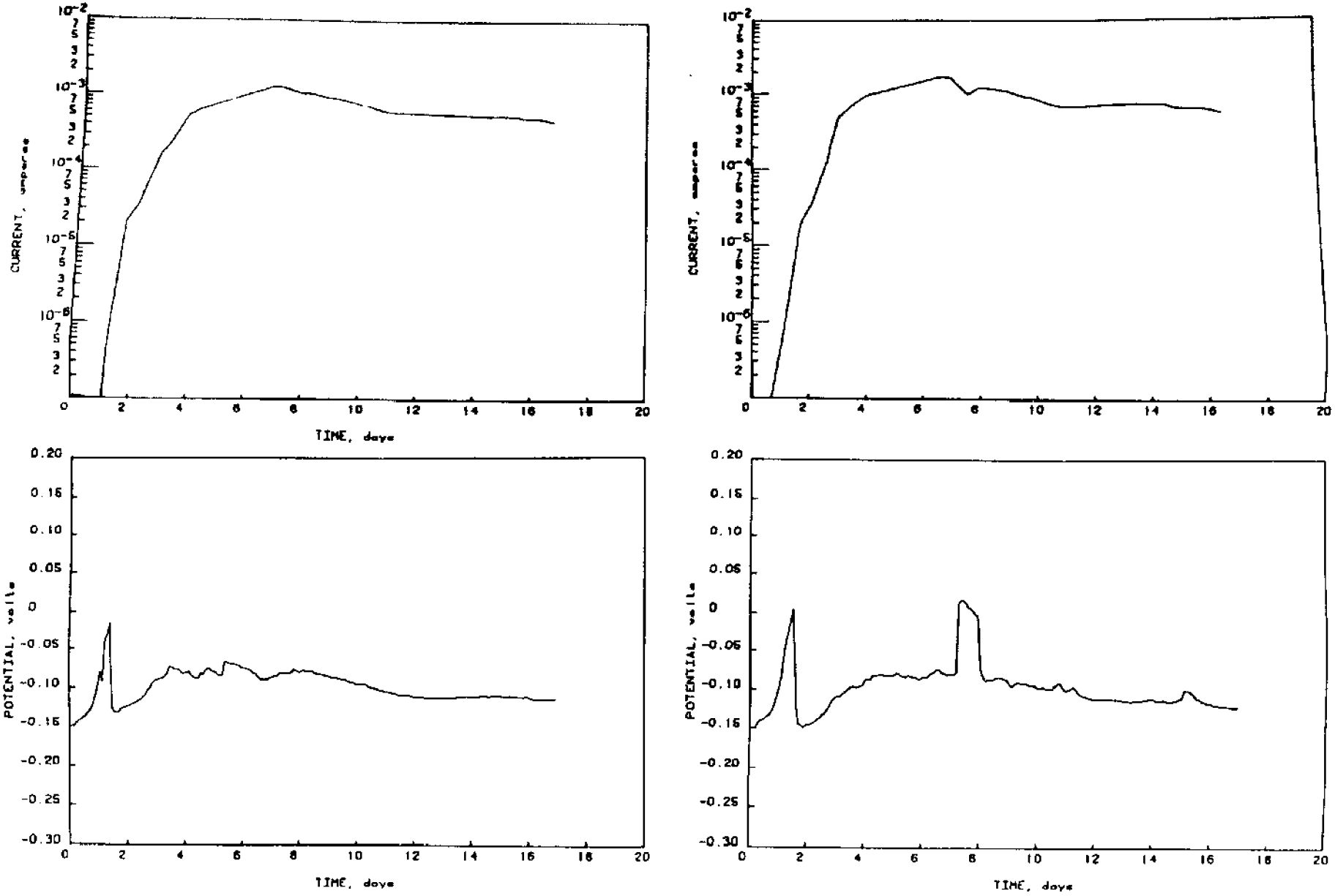

TYPE 316 (Natural Seawater)

Figure 21.

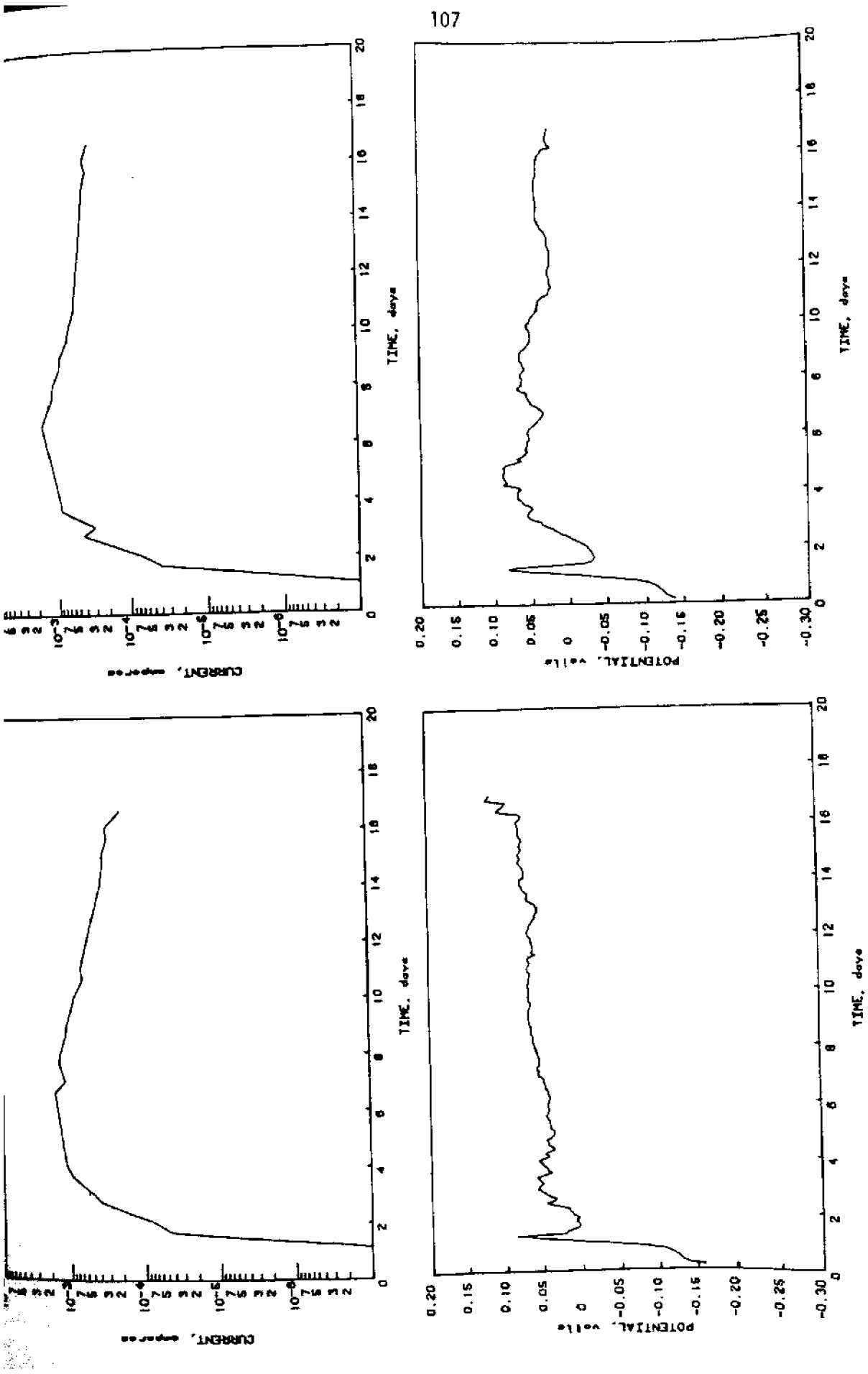

20-25-4.5-1.5 (Natural Seawater)

Figure 22.

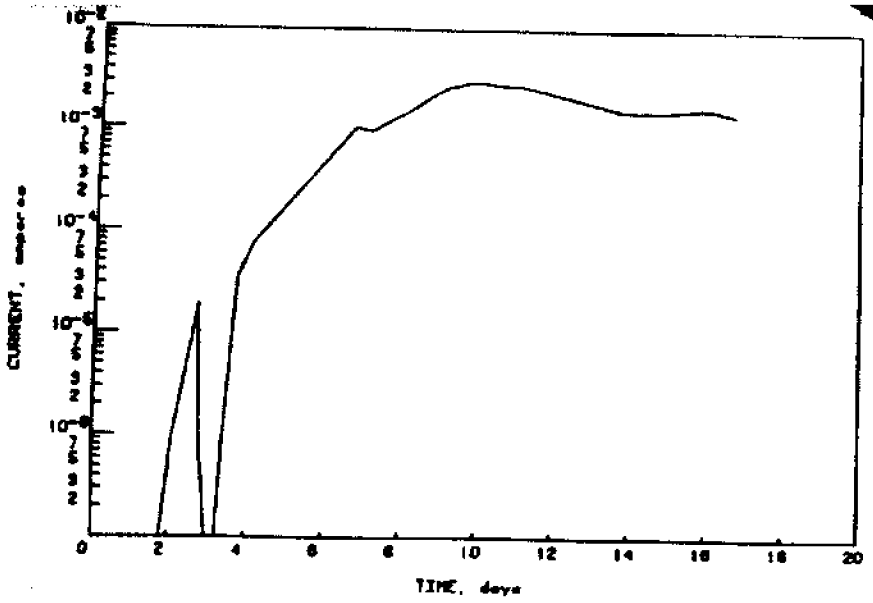

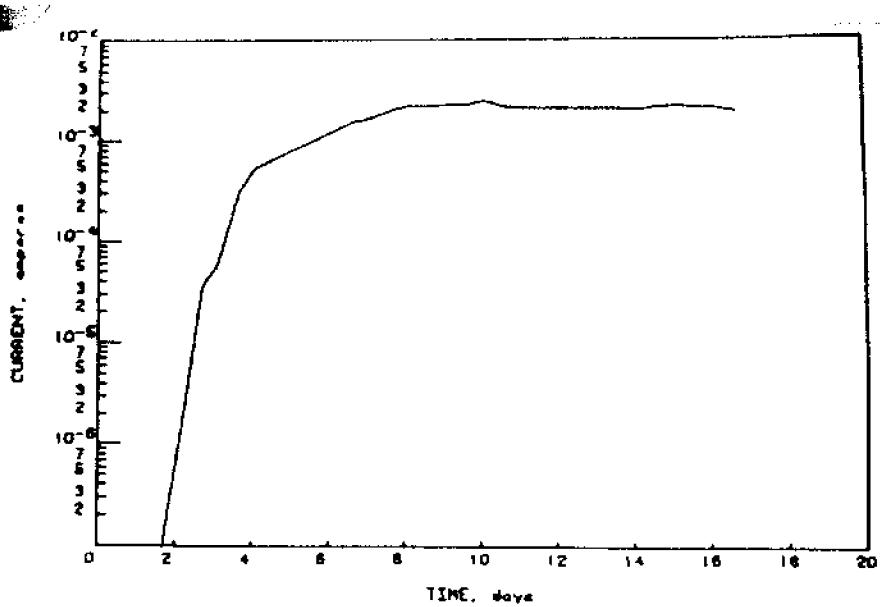

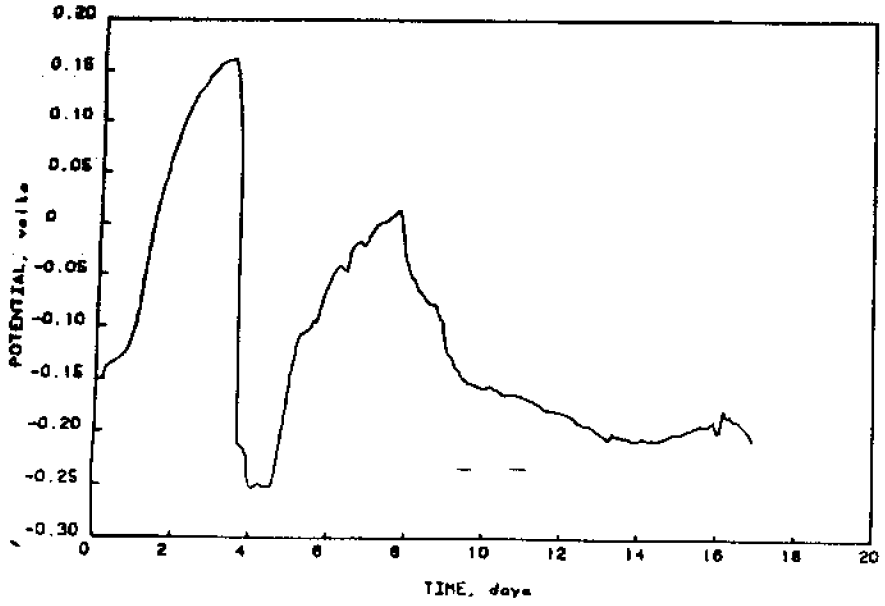

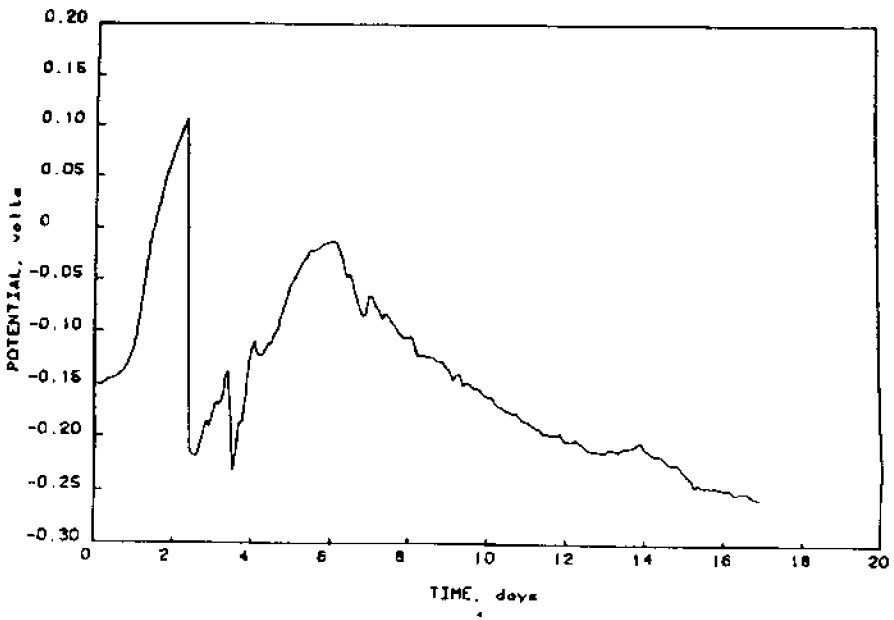

18Cr-2Mo (Natural Seawater)

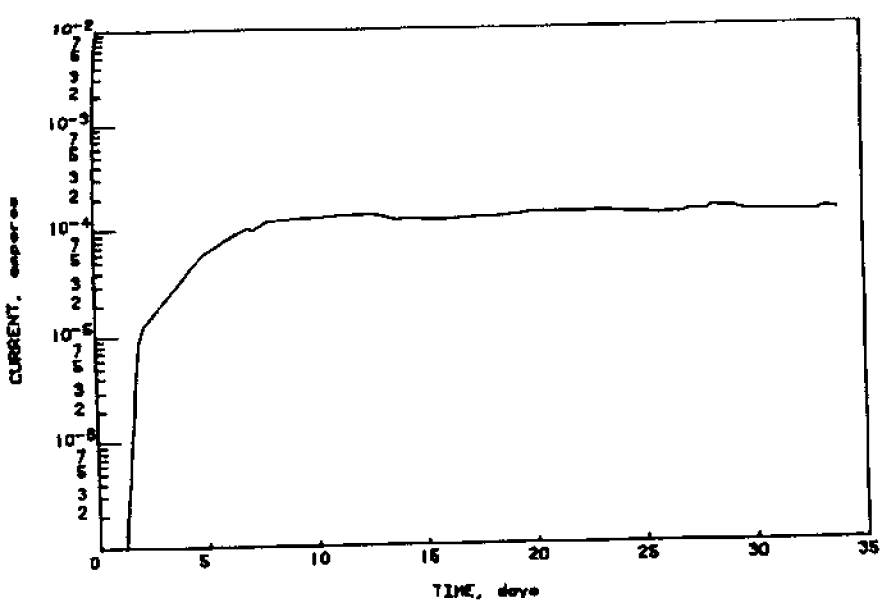

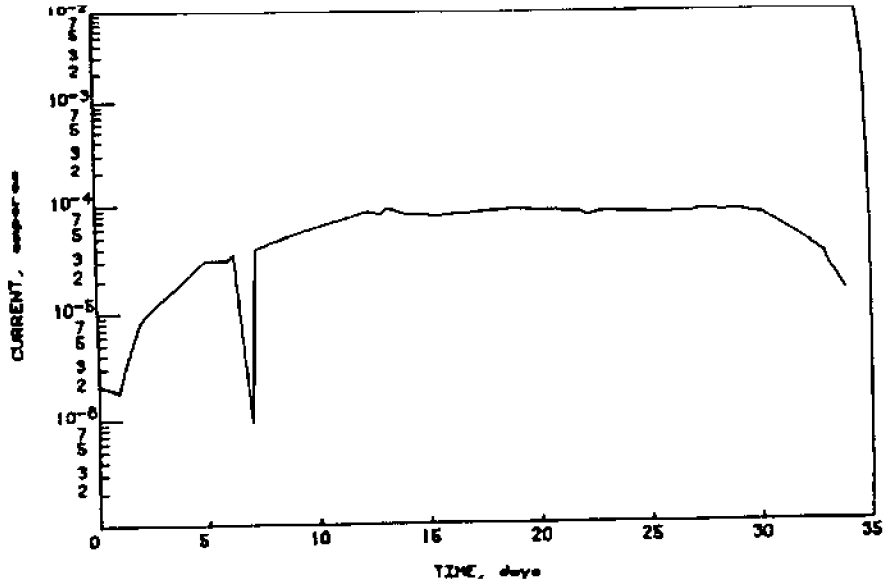

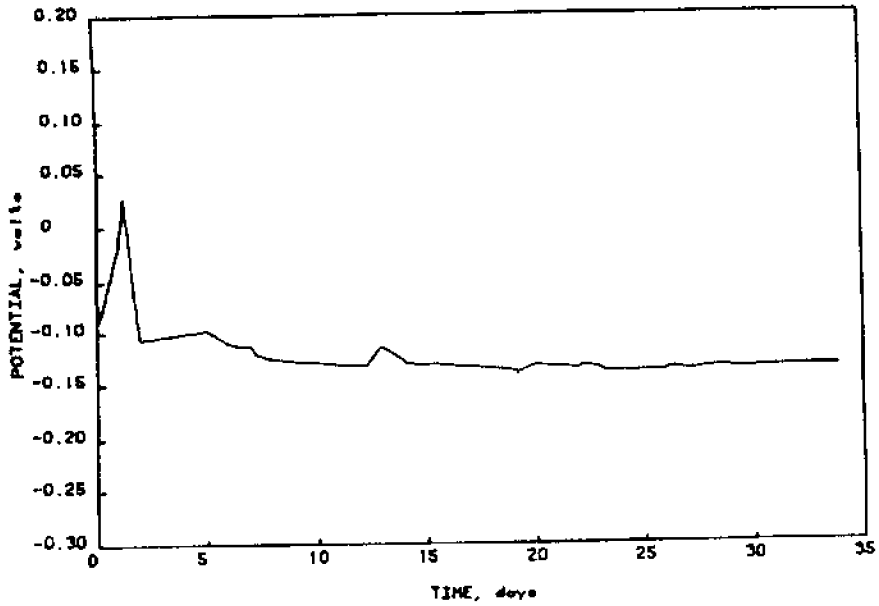

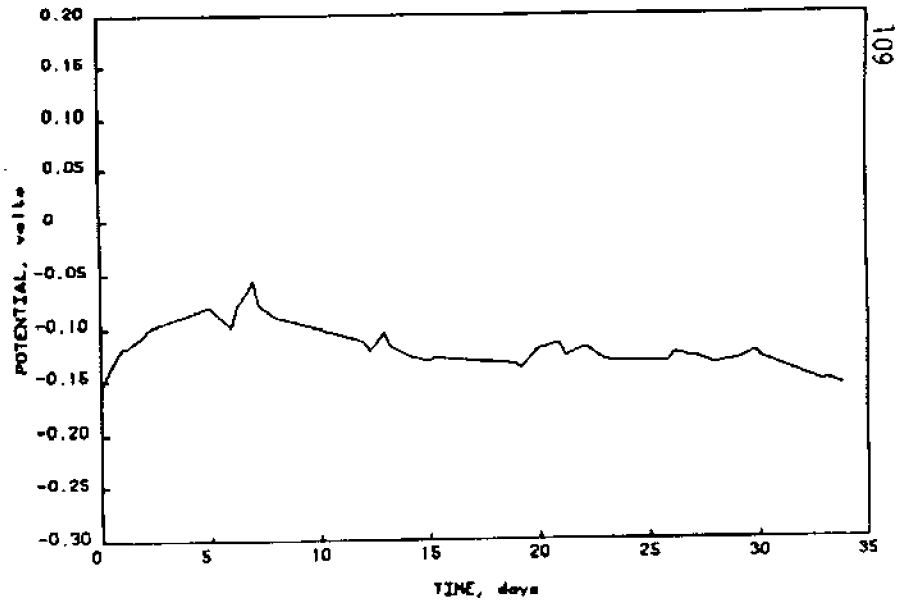

TYPE 316 (Synthetic Seawater)

Figure 24.

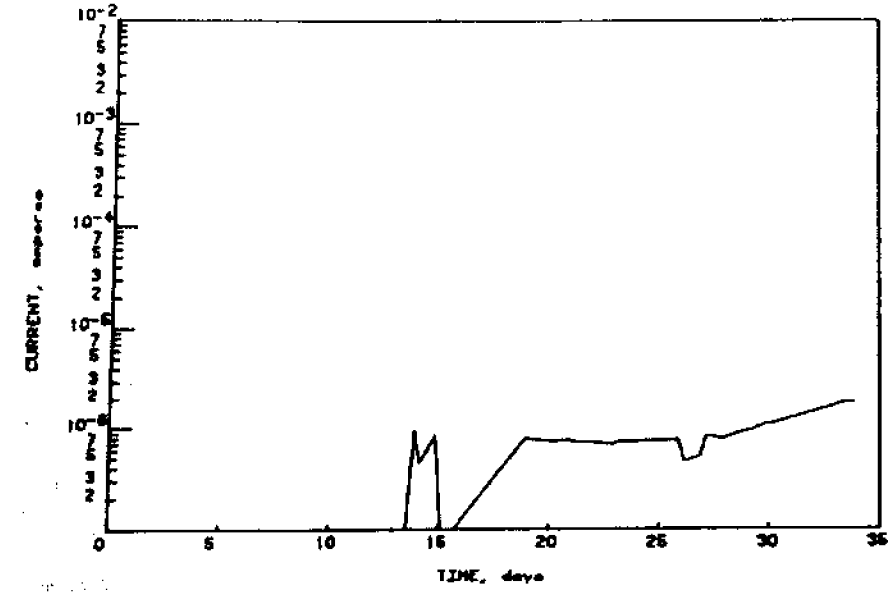

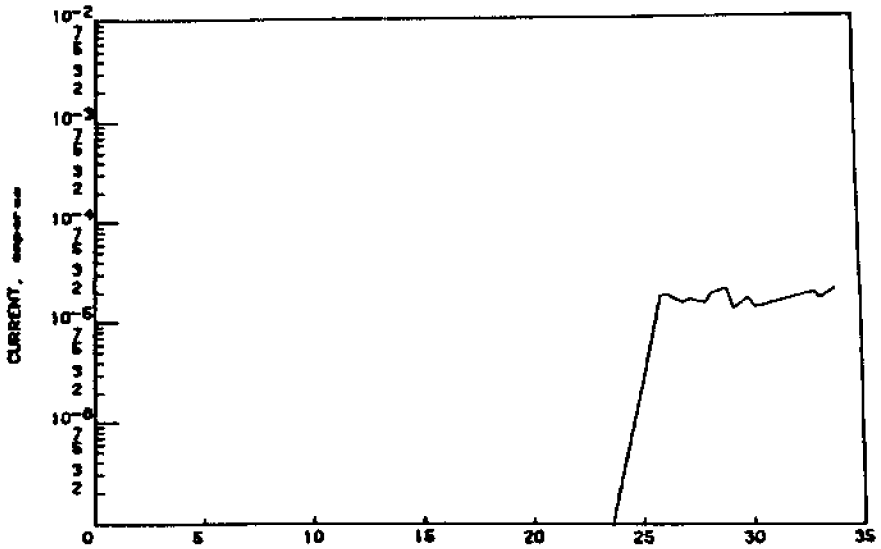

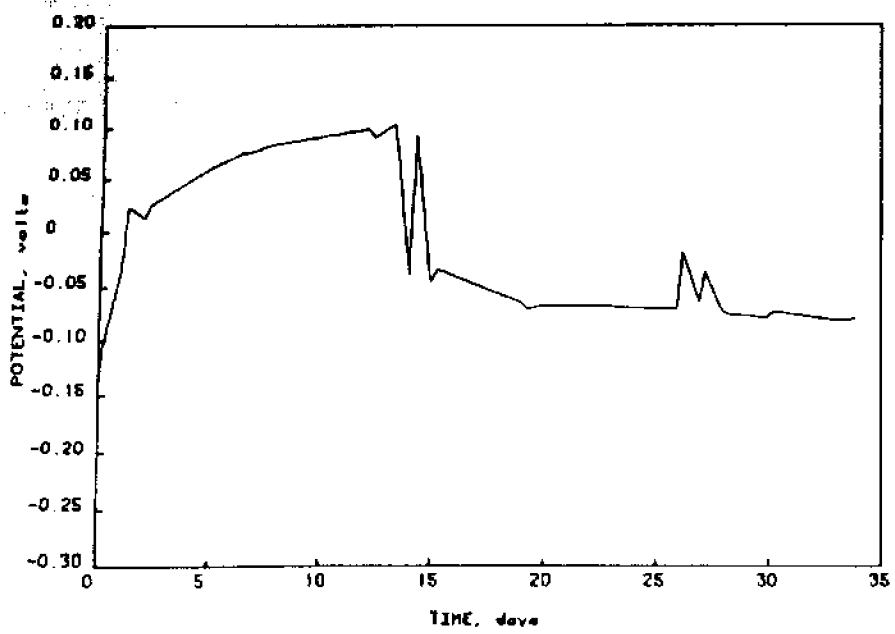

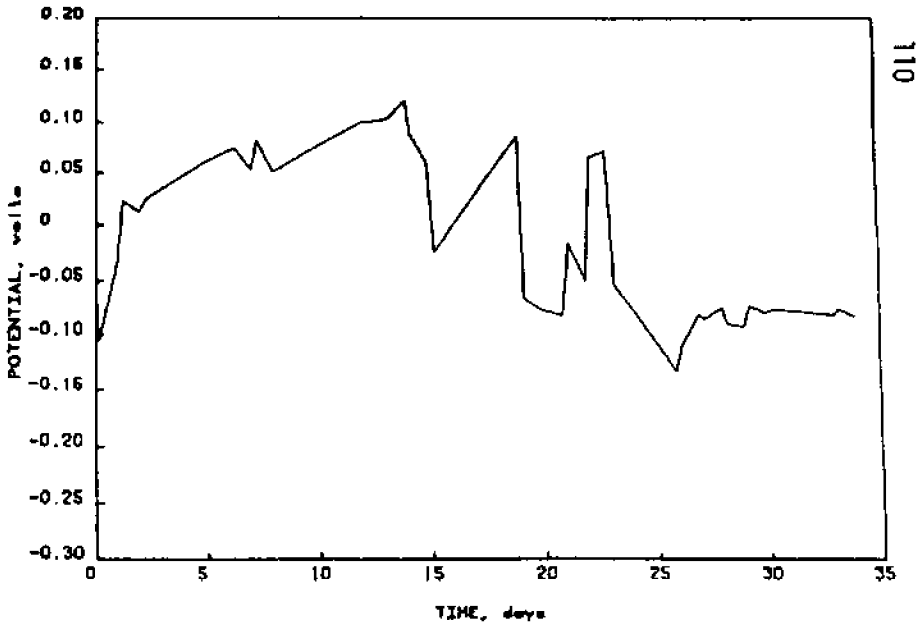

20-25-4.5-1.5 (Synthetic Seawater)

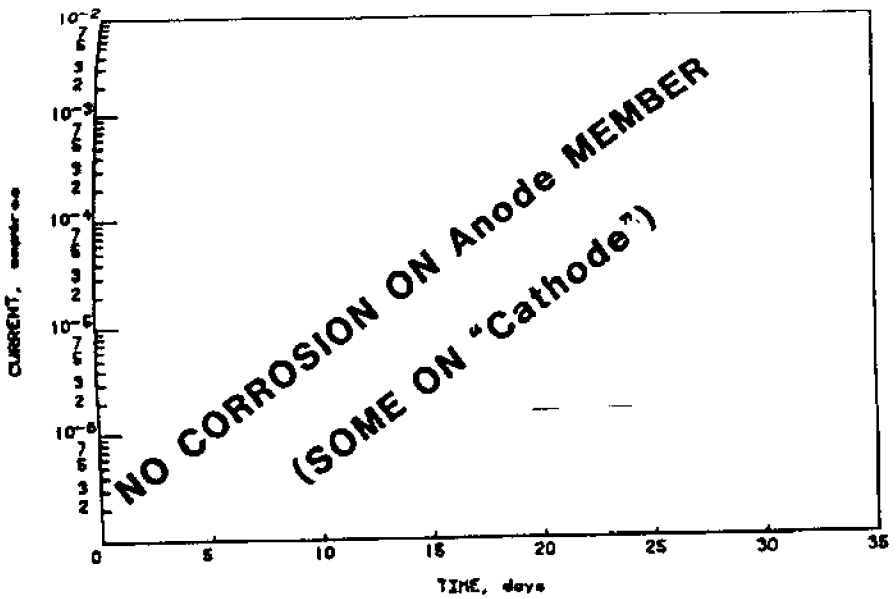

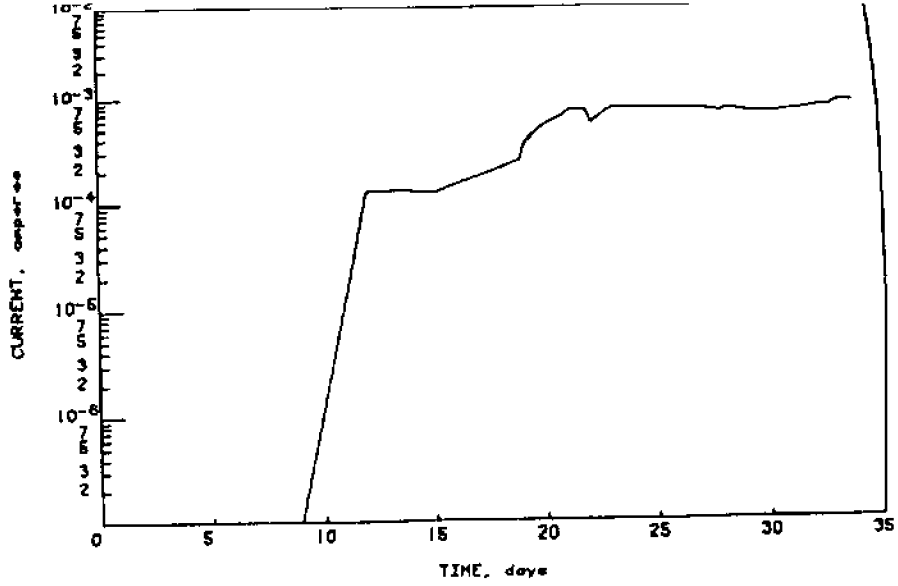

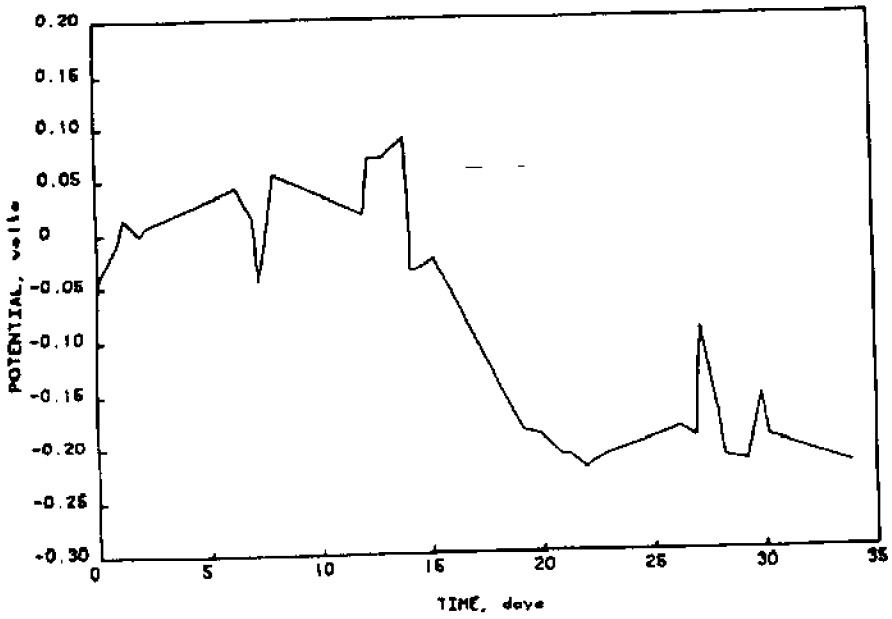

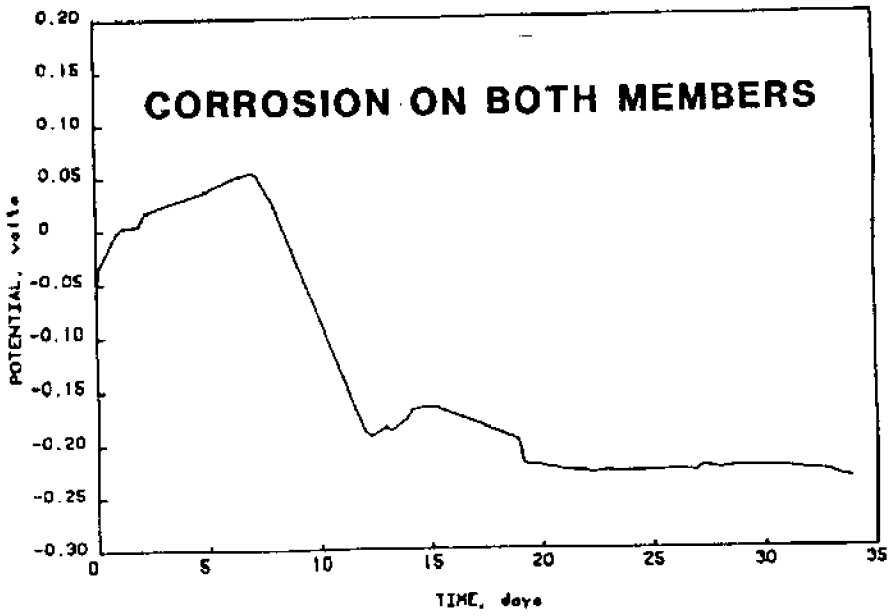

111

18Cr-2Mo (Synthetic Seawater)

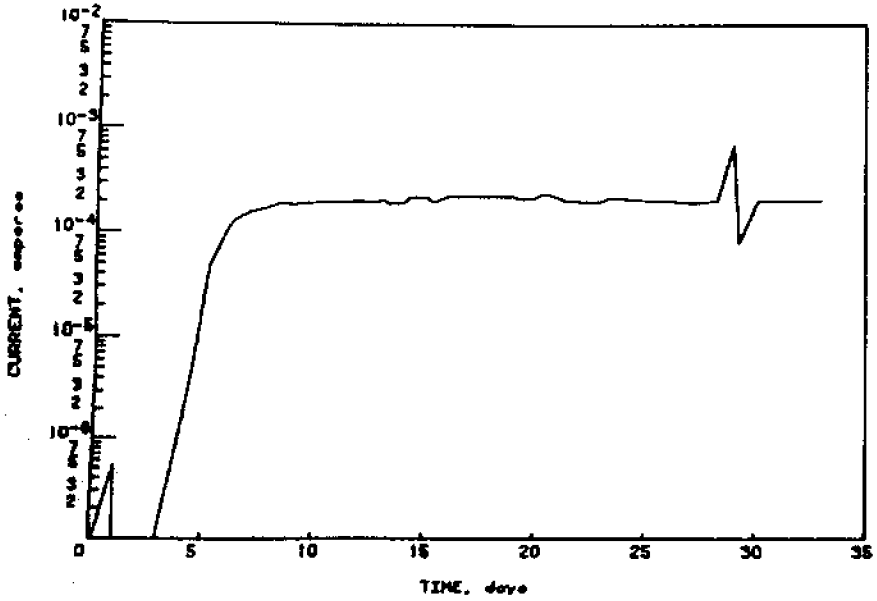

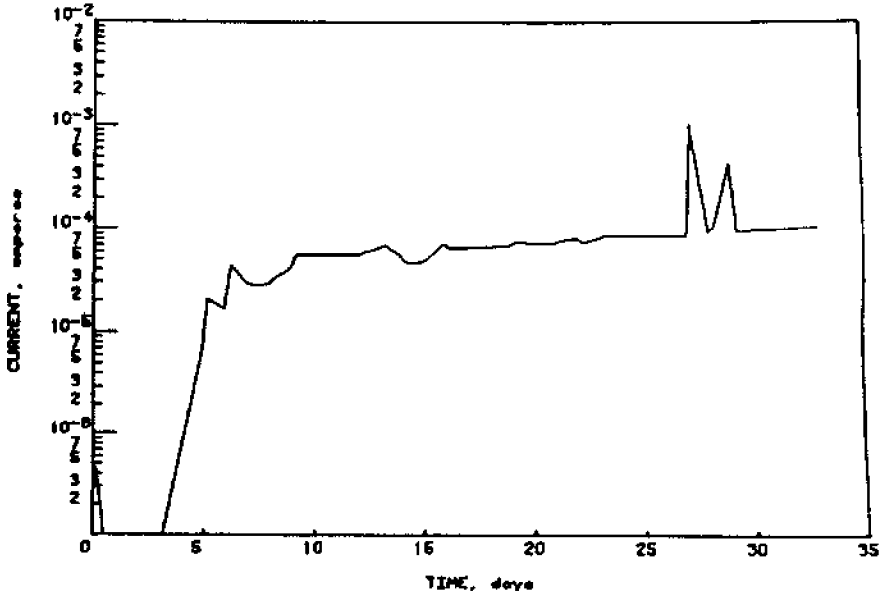

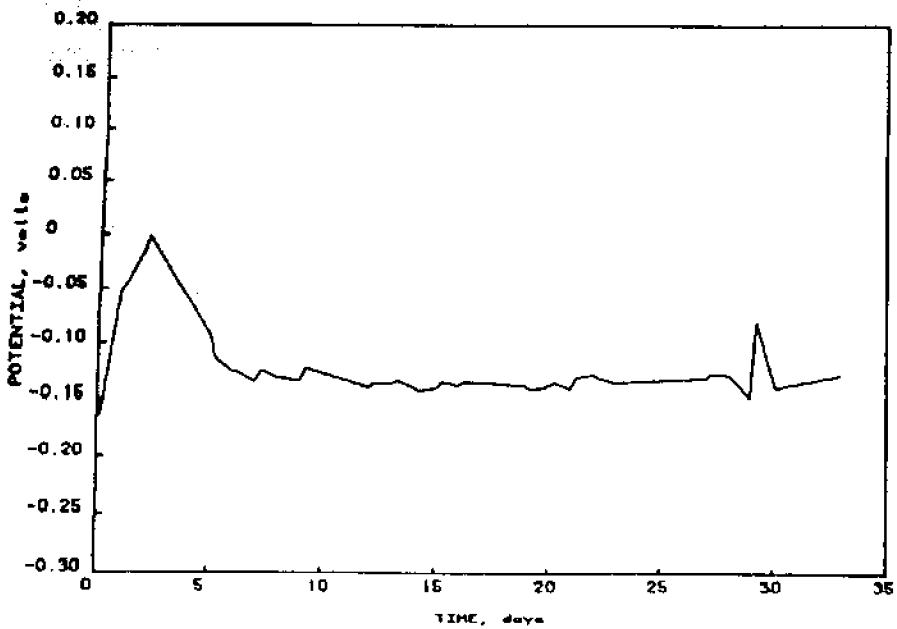

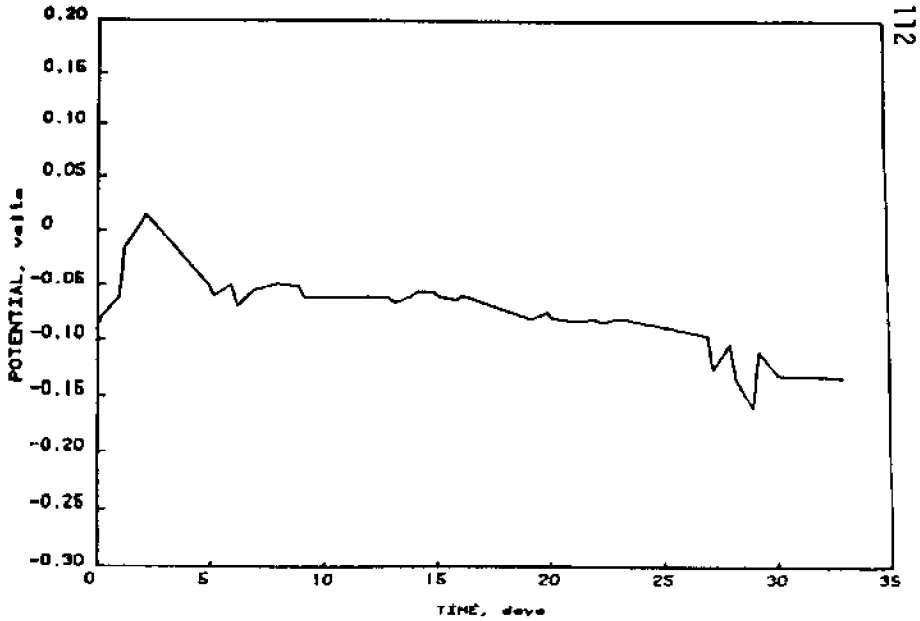

TYPE 316 (3.5% NaCl)

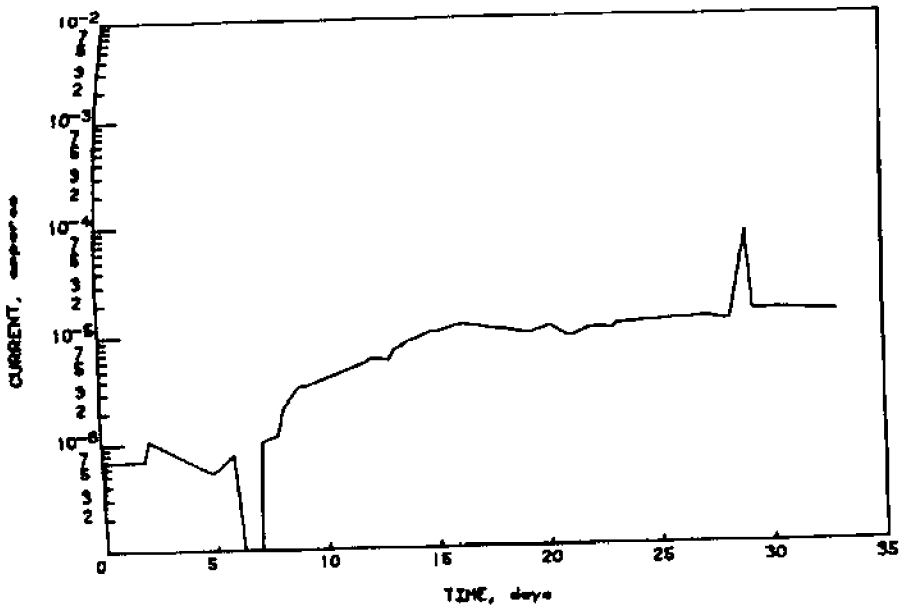

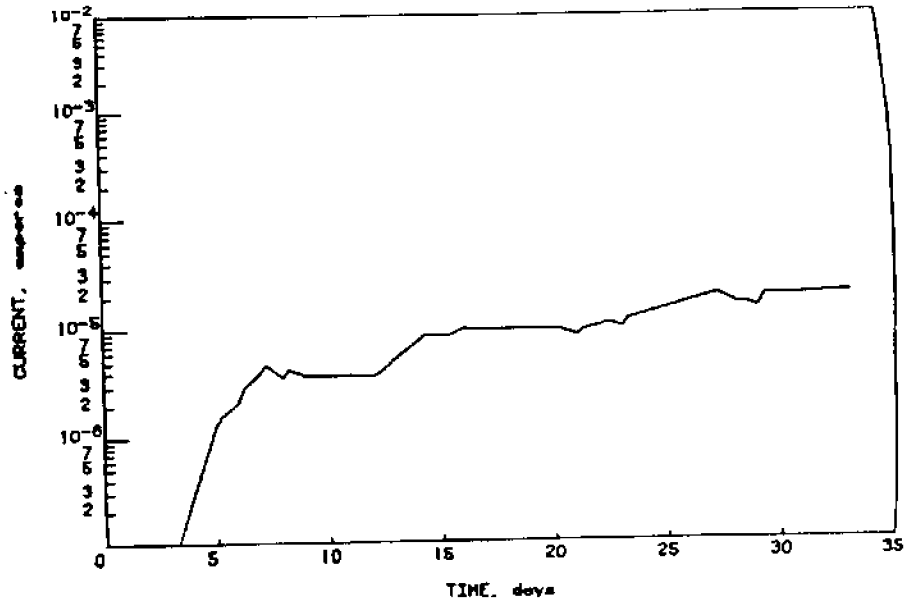

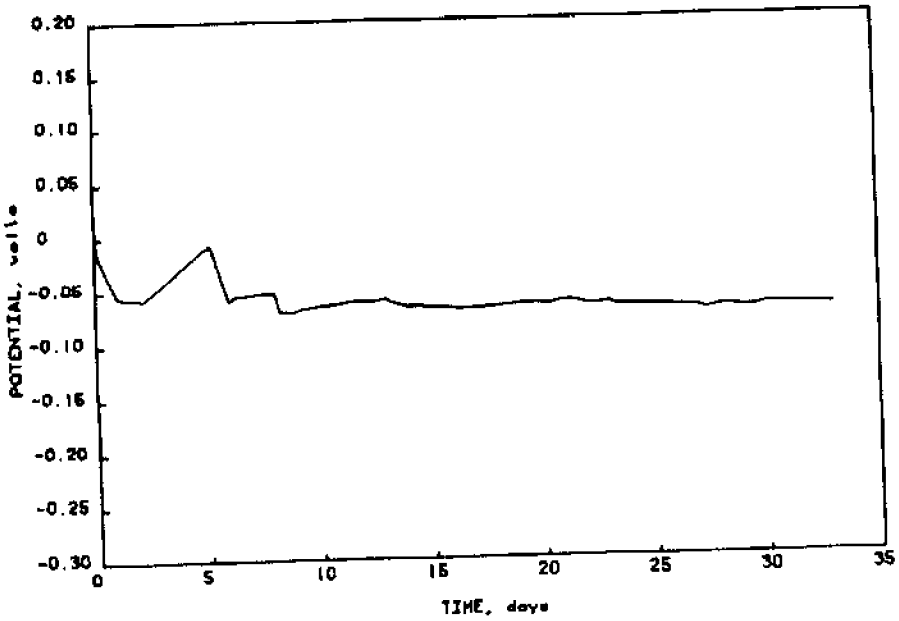

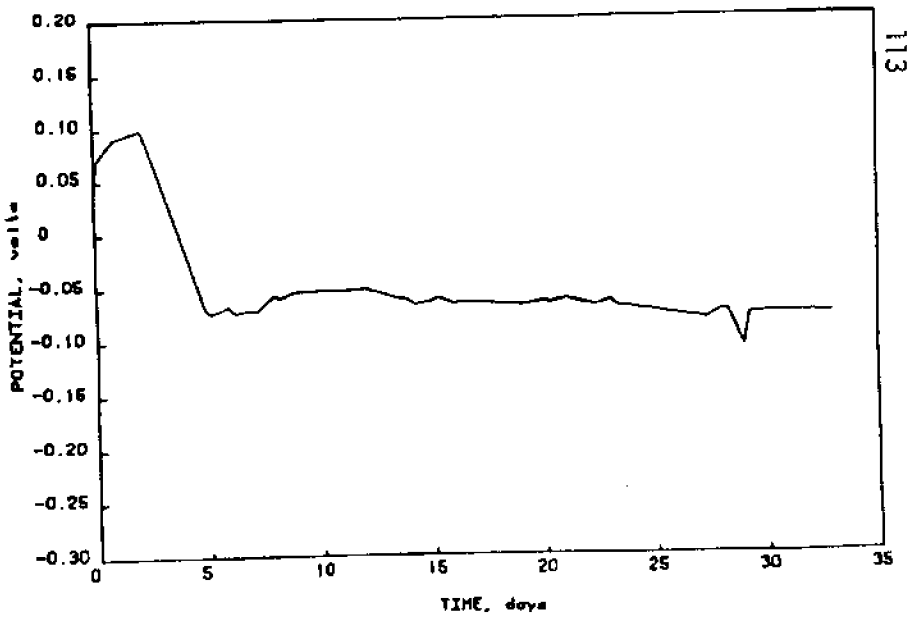

20-25-4.5-1.5 (3.5% NaCl)

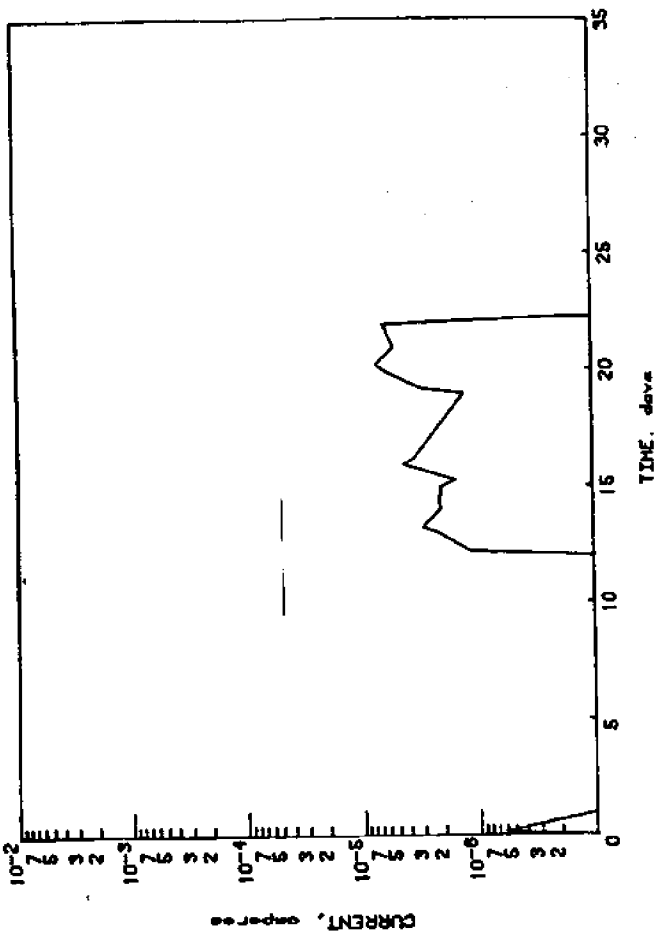

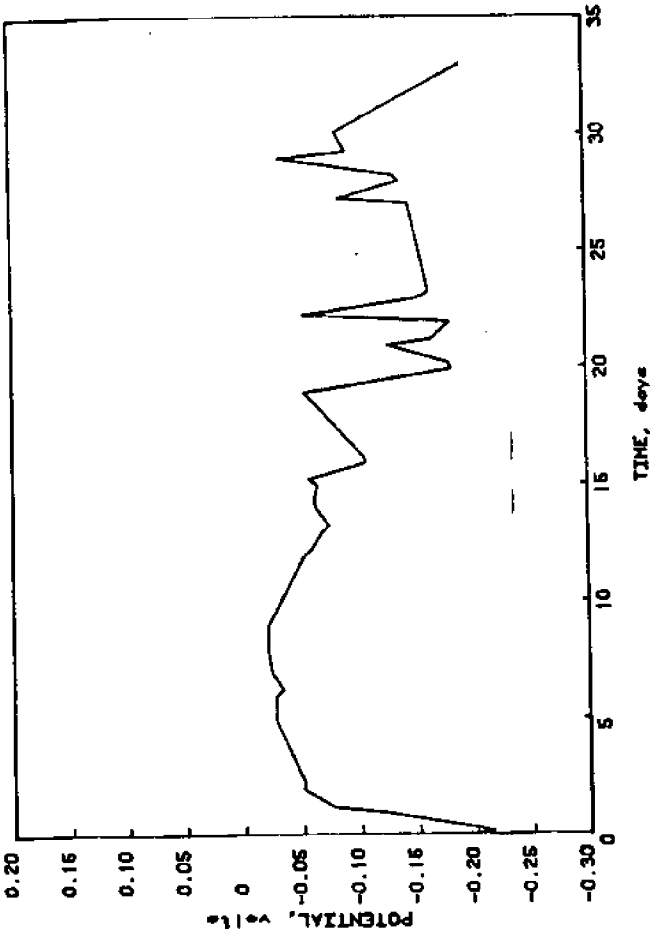

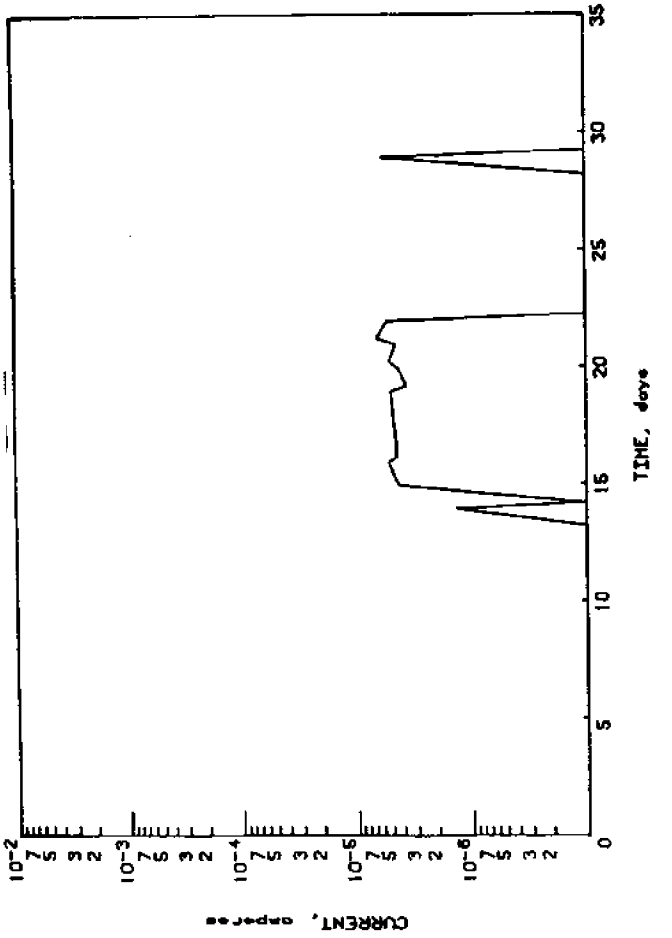

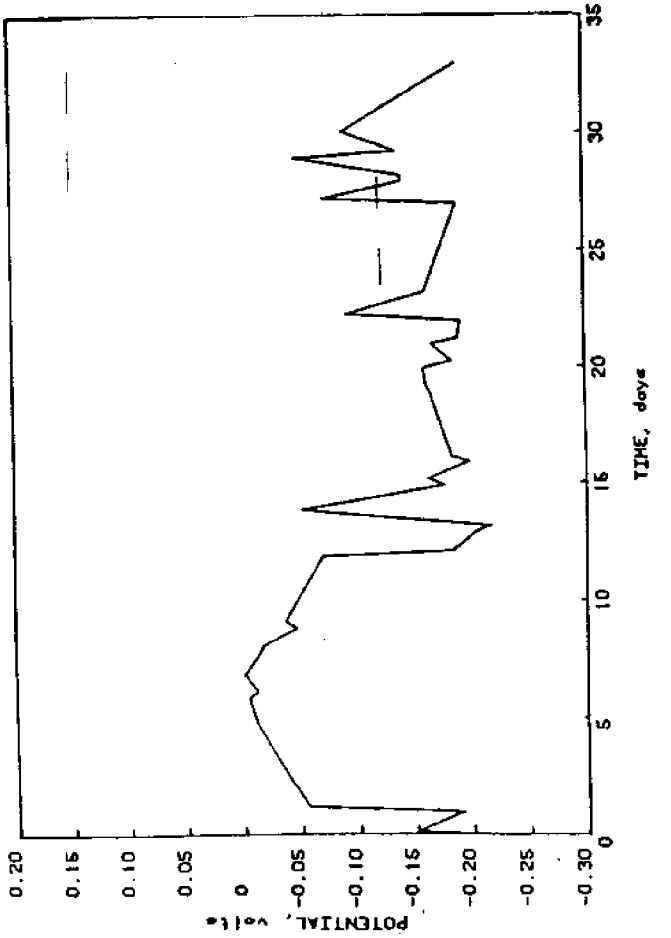

18Cr-2Mo (3.5% NaCl)

Figure 29.

TABLE 1

General Resistance to Crevice Corrosion Propagation for Several Alloys in Natural and Synthetic Environments

Environment	Stainless Alloy	Crevice Corrosion Propagation Total Charge (coulombs) 400 Hour Test	800 Hour Test
Natural Seawater	alloy 904L	1020	--
	alloy 904L	1018	--
	Type 316	927	--
	Type 316	1218	--
	18Cr-2Mo	1854	--
	18Cr-2Mo	2193	--
Synthetic Seawater	alloy 904L	0.1	2
	alloy 904L	0.1	17
	Type 316	120	324
	Type 316	64	176
	18Cr-2Mo*	6	1033
3.5% NaCl	alloy 904L	1.2	3
	alloy 904L	1.5	7
	Type 316	5.4	27
	Type 316	5.1	27
	18Cr-2Mo	196	510
	18Cr-2Mo	47	214

* Corrosion on duplicate specimen occurred on cathode stem, crevice OK after 800 hours.

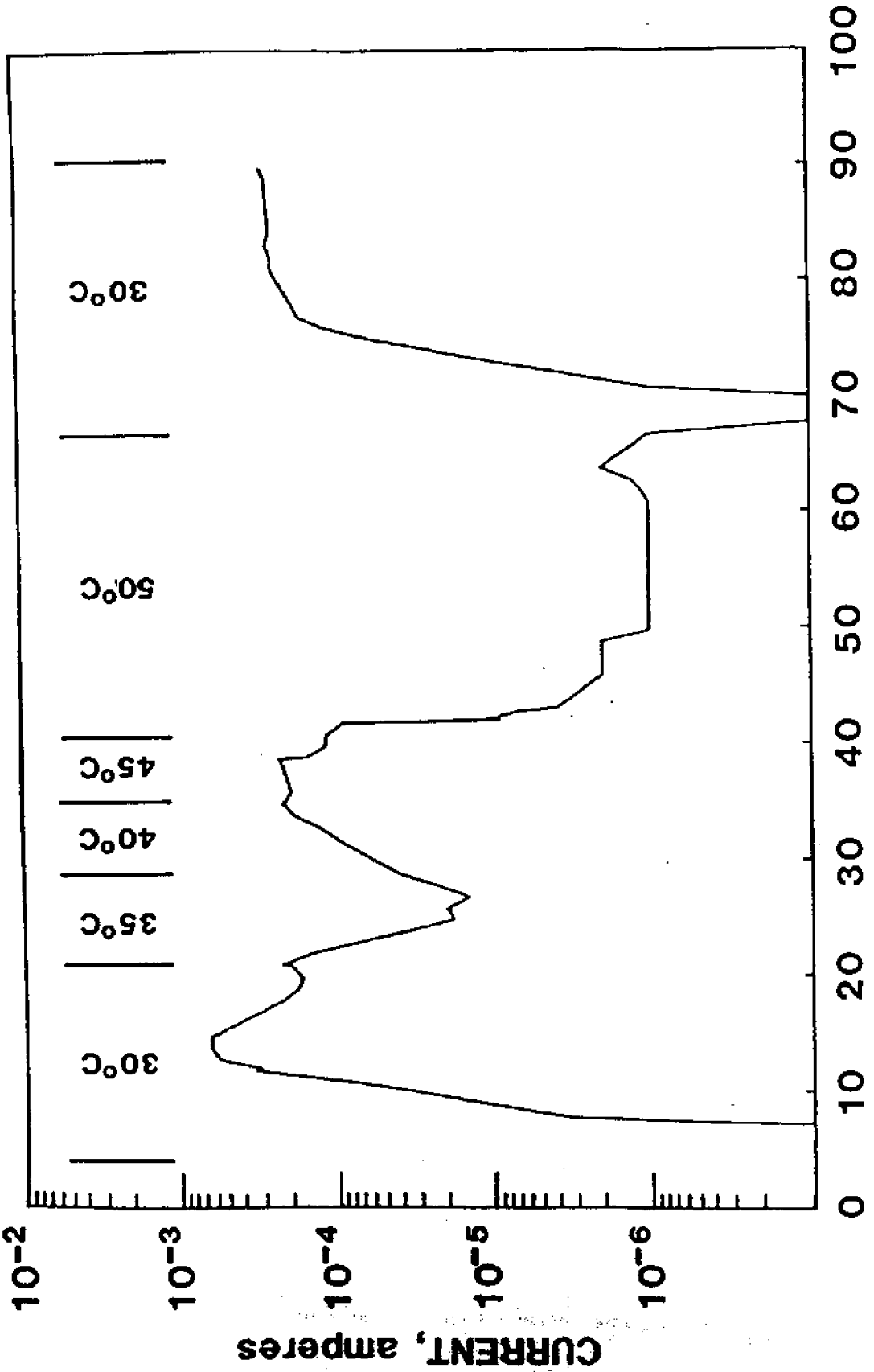

Figure 30. Monitoring crevice corrosion currents for remote crevice assembly exposed initially at 30°C. The temperature increased in 5°C increments and subsequently cooled.

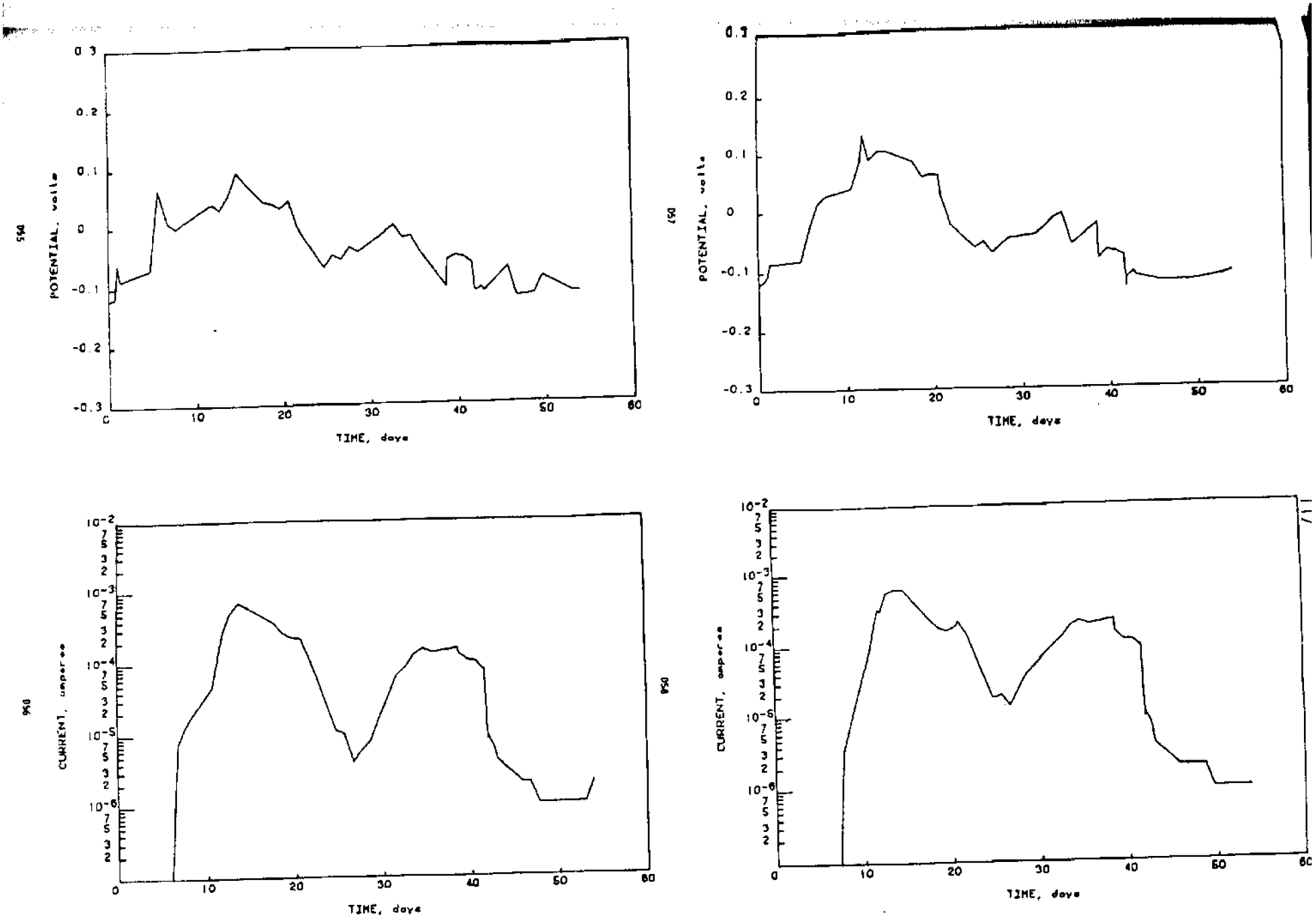

Figure 31. Monitoring potentials and crevice corrosion currents for remote crevice assembly exposed initially at 30°C. Temperature increased in 5°C increments.

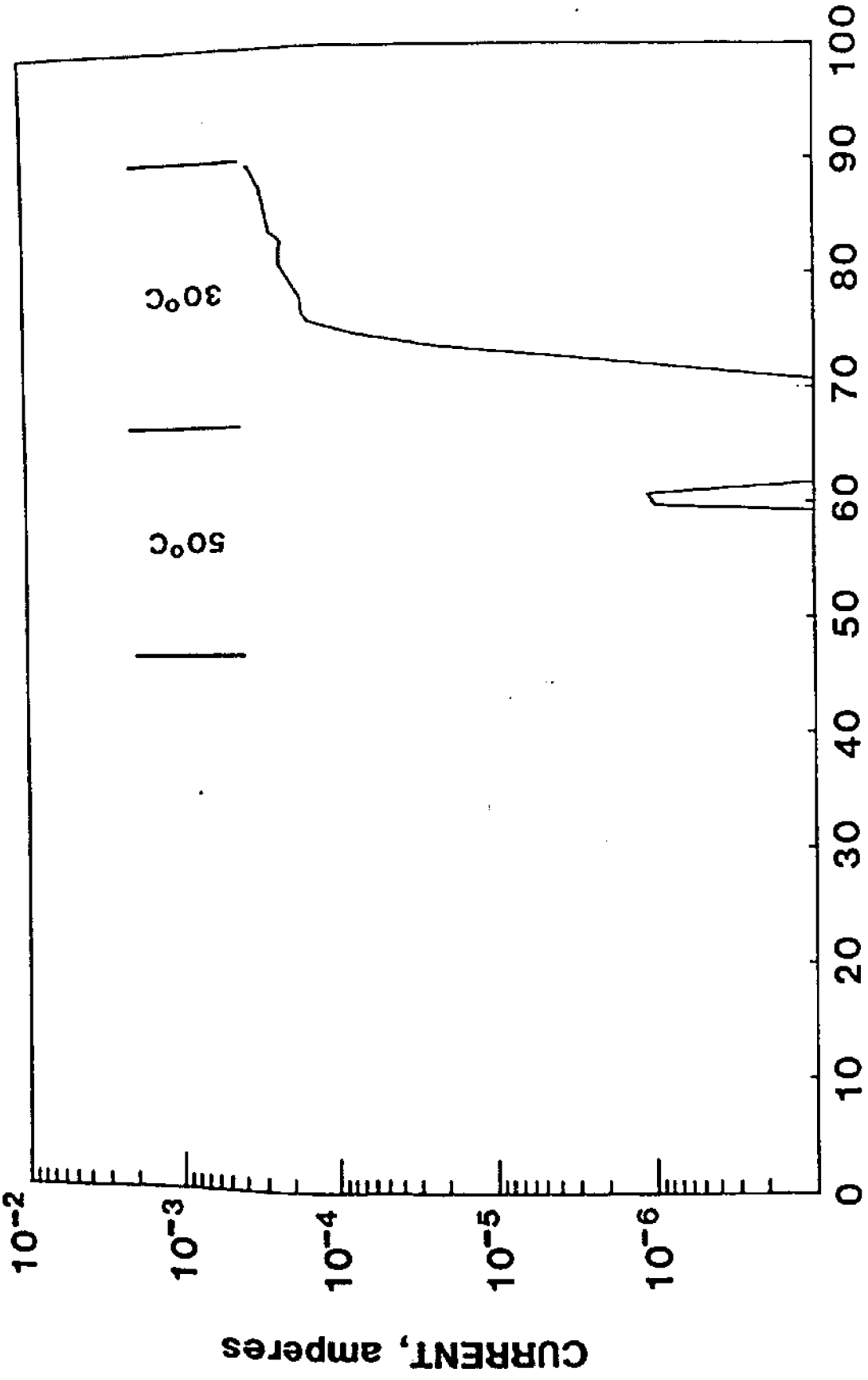

Figure 32. Crevice corrosion currents for assembly initially exposed at 50°C and subsequently

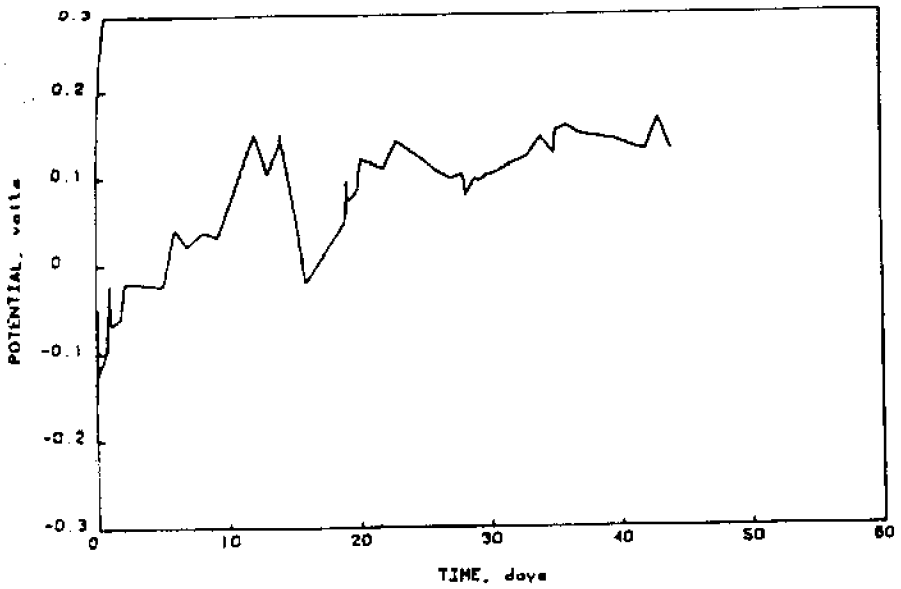

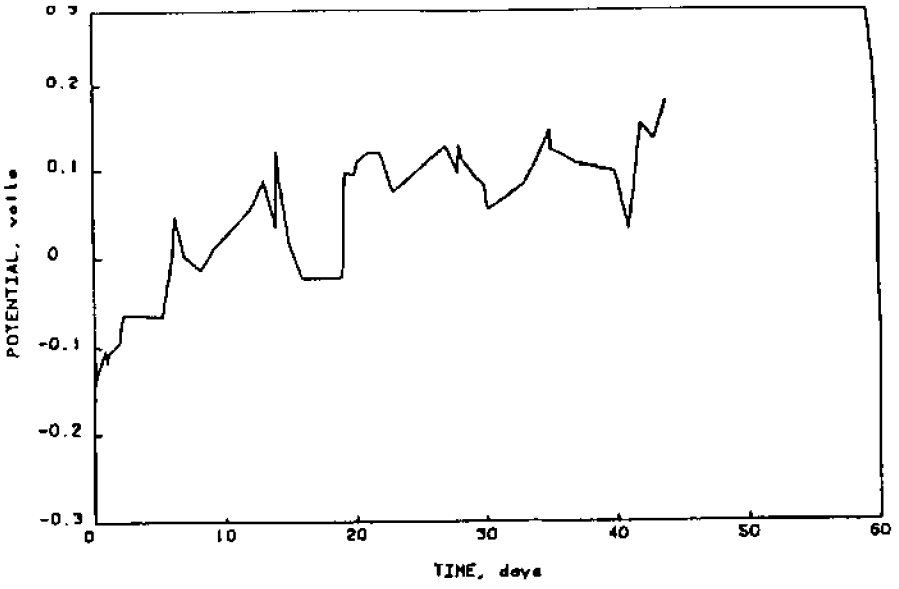

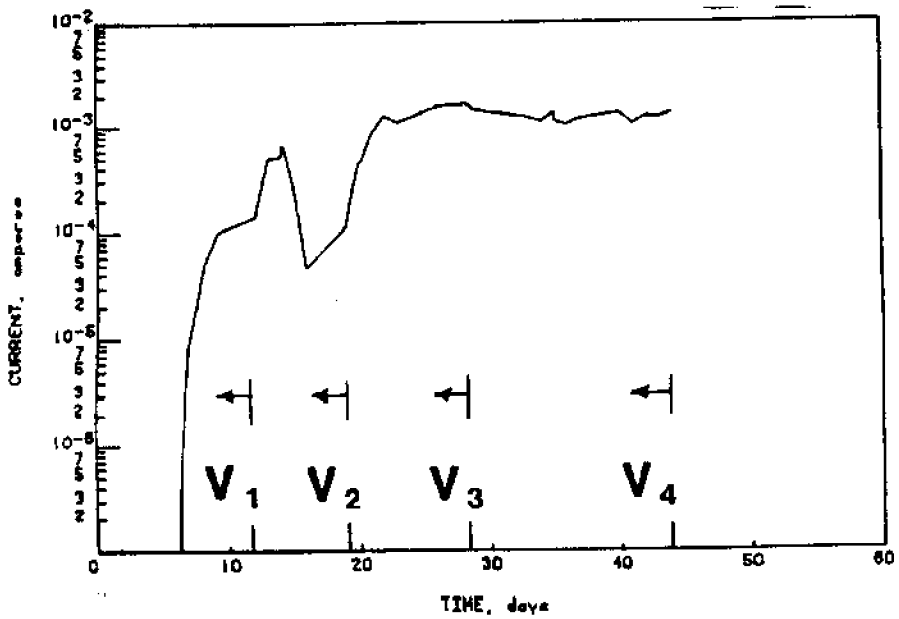

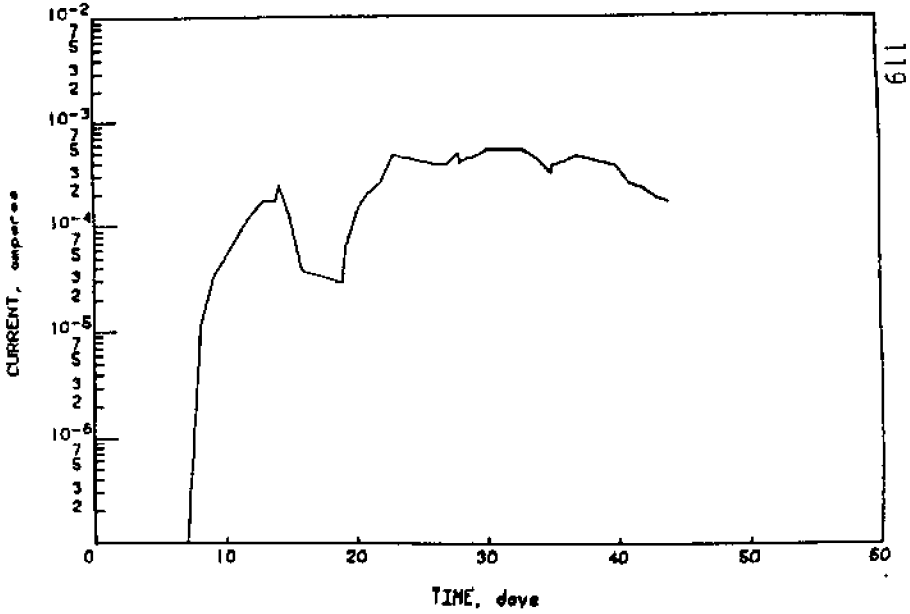

alloy 904L: Filtered Seawater at 30°C

Figure 33.

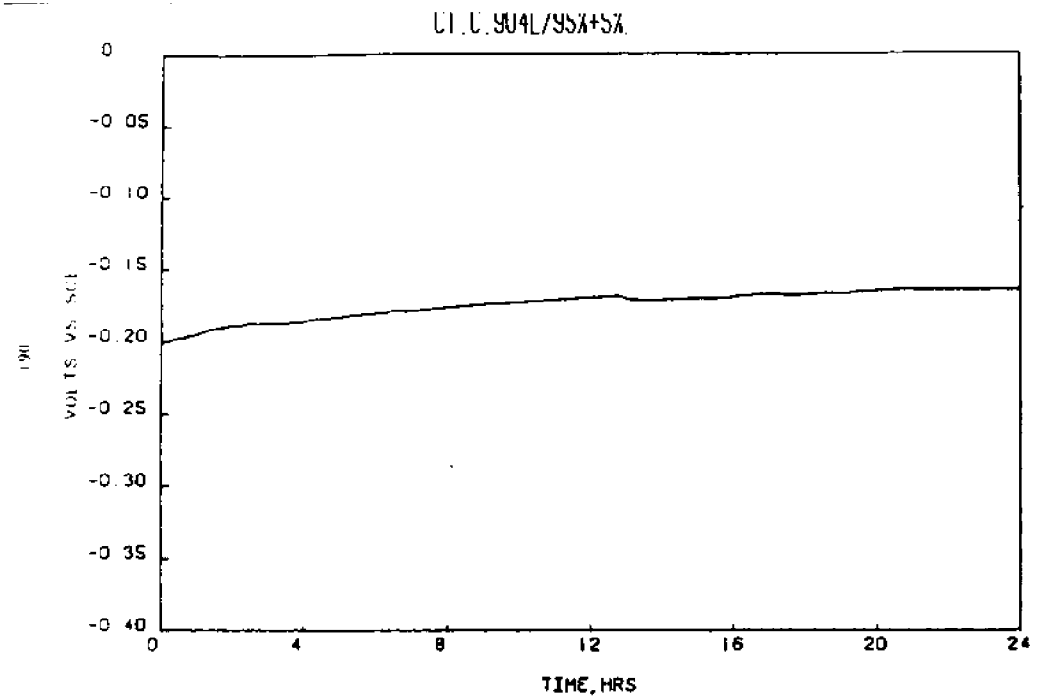
CT.C.904L/95%+5%
VOLTS VS SCE
TIME, HRS

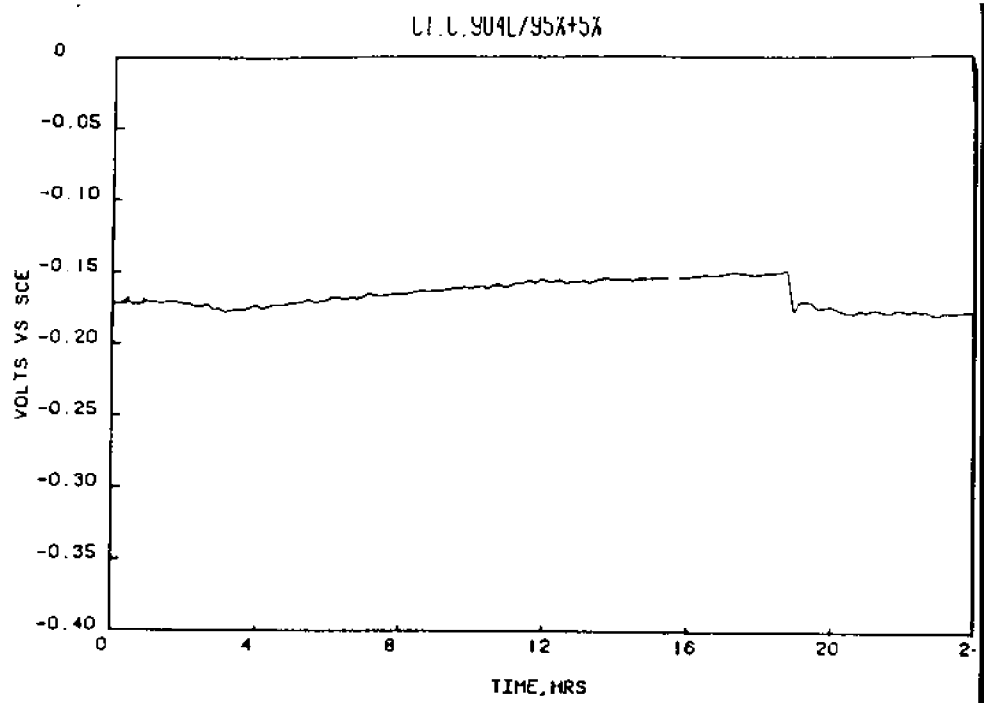
CT.C.904L/95%+5%
VOLTS VS SCE
TIME, HRS

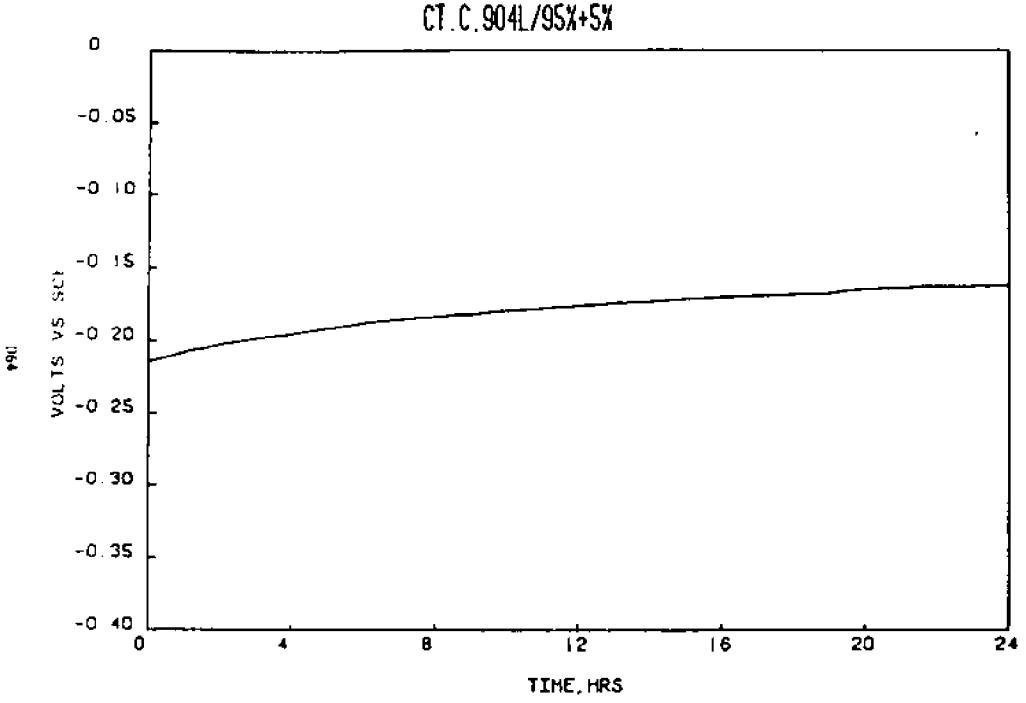
CT.C.904L/95%+5%
VOLTS VS SCE
TIME, HRS

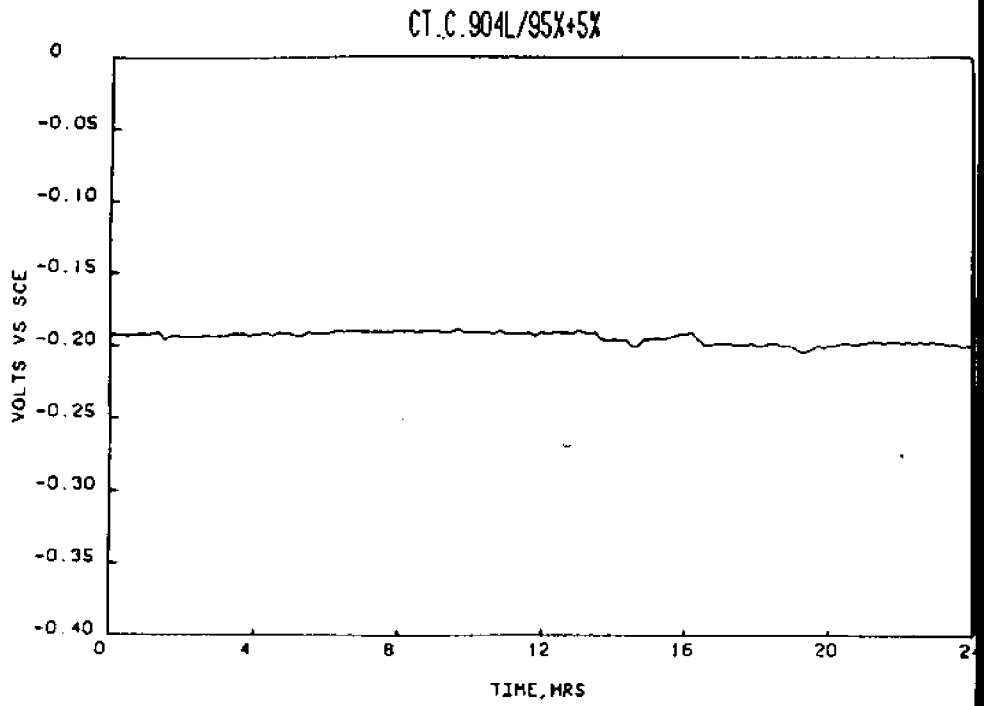
CT.C.904L/95%+5%
VOLTS VS SCE
TIME, HRS

Figure 34.

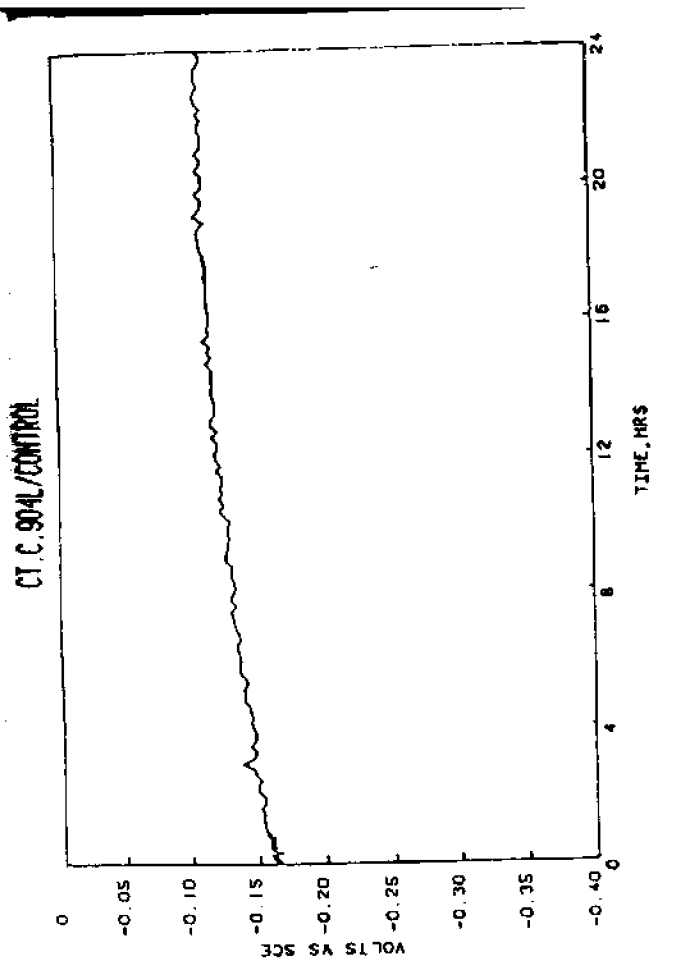
CT.C.904L/CONTROL
VOLTS VS SCE
TIME,HRS
0
-0.05
-0.10
-0.15
-0.20
-0.25
-0.30
-0.35
-0.40
4
8
12
16
20
24

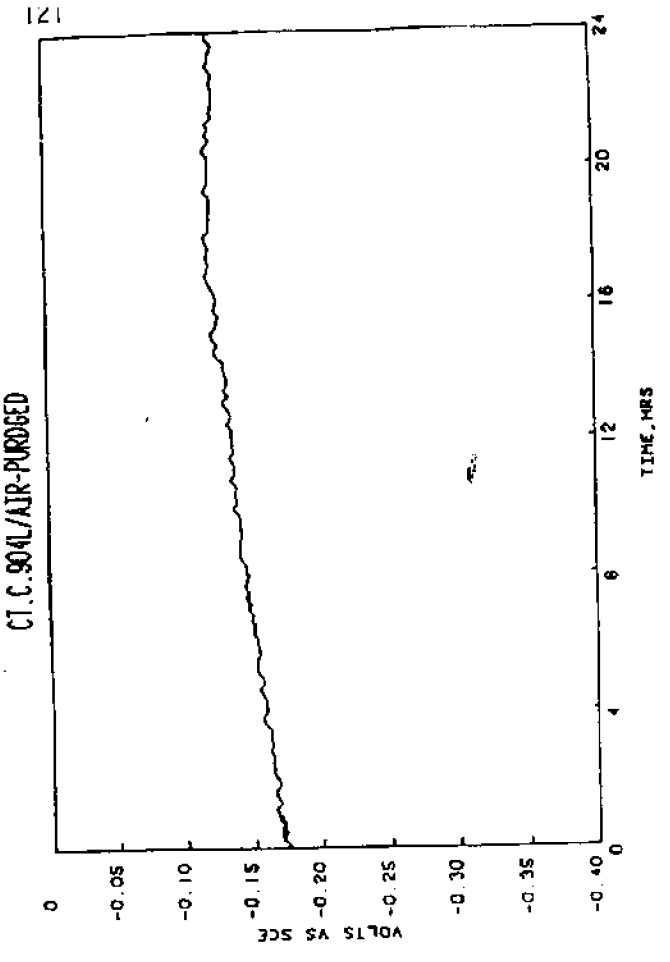
CT.C.904L/AIR-PURGED
VOLTS VS SCE
TIME,HRS
0
-0.05
-0.10
-0.15
-0.20
-0.25
-0.30
-0.35
-0.40
4
8
12
16
20
24

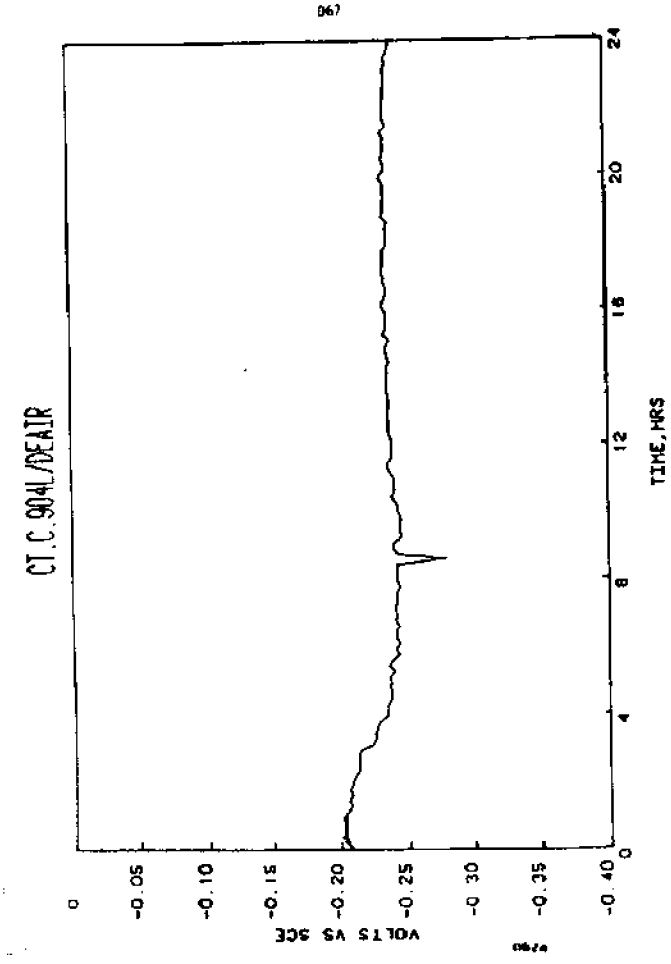
CT.C.904L/DEAIR
VOLTS VS SCE
TIME,HRS
0
-0.05
-0.10
-0.15
-0.20
-0.25
-0.30
-0.35
-0.40
4
8
12
16
20
24

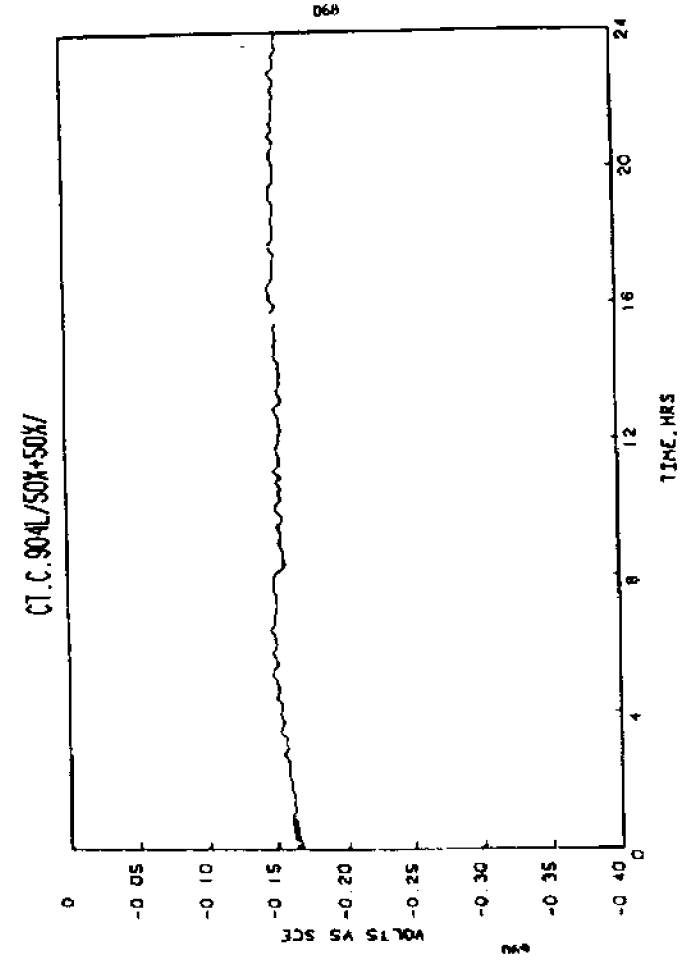
CT.C.904L/SOX+SOX/
VOLTS VS SCE
TIME,HRS
0
-0.05
-0.10
-0.15
-0.20
-0.25
-0.30
-0.35
-0.40
4
8
12
16
20
24

Figure 35.

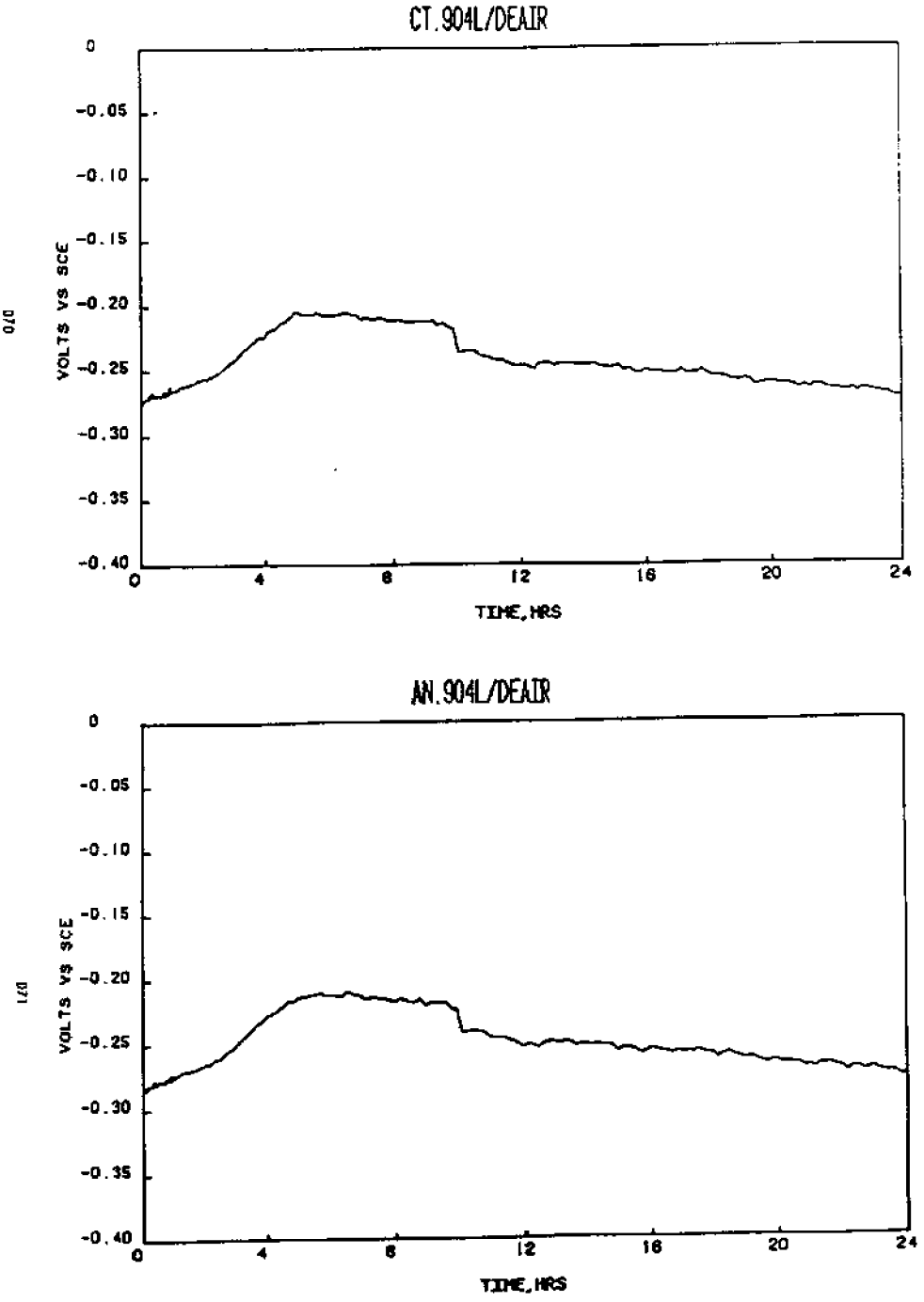
CT.904L/DEAIR
VOLTS VS SCE
0
-0.05
-0.10
-0.15
-0.20
-0.25
-0.30
-0.35
-0.40
0
4
8
12
16
20
24
TIME,HRS
AN.904L/DEAIR
VOLTS VS SCE
TIME,HRS

Figure 36.

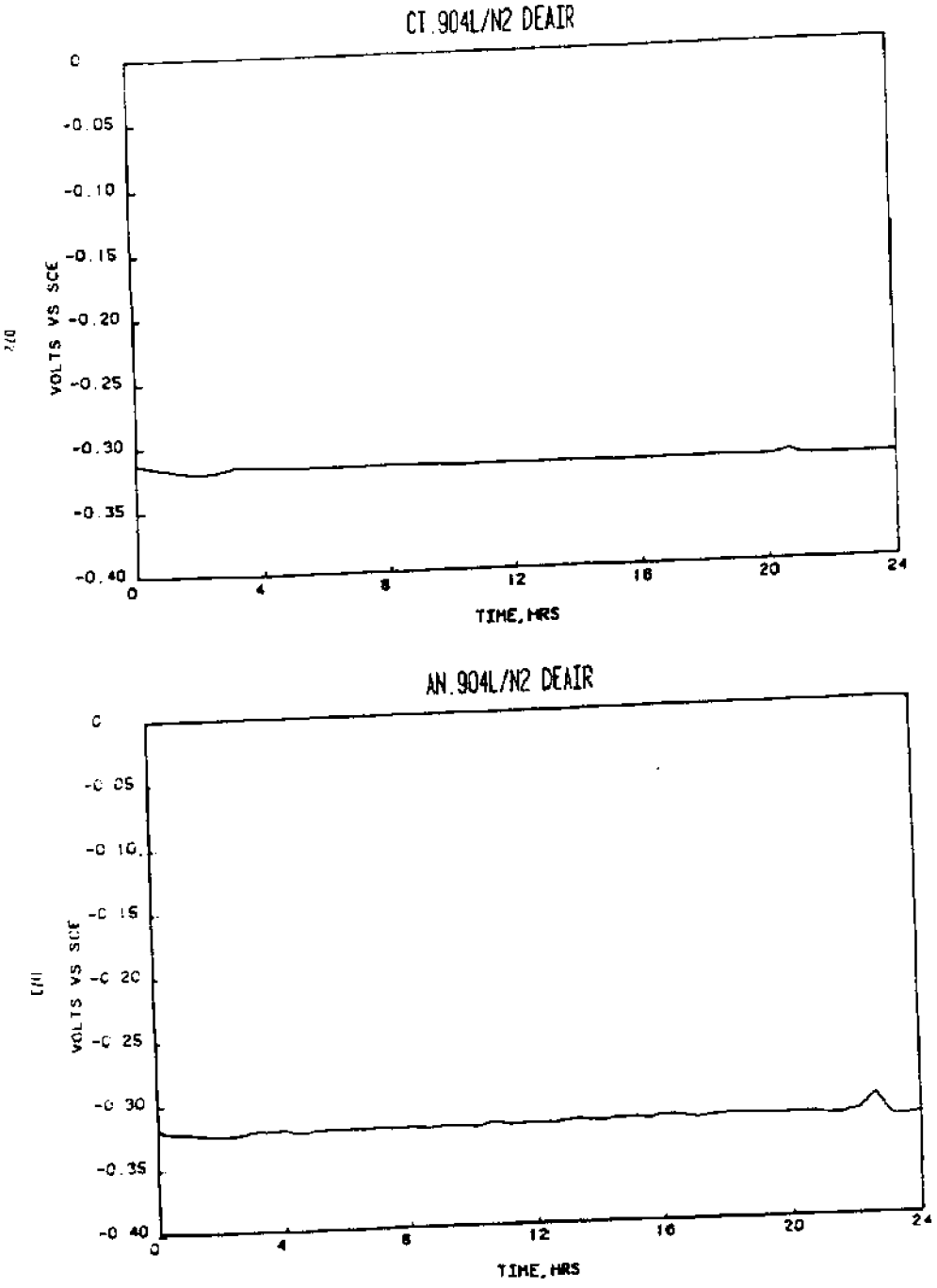
CT.904L/N2 DEAIR
VOLTS VS SCE
0
-0.05
-0.10
-0.15
-0.20
-0.25
-0.30
-0.35
-0.40
0
4
8
12
16
20
24
TIME, HRS
AN.904L/N2 DEAIR
VOLTS VS SCE
0
-0.05
-0.10
-0.15
-0.20
-0.25
-0.30
-0.35
-0.40
0
4
8
12
16
20
24
TIME, HRS

Figure 37.

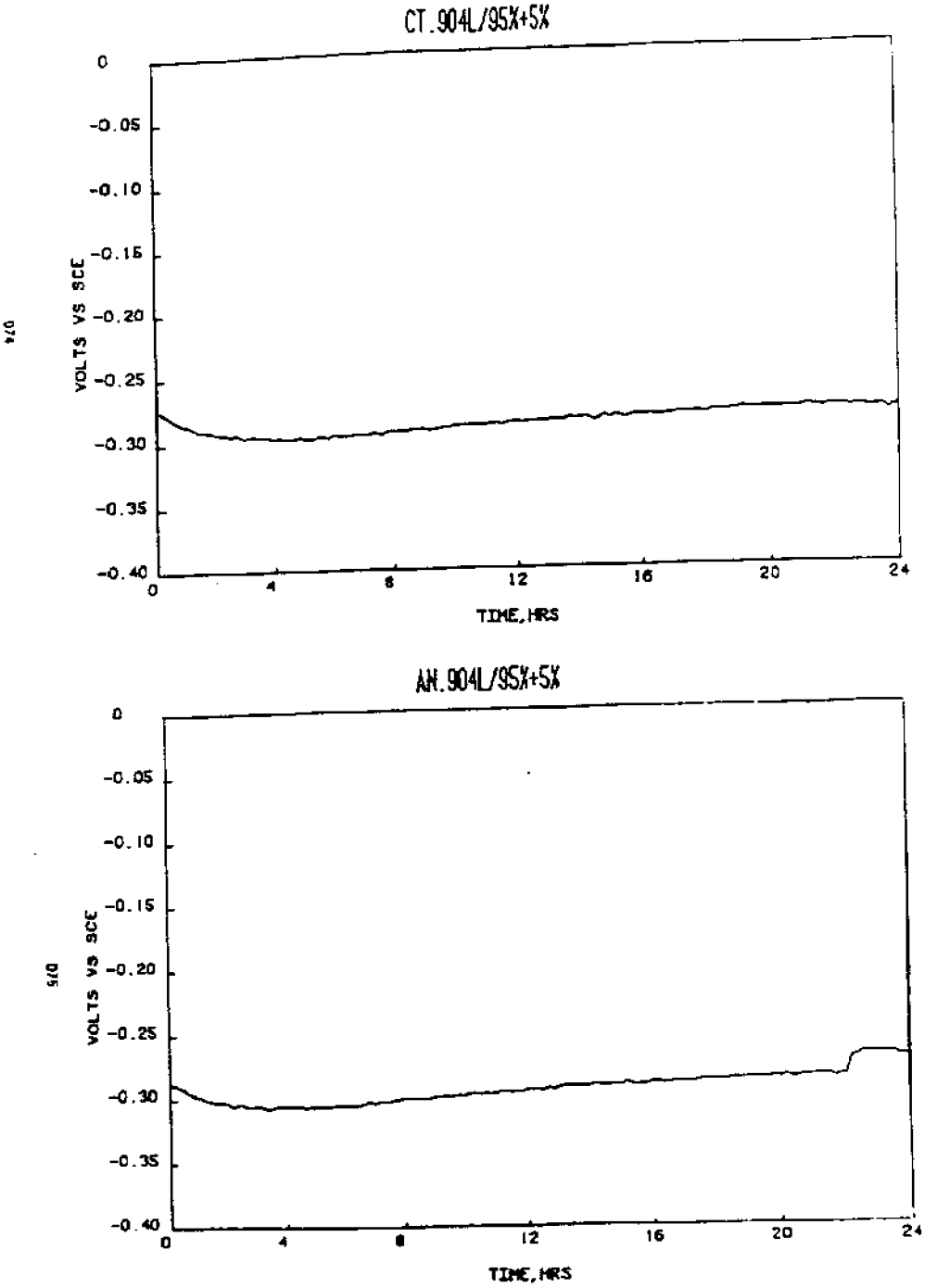
CT.904L/95%+5%
0
-0.05
-0.10
-0.15
-0.20
-0.25
-0.30
-0.35
-0.40
VOLTS VS SCE
0
4
8
12
16
20
24
TIME,HRS
AN.904L/95%+5%
0
-0.05
-0.10
-0.15
-0.20
-0.25
-0.30
-0.35
-0.40
VOLTS VS SCE
0
4
8
12
16
20
24
TIME,HRS

Figure 38.

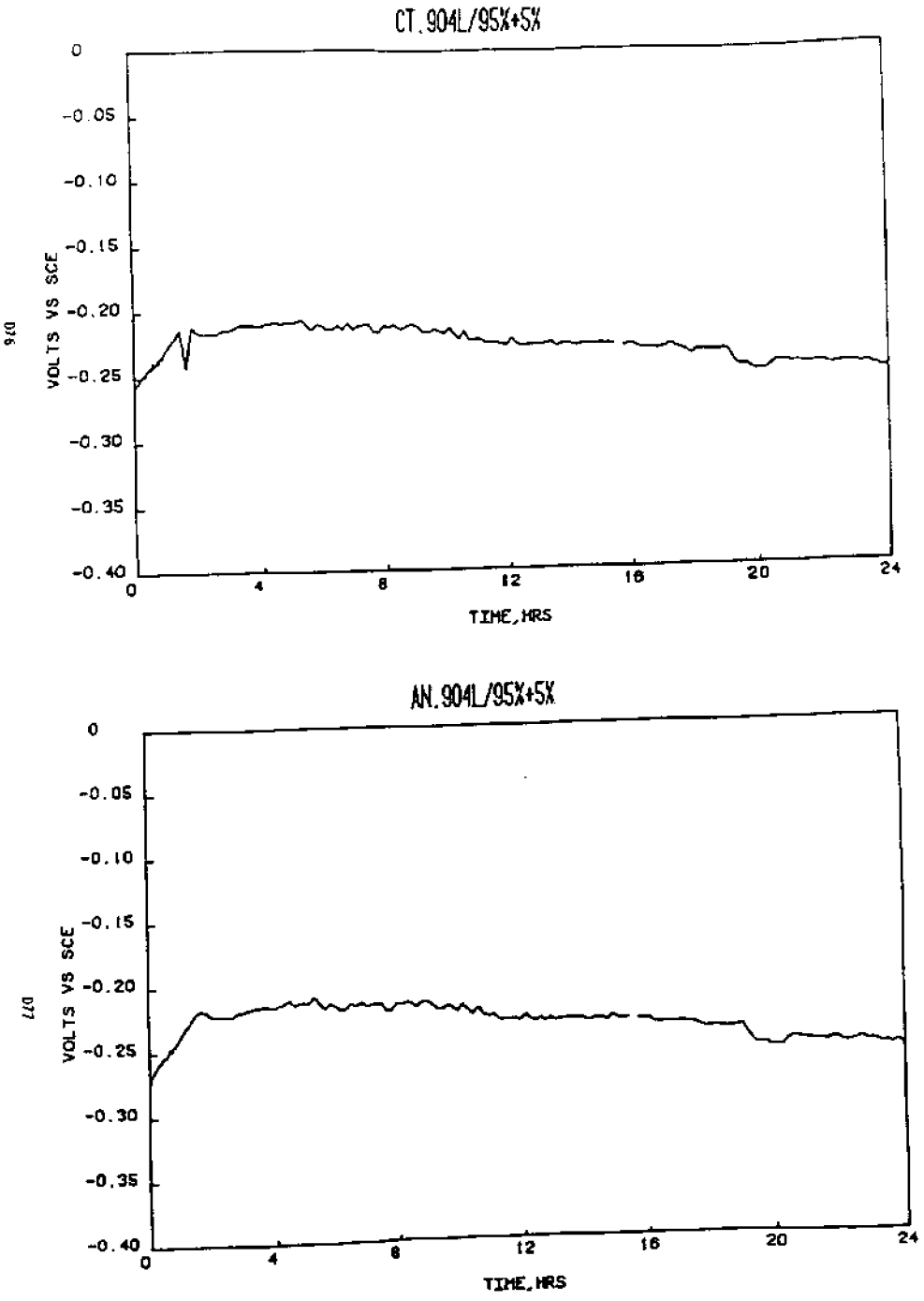
CT.904L/95%+5%
0
-0.05
-0.10
-0.15
-0.20
-0.25
-0.30
-0.35
-0.40
VOLTS VS SCE
0
4
8
12
16
20
24
TIME,HRS
AN.904L/95%+5%
0
-0.05
-0.10
-0.15
-0.20
-0.25
-0.30
-0.35
-0.40
VOLTS VS SCE
0
4
8
12
16
20
24
TIME,HRS

Figure 39.

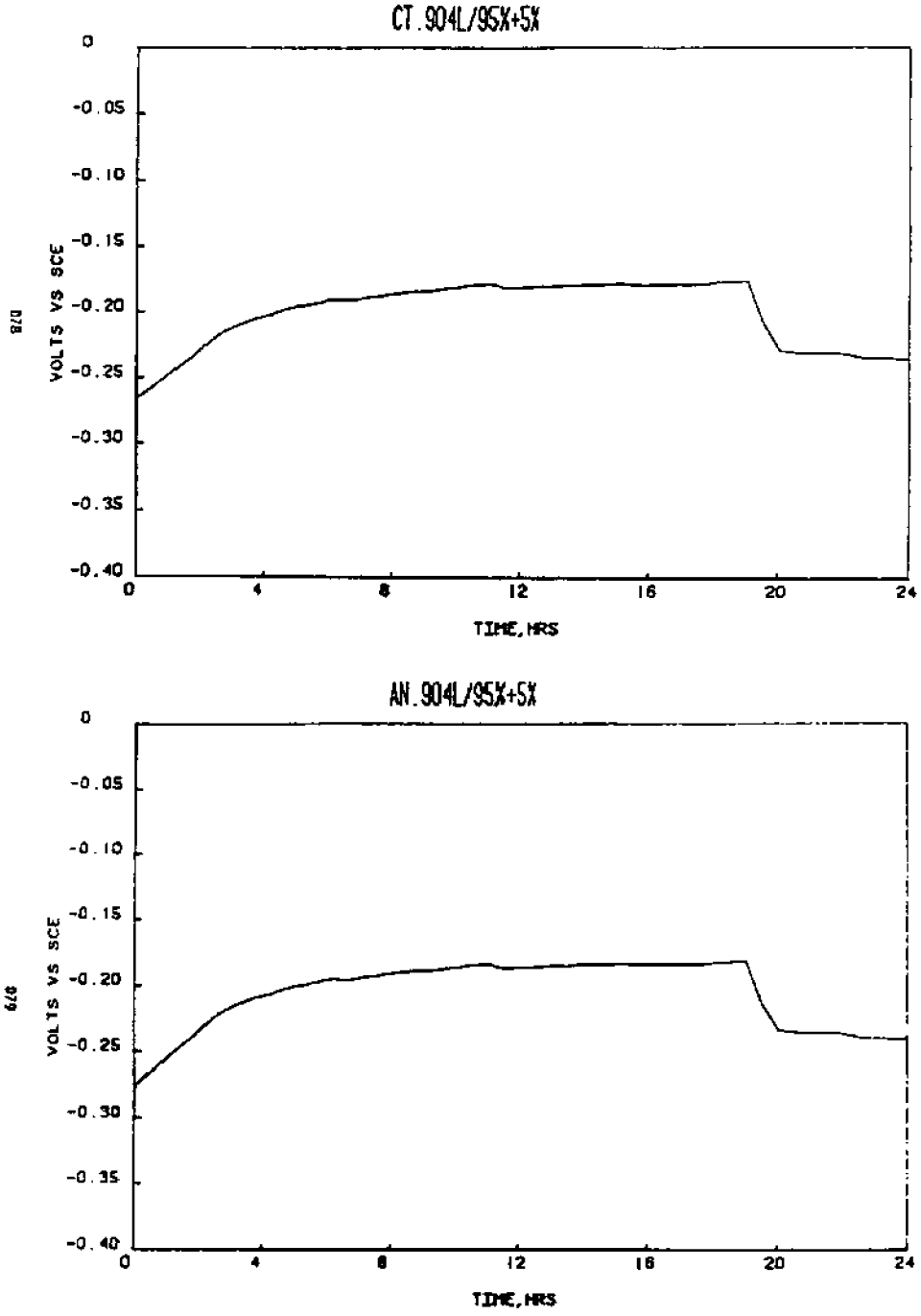
CT.904L/95%+5%
0
-0.05
-0.10
-0.15
-0.20
-0.25
-0.30
-0.35
-0.40
VOLTS VS SCE
0
4
8
12
16
20
24
TIME,HRS
AN.904L/95%+5%
0
-0.05
-0.10
-0.15
-0.20
-0.25
-0.30
-0.35
-0.40
VOLTS VS SCE
0
4
8
12
16
20
24
TIME,HRS

Figure 40.

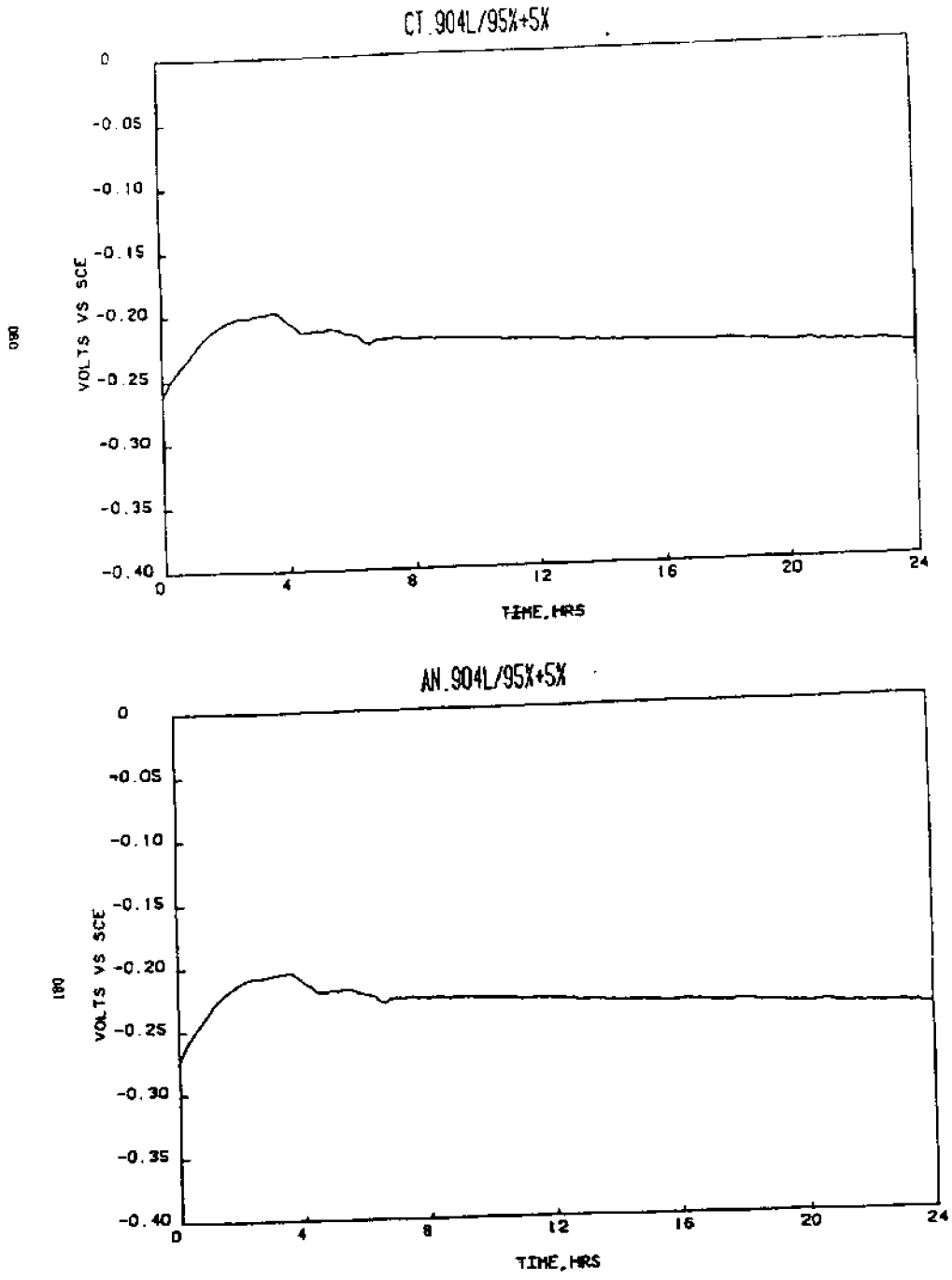
CT.904L/95%+5%
0
-0.05
-0.10
-0.15
-0.20
-0.25
-0.30
-0.35
-0.40
VOLTS VS SCE
0
4
8
12
16
20
24
TIME,HRS
AN.904L/95%+5%
0
-0.05
-0.10
-0.15
-0.20
-0.25
-0.30
-0.35
-0.40
VOLTS VS SCE
0
4
8
12
16
20
24
TIME,HRS

Figure 41.

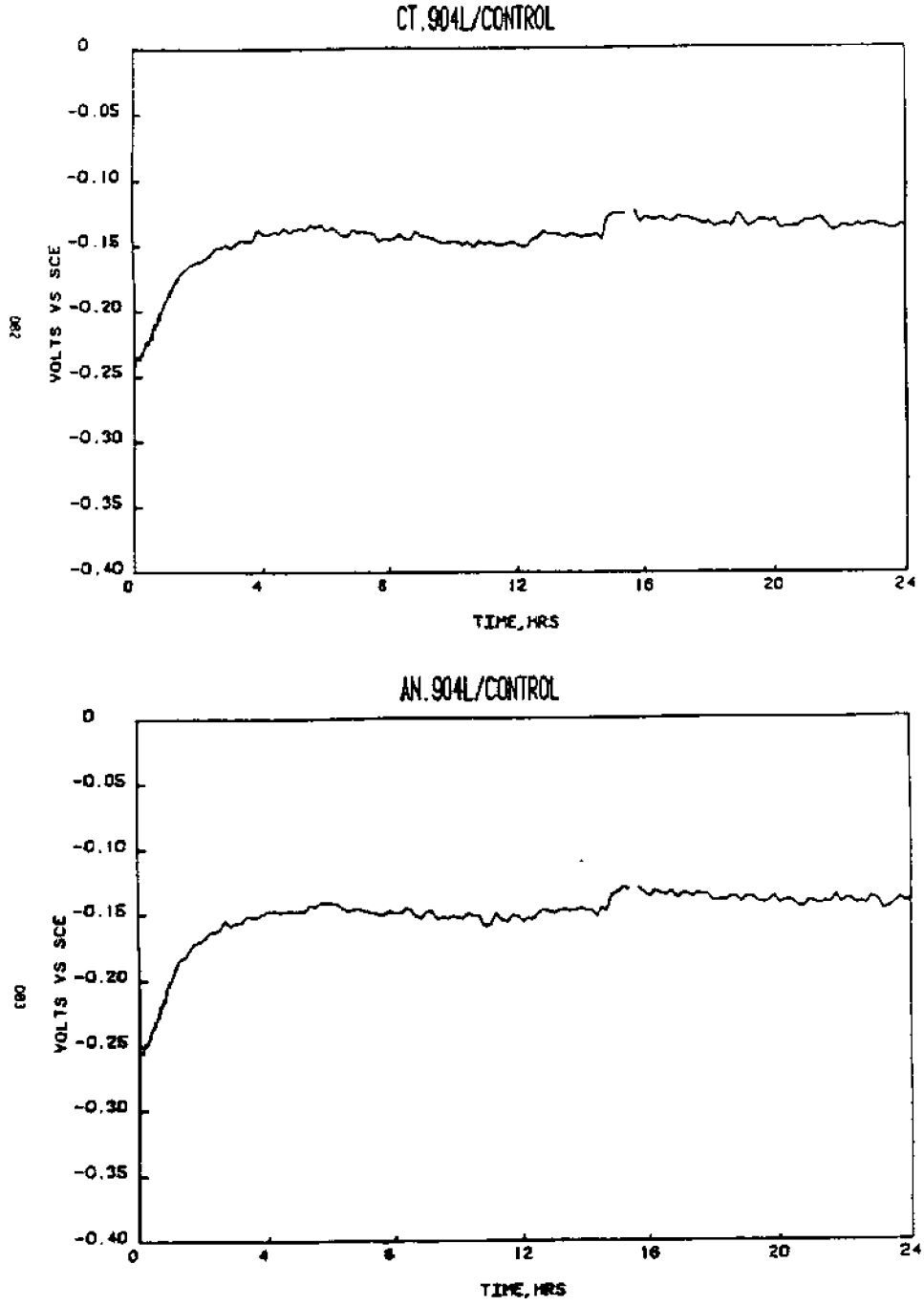
CT.904L/CONTROL
0
-0.05
-0.10
-0.15
-0.20
-0.25
-0.30
-0.35
-0.40
VOLTS VS SCE
0 4 8 12 16 20 24
TIME,HRS
AN.904L/CONTROL
0
-0.05
-0.10
-0.15
-0.20
-0.25
-0.30
-0.35
-0.40
VOLTS VS SCE
0 4 8 12 16 20 24
TIME,HRS

Figure 42.

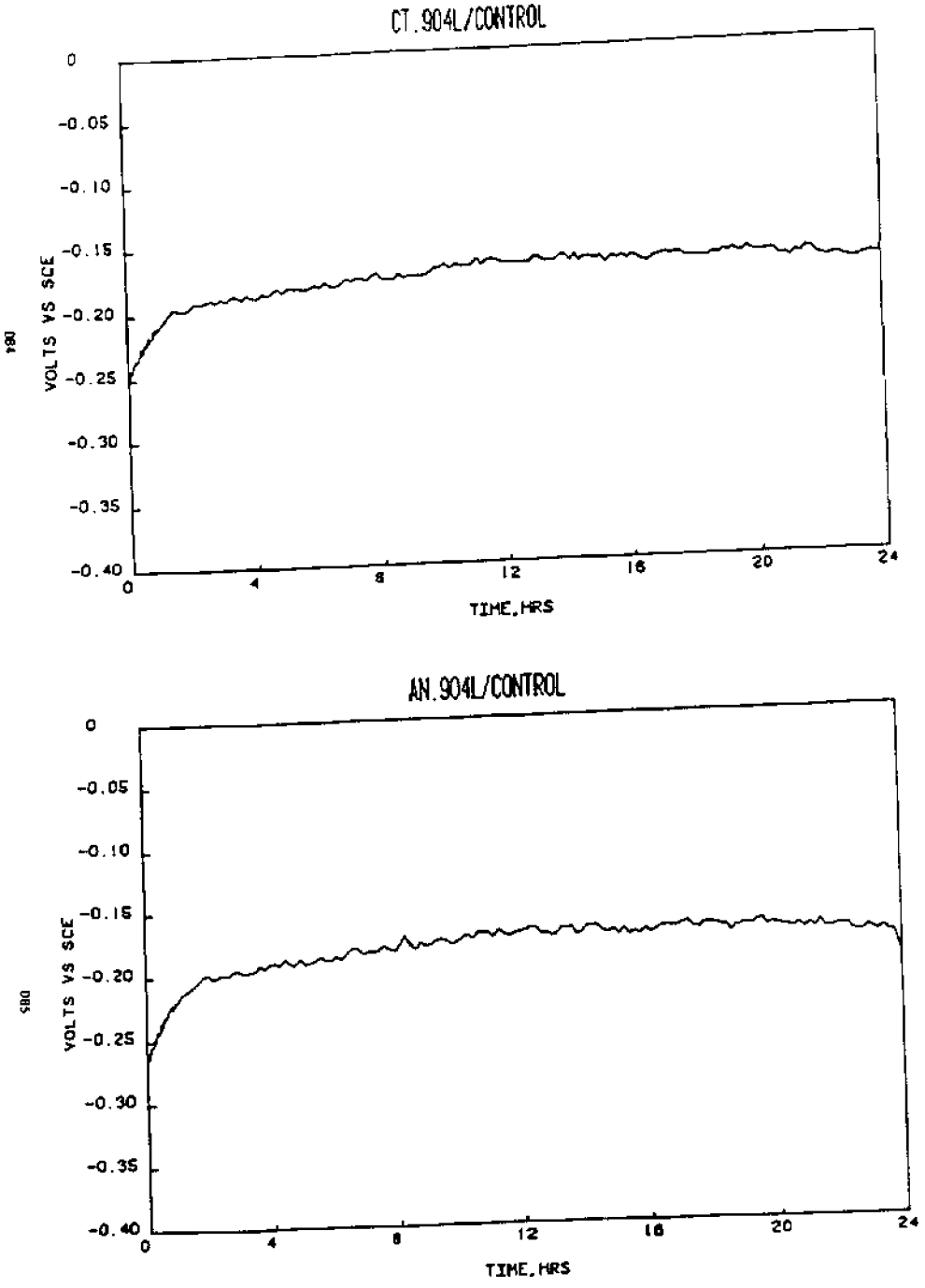
CT.904L/CONTROL
VOLTS VS SCE
0
-0.05
-0.10
-0.15
-0.20
-0.25
-0.30
-0.35
-0.40
0
4
8
12
16
20
24
TIME,HRS
AN.904L/CONTROL
VOLTS VS SCE
TIME,HRS

Figure 43.

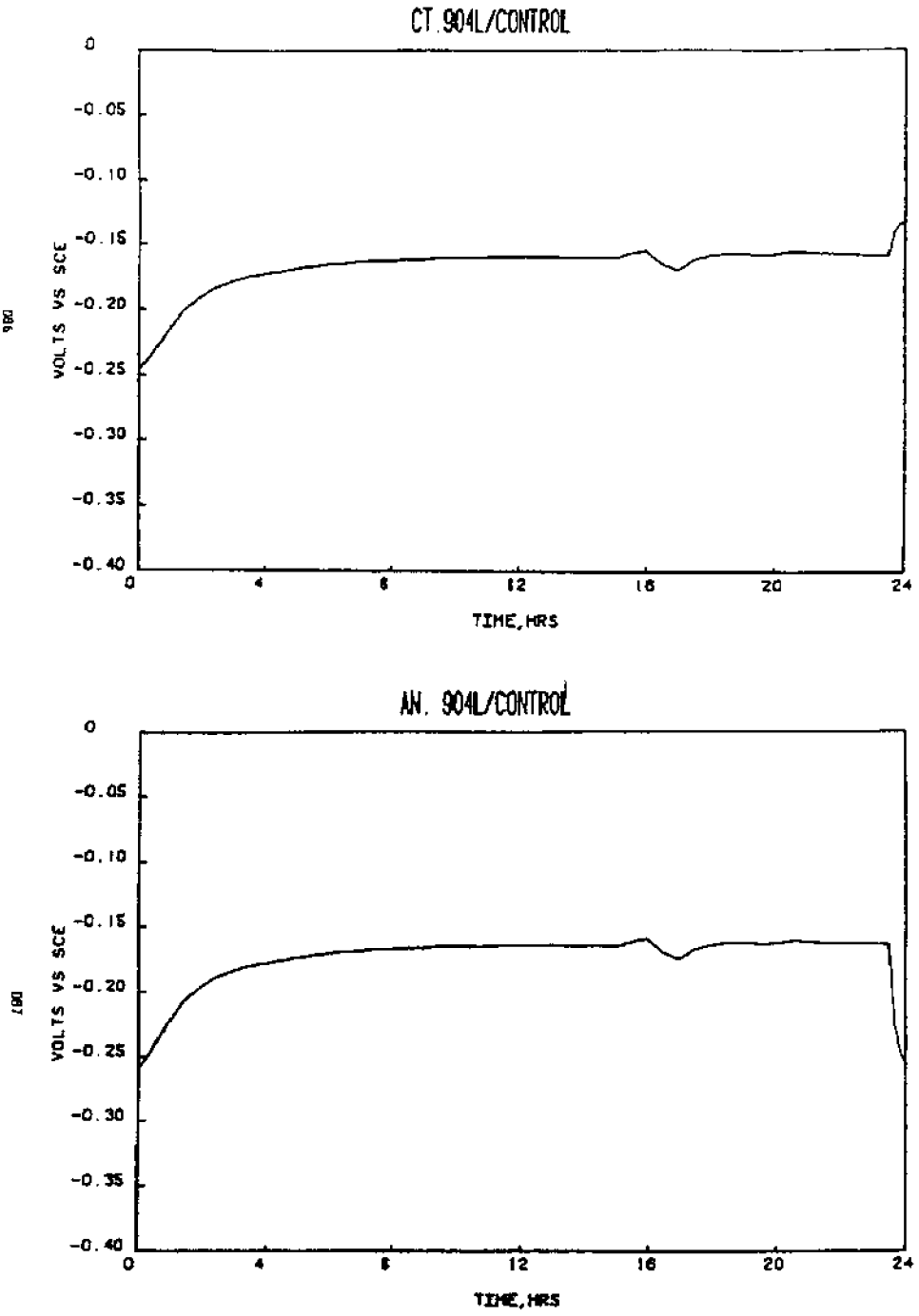
CT. 904L/CONTROL
VOLTS VS SCE
0
-0.05
-0.10
-0.15
-0.20
-0.25
-0.30
-0.35
-0.40
0
4
8
12
16
20
24
TIME, HRS
AW. 904L/CONTROL
VOLTS VS SCE
TIME, HRS

Figure 44.

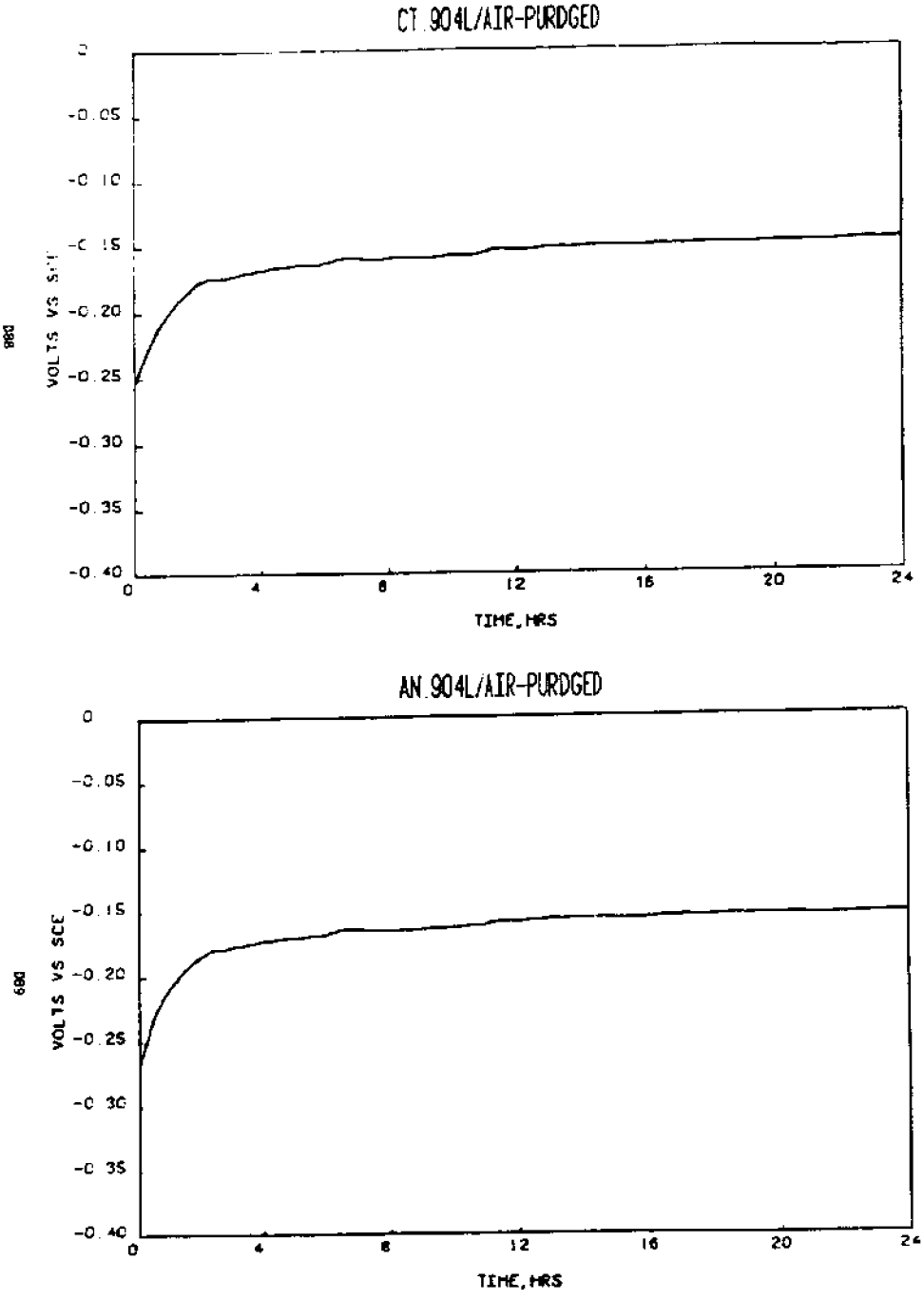
CT.904L/AIR-PURDGED
VOLTS VS SCE
0
-0.05
-0.10
-0.15
-0.20
-0.25
-0.30
-0.35
-0.40
0
4
8
12
16
20
24
TIME,HRS
AN.904L/AIR-PURDGED
VOLTS VS SCE
0
-0.05
-0.10
-0.15
-0.20
-0.25
-0.30
-0.35
-0.40
0
4
8
12
16
20
24
TIME,HRS

Figure 45.

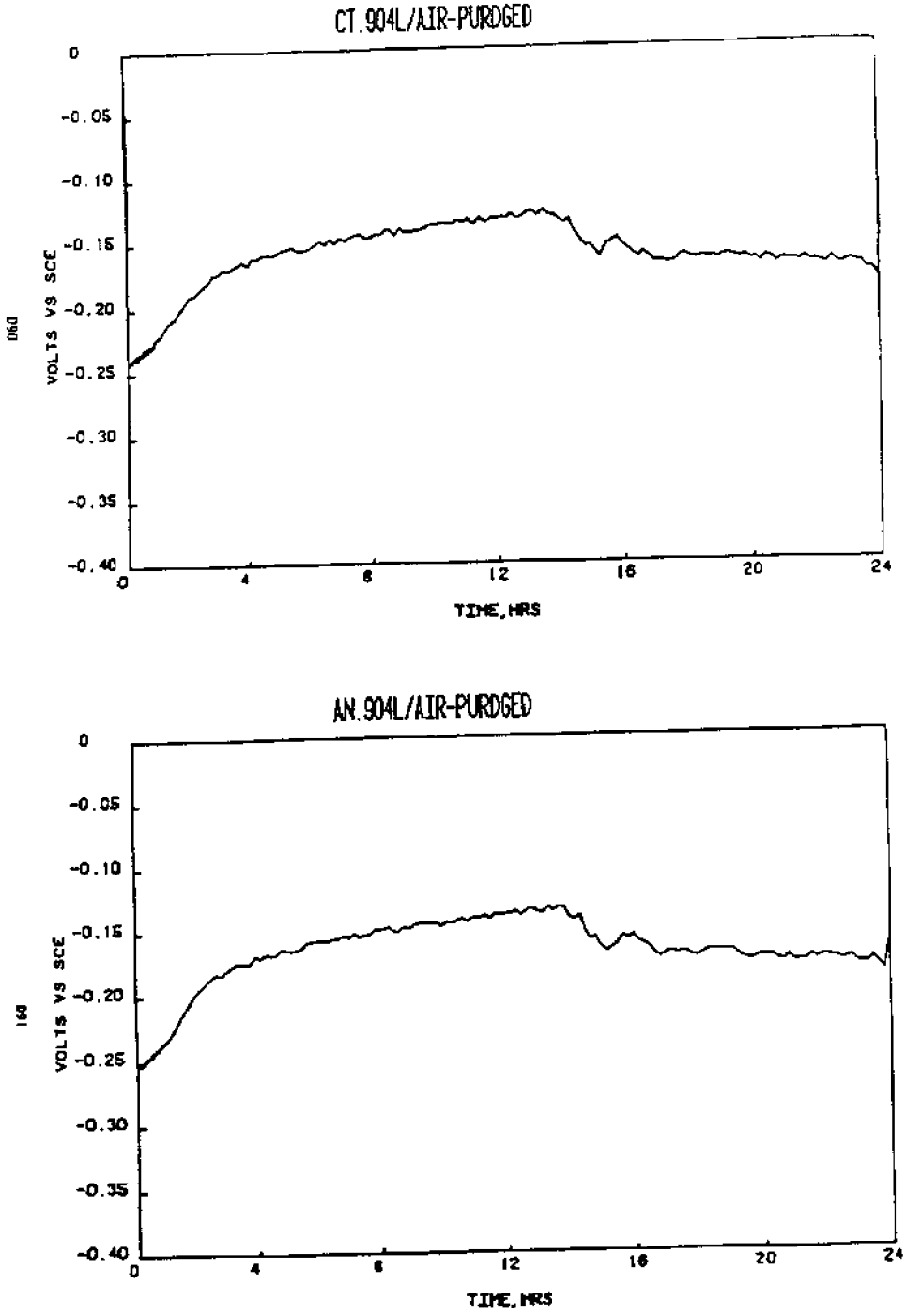
CT.904L/AIR-PURDGED
0
-0.05
-0.10
-0.15
-0.20
-0.25
-0.30
-0.35
-0.40
VOLTS VS SCE
0
4
8
12
16
20
24
TIME,HRS
AN.904L/AIR-PURDGED
0
-0.05
-0.10
-0.15
-0.20
-0.25
-0.30
-0.35
-0.40
VOLTS VS SCE
0
4
8
12
16
20
24
TIME,HRS

Figure 46.

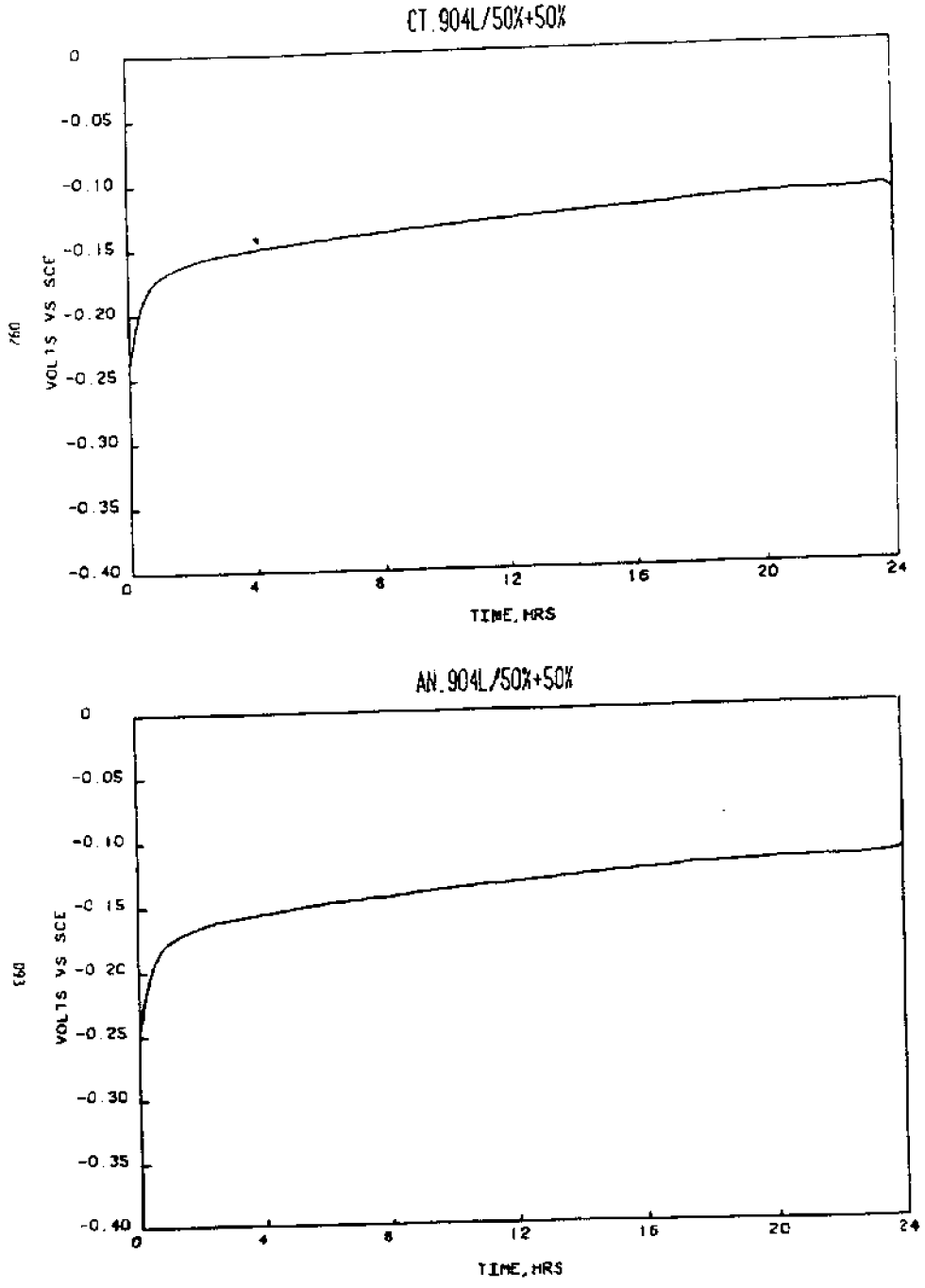
CT.904L/50%+50%
0
-0.05
-0.10
-0.15
-0.20
-0.25
-0.30
-0.35
-0.40
VOLTS VS SCE
0
4
8
12
16
20
24
TIME,HRS
AN.904L/50%+50%
0
-0.05
-0.10
-0.15
-0.20
-0.25
-0.30
-0.35
-0.40
VOLTS VS SCE
0
4
8
12
16
20
24
TIME,HRS

Figure 47.

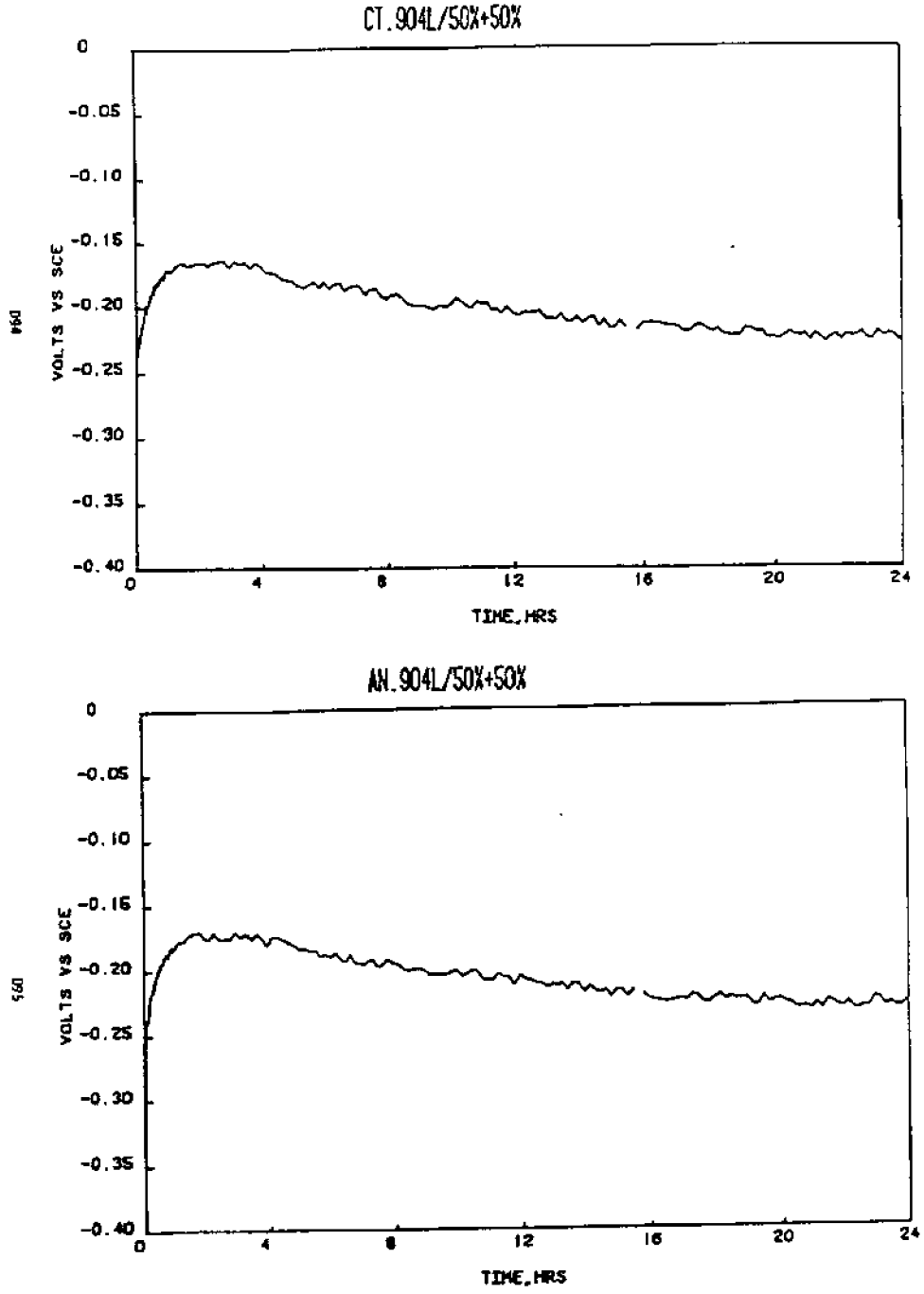
CT.904L/50%+50%
0
-0.05
-0.10
-0.15
-0.20
-0.25
-0.30
-0.35
-0.40
VOLTS VS SCE
0
4
8
12
16
20
24
TIME,HRS
AN.904L/50%+50%
0
-0.05
-0.10
-0.15
-0.20
-0.25
-0.30
-0.35
-0.40
VOLTS VS SCE
0
4
8
12
16
20
24
TIME,HRS

Figure 48.

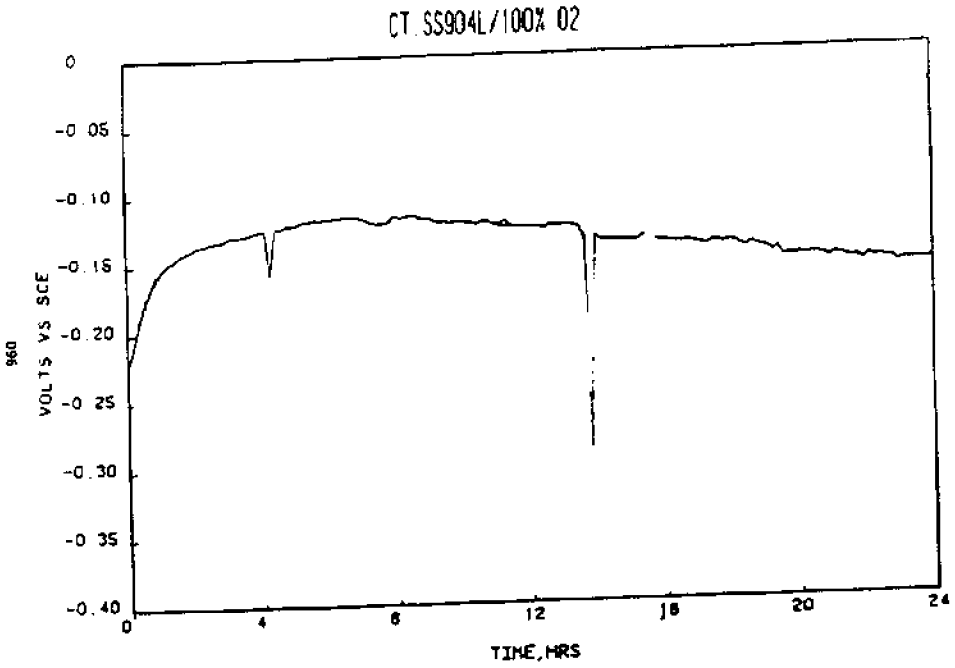
CT.SS904L/100% 02
0
-0.05
-0.10
-0.15
-0.20
-0.25
-0.30
-0.35
-0.40
VOLTS VS SCE
0
4
8
12
16
20
24
TIME,HRS

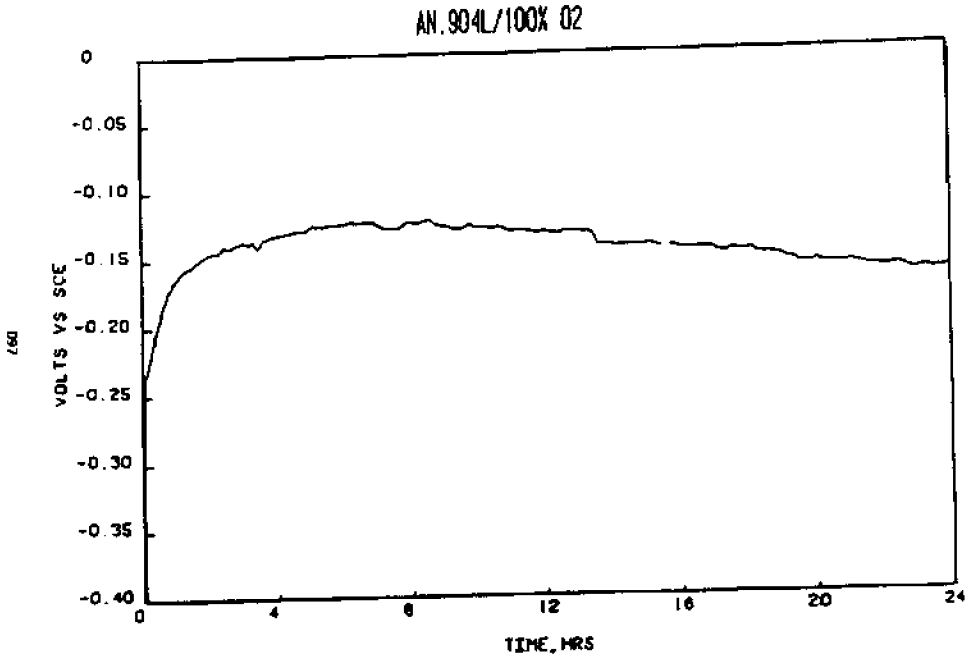
AN.904L/100% 02
0
-0.05
-0.10
-0.15
-0.20
-0.25
-0.30
-0.35
-0.40
VOLTS VS SCE
0
4
8
12
16
20
24
TIME,HRS

Figure 49.

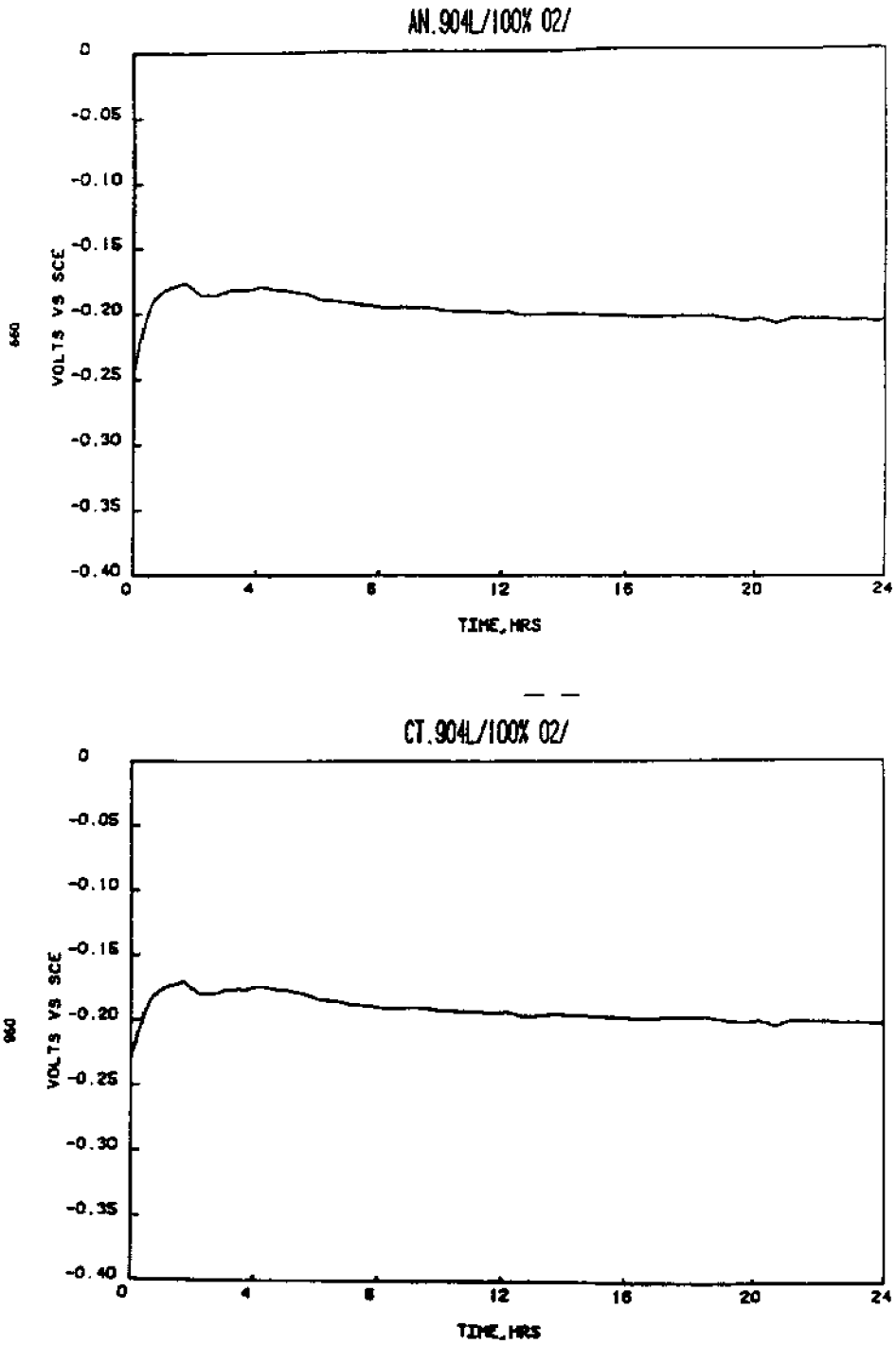
AN.904L/100% O2/
0
-0.05
-0.10
-0.15
-0.20
-0.25
-0.30
-0.35
-0.40
660
VOLTS VS SCE
0
4
8
12
16
20
24
TIME,HRS
CT.904L/100% O2/
0
-0.05
-0.10
-0.15
-0.20
-0.25
-0.30
-0.35
-0.40
960
VOLTS VS SCE
0
4
8
12
16
20
24
TIME,HRS

Figure 50.

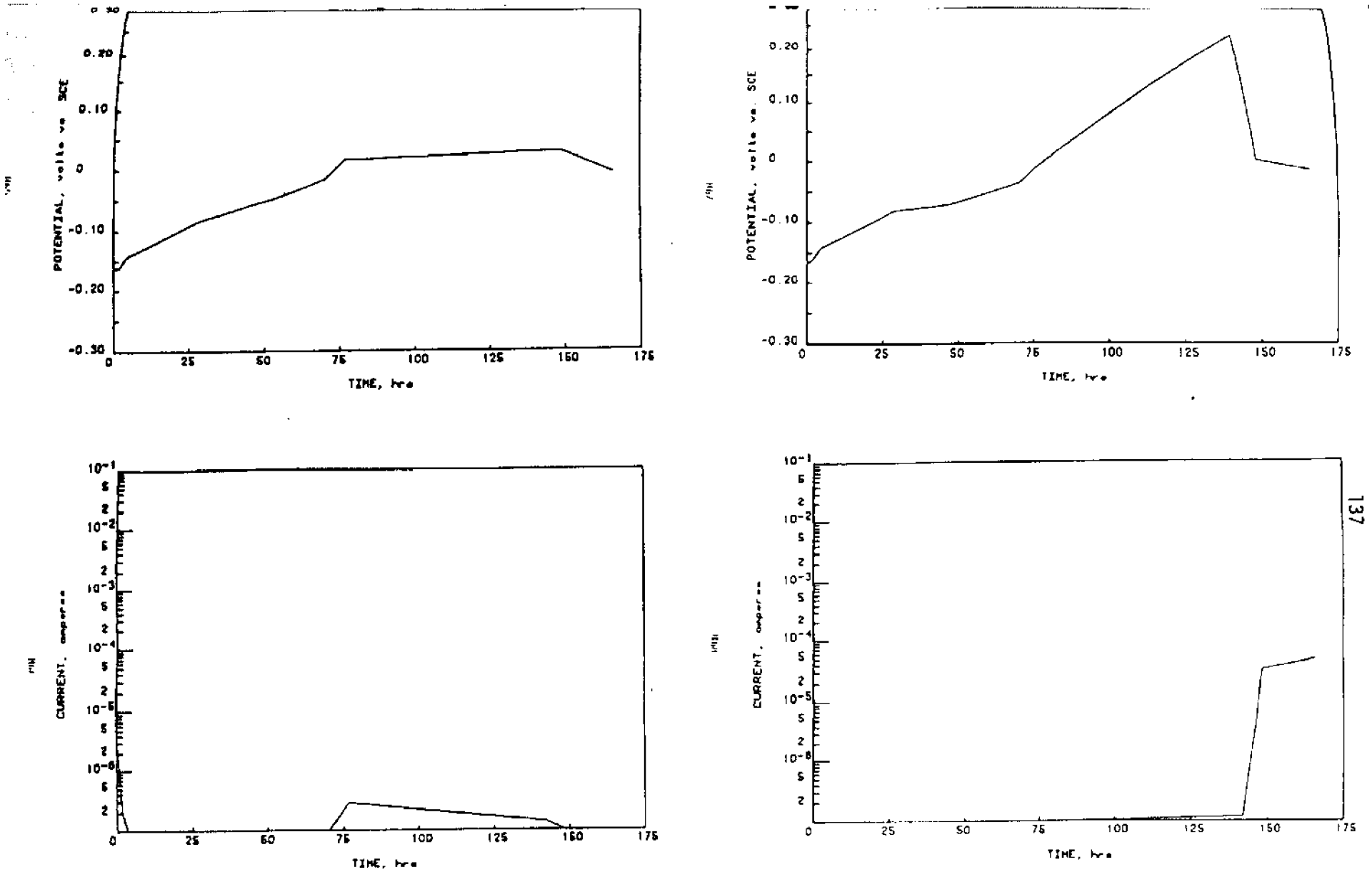

Figure 51. Comparison of couple potentials and current for Type 316 without tape inserts (load 10 psi gauge).

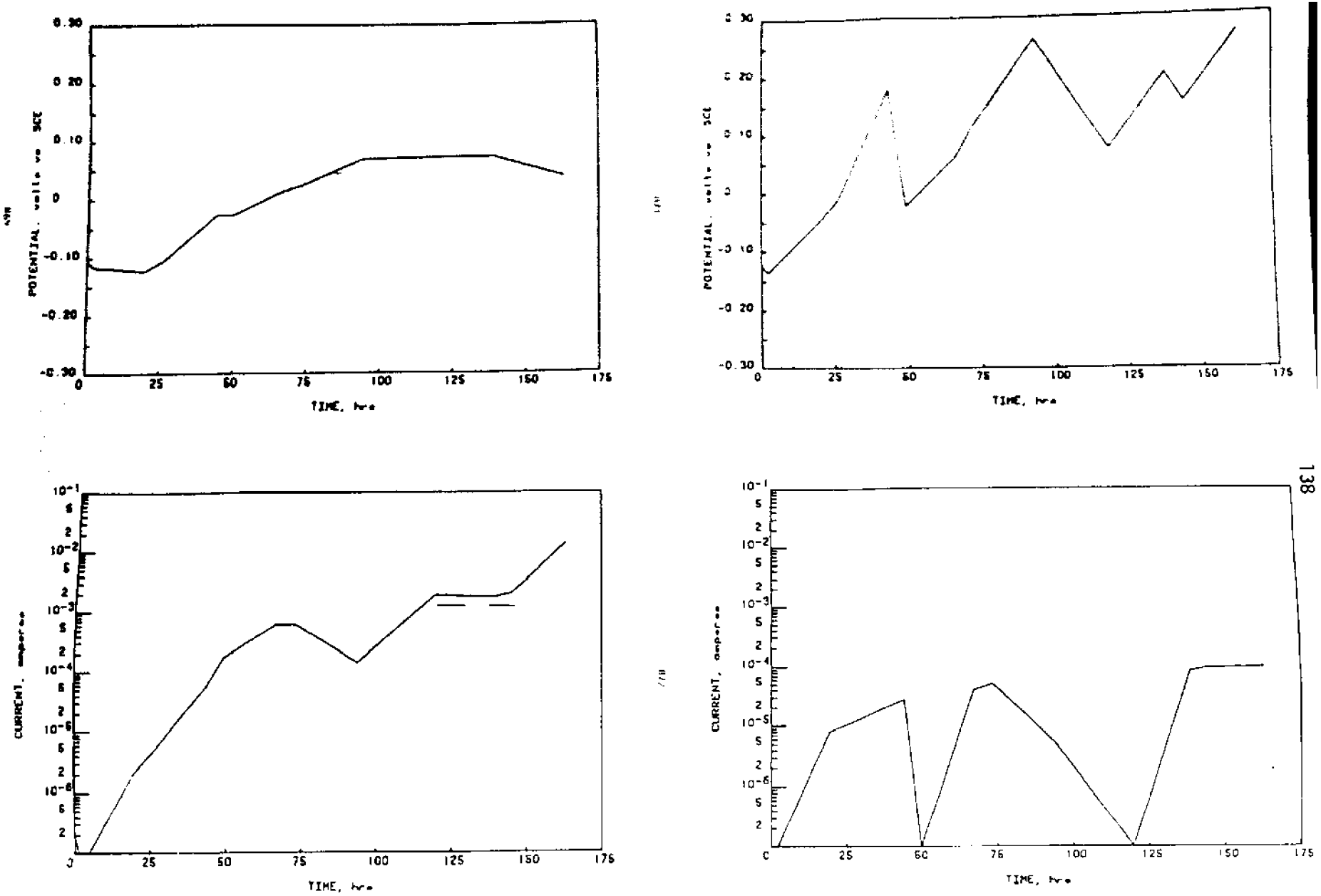

Figure 52. Comparison of couple potentials and current for Type 316 with deformable tape inserts (load 10 psi gauge).

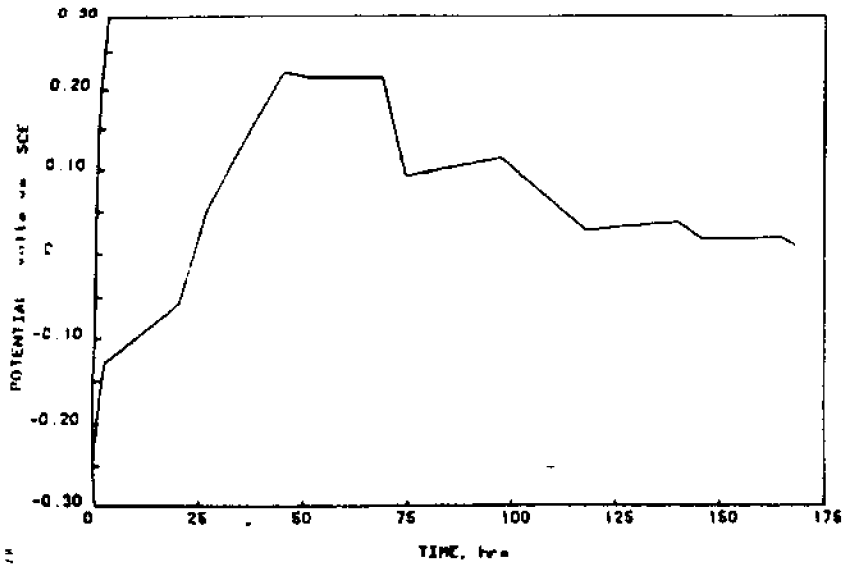

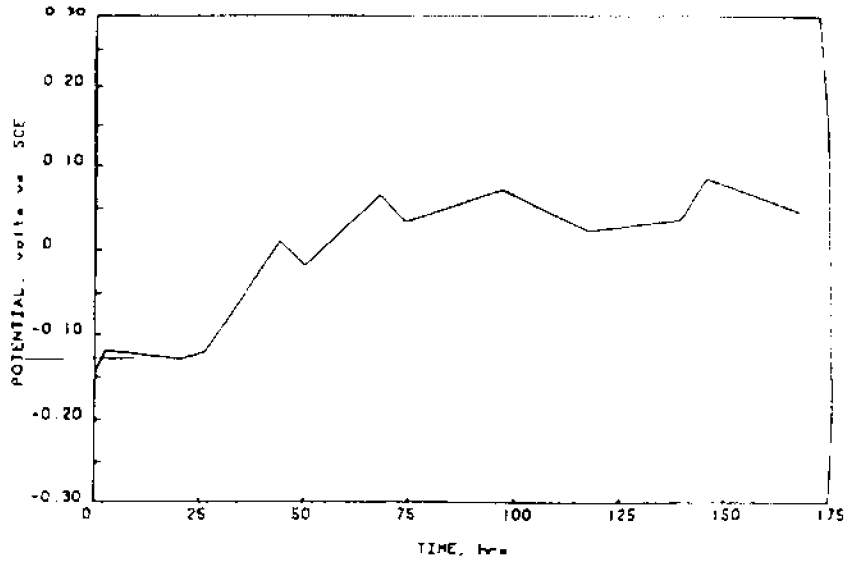

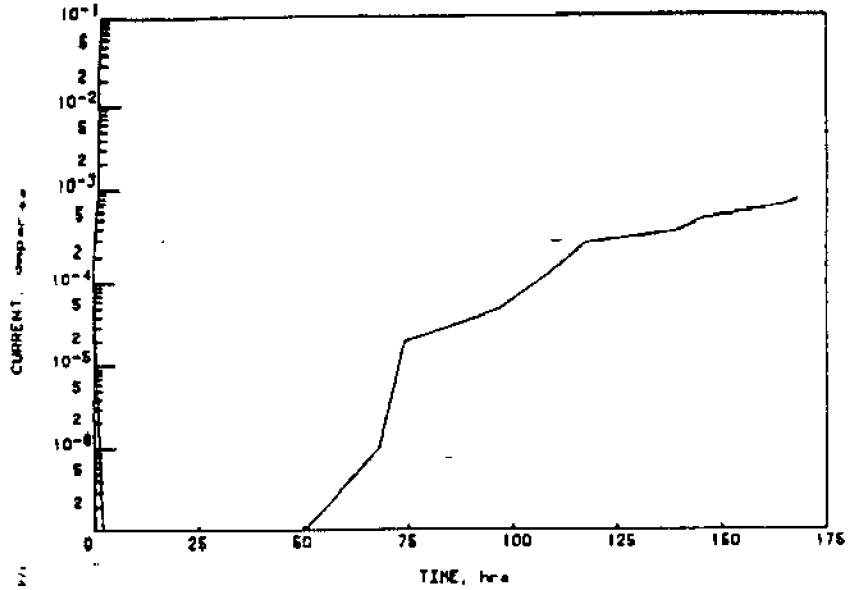

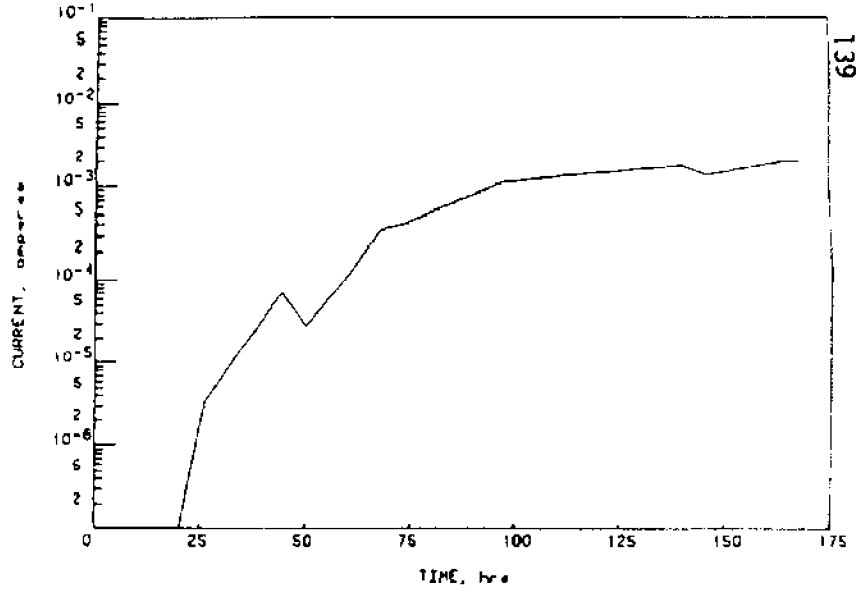

Figure 53. Comparison of couple potentials and current for Type 316 with deformable tape inserts (load 10 psi gauge).

III.B.

CREVICE CORROSION RESISTANCE OF SEVERAL IRON AND NICKEL BASE CAST ALLOYS IN SEAWATER

By

R. M. Kain

Presented at
CORROSION/82, Paper No. 66
Houston, Texas, March 1982

LaQUE CENTER FOR CORROSION TECHNOLOGY, INC.
Post Office Box 656
Wrightsville Beach, North Carolina 28480
(919) 256-2271

PAPER NUMBER

66

The International Corrosion Forum Sponsored by the National Association of Corrosion Engineers / March 22-26, 1982 / Albert Thomas Convention Center, Houston, Texas

CREVICE CORROSION RESISTANCE OF SEVERAL IRON AND NICKEL BASE CAST ALLOYS IN SEAWATER

R. M. KAIN
LaQue Center for Corrosion Technology, Inc.
Post Office Box 656
Wrightsville Beach, North Carolina 28480

ABSTRACT

Seawater crevice corrosion resistance of several iron base and nickel base cast alloys has been investigated. An expanded matrix, multiple crevice test method was used to determine any effect of assembly torque level and test duration. Results of seawater immersion tests are compared with mathematical modelling predictions describing effects of alloying and crevice geometry. Scanning electron microscopy is utilized to quantify actual crevice gap dimensions and to study the morphology of corrosion incurred by susceptible materials. While beneficial effects of alloy molybdenum content are apparent, crevice geometry consideration may have an overriding influence on resistance to crevice corrosion initiation.

INTRODUCTION

Crevice corrosion resistance of austenitic stainless steels and related nickel base alloys remains a topic of sustained interest in the technical community. While some stainless type materials are susceptible to crevice corrosion under certain conditions, there are increasing numbers of successful applications in marine environments. This is particularly true for alloys with molybdenum contents greater than the levels in AISI Type 316 stainless steel.[1]

The susceptibility to crevice corrosion beneath barnacles and other marine attachments, can limit the utility of some common grades of stainless steel, e.g., AISI Type 304 and Type 316. The development of such crevice formers is most likely to occur under low velocity conditions found upon simple exposure in nominally quiescent seawater. Field experience has shown that crevice corrosion may also occur at barnacle sites developed in seawater handling systems during prolonged shut-down periods if not drained and flushed with fresh water.[2,3] These alloys have also been shown to be susceptible to crevice corrosion in shielded areas formed by metal to metal and non-metal to metal connectors in service, as well as in laboratory controlled experiments.[4]

It has long been recognized that a realistic test is one which provides conditions most closely approximating the intended field application. Because of the many possible applications, providing a representative test is no doubt a challenging task. From the environmental standpoint, testing in an actual environment, such as natural seawater, overcomes the concerns of relevancy encountered in the use of laboratory simulations and/or accelerated test procedures.[5,6] The benefits of the latter as initial screening tests for alloy development purposes are nonetheless recognized.[7,8]

Testing in natural seawater environments has not been without problems, however, as evidenced by reports describing the "unpredictable" behavior of stainless alloys in seawater. In recent years, the understanding of crevice corrosion has been advanced by the identification of numerous metallurgical-environmental-geometric factors which affect its occurrence. In particular, the insight gained with mathematical models[9-11] to study these factors has helped to explain much of the observed variability in crevice corrosion test data.

It has been shown that crevice geometry factors, such as crevice depth and crevice gap (i.e., tightness) have significant impact on the resistance of an alloy to crevice corrosion initiation.[12,13] Modelling predictions indicate that for a given crevice depth, some critical gap dimension must exist in order for crevice initiation to occur. With the size (i.e., depth) of the specific crevice former which is utilized in controlled tests generally held constant, scatter in crevice initiation data may be due to extremely small differences in crevice gap at various sites. Such differences, in the case of multiple crevice assemblies (MCA), for example, may be of a dimension less than 0.1 μm according to modelling predictions.[13]

Multiple crevice assemblies have been frequently used in tests to identify relative alloy resistance to crevice corrosion under severe but not accelerated conditions.[13-19] The effects of crevice assembly tightness have been recently described for a series of wrought stainless alloys exposed with crevice assemblies tightened at different torque levels.[20] It was found that while many materials exhibited crevice corrosion at an assembly torque level of 8.5 Nm, the overall incidence of crevice corrosion decreased at the lower torque level of 2.8 Nm. Decreased torque level also resulted in an increase in the observed times to initiation for susceptible alloys. These observations emphasize the importance of crevice tightness.

Multiple crevice assemblies were also recently utilized by Hack[21] to evaluate the relative crevice corrosion resistance of 45 wrought and cast alloys. Six cast alloys from the above study were selected for further evaluation as described in the present paper. An expanded test matrix to assess the effects of crevice assembly torque level and test duration was applied in the evaluation of CF8M, CN7M, CN7MS, IN-862, cast alloy 625 and CW-12M-2. These alloys have similar chromium contents (18 to 21%), but range in molybdenum content from 2.5 to 18 percent and nickel content from 10 to 64 percent. To further qualify the seawater crevice corrosion test data and define its relevance to service experiences, additional electrochemical testing and mathematical modelling were employed.

EXPERIMENTAL

Materials

Table I gives the chemical analyses and heat treatments of the six cast alloys tested. CF8M is the cast counterpart to wrought AISI Type 316 stainless steel. While

CF8M is known to perform satisfactorily in flowing seawater, its susceptibility to localized corrosion under stagnant conditions is well documented.[2] CN7M is one of the most common "20 type alloys" and has been found to be resistant to numerous corrosive environments.[22] With its high nickel content and 2 to 3 percent molybdenum, this alloy is frequently used for seawater service. CN7MS has corrosion resistance similar to CN7M. The two alloys differ primarily with respect to Si and Ni contents, as shown in Table I. IN-862 is a 5 percent molybdenum alloy with a high resistance to chloride environments.[6,23]

Cast alloy 625 and CW-12M-2 are both nickel base alloys with high molybdenum contents. Their wrought counterparts, e.g., INCONEL* alloy 625 and HASTELLOY** alloy C-276, consistently exhibit excellent resistance to crevice corrosion in seawater.[6,21]

Multiple Crevice Tests

Specimens: Materials were obtained from a commercial foundry as castings in the form of individual, wedge shape panels measuring approximately 10 x 15 cm. Specimens were machined (shaper or milled) to remove the as-cast surface and to provide parallel sides for subsequent application of the crevice formers. A 13 mm diameter center hole was drilled in each specimen for the attachment of crevice assemblies. Surfaces were prepared by wet grinding with 120 grit SiC abrasive papers. Final grinding was limited to crevice areas with the intention of providing consistent surfaces. A number of replicate specimens were machined in each case. Specimen cleaning procedures and method of attachment of the multiple crevice assembly washers are identical to those described elsewhere.[20]

Test Matrix: Figure 1 describes the test matrices utilized for the various alloys. Selection of the exposure conditions was based on the alloys resistance in the initial study[21] with added consideration of alloy chemistry, e.g., molybdenum content. The matrices were selected to reveal the effects of torque level and test duration.

Apparatus and Environment: Tests were conducted in a low velocity (~0.02 m/sec) seawater trough described elsewhere.[20] Briefly, the apparatus had provisions for recirculation and introduction of fresh, filtered seawater on a continuing basis through the exposure period. During the course of the tests, the seawater was maintained at a temperature of 30°C ± 2°C. Table II provides a summary of the seawater hydrology.

Inspection and Assessments: Specimens were inspected during the course of the test for visual signs of accumulated corrosion products. Inspections were conducted on a daily basis (without disturbance or removal of the test panels) during the first 30 days. The frequency of inspection was less for exposures in excess of 30 days.

Following removal of the specimens at the conclusion of testing, crevice corrosion depths at individual crevice sites were measured with a needle point dial gauge (gauge accuracy to the nearest 0.01 mm). Because of observed selective phase attack in some cast alloys, depth of penetrations determined by this method may not be absolute.

* INCONEL is a trademark of the Inco Family of Companies.
** HASTELLOY is a trademark of Cabot Corporation.

Mathematical Modelling

The mathematical model utilized for this investigation is that described by Oldfield and others.[5,9,10,12,24] It has recently been used by the author to describe the resistance of wrought AISI Type 304 and Type 316 in seawater and related environments.[13] The model is particularly useful in examining the influence of variables, such as alloy composition, crevice geometry and bulk environment chemistry. Inputs to the model include theoretical assumptions, known quantities and experimental data.

Electrochemical Procedures: One input to the above mathematical model is the critical crevice solution (CCS) for each alloy. The CCS is defined by a pH and chloride level which is sufficiently aggressive to break down the passive film and initiate corrosion.[25] The composition of the CCS is determined from a series of potentiodynamic polarization tests in a number of concentrated, deaerated solutions. The specific solution pH and chloride level at which an anodic current peak of 10 $\mu A/cm^2$ is measured during potential scanning is identified as the CCS. CCS criteria and details of the electrochemical procedures are described elsewhere.[10]

Test electrodes for the CCS determinations were prepared from the same stock materials as those utilized for the MCA test specimens. In recognition of the variability in microstructure associated with some cast materials, polarization tests were conducted on duplicate electrodes.

RESULTS AND DISCUSSION

Crevice Corrosion Initiation Behavior

Time to Initiation: The two high molybdenum nickel base materials, cast alloy 625 and CW-12M-2, were found to be resistant to crevice corrosion in MCA tests lasting up to 90 days (see Figure 1- Matrix C). For the remaining lower alloyed materials, however, some degree of crevice corrosion was found on all specimens exposed according to Matrices A and B (Figure 1).

Table III gives the approximate time to initiation for specimens of CF8M, CN7M, CN7MS and IN-862. Initiation times are based on the first sighting of accumulated corrosion products at one or more of the multiple crevice washers. (Actual times to initiation may be shorter in some cases, since some time must elapse between breakdown and accumulation of sufficient corrosion products to be visibly detected.) In the initial test conducted at the 8.5 Nm torque level, all four of the less alloyed materials exhibited crevice corrosion within approximately 87 hours. The average time to initiation was somewhat longer for the 5 percent molybdenum alloy, IN-862.

The test at 2.8 Nm torque showed somewhat greater specimen to specimen variation in the observed times to initiation. In contrast to the previous test results, the lower assembly torque gave somewhat longer average times to initiation. This effect was most pronounced for IN-862 and CN7M.

Incidence of Crevice Corrosion: Table IV shows the number of crevice sites which initiated attack for each specimen exposed in the various tests. These data are further

summarized in Table V. Although other MCA tests have shown greater variability, the specimen-to-specimen or side-to-side differences in the number of corroded sites beneath the grooved washers in the present series are generally minimal. It has been suggested that these variations may be attributed to extremely small, but nonetheless, critical differences in crevice tightness at the individual crevice sites.[13,20] Such variation, especially in the case of cast materials, could also be attributed to segregation in the microstructure.

From Table V, it can be seen that the results of the initial test at the 8.5 Nm torque level show no significant difference between the 2 to 3 percent molybdenum containing alloys CF8M, CN7M and CN7MS. Some trend toward a lower incidence of initiation, however, is indicated by the results for IN-862. This increased resistance is further shown by the results for the 60 day test at the 8.5 Nm torque level.

Decreasing the torque level to 2.8 Nm had no apparent effect on the incidence of crevice initiation for CF8M, CN7M and CN7MS. Again all three materials exhibit similar behavior. Results from the 60 day test at the 2.8 Nm torque level again reveal the higher resistance of the 5 percent molybdenum alloy, IN-862.

It is significant to note that increasing the test duration had little, if any, effect on increasing the incidence of crevice initiation. This is evident from the results of the 60 day test of IN-862 at the 8.5 Nm torque level, as well as those for CF8M, CN7M and CN7MS in the 2.8 Nm test. Similar observations have been reported for a number of wrought materials tested under similar conditions.[20]

The crevice corrosion resistance of IN-862 has been reported previously.[7] In these earlier seawater tests, no evidence of crevice initiation was detected for IN-862. However, the torque level was not measured in this earlier work and it is possible that the crevices may have been less tight than those employed in the present study.

Mathematical Model Assessment of Initiation Times

Critical Crevice Solution Determinations: Figure 2 shows plots of anodic peak current densities for the various cast alloys as a function of the pH of the simulated crevice solution. These plots were utilized to identify the critical crevice solution (CCS) pH as previously described. Table VI gives the composition (pH and chloride concentration) of the CCS for the six materials in the present study. While it is recognized that alloy composition (particularly Cr content) and crevice geometry affect the rate of pH fall within a crevice, it generally may be viewed that the lower the CCS pH value the higher the resistance of the alloy to crevice corrosion initiation.

The CCS pH values for the three alloys containing 2 to 3 percent molybdenum are quite similar. Again, these alloys exhibited similar initiation behavior in the severe MCA test (8.5 Nm torque level). The somewhat longer initiation times and lower incidence of crevice corrosion exhibited by the 5 percent molybdenum alloy, IN-862, can be attributed in part to its lower CCS pH value. Furthermore, alloy 625 and CW-12M-2 exhibited by far the lowest CCS pH values. These alloys were resistant in the MCA tests.

Crevice Geometry and Predicted Time to Initiation: As previously noted, crevice geometry is an important factor controlling the crevice corrosion resistance of stainless type alloys. Scanning electron microscopy (Figure 3) has identified crevice gaps of at least 0.1 μm for a MCA (acetal resin) tightened to a torque of 8.5 Nm. Actual crevice

gaps are difficult to measure and the above value may or may not be representative of other plateau sites or other assemblies. A possibility exists that even tighter crevice gaps may be attainable.

Earlier mathematical modelling studies[13] indicated that with a crevice depth of 0.1 cm (crevice depth of MCA plateau), crevice gap values less than 0.1 μm were required for breakdown of passivity for AISI Type 304 and Type 316. Modelling also predicts that none of the six cast alloys in the present study will break down at 0.1 cm depth and 0.1 μm gap. However, as shown in Table VII, modelling with smaller gaps (same depth) yields predictions of a time to breakdown for CF8M, CN7M, CN7MS and IN-862. Breakdown is not predicted for the two high molybdenum containing nickel base alloys. As can be seen, this trend is consistent with the results of the 30 day MCA test at the 8.5 Nm torque level (Table III). Differences in predicted times to breakdown between IN-862 and the other three susceptible alloys may be indicative of the time difference required to achieve the respective CCS composition.

A decrease in the crevice assembly torque level would tend to produce somewhat wider crevice gaps. This, in turn, would affect the times to initiation as indicated by the results of the MCA test conducted at the 2.8 Nm torque level.

While extremely tight crevice gaps appear necessary for relatively shallow crevices (e.g., depth of MCA washer), wider crevice gaps may become more relevant when deeper crevices are considered.

Figure 4 shows a typical gasket/metal assembly prepared for scanning electron microscope determination of crevice gaps (i.e., crevice tightness). The surface roughness of the "flange" material and the asbestos and rubber gasketing materials are typical of many service applications. Figure 5 shows several views of the crevice gap attainable when tightened to a modest torque level of 2.8 Nm. Measurements at a number of locations around the outer edges revealed gaps ranging from as little as 0.1 μm to about 10 μm using both gasketing materials.

Table VIII gives additional results of mathematical modelling for the six cast alloys. Geometric input variables to the model included a number of gap values within the range of those indicated above and two crevice depths.

The mathematical model predictions are consistent with the known influence of crevice geometry. That is, the severity of crevice corrosion increases as depth increases and gap decreases (crevice becomes tighter). For a given gap dimension, increasing the crevice depth from 0.5 cm to 1.0 cm decreases the predicted time to breakdown. Conversely, for a given crevice depth, increasing the crevice gap increases the time to breakdown. For each alloy-crevice depth combination, there is a critical gap dimension above which breakdown is not predicted. For the widest gap considered (1.25 μm), none of the alloys modelled are predicted to initiate attack at either depth. As the gap is decreased, however, higher alloy contents are required for a model prediction of resistance. This can be seen for the 0.25 μm gap - 0.5 cm depth combination where breakdown is not predicted for IN-862 and the two nickel base alloys. Yet for a 0.125 μm gap, these highly resistant alloys are predicted to initiate attack at both crevice depths.

Again, the initiation results from the MCA tests are in general agreement with the trends identified by the mathematical modelling of other geometries. Cast alloy 625 is predicted to be more resistant than IN-862 which in turn is predicted to be more

resistant than the 2-3 percent molybdenum alloys. It should be emphasized, however, that while the MCA test may provide a ranking of alloys in terms of relative resistance to crevice corrosion, MCA test data can not be extrapolated to predict whether attack will occur under any given service condition unless that service condition duplicates the MCA test.

Crevice Corrosion Propagation Behavior

Depth of Penetration: The range of penetrations for crevice corrosion occurring beneath the grooved washers on each of the specimens is also given in Table IV. As can be seen, the ranges of penetration generally cover one to two orders of magnitude. These variations may be due, in part, to differences in initiation time at individual sites and are not uncommon for seawater tests of this type.[6,13,20] In the case of cast alloys which corrode preferentially, microstructural variations will also affect penetration. It is generally the maximum depth value which shows the greatest scatter. Less scatter is found at the lower end of the penetration range.

Table IX compares the average and maximum depths of penetrations for the various alloys. Again, results of the initial 30 day test indicate somewhat greater resistance for the higher alloyed materials. Average penetration values for CN7MS, CN7M and IN-862 are substantially lower than that determined for CF8M.

The data describe severe penetration for the four alloys which initiated under the described conditions. The progression of attack to the extent shown can be attributed not only to the rapid initiation but also to the limited area in which the crevice corrosion is confined. Also, it would appear that in the absence of accumulated biofouling, sufficient driving force from cathodic reduction reactions on the boldly exposed specimen surfaces was present to sustain the penetration. Penetrations reported for CN7M and CF8M tested under similar conditions are within the ranges of those determined in the present study.[7]

Electrochemical Assessment of Propagation Resistance

Slopes of the pH versus anodic peak current plots have been used as an indicator of the resistance to crevice corrosion propagation.[12] The higher the value of the slope the greater is the expected crevice corrosion penetration. Table X gives the slope of plots from Figure 2 for the six alloys. In the present study, CF8M and CN7MS exhibit the highest slope value and also show generally greater penetrations in the MCA tests than do CN7M and IN-862. Because no evidence of crevice initiation was found for cast alloy 625 and CW-12M-2, it is obviously difficult to assess the propagation resistance of these two alloys. The very low slope values indicated in Table X, however, suggest that if initiation were to occur any propagation for these two nickel base alloys would be considerably less than that described for the other materials.

Metallurgical Aspects of Crevice Corrosion Behavior

Effect of Molybdenum Content: It was previously shown in Table VI that the pH of the CCS decreased with increased molybdenum content. Figure 6 shows the predicted times to breakdown from the mathematical modelling (Table VIII) as a function of molybdenum content. It can be seen that while predicted times to breakdown increase with increasing molybdenum contents, crevice tightness (i.e., gap dimension) appears

to exert a far more dominant influence. Again, this dependency on crevice geometry helps explain the variability often observed in seawater crevice corrosion tests.

Sedriks[1] has indicated that a molybdenum content of about 6 percent in stainless type alloys is generally required to provide resistance to crevice corrosion beneath barnacle attachments in seawater. For more severe crevices, higher molybdenum contents are required. Oldfield and others have also emphasized the importance of crevice geometry/alloy chemistry relationships on the resistance to initiation.[12,16]

Morphology of Crevice Corrosion: Preferential corrosion of select phases of cast stainless steel and nickel base alloys has been previously correlated with corrosion behavior in non-marine environments. For example, Jones and Kain[23] described preferential attack of the austenitic matrix for CF8M exposed to 25% H_2SO_4 and 10% $FeCl_3$ environments. In the case of CN7M, preferential attack followed the dendritic areas in the microstructure of specimens which corroded in 10% $FeCl_3$. For IN-862, on the other hand, exposure in the above environment results in general attack related to specific crystal orientations as well as to selective attack around second phase particles.

Figures 7 to 9 show scanning electron micrographs of corroded crevice sites for the four susceptible alloys in the present seawater tests. In the case of CF8M, Figure 7, the austenitic structure corrodes preferentially. The enlarged micrograph shows the ferrite network typical of this material. For the most part, micrographs of CN7M and CN7MS (Figure 8) show similar dissolution of the dendritic areas as well as deeper attack at preferred sites which may be intermetallic particles along the interdendritic regions. The penetrations in CN7MS appear to be deeper than those in CN7M. The scanning electron micrographs for IN-862 (Figure 9) show the crystallographic orientation of attack within the dendrites and attack at sites of second phase particles. Despite the difference between the bulk seawater environment and the other environments described by Jones and Kain,[23] the morphology of attack is similar for the respective alloys. This is not surprising in view of the acidification process within the crevice area.

The preceding micrographs clearly show the limitations of conventional methods (i.e., depth gauge) for determining penetration in cast alloys. However, in light of the extensive corrosion incurred in the present tests, differences between measured and actual penetration may not be significant.

Cast versus Wrought Material

The critical crevice solution data for the cast alloys described herein indicate that a more acid solution is required for crevice corrosion initiation than for similar wrought materials.[12] Table XI compares the present results for CF8M with those for the wrought counterpart, AISI Type 316 stainless steel. The differences between the two product forms suggest that the cast version would be more resistant to initiation of crevice attack than the wrought material. This is supported by the accompanying MCA data describing the observed differences in initiation times.

Although the CCS tests indicate improved initiation resistance for the CF8M, the difference in propagation slope values suggests that it has less propagation resistance than Type 316. Again, the electrochemical indications are supported by the MCA test results. Distinct differences can be seen in the depth of penetration measurements provided.

SUMMARY AND CONCLUSIONS

The crevice corrosion resistance of several iron base and nickel base alloys in seawater has been investigated by means of the multiple crevice assembly test and mathematical modelling. Among parameters studied were the crevice assembly torque level and test duration. While two high molybdenum containing nickel base materials, cast alloy 625 and CW-12M-2, were found to be resistant in all tests, the remaining four stainless type alloys exhibited varying degrees of susceptibility. Decreased crevice assembly torque resulted in a trend toward longer times to initiation and, in some cases, increased data scatter. Decreased assembly torque had little effect on the overall incidence of crevice corrosion initiation. Increased test duration did not result in a significant increase in crevice corrosion initiation. Although IN-862 was found to be susceptible in the present series of investigations, the beneficial effects of its higher alloy content (e.g., 5% Mo) were apparent.

All four susceptible alloys in the MCA tests exhibited significant penetration in relatively short periods of time. Scanning electron microscopy showed some influence of microstructure on propagation behavior which correlated well with previous observations on corrosion in other media.

Electrochemical tests in simulated crevice solutions provided experimental input for mathematical modelling to study the effects of alloy composition and crevice geometry. The effects of crevice geometry have been previously shown to have a significant effect on the initiation resistance of stainless alloys. The present study combined the results of actual crevice geometry measurements (i.e., crevice gap determined by SEM examination) with the electrochemical data to identify conditions where resistance to crevice corrosion would be anticipated.

It must be recognized that significant differences exist between the geometric conditions assumed for the model and those encountered in service. For the model calculations, it is assumed that a uniform crevice gap exists over the entire crevice depth. In practice, this is highly unlikely as evidenced by the variation in gaps actually measured for rubber and asbestos assemblies. This may also help to explain the difference between reported service performance and MCA results.

While cast alloys, such as CF8M and CN7M, routinely exhibit crevice corrosion in seawater tests, there are many cases where these materials have performed satisfactorily in service. Resistance offered by pumps and valves of these materials can be often attributed to high velocity conditions which prevent marine attachments and also to cathodic protection frequently afforded by galvanic coupling with carbon steel piping. As an example, CN7M valves installed in seawater intake lines at the LaQue Center for Corrosion Technology, Inc. some 20 years ago are still in service today.

Seawater crevice corrosion tests can identify conditions which may cause crevice corrosion of stainless type alloys. The occurrence of crevice corrosion in these tests may not necessarily limit the use of the alloy if service conditions are less severe. Conversely, good service performance in one application should not necessarily become an endorsement for use in other applications.

REFERENCES

1. Sedriks, A. J., "Corrosion of Austenitic Fe-Cr-Ni-Mo alloys in Marine Environments," to be published in International Metals Reviews.

2. Tuthill, A. H., Schillmoller, C. M., "Guidelines for Selection of Marine Materials," An INCO publication, Originally Presented at the Ocean Science and Ocean Engineering Conference - Marine Technology Society, Washington, D.C., June 14-17, 1965.

3. Flint, G. N., "Resistance of Stainless Steels to Corrosion in Naturally Occurring Waters," Transactions of the 2nd Spanish Corrosion Congress.

4. LaQue, F. L., Marine Corrosion, Chapter 5, Wiley Interscience, John Wiley & Sons, Inc. (1975), 1975.

5. Kain, R. M., Lee, T. S., "Crevice Corrosion of Stainless Steels in Ambient and Elevated Temperature Seawater," Presented at 5th International Congress on Marine Corrosion and Fouling, Barcelona, Spain, May 1980.

6. Kain, R. M., "Localized Corrosion Behavior in Natural Seawater: A Comparison on Electrochemical and Crevice Testing of Stainless Alloys," CORROSION/80, Paper No. 74.

7. Jones, R. M. F., "Cast Stainless Steel for Chloride Environments," AFS Transactions, American Foundryman's Society, Vol. 81, pg. 349-352 (1973).

8. Jackson, R. P., Van Royen, D., Localized Corrosion - Cause of Metal Failure, ASTM, STP 516, pg. 210.

9. Oldfield, J. W., Sutton, W. H., British Corrosion Journal, Vol. 13, pg. 13 (1978).

10. Oldfield, J. W., Sutton, W. H., British Corrosion Journal, Vol. 13, pg. 104 (1978).

11. Bernhardson, et al., "Crevice Corrosion of Stainless Steels, Calculations of Concentrations and pH Changes," Presented at the 8th International Congress on Metallic Corrosion, Mainz, West Germany, 1981.

12. Oldfield, J. W., "Crevice Corrosion of Stainless Steels - The Importance of Crevice Geometry and Alloy Composition," Presented at 19th Journees de Aciers Speciaux, Staint-Etienne, May 1980.

13. Kain, R. M., "Crevice Corrosion of Stainless Steels in Seawater and Related Environments," CORROSION/81, Paper No. 200. Submitted for Publication to CORROSION.

14. Anderson, D. B., Galvanic and Pitting Corrosion, ASTM STP 576, pg. 261.

15. Sydberger, T., Werkstoffe and Korrosion, Vol. 32, p. 119-128 (1981).

16. Bernhardson, S., Mellstrom, R., "Stainless Steel for Seawater Service," Presented at the 5th International Congress on Marine Corrosion and Fouling, Barcelona, Spain, May 19-23, 1980.

17. Kovach, C. W., Redmerski, L. L., "Crevice Corrosion of Type 316 and Highly Alloyed Stainless Steels in Simulated Natural Environments Using the Multiple Crevice Assembly," CORROSION/81, Paper No. 123.

18. Krougman, J. M., Ijsseling, F., "Crevice Corrosion of Stainless Steels and Nickel Alloys in Seawater," Presented at the 5th International Congress on Marine Corrosion and Fouling, Barcelona, Spain, May 19-23, 1980.

19. Kain, R. M., "Crevice Corrosion Resistance of Austenitic Stainless Steels in Ambient and Elevated Temperature Seawater," CORROSION/79, Paper No. 230.

20. Kain, R. M., "Crevice Corrosion and Metal Ion Concentration Cell Corrosion Resistance of Candidate Materials for OTEC Heat Exchangers, Parts I and II, U.S. Department of Energy, Report No. ANL/OTEC-BCM-022.

21. Hack, H. P., "Crevice Corrosion Behavior of 45 Molybdenum Containing Stainless Steels in Seawater," To be presented at CORROSION/82, Houston, Texas.

22. "Properties and Selection: Stainless Steels, Tool Materials and Special Purpose Metals," Metals Handbook, Ninth Edition, Vol. 3, American Society for Metals (1980).

23. Jones, R. M. F., Kain, R. M., "The Effect of Microstructure on the Corrosion Resistance of Several Cast Alloys," CORROSION/75, Paper No. 67.

24. Oldfield, J. W., Lee, T. S., Kain, R. M., "Mathematical Modelling of Crevice Corrosion of Stainless Steels, Corrosion and Corrosion Protection," Corrosion and Corrosion Protection - H. H. Uhlig Birthday Symposium, Corrosion Division Proceedings, Vol. 81-8, The Electrochemical Society, pg. 213.

25. Crolet, J. L., Seraphin, L., Tricot, R., Revere Metallurgie, pg. 937 (1975).

TABLE I

Composition of Several Corrosion Resistant Cast Alloys

Alloy Designation		Chemical Analysis - Percent by Weight										
ACI	Other	C	Cr	Ni	Mo	Cu	Si	Mn	S	P	Fe	Other
CF8M	--	0.04	19.30	10.06	2.36	--	0.79	0.95	0.019	0.015	Bal.	--
CN7M	--	0.04	20.01	28.18	2.51	3.12	0.76	0.18	0.025	0.007	Bal.	--
CN7MS	--	0.05	19.37	22.10	2.93	1.55	3.00	1.00	0.010	0.006	Bal.	--
--	IN-862	0.03	20.92	24.46	5.00	--	0.52	0.47	0.009	0.007	Bal.	--
--	alloy 625	0.02	20.58	Bal.	8.53	--	0.01	0.20	0.011	0.006	3.62	3.48 Cb
CW-12M-2	--	0.01	18.10	Bal.	17.58	0.08	0.56	0.54	0.007	0.010	0.29	--

Alloy Casting Heat Treatments

Alloy	Heat Treatment
CF8M	1 hr at 1120°C and WQ
CN7M	1 hr at 1150°C and WQ
CN7MS	1 hr at 1150°C and WQ
Alloy 625	1 hr at 1150°C and WQ
IN-862	1 hr at 1160°C and WQ
CW-12M-2	2 hrs at 1125°C and WQ

WQ - Water Quenched

TABLE II

Seawater Hydrology*

	pH	Chloride (g/L)	Salinity (g/L)	Dissolved Oxygen (mg/L)
Initial 30 day test	7.9 to 8.1	19.5 to 20.1	35.1 to 36.3	5.8 to 7.4
Expanded Test Matrix				
60 days	8.0 to 8.2	18.9 to 19.5	34.1 to 35.2	5.0 to 6.1
90 days	8.0 to 8.2	18.9 to 19.5	34.1 to 35.2	5.0 to 6.3

* Weekly analyses of filtered seawater in controlled temperature test trough.

TABLE III

Observed Times to Initiation in Multiple Crevice Tests Conducted in 30°C Seawater*

Test Conditions	Time (hrs)	CF8M	CN7M	CN7MS	IN-862
8.5 Nm - 30 days	Earliest	87	87	87	87
	Average	87	87	87	145
	Deviation (n)	0(5)	0(5)	0(6)	59(2)
- 60 days	Earliest				109
	Average				162
	Deviation (n)				36(4)
Combined (8.5Nm)	Earliest				87
	Average				157
	Deviation (n)				45(6)
2.8 Nm - 30 days	Earliest	36	109	109	
	Average	97	321	109	
	Deviation (n)	27(6)	141(4)	0(6)	
- 60 days	Earliest	109	109	36	109
	Average	109	302	113	230
	Deviation (n)	0(6)	193(4)	40(6)	158(4)
Combined (2.8Nm)	Earliest	36	109	36	
	Average	103	312	111	
	Deviation (n)	19(12)	169(8)	28(12)	

(n) number of observations

* No evidence of crevice corrosion found on any of the cast alloy 625 and CW-12M-2 in test lasting up to 90 days at 8.5 Nm torque level.

TABLE IV

Expanded Matrix-Multiple Crevice Test Results for Several Cast Alloys*

Alloy	Test Conditions	No. of Sites Initiated		Penetration Range (mm)	
		Side 1	Side 2	Side 1	Side 2
IN-862	30 day-8.5 Nm	3	1	0.12 to 0.22	0.29
		9	13	0.24 to 0.72	0.18 to 0.91
		16	10	0.18 to 1.17	0.12 to 1.22
	60 day-8.5 Nm	6	7	0.20 to 1.75	0.25 0.68
		4	14	0.24 to 0.72	0.23 to 1.05
	60 day-2.8 Nm	7	8	0.17 to 0.99	0.30 to 0.68
		7	2	0.08 to 4.31	0.13 to 0.26
		7	8	0.15 to 1.23	0.15 to 0.86
CN7M	30 day-8.5 Nm	14	17	0.18 to 0.76	0.28 to 2.33
		18	18	0.29 to 1.03	0.22 to 0.91
		17	13	0.18 to 1.17	0.15 to 0.70
	30 day-2.8 Nm	17	17	0.04 to 1.27	0.28 to 1.95
		18	16	0.16 to 2.24	0.08 to 1.89
	60 day-2.8 Nm	15	1	0.20 to 2.00	0.42
		19	20	0.17 to 0.97	0.08 to 2.93
CN7MS	30 day-8.5 Nm	16	19	0.18 to 2.34	0.26 to 2.06
		19	14	0.14 to 3.82	0.17 to 1.46
		14	20	0.08 to 2.47	0.12 to 2.95
	30 day-2.8 Nm	15	19	0.10 to 3.01	0.15 to 2.37
		16	18	0.13 to 2.71	0.13 to 2.72
		20	18	0.20 to 3.18	0.13 to 2.20
	60 day-2.8 Nm	19	13	0.06 to 1.73	0.21 to 2.17
		20	19	0.10 to 3.53	0.11 to 2.67
		11	19	0.10 to 2.16	0.11 to 2.29
CF8M	30 day-8.5 Nm	12	14	0.19 to 0.69	0.16 to 3.06
		17	4	0.45 to 3.77	0.45 to 0.83
		17	10	0.27 to 3.13	0.33 to 2.28
	30 day-2.8 Nm	19	12	0.18 to 3.92	0.10 to 4.04
		20	12	0.23 to 3.22	0.24 to 3.59
		18	20	0.07 to 2.86	0.10 to 3.93
	60 day-2.8 Nm	15	18	0.06 to 2.03	0.17 to 3.08
		15	13	0.14 to 1.55	0.15 to 2.24
		15	12	0.13 to 3.59	0.07 to 1.31

* 30 day-8.5 Nm test results from initial investigation (after Hack[21])

TABLE V

Comparison of the Incidence of Crevice Corrosion in Multiple Crevice Tests

Test Conditions	Mean No. of MCA Sites Initiated on Each Specimen (20 max/side)*					
	2-3% Mo			5% Mo	8% Mo	
	CF8M	CN7M	CN7MS	IN-862	alloy 625	CW-12M-2
8.5 Nm - 30 days	12(5)	16(2)	17(2)	9(5)	0	0
8.5 Nm - 60 days	+	+	+	8(4)	0	0
8.5 Nm - 90 days	+	+	+	+	0	0
2.8 Nm - 30 days	17(4)	17(1)	18(2)	+	+	+
2.8 Nm - 60 days	15(2)	14(6)	17(4)	7(2)	+	+

* Numbers in parenthesis indicate standard deviation.

\+ Not tested

TABLE VI

Critical Crevice Solutions Derived from Electrochemical Tests

Alloy	Percent Cr	Percent Mo	CCS Concentrations pH	CCS Concentrations Chloride (M)
CF8M	19	2.5	1.30	4.5
CN7MS	19	3.0	1.25	4.5
CN7M	20	2.5	1.25	4.5
IN-862	21	5.0	0.80	6.0
Cast alloy 625	21	8.5	0.30	6.0
CW-12M-2	18	17.5	0.10	6.0

TABLE VII

Mathematical Modelling Predictions Based on MCA Geometry Inputs*

Alloy	Predicted Hours to Breakdown in Non-metal to Metal Crevice Gap	
	0.1 μm	0.01 μm
CF8M	No Breakdown	8
CN7M	"	8
CN7MS	"	8
IN-862	"	130
alloy 625	"	No Breakdown
CW-12M-2	"	"

* crevice depth 0.1 cm

TABLE VIII

Effect of Crevice Geometry on the Predicted Time to Breakdown for Several Cast Alloys in Seawater

Alloy	Crevice Depth (cm)	Predicted Hours to Breakdown in Non-metal to Metal Crevice Gap			
		0.125 μm	0.250 μm	0.500 μm	1.250 μm
CW-12M-2	0.5	791	NB	NB	NB
	1.0	191	465	NB	NB
alloy 625	0.5	284	NB	NB	NB
	1.0	149	342	NB	NB
IN-862	0.5	147	NB	NB	NB
	1.0	106	232	590	NB
CN7MS	0.5	83	254	NB	NB
	1.0	70	147	333	NB
CN7M	0.5	80	238	NB	NB
	1.0	68	143	322	NB
CF8M	0.5	85	261	NB	NB
	1.0	71	149	338	NB

NB - No breakdown.

TABLE IX

Crevice Corrosion Propagation Resistance

Test Conditions	Depth of Crevice Penetration (mm)											
	CF8M		CN7MS		CN7M		IN-862		alloy 625		CW-12M-2	
	avg.	max.	avg.	max.	avg.	max.	avg.	max.	avg.	max.	avg.	max.
8.5 Nm-30 days	0.97	3.77	0.59	3.82	0.50	2.33	0.42	1.22	0	0	0	0
-60 days	+	+	+	+	+	+	0.63	1.75	0	0	0	0
-90 days	+	+	+	+	+	+	+	+	0	0	0	0
2.8 Nm-30 days	0.63	4.04	0.75	3.18	0.60	2.24	+	+	+	+	+	+
-60 days	0.83	3.59	0.58	3.53	0.66	2.93	0.52	4.31	+	+	+	+

+ Not tested

TABLE X

Slopes of pH Versus Anodic Peak Current Plots*

Alloy	$\frac{d(\log I_{peak})}{dpH}$
CF8M	1.9
CN7MS	1.8
CN7M	1.4
IN-862	1.4
Cast alloy 625	0.3
CW-12M-2	0.3

*after Figure 2

TABLE XI

Comparison of Initiation and Propagation Resistance of Cast and Wrought Versions of Type 316 Stainless Steel

	Electrochemical Tests				Multiple Crevice Tests*			
	CCS Concentration		d (log I peak)		Initiation Time (hrs)		Depth of Penetration (mm)	
	pH	Cl⁻(M)	dpH		Earliest	Avg.	Avg.	Max.
CF8M	1.3	4.5	1.9		87	87	0.97	3.77
AISI Type 316	1.65	4.0	1.3	Test 1	6	122	0.45	0.88
				Test 2	15	56	0.61	1.93
				Combined	6	89	0.53	1.93

*All 30 days exposures in 30°C, low velocity filtered seawater. Crevice assembly torque is 8.5 Nm.

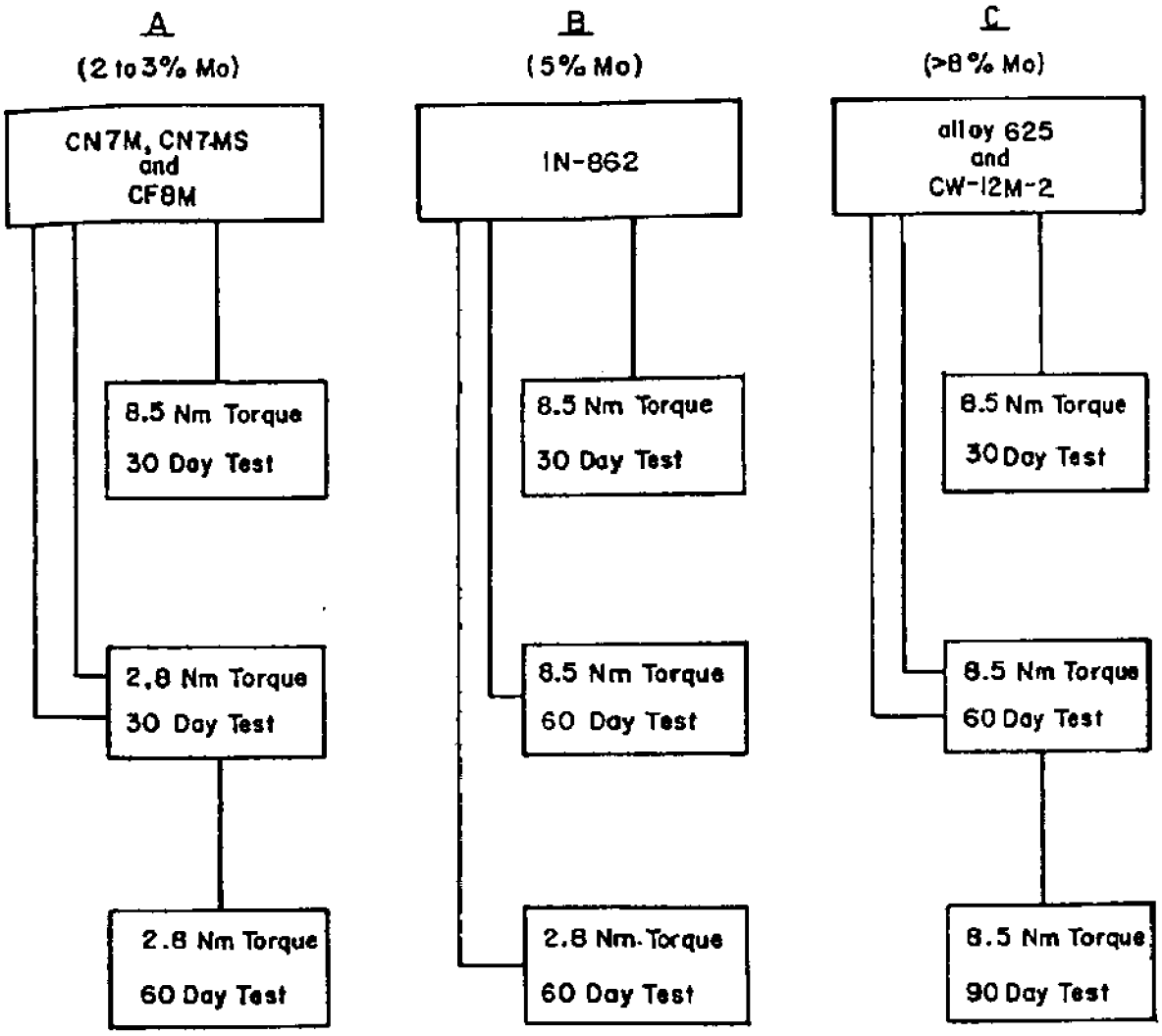

Figure 1. Multiple crevice assembly test matrices for evaluating several cast alloys in low velocity, filtered seawater at 30°C.

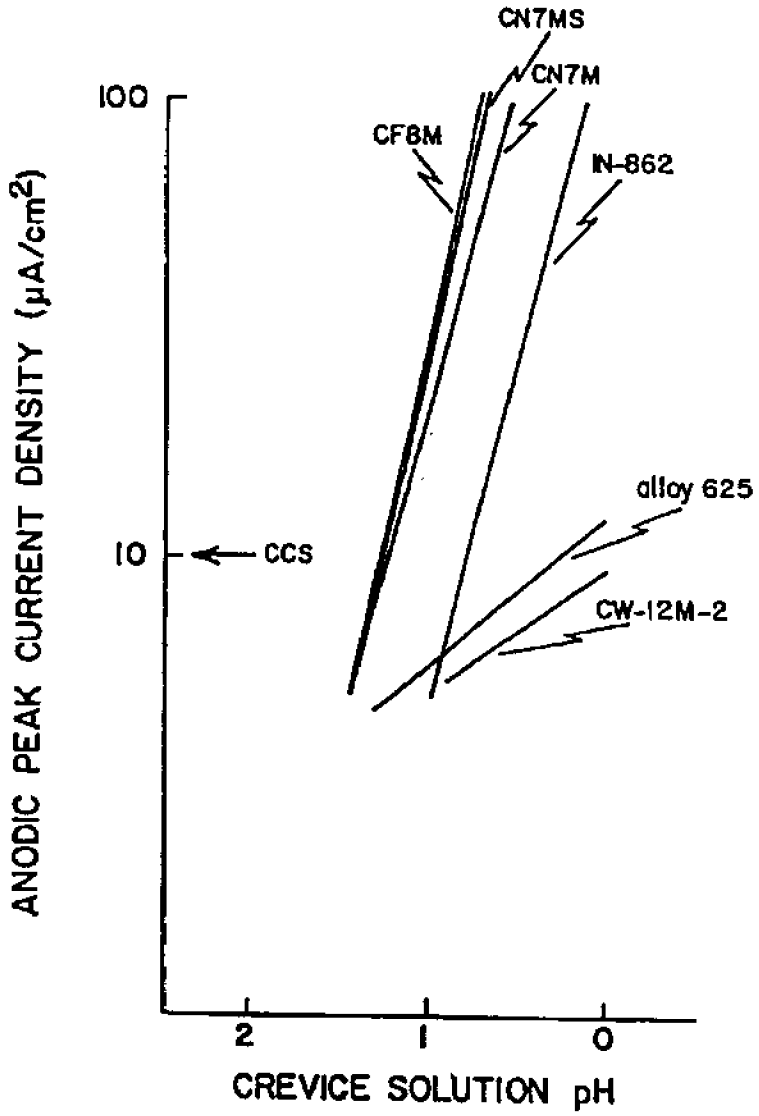

Figure 2. Plot of anodic peak current density versus simulated crevice solution pH used to determine composition (pH) of CCS according to the 10 $\mu A/cm^2$ criterion.

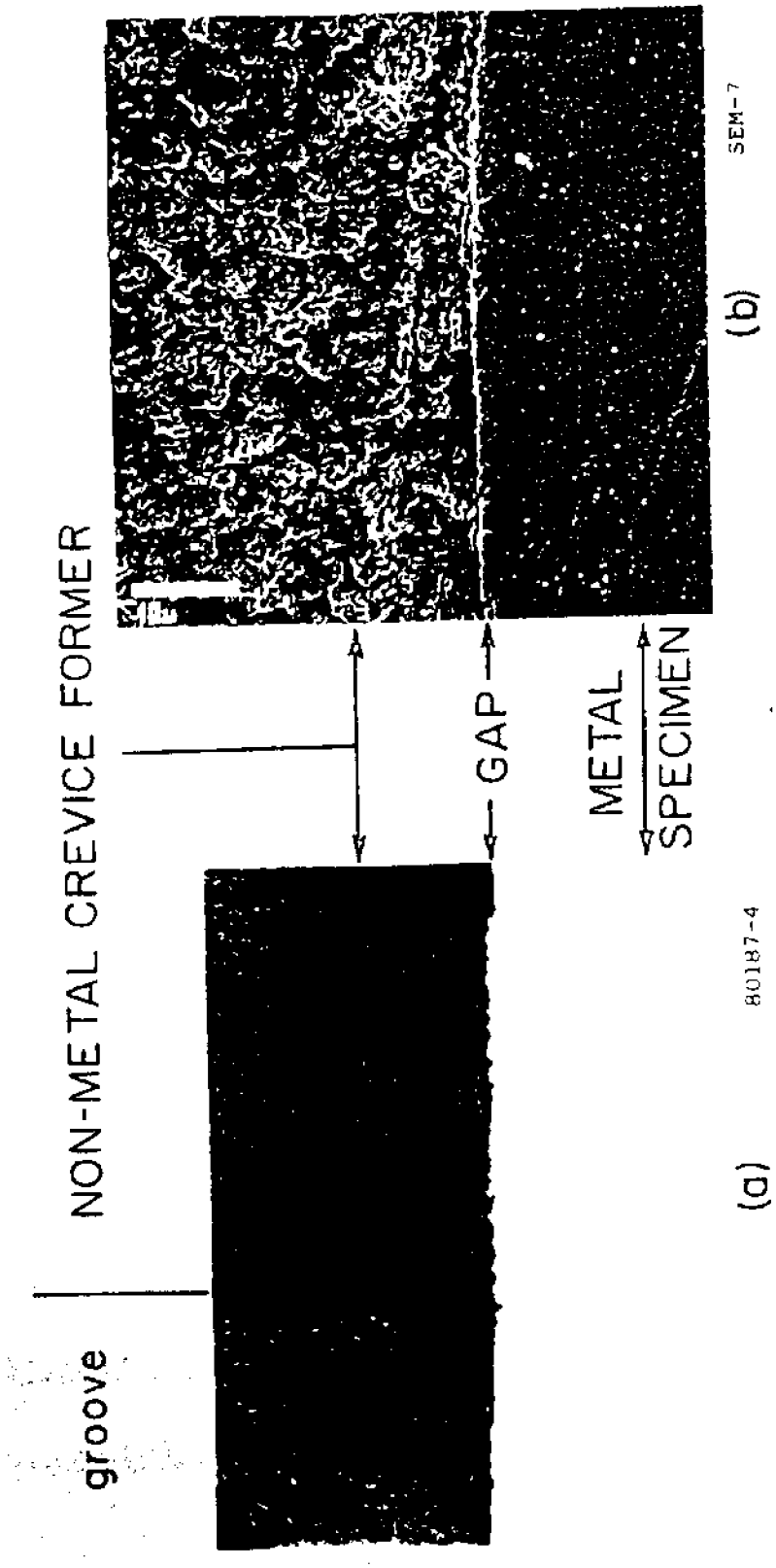

Figure 3. Cross-sectional view of crevice formed by plateau of non-metallic multiple crevice washer fastened to stainless steel specimen: a) photomicrograph, original magnification 400X, b) scanning electron micrograph.

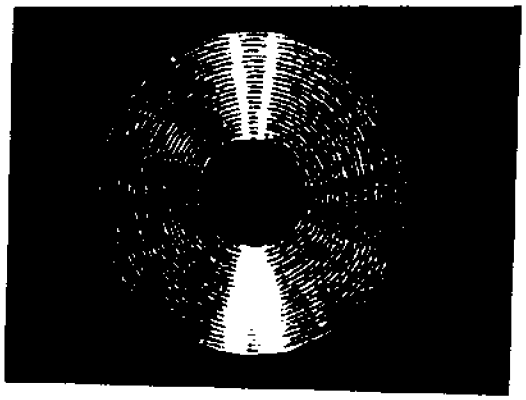

81079-2A

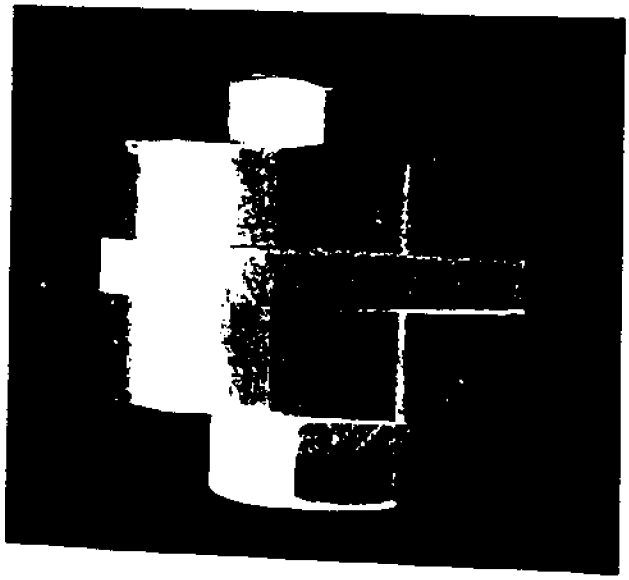

81079-6A

Figure 4. Surface finish (~125 RMS: machine turned) provided for metal component (top) and completed assembly prepared for scanning electron microscope examination of crevice gaps. 2.5X

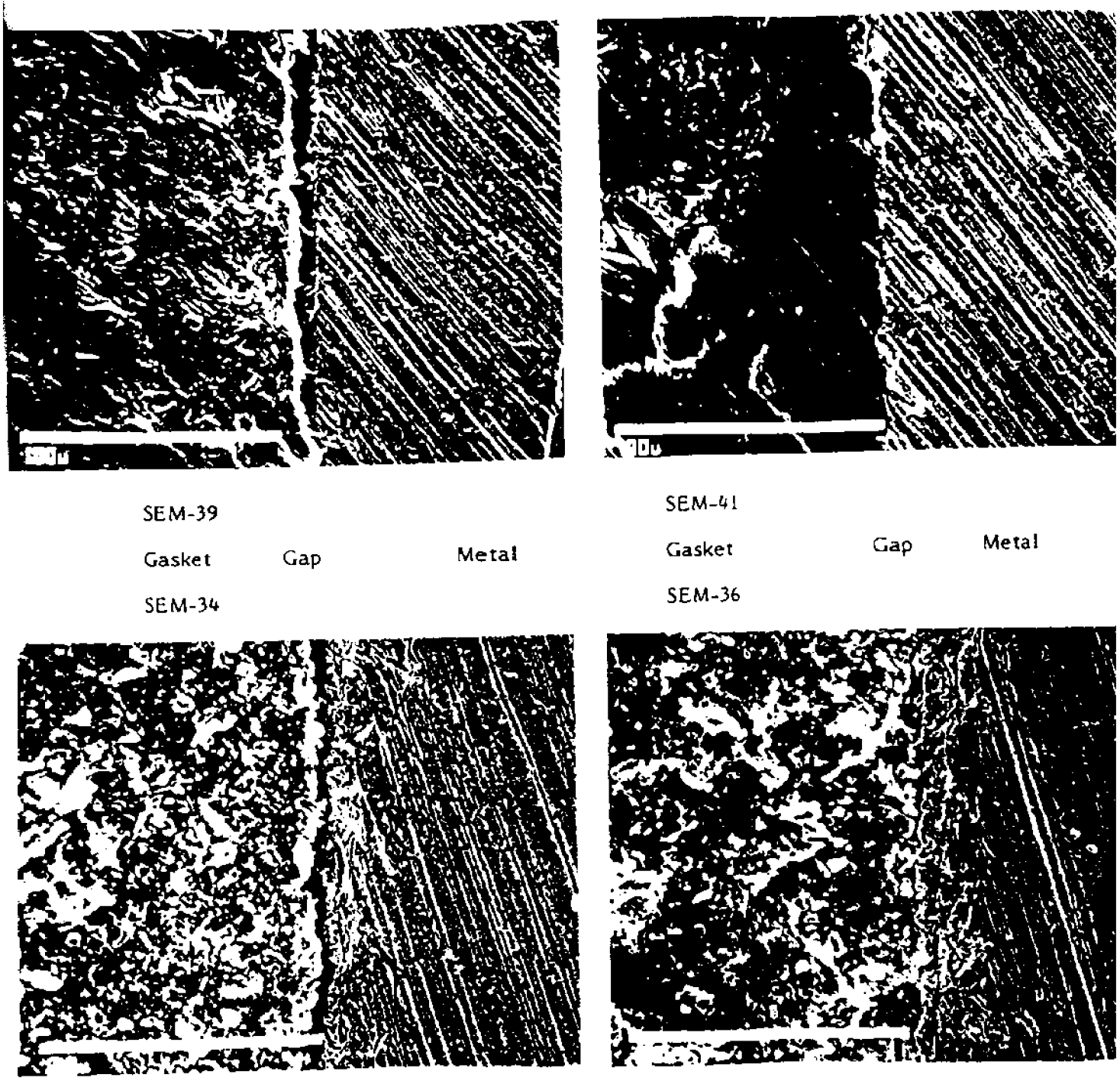

Figure 5. Scanning electron micrographs showing variations in crevice gap for asbestos gasket/stainless steel (top left and right) and rubber gasket/stainless steel (bottom left and right) assemblies at 2.8 Nm torque level.

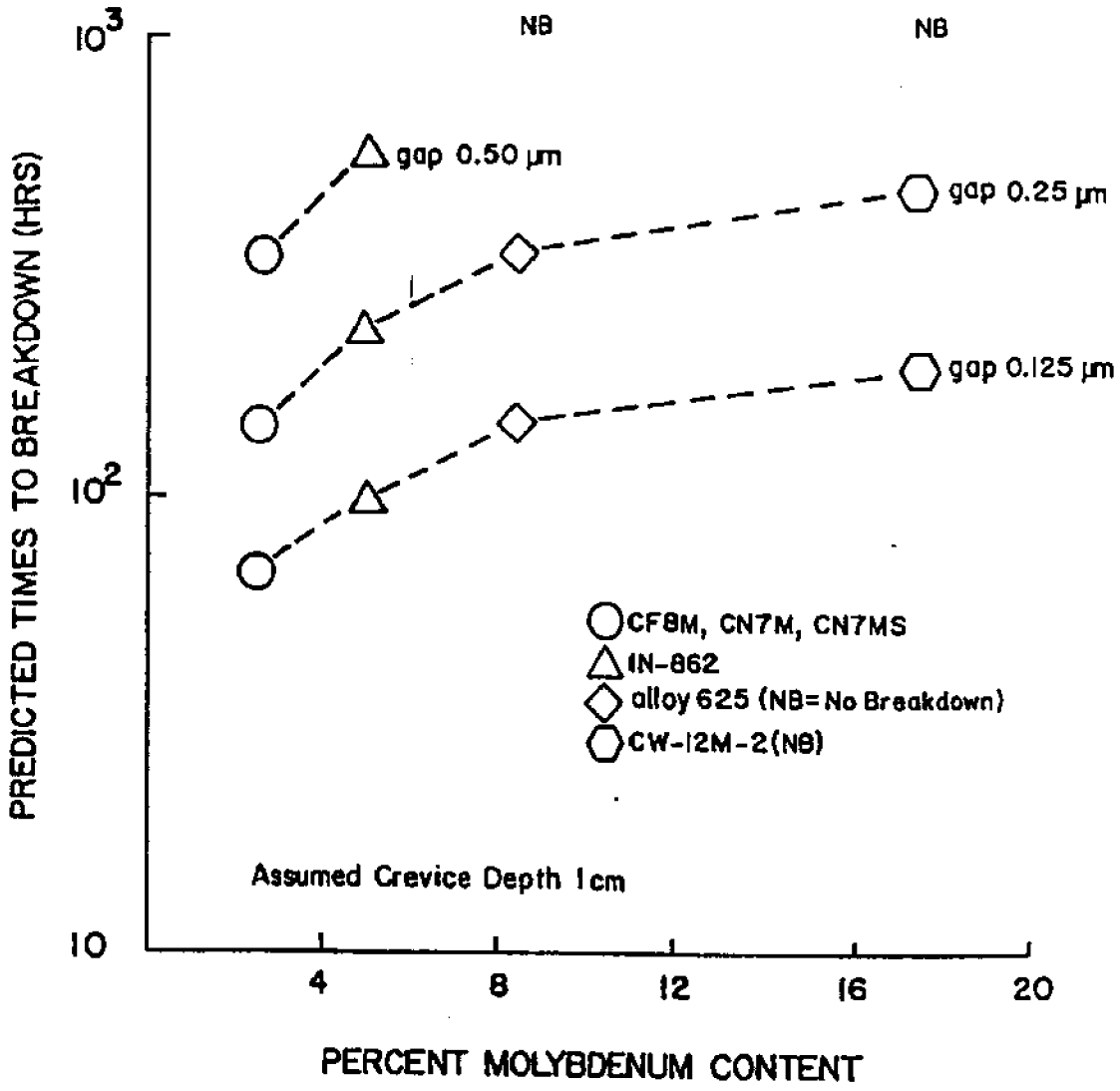

Figure 6. Predicted time to breakdown for several cast alloys in seawater as a function of molybdenum content: mathematical modelling for non-metal to metal crevice geometries.

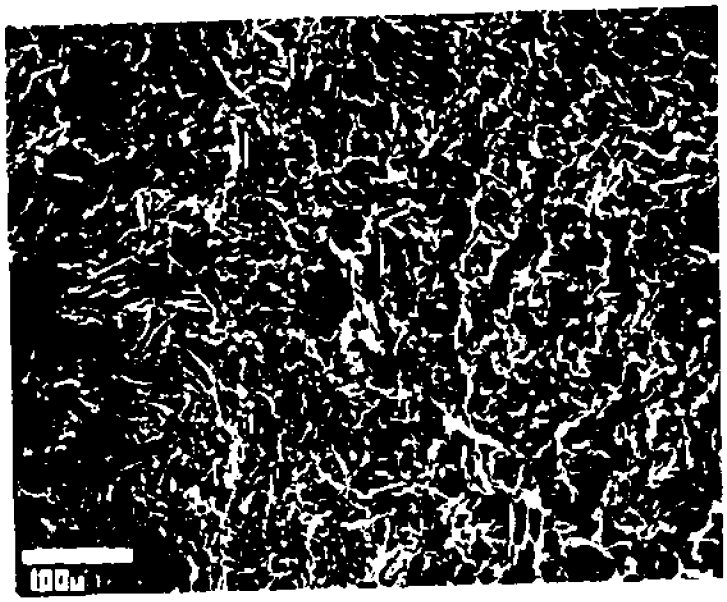

SEM-74

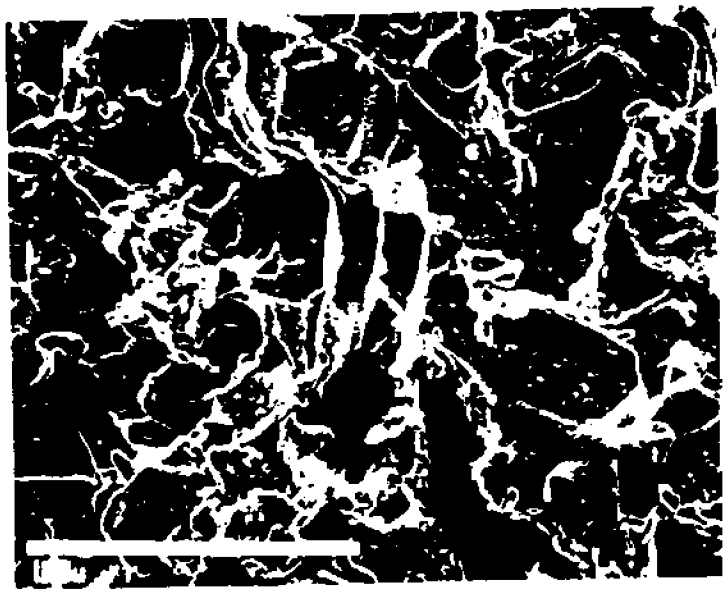

SEM-75

Figure 7. Scanning electron micrographs of CF8M showing preferential corrosion of austenite matrix at initiated crevice sites.

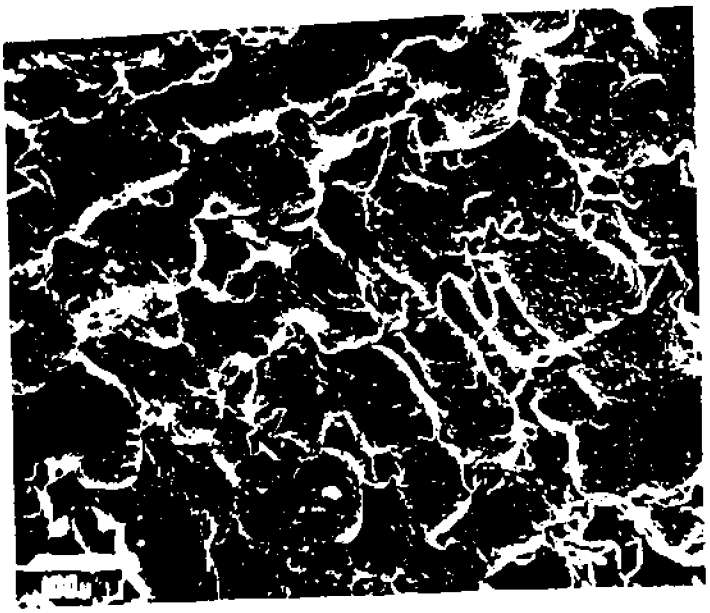

a) SEM-63

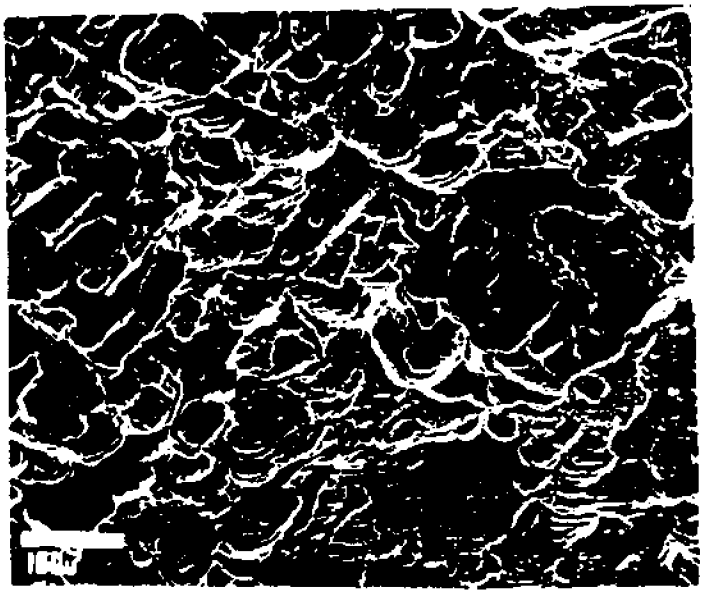

b) SEM-69

Figure 8. Scanning electron micrographs of corroded crevice sites for CN7M (a) and CN7MS (b).

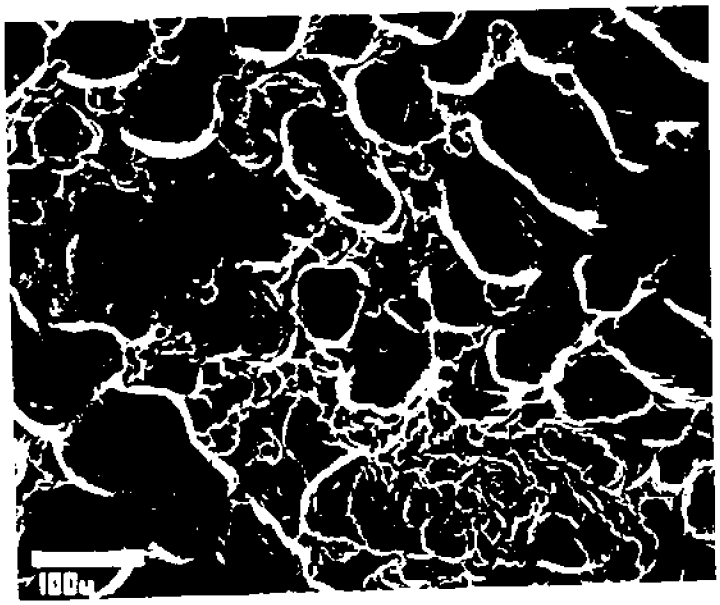

SEM-76

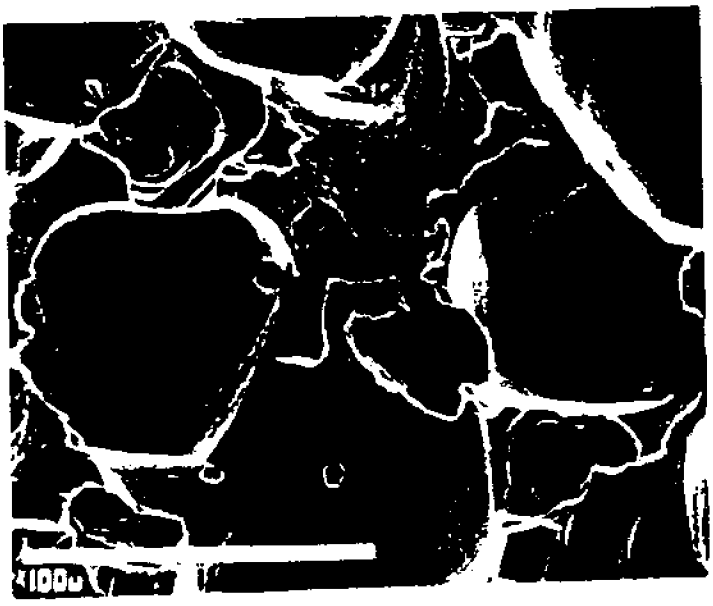

SEM-77

Figure 9. Scanning electron micrographs of IN862 showing preferred orientation of corrosion at initiated crevice sites.

III.C.

CREVICE CORROSION RESISTANCE OF TYPE 316 STAINLESS STEEL IN MARINE ENVIRONMENTS

By

R. M. Kain

and

T. S. Lee

To Be Presented At

9th International Congress on Metallic Corrosion
Toronto, Canada, June 3-4, 1984

LaQUE CENTER FOR CORROSION TECHNOLOGY, INC.
POST OFFICE BOX 656
WRIGHTSVILLE BEACH, NORTH CAROLINA 28480
(919) 256-2271

CREVICE CORROSION RESISTANCE OF TYPE 316 STAINLESS STEEL IN MARINE ENVIRONMENTS

R. M. Kain and T. S. Lee
LaQue Center for Corrosion Technology, Inc., Wrightsville Beach, NC 28480

J. R. Scully
David W. Taylor Naval Ship, R&D Center, Bethesda, MD 20084

ABSTRACT - Because of its two percent molybdenum content, Type 316 stainless steel has long been a material specified for service in chloride-containing environments. Its improved resistance to pitting and atmospheric corrosion, as compared with Type 304 and other stainless steels, is well documented. However, in seawater, the presence of crevices, such as those created by the attachment of barnacles or other sources, may severely limit the alloy's utility. Crevice corrosion resistance of Type 316 as determined from reported laboratory tests and service experience in marine environments ranging from aggressive coastal atmospheres to low velocity seawater and diluted seawater typical of some estuarian conditions is reviewed.

INTRODUCTION

There are many stainless steels which have been developed in recent years for service in marine environments. These alloys have evolved from AISI standard grades and generally have higher alloying contents of molybdenum, chromium and nickel. There are, however, standard grades of stainless steel which have seen application in chloride-containing environments. In some cases, these applications have been successful while, in others, the materials have not given satisfactory service. In seawater environments, the principal mode of corrosion failure of stainless steels is crevice corrosion.

This paper describes the crevice corrosion resistance of a standard stainless steel which has been frequently employed in chloride environments. The behavior of Type 316 stainless steel is reviewed in terms of the principal factors which affect crevice corrosion including crevice geometry, environmental factors, metallurgical factors and electrochemical factors.

All natural exposure tests were conducted at the LaQue Center for Corrosion Technology, Inc. at Wrightsville Beach and Kure Beach, NC. Except for tests involving alloy modifications (Mn and S levels), all other data are for commercially produced material of nominal composition. Details of various test procedures using multiple crevice assemblies and other crevice formers and electrochemical techniques for determination of anodic polarization behavior and critical crevice solution (CCS) concentrations are described elsewhere.[1-3] Also, the various inputs and outputs of the mathematical model of crevice corrosion which is utilized in the current work are discussed in detail in previous articles.[4,5]

EFFECTS OF CREVICE GEOMETRY

Utilization of the recently developed mathematical model of crevice corrosion[3,4] has provided insight into the factors affecting the resistance of stainless steels and related iron base and nickel base alloys in chloride containing environments. Among these factors, the impact of crevice geometry variables, such as crevice depth and particularly crevice gap, is of topical interest. It has long been recognized that if crevices are unavoidable, they should be kept as open and as shallow as possible. However, it is only recently that the criticality of these dimensions has been explored.

Mathematical modelling and scanning electron microscopy of actual crevices[6,7] indicate that differences in alloy performance from one application to another can probably be attributed to differences in the type and geometry of the crevice former. It has also been suggested[6,8] that variability in laboratory tests might be explained by relatively minor differences in the actual crevice gap as affected by the degrees of flatness and tightness between the subject material and the crevice former. In some cases, the model predicts that a variation in crevice gap by a fraction of a micron could be the difference between resistance and susceptibility for a given alloy/environment combination.

Earlier mathematical modelling has shown the beneficial effects of increased crevice gap and decreased crevice depth on the predicted crevice corrosion initiation resistance of Type 304 and Type 316 in seawater.[1] Additional modelling covering a broader range of conditions of practical significance has been conducted for several alloys including Type 316.[7] Figure 1 summarizes predictions of crevice geometries where Type 304, Type 316 and Type 317 stainless would be expected to be resistant to crevice corrosion. These geometries are those combinations of gap and depth above and to the left of the line for each alloy.

The various combinations of crevice depths and crevice gap which were modelled cover 196 combinations. The depth dimensions are applicable for either open or blind crevices as depicted schematically in Figure 2. Similarly, the gap dimensions apply to both non-metal to metal crevices and metal to metal crevices as shown in Figure 2. Metal to metal crevice geometries result in the introduction of metal ions into the crevice solution from both surfaces. Thus a metal to metal crevice of twice the gap dimension of a non-metal to metal crevice will result in the same ultimate

crevice environment chemistry and equivalent times to initiation of crevice corrosion.

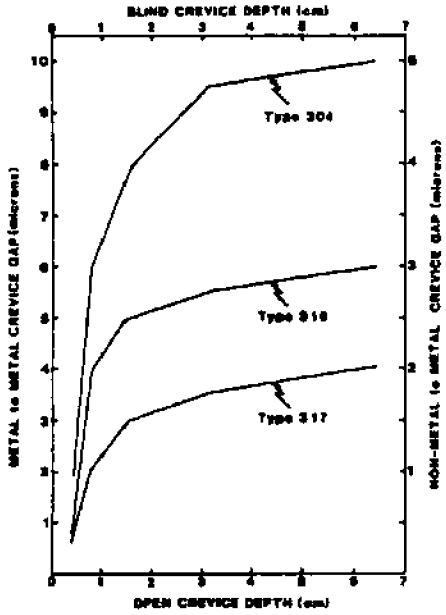

Figure 1. Predicted geometric conditions for resistance (above and to the left of the line for each alloy) and susceptibility (below and to the right of each line) to crevice corrosion.

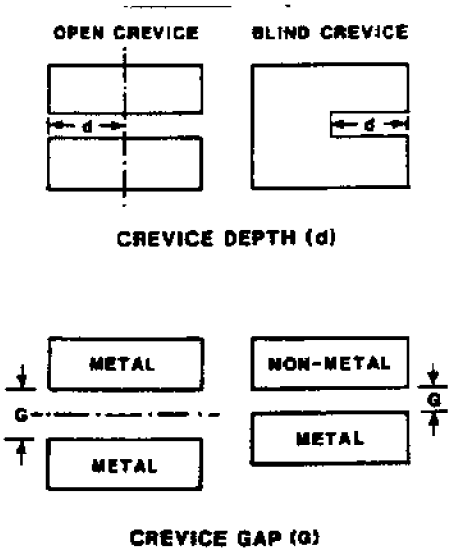

Figure 2. Schematic of crevice geometry factors.

In reviewing the data in Figure 1, it is clear that an alloy ranking of relative alloy resistance is possible. Type 304 stainless steel is predicted to be susceptible to crevice corrosion over the broadest range of crevice geometry conditions. Type 317 stainless steel is shown to be susceptible over the smallest range of conditions. The performance of Type 316 stainless steel lies between these two materials, but is more nearly like Type 317 in expected performance. For the range of crevice gaps and depths considered, Type 316 is predicted to be resistant to crevice corrosion for nearly half of the geometry combinations modelled.

ENVIRONMENTAL EFFECTS

Resistance to Dilute Seawater

Type 316 stainless steel has been frequently utilized for service in brackish waters of varying chloride concentrations. A greater degree of resistance to crevice corrosion would be expected with decreased chloride levels in the bulk environment. However, actual resistance would be dependent, in part, on the severity of the crevice geometry present. Mathematical modelling predictions indicate that as the bulk chloride level increases, crevice corrosion initiation of Type 316 (as well as others) is likely to occur over a broader range of geometric conditions.[1]

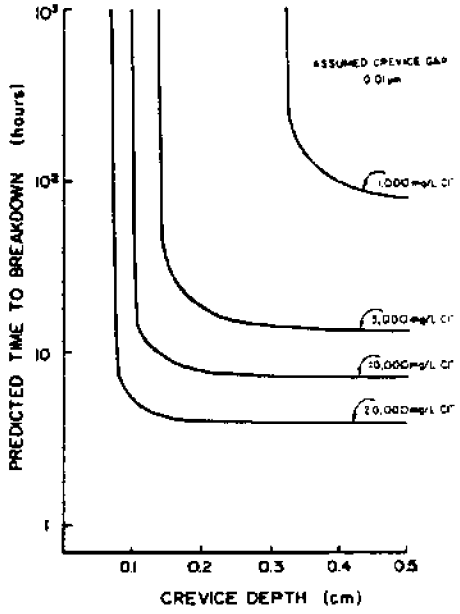

Figure 3. Effect of crevice geometry and bulk environment chloride concentration on resistance of Type 316 stainless steel.

Figure 3 describes the relationship between bulk chloride concentration and crevice depth on the predicted resistance of Type 316 stainless steel with a fixed crevice gap geometry. Under severe conditions, i.e., crevice depth of 0.5 cm, initiation is predicted over the full range of chloride concentrations considered. Time to breakdown is shown to decrease with increased chloride concentration. It can also be seen that for each chloride concentration, some critical value of crevice depth exists where initiation is no

longer predicted (i.e., depth values less than those indicated by the vertical segment of the curves). In contrast to a critical depth of about 0.3 cm in dilute seawater at 1,000 mg/L Cl^-, the critical depth dimension is predicted to be to less than 0.1 cm in full strength seawater (~20,000 mg/L Cl^-). For a given chloride concentration, the degree of propagation would also be governed by crevice geometry and its effect on crevice solution concentration.

Results of multiple crevice assembly tests in dilute seawater environments in the 1,000 to 10,000 mg/L chloride range indicate depths of penetration for Type 316 to be an order of magnitude less than the penetrations incurred in full strength (~19,000 mg/L Cl^-) seawater.(1) Additional studies in seawater diluted by 10 and 25 percent indicate behavior similar to that typically identified in full strength seawater, but with some slight decrease in the maximum depth of attack. The combined data, shown in Figure 4, suggest that some critical dilution level may exist which contributes to an abrupt change in propagation behavior.

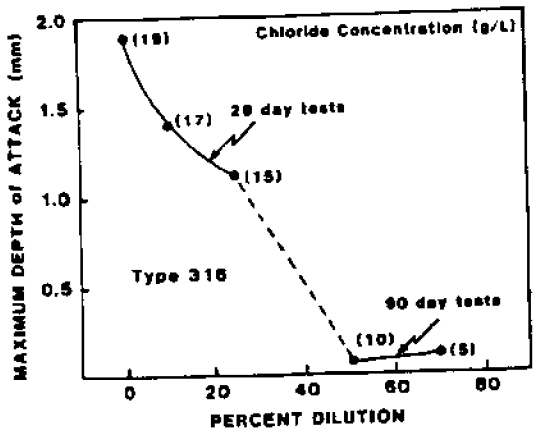

Figure 4. Effect of seawater dilution on crevice corrosion penetration.

Atmospheric Crevice Corrosion Behavior

While stainless steels offer considerably greater resistance to general atmospheric corrosion than ordinary steel, rust staining and mild pitting can be expected for some grades in aggressive coastal environments.(9) For this reason, Type 316 stainless steel with its beneficial two percent molybdenum content is frequently recommended. Little information, however, appears in published literature documenting the alloy's resistance to crevice corrosion under atmospheric conditions. This would be of concern in such applications as coastal construction, surface cargo containers and offshore platforms where crevices are likely to be created during fabrication and assembly.

To develop some insights into the behavior of Type 316, a series of crevice corrosion tests were conducted at distances of 25 and 250 meters from the ocean at Kure Beach, NC. Using both multiple crevice assemblies and an acrylic crevice former, crevice corrosion was detected within ten weeks for both Type 316 and Type 304 panels exposed at the two locations. While the extent of rust staining emmanating from beneath the crevice formers was greatest for Type 304 in the 25 meter lot, both materials exhibited a similar appearance in the 250 meter lot at that time.

After six months, crevice corrosion was found beneath all crevice assemblies (skyward and groundward sides) for both alloys in the two test locations. In the case of the multiple crevice assembly tests, corrosion initiated at all 20 available sites beneath each washer in the 25 meter lot exposures. Overall, slightly fewer sites, particularly for Type 316, corroded in the 250 meter lot exposures.

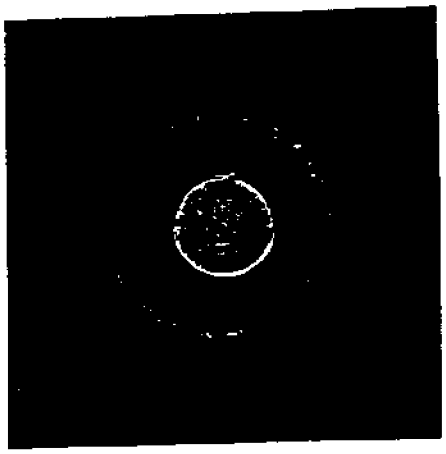

Figure 5. Crevice corrosion incurred by Type 316 stainless steel in 6 month test in the 25 meter marine atmospheric test lot.

While corrosion at the smaller, multiple crevice assembly sites was generally uniform, corrosion beneath the acrylic crevice formers occurred as discrete pits along with some uniform dissolution. Figure 5 shows a view of one of the acrylic washer crevice sites for Type 316 exposed in the 25 meter lot. This localized behavior is consistent with service experience for Type 316. Figure 6 shows examples of the extent of crevice corrosion found at metal-to-metal lap joints of Type 316 test rack frames with over 10 years exposure in the 25 meter lot at Kure Beach.

Table I summarizes the maximum depth of penetration for the various alloy/environment/crevice former combinations. For the acrylic washer tests, maximum depths of pitting within the crevice are indicated in parentheses. Approximately 80 percent of the pit depth measurements were <0.01 mm. Likewise, more than 80 percent of corroded multiple crevice assembly sites measured <0.01 mm in depth. Regardless of the type of crevice former or mode of attack, penetration was generally limited to a few hundredths of a millimeter.

From the penetration data, little difference in resistance can be discerned between Type 316 and Type

304. Results from the multiple crevice assembly tests, however, clearly quantify differences in penetration as a function of distance from the ocean.

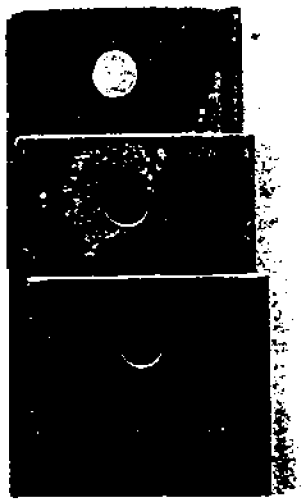

Figure 6. Crevice corrosion at test rack lap joints after 10 years service in the 25 meter marine atmospheric test lot.

TABLE I
Crevice Corrosion Penetration Resistance Exhibited by Type 316 and Type 304 Stainless Steels in Six Month Exposures at Kure Beach

		Maximum Depth of Penetration (mm)			
		Acrylic Crevice Washers[1]		Multiple Crevice Assemblies	
Test Site	Alloy	Sky-ward	Ground-ward	Sky-ward	Ground-ward
25m	Type 316	0.02 (0.02)	0.02 (0.02)	0.03	0.02
25m	Type 304	0.01 (0.03)	0.01 (0.04)	0.03	0.02
250m	Type 316	0.01 (0.02)	0.01 (0.02)	0.01	0.01
250m	Type 304	0.01 (0.01)	0.01 (0.02)	0.01	0.01

(1) pit depth measurements in parentheses

In comparison to exposure in seawater where depths of crevice corrosion can exceed 1 mm in 30 days (Figure 4), crevice corrosion of Type 316 stainless steel (as well as other stainless steels) in marine atmospheres is orders of magnitude less severe under similar crevice formers. This can be attributed to a lack of any substantially effective cathodic surface due to the high electrical resistance of surface moisture films during time of wetness as well as the absence of any continuous aqueous environment in drier periods.

METALLURGICAL EFFECTS

Effect of Mn and S Levels

Decreased levels of manganese and sulfur in stainless steel have been reported to contribute to increased pitting.[10] Improved resistance to initiation of crevice corrosion by lowering the manganese content to 0.2 percent has also been reported.[11] Such reductions correspond to the same positive effect obtained by the addition of at least 1.5 percent molybdenum. To further assess the effects of Mn and S levels on expected seawater crevice corrosion behavior, a series of tests were conducted.

One test involved an electrochemical determination of the critical crevice solution (CCS) composition required to initiate crevice corrosion.[3] In this test, an alloy is defined as being more resistant if the CCS is at a lower pH/higher chloride value. Table II summarizes CCS values for several alloys of varied Mn and S levels.

TABLE II
Critical Crevice Solutions for Stainless Steels

	Percent Content		Critical Crevice Solutions (CCS)	
Alloy	Mn	S	pH	Cl^-(M)
Type 304	0.16	0.005	2.00	1.5
	0.18	0.017	2.05	1.5
	1.20	0.006	2.00	1.5
	1.11	0.015	2.10	1.5
Type 316	0.18	0.003	1.70	3.5
	0.25	0.014	1.70	3.5
	1.48	0.004	1.65	3.5
	1.46	0.019	2.05	2.5
20Cr-25Ni-4.5Mo-1.5Cu	1.48	0.004	1.35	4.5
	0.18	0.013	1.30	4.5

In the case of Type 304, relatively little difference in the CCS composition can be seen as a function of Mn and S levels. A slightly higher pH, however, is noted for the high Mn-high S version (i.e., less resistant). While generally similar findings were determined for Type 316, a more substantial difference is shown between the CCS for the high Mn-high S heat and that for the other Mn-S combinations. Reducing Mn and S levels in the 20Cr-25Ni-4.5Mo-1.5Cu alloy had no significant effect on CCS composition.

The CCS values identified in Table II were used as inputs for mathematical modelling. Figure 7 gives modelling predictions for the times to crevice corrosion initiation as a function of crevice geometry. In this example, crevice depth (0.1 cm) is fixed and crevice gap or tightness for a non-metal to metal assembly is

varied. Alloy resistance is compared for high Mn-high S and low Mn-low S heats of Type 304 and Type 316. Predictions for the two heats of the 20Cr-25Ni-4.5Mo-1.5Cu alloy having similar CCS values are typified by one curve.

These curves indicate that as crevice gap is increased, the time to initiation of crevice corrosion is increased. For each material, some crevice gap exists where crevice corrosion is no longer predicted. For both Type 304 and Type 316, it can be seen that the high Mn-high S versions are predicted to be susceptible to corrosion over a wider range of tight crevices than the corresponding low Mn-low S version. In this regard, the beneficial effects of decreased Mn and S content are more pronounced for Type 316. As shown, the resistance of the low Mn-low S heat of Type 316 approaches the resistance of the higher alloyed stainless steel.

The modelling predictions in Figure 7 also show that for extremely tight crevices (e.g., 0.01 m gap), any effect of alloy content would be less noticeable. This was confirmed in actual tests conducted in 25°C, filtered seawater. Evidence of ongoing crevice corrosion beneath multiple crevice assemblies fastened to 5 cm x 5 cm specimens was detected for all materials within three days of exposure. After ten days, all materials, regardless of Mn and S levels, exhibited substantial penetration as indicated in Table III.

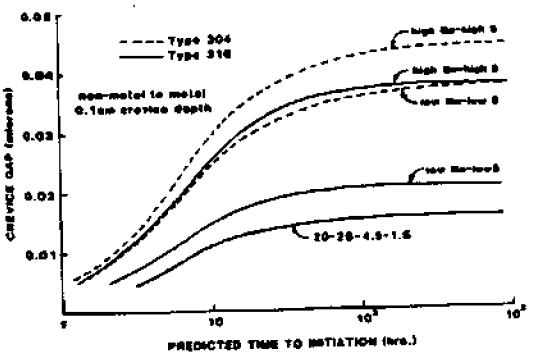

Figure 7. Effect of alloy Mn and S content on resistance to crevice initiation.

Variations in depth of penetration can be attributed to differences in the actual time to crevice corrosion initiation at individual sites beneath the multiple crevice assemblies, as well as site to site differences in the crevice solution concentration. Less severe crevice geometries than those created in the multiple crevice assembly test may allow for greater distinction of any positive effect of controlled Mn and S levels. However, since it is unlikely that crevice geometry can be controlled to the extent suggested by mathematical modelling, differences in behavior from one application to another should be expected.

TABLE III
Range of Crevice Corrosion Penetration in Ten Day Multiple Crevice Assembly Tests in 25°C Filtered Seawater

Mn-S Variation	Depth of Penetration (mm) Type 316	Type 304	20Cr-25Ni-4.5Mo-1.5Cu
Low Mn-Low S	0.01 to 0.48	0.02 to 0.51	--
Low Mn-High S	0.02 to 0.48	--	0.05 to 0.56
High Mn-Low S	0.01 to 0.60 0.01 to 0.38	0.05 to 0.71 0.10 to 0.58	--
High Mn-High S	0.02 to 0.43	0.02 to 0.51 0.09 to 0.38	--

ELECTROCHEMICAL EFFECTS

Protection of Type 316 Stainless Steel

Galvanic coupling with steel has been previously recognized[12] as a viable means of affording protection to stainless steel. A recent study[13] has quantified the effectiveness of this technique for control of crevice corrosion of Type 304 and Type 316 in seawater. Carbon steel anodes which are 1/10 and 1/100 the area of the stainless steel surface area have been shown to prevent crevice corrosion of Type 316 in 28 day tests in low velocity seawater at 14°C. Unprotected samples corroded to a depth of up to 1.27 mm. Similar tests conducted in somewhat warmer seawater (i.e., 22-28°C) were also successful in controlling crevice corrosion for stainless steel to steel area ratios of 50:1. While some initiation and slight penetration (0.02 mm maximum in 30 days) was measured at the 50:1 area ratio, the extent of penetration was more than two orders of magnitude less than that reported for uncoupled specimens.

Potential data reported[13] for the 14°C seawater test are plotted in Figure 8 as a function of the stainless steel to steel area ratio. Values for the unprotected specimens (-0.030 V) approximate potentials reported elsewhere for Type 316 undergoing crevice corrosion.[7,14] As can be seen, coupling with carbon steel resulted in an expected shift to more active potentials. Increasing the stainless steel area reduced the degree of polarization in the active direction. These couple potentials are more active to, or closely approximate, the corrosion potential for Type 316 exposed in deaerated, simulated crevice solutions (25°C) in the pH range 0.8 to 1.5.[14,15]

Figure 9 describes the anodic polarization behavior for Type 316 as determined by potentiodynamic polarization tests in a deaerated, 6M Cl^-, pH=0.8 solution.[14] As can be seen, any polarization resulting in potentials more negative to about -0.4 V would cathodically protect Type 316 in an aggressive crevice solution. Uncoupled material undergoing crevice

corrosion could corrode in the active potential regime (i.e., -0.3 to -0.4 V, approximately) or at potentials more noble to the breakthrough potentials, i.e., -0.15 V in this case.

In cases where polarization due to coupling with carbon steel is not sufficient to adjust the potential of the stainless steel to the cathodic region, reduction in crevice corrosion propagation is still possible. This could result should the crevice potential be maintained in the passive region or at low currents associated with potentials more active to the anodic peak. This was apparently the case where some slight penetration was observed in the warm seawater tests at the 50:1 stainless steel to steel area ratio.

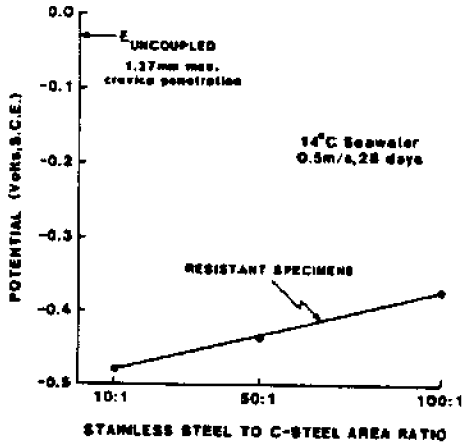

Figure 8. Polarization of stainless steel by coupling with carbon steel.

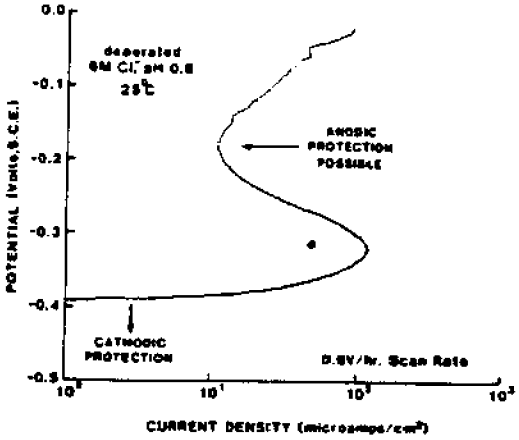

Figure 9. Polarization behavior of Type 316 in simulated crevice solution.

SUMMARY

Accurately assessing the crevice corrosion resistance of Type 316 and other stainless alloys requires a recognition of many factors. A review of previous and ongoing research has shown that in seawater and related chloride-containing environments, metallurgical, environmental and design factors are important. Testing in natural marine environments with additional support of laboratory electrochemical methods and mathematical modelling have been employed to identify factors affecting the behavior of Type 316 stainless steel. The present paper has described the interrelationship between crevice geometry factors of crevice gap and crevice depth on predicted resistance in full strength and diluted seawater. Results of multiple crevice assembly tests describe a substantially lower degree of crevice corrosion in diluted environments and suggest some critical level of dilution which will affect propagation.

The crevice corrosion resistance of Type 316 in aggressive coastal atmospheres has been quantified and compared to long term service experience. While some attack can be encountered, especially at locations closest to the ocean, depths of penetration are minimal in comparison to seawater.

Electrochemical testing and mathematical modelling confirm the reported beneficial effects of reduced Mn and S levels in stainless steels. However, because of the apparent narrow margin of improvement, it is uncertain that any noticeable benefit can be derived if crevice conditions are severe.

Crevice corrosion protection by sacrificial anode coupling methods is shown to be effective. Results from multiple crevice assembly tests with stainless steel coupled to carbon steel at different area ratios were correlated with results of electrochemical test results. Crevice corrosion was reduced or prevented by polarization near to or within the cathodic region described by polarization curves developed in simulated crevice solutions.

With an understanding of the operative mechanism of crevice corrosion, a combination of theoretical treatments and natural exposures can be utilized to define conditions where Type 316 is likely to resist corrosion.

REFERENCES

1. Kain, R. M., "Crevice Corrosion Behavior of Stainless Steels in Seawater and Related Environments," Paper No. 200, CORROSION/81, Toronto, Canada, April 1981.

2. Oldfield, J. W., "Crevice Corrosion of Stainless Steels - The Importance of Crevice Geometry and Alloy Composition," Presented at the 19th Journees de Aciers Speciaux, Saint-Etienne, May 1980.

3. Oldfield, J. W. and Sutton, W. H., "Crevice Corrosion of Stainless Steels. II. Experimental Studies," British Corrosion Journal, Vol. 13, p. 104, 1978.

4. Oldfield, J. W. and Sutton, W. H., "Crevice Corrosion of Stainless Steels. I. A Mathematical Model," British Corrosion Journal, Vol. 13, p. 13, 1978.

5. Oldfield, J. W., Lee, T. S. and Kain, R. M., "Mathematical Modelling of Crevice Corrosion of Stainless Steels," Corrosion and Corrosion Protection, Vol.81-8, The Electrochemical Society, 1981, pp. 213-224.

6. Kain, R. M., "Crevice Corrosion Resistance of Several Iron Base and Nickel Base Cast Stainless Alloys in Seawater," Paper No. 66, CORROSION/82, Houston, Texas, March 1982.

7. Lee, T.S. and Kain, R.M., "Factors Influencing the Crevice Corrosion Behavior of Stainless Steels in Seawater," Paper No.69, CORROSION/83, Anaheim, California, April 1983.

8. Kain, R. M., "Crevice Corrosion and Metal Ion Concentration Cell Corrosion Resistance of Candidate Materials for OTEC Heat Exchangers, Parts I and II," ANL/OTEC-BCM-022, May 1981.

9. "Marine Atmospheric Corrosion," The International Nickel Company, Inc., Publication A-1275.

10. Degerbeck, J. and Wold, E., Werkstoffe un Korrosion, Vol. 25, p. 172, 1974.

11. Degerbecker, J., "The Influence of Mn Compared to That of Cr, Mo and S on the Resistance to Initiation of Pitting and Crevice Corrosion in Austenitic Stainless Steels," Werkstoffe un Korrosion, Vol. 29, p. 179-188, 1978.

12. Moller, G. E., "The Successful Use of Austenitic Stainless Steels in Seawater," Society of Petroleum Engineers, April 1977.

13. Lee, T.S. and Tuthill, A.H., "Use of Carbon Steels to Mitigate Crevice Corrosion of Stainless Steels in Seawater," Materials Performance, Vol. 22, No. 1, January 1983.

14. Kain, R. M. and Lee, T. S., "Recent Developments in Test Methods for Investigating Crevice Corrosion, Presented at International Symposium on Laboratory Corrosion Tests and Standards, ASTM, Bal Harbour, Florida, November 1983.

15. Kain, R.M. and Lee, T.S., "The Effect of Crevice Solution pH on Corrosion Behavior of Stainless Alloys," Paper No. 27, CORROSION/84, New Orleans, Louisiana, April 1984.

III.D. THE EFFECT OF CREVICE SOLUTION PH ON CORROSION BEHAVIOR OF STAINLESS ALLOYS

By

R. M. Kain

and

T. S. Lee

To Be Presented At

CORROSION/84, T-5F Symposium
New Orleans, Louisiana, April 2-6, 1984

LaQUE CENTER FOR CORROSION TECHNOLOGY, INC.
POST OFFICE BOX 656
WRIGHTSVILLE BEACH, NORTH CAROLINA 28480
(919) 256-2271

PAPER NUMBER
27

CORROSION 84

The International Corrosion Forum Devoted Exclusively to The Protection and Performance of Materials

April 2-6, 1984/New Orleans Hilton Hotel/Rivergate Exhibition Center/New Orleans, Louisiana

THE EFFECT OF CREVICE SOLUTION PH ON CORROSION BEHAVIOR OF STAINLESS ALLOYS

R. M. Kain and T. S. Lee
LaQue Center for Corrosion Technology, Inc.
Post Office Box 656
Wrightsville Beach, North Carolina 28480

ABSTRACT

Crevice corrosion initiation and propagation are controlled, in part, by the pH of the crevice solution. Variations in pH can be attributed to differences in crevice geometry, alloy composition and bulk environment chemistry. Comparisons are detailed for tests in natural seawater and other chloride containing waters. The utility of electrochemical tests and mathematical modelling are also discussed.

INTRODUCTION

Resistance of stainless steels and related alloys to crevice corrosion is dependent on whether the crevice electrolyte becomes sufficiently aggressive to cause breakdown of passivity. Alloy composition, bulk solution chemistry, crevice geometry and other related factors contribute to an increase in the acidity and chloride concentration of this oxygen deprived electrolyte.[1] Breakdown is likely to occur if these concentrations exceed some critical level, specific to that alloy. This concentration has been designated as a critical crevice solution (CCS).[2,3]

The impact of these factors on the resistance to crevice corrosion initiation and propagation is being investigated by various electrochemical and mathematical methods.[2-11] Modelling of chemistry changes in the crevice electrolyte indicates a strong dependency on crevice gap and crevice depth dimensions. In addition, for each alloy-geometry combination, the bulk environment chloride level will affect the ultimate crevice electrolyte pH. Accordingly, a given stainless steel may encounter a range of crevice solutions of varying pH and chloride level dependent upon the crevice geometry and bulk environmental conditions encountered.

Previous and on-going crevice corrosion research at the LaQue the Center for Corrosion Technology, Inc. (LCCT) has utilized a remote crevice assembly (RCA) to

quantify differences in the propagation resistance of stainless steels as affected by alloy content and bulk environment chemistry.[4,5] This technique enables measurement of current to a physically separated but electrically connected anode member (crevice area) exposed in the same bulk environment with a larger cathode member (crevice free area). While the remote crevice technique has proved a valuable tool, it nonetheless is subject to some of the same crevice geometry related problems identified for other applied crevice former test methods. Specifically, the limits to which the critical crevice gap dimensions can be accurately reproduced pose some limitations in obtaining reproducible crevice test results.

The following describes the use of a compartmentalized cell to study the effects of differences in the cathode and anode electrolytes on propagation and cessation of crevice corrosion.[11] While the technique is similar to the RCA procedure in that the respective cell members are physically separated but electrically connected, the anode member is exposed without a crevice in a deaerated, simulated crevice solution. The crevice solutions selected are more concentrated than the measured CCS for the given alloy, hence the crevice geometry effects on development of the CCS are eliminated.

EXPERIMENTAL

Apparatus

A test cell was constructed to separate the stainless steel cathode and anode members in their respective environments. The cell partition between the compartments consists of an agar gel sandwiched between two fritted glass discs held in place with a nylon compression fitting. In each case, the gel is prepared with the crevice electrolyte selected for the given test. Earlier attempts with fritted discs, singly or in combination with compressed layers of filter paper, either did not sufficiently suppress chloride diffusion from the more concentrated crevice solution or, if effective, resulted in excessively high electrical resistance.

As shown schematically in Figure 1, the cathode compartment contained provision for recirculation of the bulk environment from a larger 20 liter reservoir. In addition to providing room for a control specimen, the large volume enabled control of the bulk environment chemistry by minimizing the effect of any remaining chloride diffusing through the partition from the more concentrated anode compartment.

Specimens

Cathode and anode members were approximately 170 cm^2 and 10 cm^2 in surface area respectively. Commercial Type 316 stainless steel was utilized for these studies. Cathodes of the 3mm thick stainless steel material were exposed with the as-produced mill finish intact (edges were machined and ground). In each case, the smaller anode members were wet ground to a 600 grit finish with SiC papers.

Prior to testing, specimens were degreased with acetone, bristle brush scrubbed with pumice, rinsed with water and then rinsed with fresh acetone and dried. Anode specimens were weighed to the nearest 0.1 mg.

Environments

Natural seawater (filtered) and a 15,000 mg/L chloride solution at pH=3 (simulated process environment) were selected as cathode (bulk) environments. These environments were open to the atmosphere and further aerated by stirring and fluid recirculation. Table 1 identifies the composition of the crevice solutions used in the compartments. Sodium chloride and hydrochloric acid were added to a synthetic seawater stock solution to give the desired chloride level and pH. The mathematical model for crevice corrosion initiation[2] was used to identify geometric and bulk environment conditions yielding this range of limiting pH values within the crevice. This identification and selection of a series of crevice solutions at limiting pH values has the advantage of enabling propagation studies under steady state environmental conditions. The simulated crevice solutions were deaerated by purging with nitrogen gas prior to being introduced to the anode cell (pressurized delivery) and vigorous purging was continued during the test. All tests were conducted at 25°C $\pm$ 2°C.

Procedure and Instrumentation

In addition to the cathode and anode members of the crevice corrosion cell, uncoupled control specimens of the same dimensions were placed in the respective compartments. Upon immersion, the anode and cathode members were allowed to freely corrode for one hour prior to being electrically coupled through a zero resistance ammeter for 24 hours. Corrosion potentials were measured using saturated calomel reference electrodes placed directly in both compartments. At the end of the test period, the cathode and anode cell members were uncoupled for one hour to re-establish their respective corrosion potentials relative to the control specimens.

Polarization Tests

Potentiodynamic polarization curves were also developed in the same simulated crevice solutions at a polarization scan rate of 0.6 V/hour. Specimens were surface ground with wet 120 SiC paper prior to test. The polarization was initiated at a potential of -0.6 V_{SCE} and proceeded to more noble potentials.

RESULTS AND DISCUSSIONS

Selection of Crevice Solutions Via Mathematical Modelling

Previous studies have identified the CCS composition for initiation of crevice corrosion of Type 316 stainless steel in seawater to be at a pH level of about 1.65 with a corresponding chloride concentration of about 4.0 M.[3] The present compartmentalized cell investigations considered three crevice solutions at pH levels 1.5, 1.3 and 1.1; all of which are more concentrated than the above CCS pH. Mathematical modelling was used to identify crevice geometries, which, in practice, would yield these concentrations as limiting values. Seawater and a process environment containing 15,000 mg/L Cl^- at pH=3 were considered as bulk environment inputs. Two fixed values for crevice depth and a range of crevice gap dimensions were entered as geometric inputs to the model. The depth dimensions of 0.30 cm and 0.75 cm are typical of those for laboratory applied crevice formers, e.g., remote crevice assemblies. Model predictions for the respective crevice gap dimensions at each of the environment-crevice depth combinations are shown in Table 2. These tight crevice gaps are within the quantified range determined earlier by

scanning electron microscopy examination of assembled crevice components.[6] From Table 2, it can be seen that tighter crevices (smaller gap) are required with the shallower crevice depths in order to produce the same limiting pH values as deeper crevices.

These data indicate a relative effect of crevice geometry (gap dimension) in the seawater tests which is greater than the differences in behavior predicted between the two bulk environments. Inter-relationships between the crevice geometry factors and bulk environment chemistry have been previously presented by the authors.[10,11] While more than one bulk environment-geometry combination can produce the same limiting pH value of the crevice solution, the rate of pH fall and hence the time to breakdown may vary.

Figure 2 shows modelling predictions for the fall in pH within two different crevices formed by a non-metal to Type 316 stainless steel assembly. In both cases, a limiting pH value of 1.1 ± 0.05 has been predicted. Assuming a CCS value of 1.65, it can be seen that the 0.3 cm depth/0.1 μm gap crevice conditions would cause more rapid initiation. Laboratory experiments with RCA devices have resulted in crevice corrosion in as little as 48 hours.[4,5] The possibility of other crevice geometries of greater severity, e.g., tighter gaps, would enable the production of crevice solutions of even lower limiting pH values. Evidence in this regard has been recently established by the authors with sensitive pH indicating papers applied to freshly disassembled crevice components. Numerous measures of pH values approximating 0.8 and less have been made.

Control Specimens

Table 3 gives the test results for the control samples exposed in both the seawater and simulated process environment compartmentalized cell tests. While these data show relatively low rates of corrosion, the detrimental effect of decreasing crevice solution pH is clearly evident. As can be seen, decreasing the crevice solution pH from 1.5 to 1.1 resulted in a fourfold increase in mass loss.

Anode/Cathode Behavior in Compartmentalized Cell Tests

Coupling of the larger cathode members in the bulk seawater and process environment to the smaller anode members in the deaerated crevice solutions produced a variety of responses. Each, however, was typified by a shift in the cathode potentials to more active values and a shift in the anode potentials to more noble values in comparison to the respective freely corroding controls. Active shifts in potentials measured for compartmentalized cell cathode members are analogous to those sometimes observed in remote crevice tests at the onset of crevice corrosion.[5]

As would be expected, the difference in potential between cathode and anode members produced a flow of current upon coupling. Figure 3 shows the current data for tests utilizing filtered seawater in the cathode compartment. In each case, the total current decayed with time with several abrupt changes in magnitude being recorded. The significance of these changes will be correlated later with the polarization characteristics of the anode. It is also evident that the total current increased as the pH of the crevice solution decreased with more than an order of magnitude difference being recorded between the pH=1.5 and pH=1.1 tests after 24 hours.

Current data for tests utilizing the simulated process solution in the cathode compartment are shown in Figure 4. Again, differences as a function of crevice solution

pH are evident. Data for both the pH=1.1 and pH=1.3 tests are comparable to those described for the seawater tests. However, the current after 24 hours in the pH=1.5 test is somewhat greater than that previously indicated in Figure 4. Additional data from these experiments are provided in Table 4.

Figure 5 compares the magnitude of these current measurements for the various bulk environment-crevice solution combinations after only a few seconds of test. These results show that while decreasing crevice solution pH contributed to higher anodic current, the impact of differences in the cathode environment was, at least at the start, substantially greater. As will be discussed later, this difference can be attributed to differences in the initial polarization toward the potential corresponding to the anodic peak current maxima determined from the polarization curves. In each case, the potentials of the anodes in the seawater test were closest to the measured anodic peak potential and, hence, greater currents would be expected.

The effect of difference in the bulk environment is more apparent from the calculated total charge data. As evidenced by the graph in Figure 6, the total charge determined for tests utilizing the cathodes in seawater was greater in all cases. These differences are obviously directly related to the differences in current decay behavior previously described by Figures 4 and 5. As can be seen in Figure 7, there was excellent agreement between anode mass loss values calculated from the total charge data (amperometric) and that obtained by the more conventional gravimetric method. The slight deviation noted in the process environment experiments may be attributed to the initiation of small areas of corrosion found at the waterline of those cathode members.

Figure 8 compares the calculated corrosion rates for Type 316 stainless steel exposed to the more aggressive pH=1.1 crevice solution. Coupling to the larger cathode areas in the bulk environment substantially increased the rate of corrosion of the anode. Again, the greatest effect was produced by coupling to the seawater cathode.

Corrosion Potentials and Polarization Behavior

Table 5 lists the corrosion potentials for the various cathode and anode members exposed to the respective bulk environments and crevice solutions for one hour. Data include potentials for the control specimens and other cell members immediately prior to coupling. For the cathode samples, potentials varied by as much as 0.030 V in the aerated bulk environments. After the initial one hour exposure, potentials for cathodes in the seawater environment were more noble to those in the acid-chloride process environment. Averaging the data for six specimens in each of the two bulk environments shows a potential difference of about 0.050 V.

As would be expected, corrosion potentials in the deaerated crevice solutions were considerably more active than those in the bulk environment, approximating an overall average of -0.395 V_{SCE}. A maximum difference of 0.009 V was recorded between samples in the same crevice solution. The average potential for the anode members was 0.225 V and 0.173 V more active to the cathodes exposed to the seawater and process environment, respectively.

Corrosion potentials for the various coupled and freely corroding members at the end of the 24 hour test are given in Table 6. The direction of polarization, i.e, a shift to more active values for cathodes and to more noble values for anodes, is again evident. It can be seen that both the potentials of the anode and cathode members are clearly affected by the concentration of the crevice solution. The lower pH crevice solutions

yield more active potentials in each case. In contrast to potential differences noted for the freely corroding members in their respective environments, a maximum of 0.015 V separated the coupled cathode and anode members. Little effect of bulk environment is evident from these final potential data.

To more clearly describe the corrosion behavior as indicated by the electrochemical and mass loss data, attention is redirected to the current decay plots shown previously in Figure 4. In each case, one or more stepwise decreases in current are evident. Note, for example, the changes occurring in the pH=1.3 test at about 16 days and also the initial decay in the pH=1.5 test. These changes correspond to changes in the anode potential which are controlled by the ability of the cathode to polarize the anode from one potential-current regime to another.

Figure 9 shows segments of potential-time plots from the various tests utilizing seawater in the cathode compartment. While uncoupled anode members in the three crevice solutions remained at active potentials with little change from their respective initial values, the uncoupled cathode members achieved somewhat more noble potentials with time.

For the coupled anodes, differences in behavior as a function of crevice solution pH are evident. Note that while the potentials in the more concentrated pH=1.1 crevice solution remained active, those at the higher pH became more noble. The abrupt change in the curve for the pH=1.3 data at about 16 hours corresponds to the decrease in current noted earlier. In the case of the pH=1.5 data, polarization to the more noble values occurred early in the test.

Figure 10 compares the spontaneous polarization behavior of the anode member in the pH=1.5 crevice solution (seawater cathode) with a potentiodynamic polarization curve developed at a scan rate of 0.6 V/hr. Coupling of the anode and cathode members resulted in a shift to a potential corresponding to the anodic peak current maxima with subsequent rapid polarization to more noble potentials. The potential-current graphs obtained by the two methods are in excellent agreement up to a potential of -0.275 V. As would be expected, the longer exposure times in the compartmentalized cell resulted in lower passive currents at the more noble potentials. Potentials identified by the inflection of the curves at about -0.300 V correspond to those at the onset of the changes in potential and current data described for the compartmentalized cell test at pH=1.5. In the pH=1.3 solution, longer times were required to polarize the anode members beyond this potential region with the resultant reduction in current. Again, in the pH=1.1 test, polarization to this potential did not occur within the 24-hour test period and there was no stepwise decrease in current.

These results show that while aggressive crevice solutions were more concentrated than that required for breakdown of passivity (CCS value), spontaneous anodic protection is possible. Accordingly, the degree of propagation may be affected by the limiting pH within the crevice and the ability of the cathode to polarize the crevice into a low passive current regime.

These findings are consistent with recent work by others[12] who have also reported that anodic protection is possible in crevice solutions more concentrated than the depassivation pH. In Figure 11, for example, data for Type 304 stainless steel indicates that passivity can be established in crevice environments if the corrosion potential can be made more noble to the Flade potential. For the present compartmentalized cell crevice environments, the Flade potential, allowing for some possible difference between Type 304 and Type 316, corresponds to a potential of approximately -0.3 V.

Additional Investigations

Numerous remote crevice assembly tests in natural seawater have indicated that stainless steels may exhibit on-going crevice corrosion at potentials more noble to those described herein.[13] This difference may be attributable to the presence of more concentrated solutions within actual crevices, e.g., pH=0.8, and to larger, more effective cathode to anode area ratios. These and other aspects are topics of continuing investigations using the compartmentalized cell technique. Preliminary results indicate that crevice corrosion can propagate at potentials typical of those associated with the breakdown regime in deaerated, acid-chloride solutions. Well established cathode members in fully aerated seawater can polarize small anodic areas into this domain of more accelerated corrosion.

SUMMARY AND CONCLUSIONS

A compartmentalized cell technique has been used to study the effects of differences in cathode and anode electrolyte on propagation and cessation of crevice corrosion of Type 316 stainless steel. A test cell was constructed to separate the stainless steel cathode and anode members in their respective environments. The compartments were joined by an agar-plug prepared with the selected crevice solution. The plug provided a relatively low resistance barrier which minimized ion migration during the tests. Aerated seawater and acid-chloride solutions were utilized in the cathode compartment. Simulated crevice solutions (deaerated) for the anode compartment were prepared based on predictions by mathematical modelling for Type 316 stainless steel. In order to study propagation behavior, the selected crevice electrolytes were more concentrated than that assumed to be the critical crevice solution (e.g., $4MCl^-$, pH=1.65). Hence, the compartmentalized cell approach eliminated the crevice geometry aspects which are difficult to control.

Increases in crevice solution acidity resulted in an increase in corrosion rate for anode members. Observed shifts of the cathode members to more active potentials after coupling were in general agreement with other data from stainless steel specimens undergoing crevice corrosion. Resulting polarization of the anode member to more noble potentials in some cases increased the corrosion rates as compared to those for freely-corroding electrodes. Depending on the crevice solution concentration and hence the magnitude of the anodic peak current density, polarization was sometimes sufficient to cause a decrease in corrosion rate by a shift to passive potentials more noble than the primary passive potential.

These observations further explain the variability sometimes noted in actual crevice corrosion penetration data.

REFERENCES

1. Kain, R. M., Lee, T. S., "Observations on the Localized Corrosion Behavior of Stainless Steel in Ambient and Elevated Temperature Seawater," Proceedings, ICMCF, 5th International Congress on Marine Corrosion and Fouling, Barcelona, Spain, May 1980.

2. Oldfield, J. W., Sutton, W. H., British Corrosion Journal, p. 13 (1978).

3. Oldfield, J. W., Sutton, W. H., British Corrosion Journal, p. 104 (1978).

4. Lee, T. S., ASTM STP 727, Electrochemical Corrosion Testing, p. 43 (1981).

5. Kain, R. M., "Electrochemical Measurement of the Crevice Corrosion Propagation Resistance of Stainless Steels: Effect of Environmental Variables and Alloy Content," Presented at CORROSION/83, Paper No. 203, Anaheim, California, April 1983.

6. Lee, T. S., Kain, R. M., "Factors Influencing the Crevice Corrosion Behavior of Stainless Steels in Seawater," Presented at CORROSION/83, Paper No. 69, Anaheim, California, April 1983.

7. Oldfield, J. W., Lee, T. S., Kain, R. M., "A Mathematical Model of Crevice Corrosion Propagation of Stainless Steel," CORROSION/81 - Research in Progress Symposium, Toronto, Canada, April 1981.

8. Oldfield, J. W., Lee, T. S., Kain, R. M., "Mathematical Modelling of Crevice Corrosion of Stainless Steels," Corrosion and Corrosion Protection, Proceedings, Vol. 81-8, The Electrochemical Society, p. 213 (1981).

9. Lee, T. S., Oldfield, Kain, R. M., O'Dell, C. S., "Assessing Crevice Corosion Behavior of Stainless Steels in Natural Waters Via Mathematical Modelling" CORROSION/82 - Research in Progress Symposium, Houston, Texas, April 1982.

10. Kain, R. M., "Crevice Corrosion Resistance of Type 304 and Type 316 Stainless Steels in Seawater and Related Environments," To be published in Corrosion, Paper No. 200, CORROSION/81, Toronto, Canada, March, 1981.

11. Kain, R. M., Lee, T. S., "Polarization Characteristics of Stainless Steel Cathode and Anode Areas Involved in Crevice Corrosion," Presented at 162nd Meeting of Electrochemical Society, October 18, 1982, Detroit, Michigan.

12. Azzerri, N., Mancia, F., Tomba, A., "Electrochemical Prediction of Corrosion Behavior of Stainless Steel in Chloride-Containing Water," Corrosion Science, Vol. 22, No. 7, 1982.

13. Kain, R. M., Lee, T. S., "Recent Developments in Test Methods for Investigating Crevice Corrosion," Presented at ASTM International Symposium on Laboratory Corrosion and Standards, Bal Harbour, Florida, November 14-16, 1983.

TABLE 1

Test Environments

Bulk Solutions (cathodes)

Natural Seawater 0.56M Cl^-, pH 8

"Process Solution" 0.42M Cl^-, pH 3

Crevice Solutions (anodes)

4.0M Cl^-, pH 1.5

4.5M Cl^-, pH 1.3

5.0M Cl^-, pH 1.1

TABLE 2

Mathematical Modelling Predictions for Limiting Crevice Solution pH Values and Several Bulk Environment-Crevice Geometry Combinations

Limiting Crevice Solution pH (±0.05 units)	Seawater Environment		Process Environment[1]	
	Crevice Gap[2] (μm)	Crevice Depth (cm)	Crevice Gap[2] (μm)	Crevice Depth (cm)
1.5	0.09 0.15	0.75 0.30	— 0.12	— 0.30
1.3	0.70 0.13	0.75 0.30	— 0.09	— 0.30
1.1	0.60 0.10	0.75 0.30	— 0.08	— 0.30

1 0.42 M Cl^-, pH=3

2 Non-metal to metal crevices

TABLE 3

Results for Freely Corroding Type 316 Stainless Steel Exposed to Anode Compartment Crevice Solutions at Varying pH and Chloride Levels

Simulated Crevice Solution		Mass Loss (mg)		Average Corrosion Rate ($mg/cm^2/d$)
Cl^- M	pH	Seawater Test Controls	Process Test Controls	
4.0	1.5	0.3	0.4	0.03
4.5	1.3	0.6	0.8	0.06
5.0	1.1	1.3	1.8	0.14

TABLE 4

Differences in Anode Behavior as Affected by Crevice Solution Concentration and Cathode Member Bulk Environment

Cathode Environment	Anode Environment pH	Anodic Currents (amps) t= 0.5 min.	Anodic Currents (amps) t= 1440 min.	Total Charge (Coulombs)	Anode Mass Loss (g) Amperometric	Anode Mass Loss (g) Gravimetric
Seawater	1.5	4.5×10^{-4}	0.4×10^{-5}	3.1	0.0008	0.0008
	1.3	4.7×10^{-4}	2.6×10^{-5}	11.5	0.0030	0.0029
	1.1	5.4×10^{-4}	8.5×10^{-5}	15.6	0.0041	0.0047
Process Environment 0.42 M Cl^-, pH=3	1.5	1.5×10^{-4}	1.1×10^{-5}	2.5	0.0006	0.0010
	1.3	1.7×10^{-4}	2.6×10^{-5}	3.9	0.0010	0.0014
	1.1	2.3×10^{-4}	8.1×10^{-5}	8.4	0..0022	0.0032

TABLE 5

Corrosion Potentials for Various Cathode and Anode Cell Members After One Hour Exposure to Respective Environments

Bulk Environment	Corrosion Potential (V_{SCE}) Most Noble	Most Active	Average
Seawater	-0.160	-0.190	-0.175
Process Solution	-0.211	-0.237	-0.224
Crevice Solution			
pH 1.5	-0.387	-0.396	-0.395
pH 1.3	-0.394	-0.400	-0.398
pH 1.1	-0.394	-0.398	-0.395

TABLE 6

Corrosion Potentials Exhibited by Coupled and Freely Corroding Members of Type 316 Stainless Steel After 24 Hours

Environments Bulk (Cathode)	Crevice (Anode)	Corrosion Potentials (Volts, SCE) Cathodes[1] Coupled	Cathodes[1] Uncoupled	Anodes[2] Coupled	Anodes[2] Uncoupled
Seawater	pH = 1.5	-0.173	-0.095	-0.182	-0.378
	1.3	-0.224	-0.044	-0.236	-0.386
	1.1	-0.299	-0.086	-0.314	-0.382
Process Solution	pH = 1.5	-0.182	-0.006	-0.192	-0.372
	1.3	-0.216	-0.064	-0.224	-0.367
	1.1	-0.297	-0.062	-0.312	-0.380

1 Reference electrode in bulk environment
2 Reference electrode in crevice solution

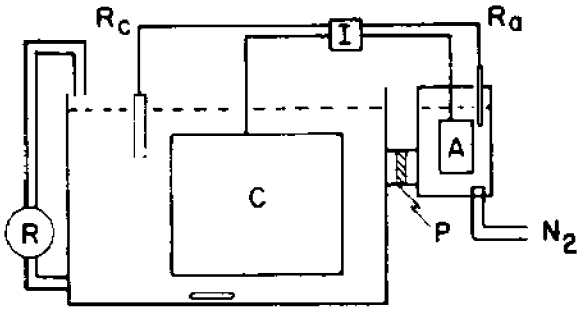

COMPARTMENTALIZED CELL

A=Anode Cell
C=Cathode Cell
R_a,R_c=Reference Electrodes
P=Cell Partition
I=Instrumentation
R=Recirculation Pump/Reservoir

Fig. 1 - Schematic identifying various components of the compartmentalized cell apparatus.

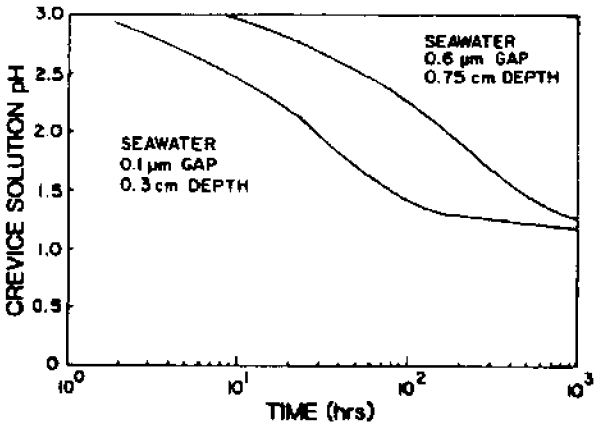

Fig. 2 - Mathematical model predictions for the fall in crevice solution pH as affected by crevice geometry.

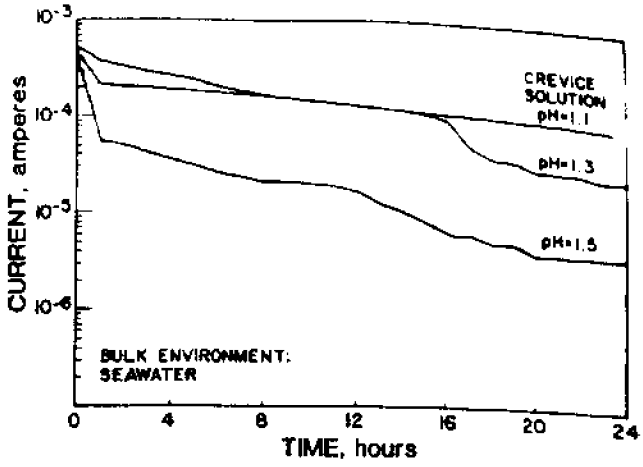

Fig. 3 - Current versus time data for tests utilizing seawater in the cathode compartment.

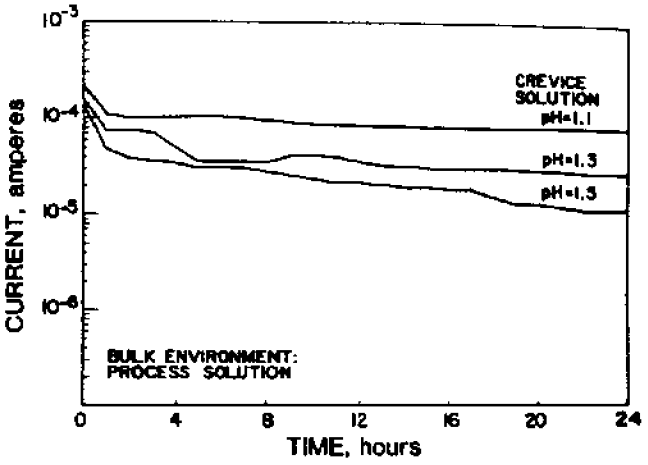

Fig. 4 - Current versus time data for tests utilizing simulated process solution in the cathode compartment.

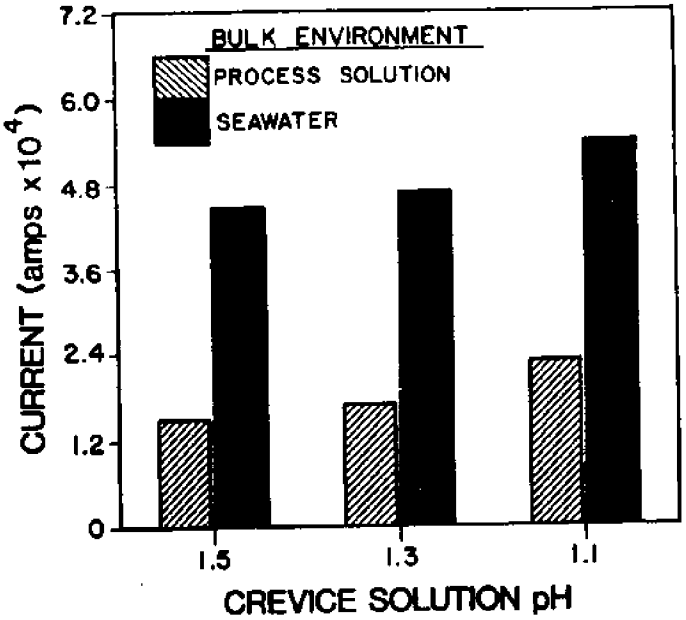

Fig. 5 - Effect of anode and cathode environments on the magnitude of initial currents.

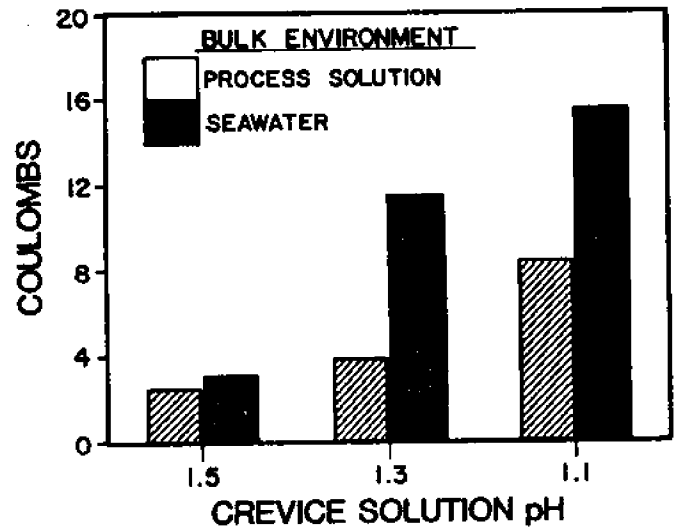

Fig. 6 - Effect of anode and cathode environments on the magnitude of total charge calculated after 24 hours.

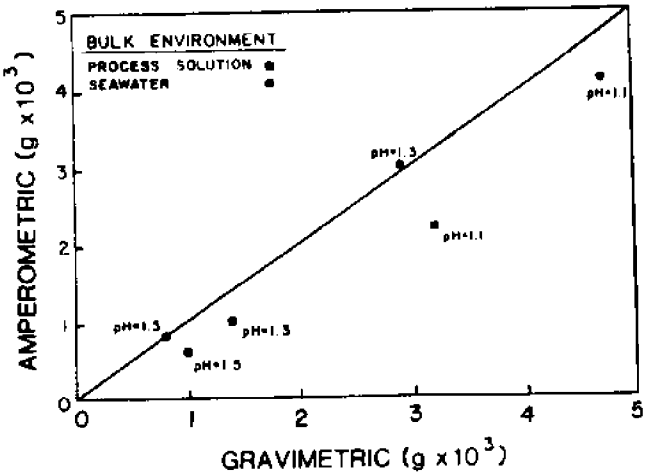

Fig. 7 - Comparison of amperometric and gravimetric mass loss data from comparmentalized cell tests.

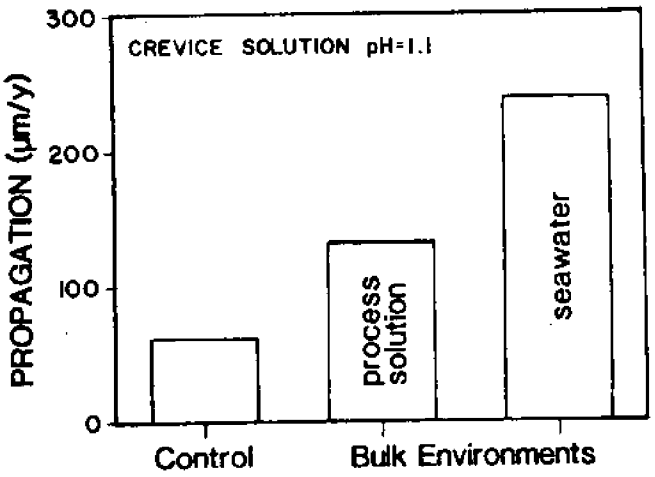

Fig. 8 - Effect of bulk environment on increased crevice corrosion propagation under low pH conditions.

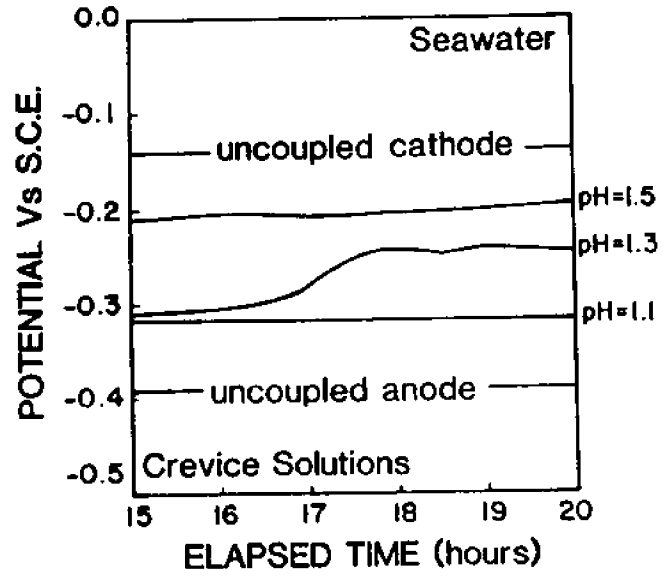

Fig. 9 - Segments of corrosion potential versus time plots for freely corroding and coupled anode and cathode members in compartmentalized cell tests with seawater as the bulk environment.

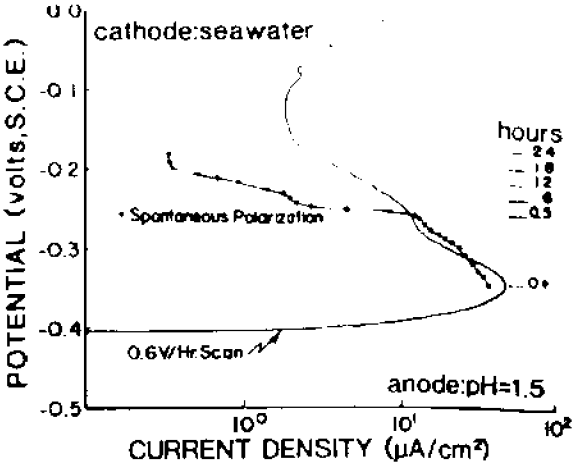

Fig. 10 - Comparison of the spontaneous polarization behavior of Type 316 stainless steel in a pH=1.5 crevice solution with a potentiodynamic polarization curve.

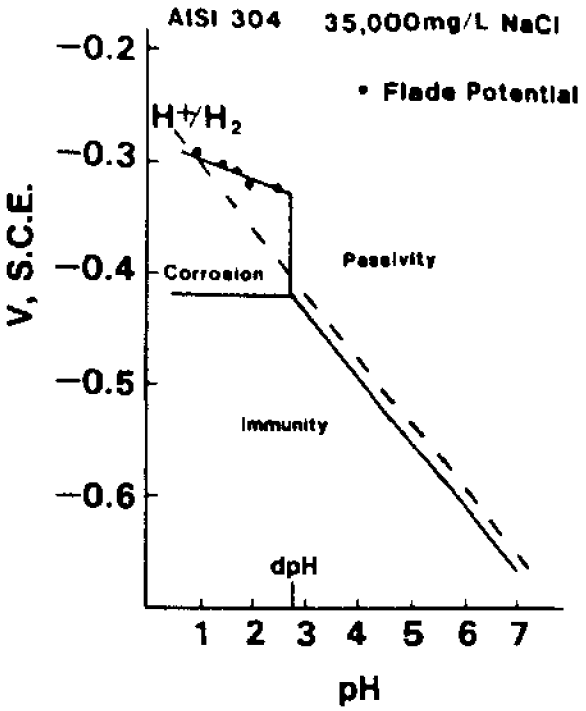

Fig. 11 - Relative potential-pH domains for immunity, corrosion and passivity of Type 304 stainless steel: after Azzerri, Mancia and Tamba, Corrosion Science, Vol. 22, No. 7, 1982.

IV. THE ROLE OF BACTERIA IN CREVICE CORROSION INITIATION

A. Introduction

The initial step in the nucleation of crevice corrosion is depletion of dissolved oxygen in the crevice water. One critical input to the Oldfield model of crevice corrosion is the calculation of the time for oxygen depletion. The mechanism of depletion has usually been assumed to be electrochemical wastage of the metal within the crevice at the passive current density, i_p, but the question has been raised as to whether marine bacteria in the crevice water could make a significant contribution to the depletion process. Such a suggestion is made credible by data generated at the LaQue Center and shown in Table AI. The initiation of crevice attack on alloy 825 at 25°C was more than four times as severe in natural seawater as it was in synthetic seawater. When both media were heated to 50°C, killing the oxygen utilizing bacteria in the natural seawater, the initiation rates were the same. These results are not definitive because the data for type 316 stainless steel show the opposite trend.

The Oldfield model predicts that the electrochemical mechanism alone is capable of depleting the oxygen in less than 15 minutes. Therefore, it may not matter in a practical sense whether or not microorganisms in the crevice water contribute much to the overall rate of oxygen utilization. However, it is important to our understanding of the mechanism of crevice corrosion to measure the relative contributions of the two mechanisms.

B. Experimental

The well-known active shift in corrosion potential of a platinum electrode with decreasing dissolved oxygen concentration has been utilized to make the desired measurements. Special cells have been

constructed out of either AISI type 316 stainless steel or polytetrafluoroethylene (TFE) as described below. The platinum electrode, along with a silver-silver chloride reference electrode, was mounted in the cap of the cell. The seawater in the cell was either left natural or sterilized. Thus, the following sets of conditions could be achieved: 1) electrochemical oxygen utilization alone using sterile water in the stainless steel cell, 2) biological utilization alone using natural seawater in the TFE cell, 3) electrochemical and biological utilization together using natural seawater in the stainless cell, or 4) no mechanism for utilization at all (other than passive wasting on the platinum and reference electrodes) using the TFE cell with sterile seawater.

The special cells were constructed as shown in Figure 1. The cell bodies were machined from 2.54 cm (1 inch) diameter rod of either type 316 stainless steel or TFE. A 2.5 cm length of rod was cut to make the body of the cell, and then a cylindrical cavity 0.25 cm (3/8 inch) diameter by 0.95 cm deep was milled into one end of the rod. The volume of the cell cavity, including the extra height introduced by the "o-ring" was 0.71 cm^3. The surface area of the inside of the cell, exclusive of the lid was 3.6 cm^2.

The cell lids were cast of Buehler Epo-Quik epoxy mounting compound in standard cylindrical metallurgical mounts. The platinum and silver electrodes and the "o-ring" were cast right into the lid as shown in the diagram. When the epoxy had fully cured, the bottom surface of the lid was ground on a belt sander to one half the depth of the "o-ring". and polished through 600 grit silicon-carbide metallurgical paper. The damaged "o-ring" was then removed, leaving a perfectly molded "o-ring"

groove. After polishing, the 20-gage platinum and 18-gage silver wires were exposed only in cross-section, and were flush with the bottom surface of the lid. The cross-sectional areas of platinum and silver exposed were 0.0052 cm^2 and 0.0081 cm^2 respectively. The sum of these areas was less than 0.4% of the inside surface area of the stainless steel cell.

In preparation for each run, the cell was washed in 10% HCl, rinsed with sterile distilled water, autoclaved at 220°C and 12 psi for 30 min., and filled with the appropriate test solution. The lid was prepared by abrading lightly with the 600-grit paper, and pickling for about 5 minutes in 70% HNO_3 diluted 1:1 with distilled water. This treatment cleaned the epoxy and platinum surfaces, and it prepared the silver surface for conversion to silver chloride. The silver was then polarized anodically in 0.1N HCl until it turned dark grey, indicating that the silver chloride layer had formed. The anodic polarization usually took between 15 and 30 minutes. Using the above procedure, a fresh platinum surface and a fresh silver-silver chloride electrode were provided at the start of each run. We found that this was important because, if not renewed, the behavior of the platinum and silver chloride electrodes would change from run to run, presumably due to organic film formation on the metal surfaces.

Natural seawater was taken either from the recirculating seawater system in the Cannon Marine Studies Building, or from a special supply of water brought to our laboratory from the open Atlantic Ocean 40 to 100 miles East of the Delaware coast. The results of these experiments did not vary significantly with the type of seawater used. Both types of water were filtered to remove suspended particulate material. For

the runs using natural seawater, the water was not treated further except for keeping it aerated. The sterile water was prepared by filtering further through a 0.2 micrometer membrane filter (Millipore) to remove most bacteria, and then autoclaving as described above. No attempt was made in these experiments to enumerate the concentration of bacterial cells in the water, nor to measure the total biomass, nor to determine the bacterial species or morphological types involved. We have assumed that: 1) oxygen utilizing bacteria were plentiful in all our waters except when a definite attempt was made to remove them, 2) the bacteria that were present were either representative of those to be found in any natural seawater, or the differences in species present would not be important as long as some kind of aerobic bacteria were abundant, and 3) if bacterial utilization of oxygen in the crevice water is of major importance in the initiation of crevice corrosion, the effect will be apparent in our experiments regardless of the species of bacteria involved.

After preparing the water, the cell was filled using a sterilized 10 ml pipette. Water was added until a convex meniscus was formed. The lid was then carefully placed over the convex water surface in such a way that no air was trapped in the cell. The absence of air bubbles was verified by visual inspection through the transparent epoxy lid.

Response of the platinum electrodes to changes in dissolved oxygen concentration was calibrated by determining the corrosion potential of the platinum in seawater solutions of predetermined oxygen contents contained in a standard polarization flask. Oxygen concentrations of 7.2 (air saturation), 3.1, 1.2 and 0.6 ppm were achieved by bubbling appropriate oxygen-nitrogen mixtures through the cell from premixed

compressed gas cylinders. The lowest oxygen concentration (about 0.1 ppm) was obtained by purging the cell with prepurified nitrogen passed over copper turnings at 500°C. The corrosion potential of the platinum was recorded after bubbling the solution with the appropriate oxygen mixture for 2 to 3 hours, or until the platinum potential stabilized.

C. Results

Results of the experiments run to date are shown in Figures 2 through 4. Figure 2 presents the results of the calibration runs for the platinum electrode as a function of dissolved oxygen concentration. At air saturation, the platinum potential (some would call it the Eh, or the redox potential of the electrolyte) was about 120 mv postive to Ag/AgCl. In the calibration runs, the platinum potential showed a nearly linear response to the oxygen concentration down to 3 ppm. Below that value, the calibration curve becomes nonlinear, and the response to changes in oxygen pressure becomes more sluggish. The vertical error bars in Figures 2 through 4 represent the envelope of all data points taken (usually five) at that condition, while the plotted point represents the mean value.

Figure 3 gives the results for the TFE cell (upper curve) and for the stainless steel cell (lower curve) with the sterile seawater. Thus, the upper curve shows the platinum potential, or the dissolved oxygen concentration when neither the electrochemical nor the biological oxygen utilization mechanisms are operative. Within the first twenty minutes, the potential changes to a value representing an oxygen concentration of about 6.8 ppm, and thereafter, it remains constant. The mechanism of the initial decrease in oxygen was not determined. The lower curve

shows the decrease in oxygen concentration caused by electrochemical reduction at the walls and bottom of the 316 stainless steel cell. The first twenty minutes saw a reduction in dissolved oxygen to 6 ppm, and within 100 minutes, the oxygen concentration was down to about 2 ppm. At this point, we have only let one run go longer than 100 minutes. In that run, the platinum potential bottomed out at about -150 mv, corresponding to nearly zero oxygen.

Figure 4 shows the results for the TFE cell (upper curve) and the stainless cell (lower curve) with the natural seawater. The two shaded bands in Figure 4 represent the outlines of the error bars from Figure 3 for comparison. The upper curve in Figure 4 shows how the oxygen utilization proceeds when only the biological mechanism is operative. During the first 40 minutes, the curve is nearly identical to that for the electrochemical mechanism. Beyond that point, the biological mechanism is slower. One might expect that when both electrochemical and biological mechanisms were operative together, their effects would be additive. The lower curve in Figure 4 shows that this probably is the case. In the experiments represented by the lower curve, both electrochemical reduction of oxygen at the stainless cell walls and bacterial uptake of oxygen in the cell water were operating. These combined mechanisms gave the most rapid oxygen depletion over the first hour of the test. It is interesting, however, that the high rate was not maintained to the end of the experiment.

D. Discussion

At first glance, our results would seem to indicate that the biological and electrochemical mechanisms produce roughly equivalent rates

of oxygen utilization. It should be remembered, however, that the biological mechanism takes place in the volume of the crevice water, while the electrochemical mechanism takes place on the metal surface. Thus, the biological mechanism is a volume effect, and the electrochemical mechanism is a surface effect. Our results, then cannot be transferred directly to the case of crevice initiation without taking into account the difference in surface-to-volume ratio between our cell and a typical crevice. As has already been stated, the surface area of stainless steel in our metallic cell was 3.6 cm^2, while the volume of the cell was 0.71 cm^3. The surface-to-volume ratio in our cells is, therefore, $(3.6)/(.71) = 5\ cm^{-1}$.

A typical crevice in marine hardware will have a crevice gap of 2.54×10^{-3} cm (1 mil). If that crevice was circular in shape and had the same volume as that of our cell, the crevice diameter would be 18.9 cm. The surface area of the crevice, considering the top and bottom surfaces but neglecting the edges, would be 561 cm^2. Thus, the surface-to-volume ratio for the crevice would be $(561)/(.71) = 787\ cm^{-1}$.

This difference in the surface-to-volume ratio would bias our cell results by a factor of (787)/(5), or by over 150 to one in favor of the electrochemical mechanism, when applying them to a typical crevice. We have stated above that, for our cell geometry, it took about 24 hours for either of the two mechanisms to bring the dissolved oxygen all the way to zero. When translating those results to a crevice geometry, one would expect that the biological mechanism, being a volume effect, would not change much if the concentration of bacterial cells in the water was not changed. On the other hand, the electrochemical mechanism should be accelerated by a factor of about 150 due to the increase in the surface-to-volume ratio. Thus, our results predict that electrochemical oxygen

depletion in the crevice should be complete in about (24)/(150) = 0.16 hours, or about 10 minutes. This value is in excellent agreement with predictions from the Oldfield model quoted earlier.

It should be noted that our results were all generated on carefully cleaned laboratory surfaces. Most stainless steel surfaces in service will not be as clean as those we have used. Moreover, we did notice that our data became less reproducible if we did not clean our surfaces carefully between each run. It is possible that the presence of dirt, oils, greases and organic films on the surfaces would decrease the rate of electrochemical oxygen reduction and bias the total rate toward the biological mechanism.

There is certainly room for additional research in several areas. First, the rates of the two competing mechanisms should be measured on surfaces whose state of cleanliness is more representative of service conditions. Second, this work should probably be repeated under conditions in which the species of microorganisms present, and their numbers per unit volume of crevice water, are known. Third, the design of our cell lid evolved during the course of the work. The shape of the cell body was dictated by our original lid design, which had the electrodes protruding down into the liquid from the lid. With the new design, in which the electrodes are mounted flush with the lower surface of the lid, the cell body could be made very shallow. Thus, it should be easy to check on the predicted effect of the surface-to-volume ratio.

Based on the results presented here, we can conclude that:

1) For clean stainless steel surfaces and natural seawater, the rates of electrochemical and biological utilization of dissolved oyxgen

are about equal for the geometry of the cells used in these experiments, that is, when the surface-to-volume ratio is less than about 10.

2) When the surface-to-volume ratio is 500 to 1000, as is probably typical for crevices in marine service, the electrochemical mechanism for oxygen utilization dominates by a factor of about 150.

3) Based on our experimental data, the estimated time for oxygen depletion by electrochemical reduction, as corrected for crevice geometry, is in excellent agreement with predictions from the mathematical model of Oldfield.

TABLE AI.

Comparative Crevice Corrosion Resistance of Stainless Alloys in Natural and Synthetic Seawater Using a Multiple Crevice Assembly

Exposure Duration: 30 Days
Torque: 10 Nm

		Synthetic SW		Natural SW	
Alloy	Temperature (C°)	% Sites Attacked*	Max. Depth of Attack(mm)	% Sites Attacked*	Max Depth of Attack
T304SS	25	31	0.11	42	2.91
T316SS	25	38	0.08	4	1.12
Alloy 825	25	8	0.01	36	1.62
T304SS	50	31	0.15	33	0.18
T316SS	50	28	0.13	35	0.08
Alloy 825	50	3	0.05	3	0.03

* % Sites Attacked = $\frac{\text{No. Sites Attacked}}{\text{120 Possible Sites}} \times 100$

Figure 1 Drawing of the lid and cell body for the stainless steel and teflon cells.

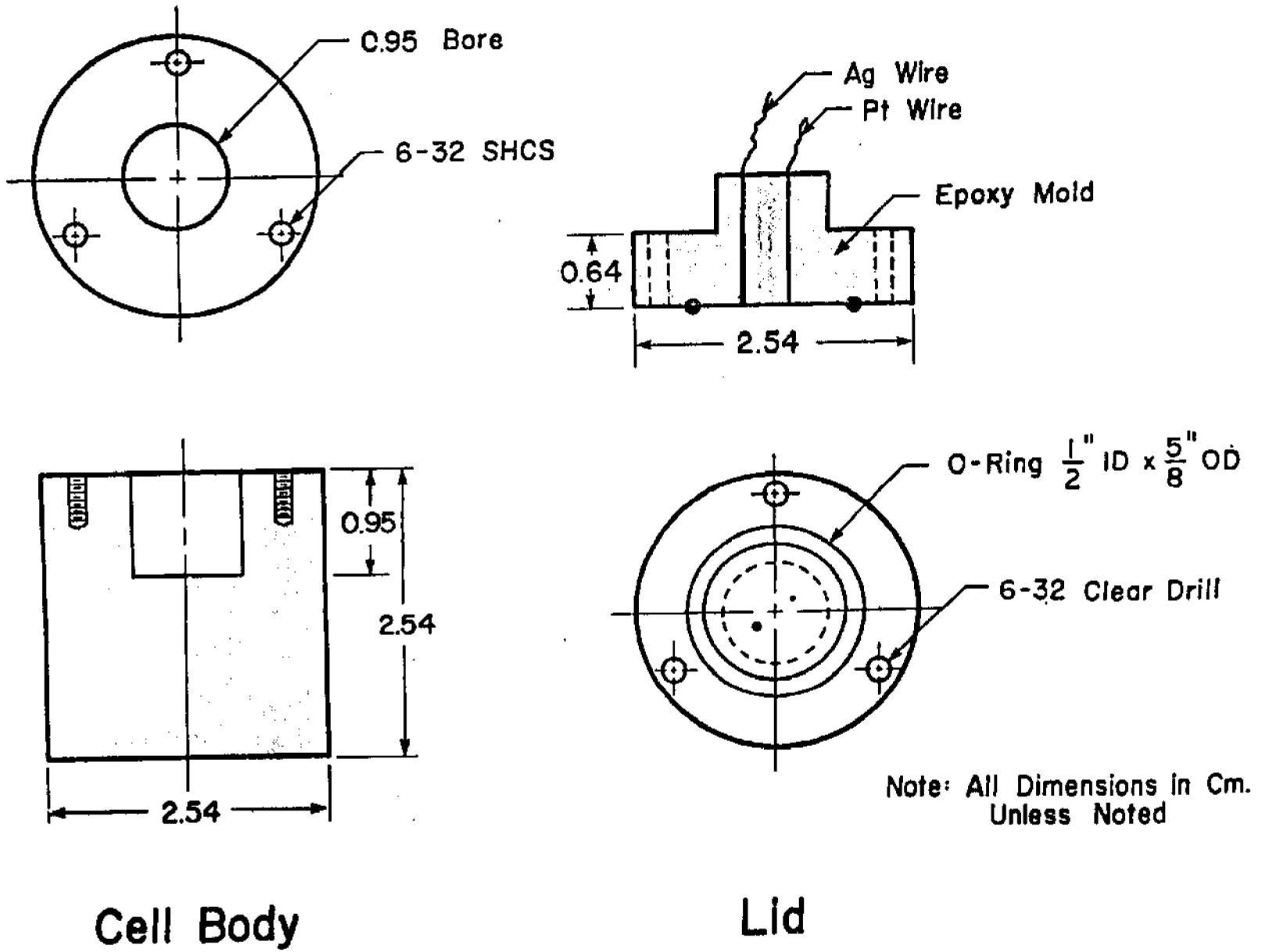

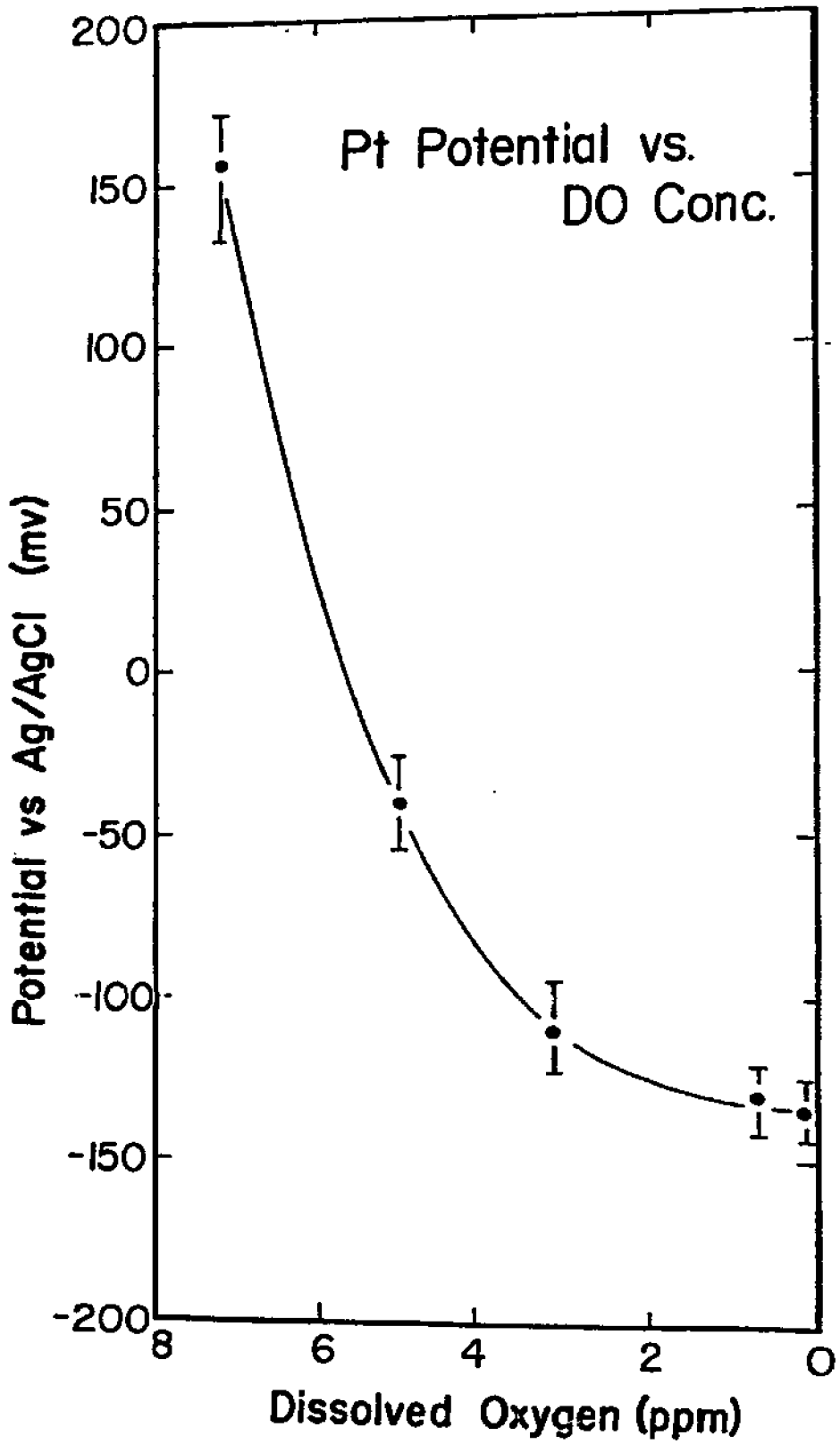

Figure 2 Platinum electrode potential as a function of dissolved oyxgen concentration in the cell.

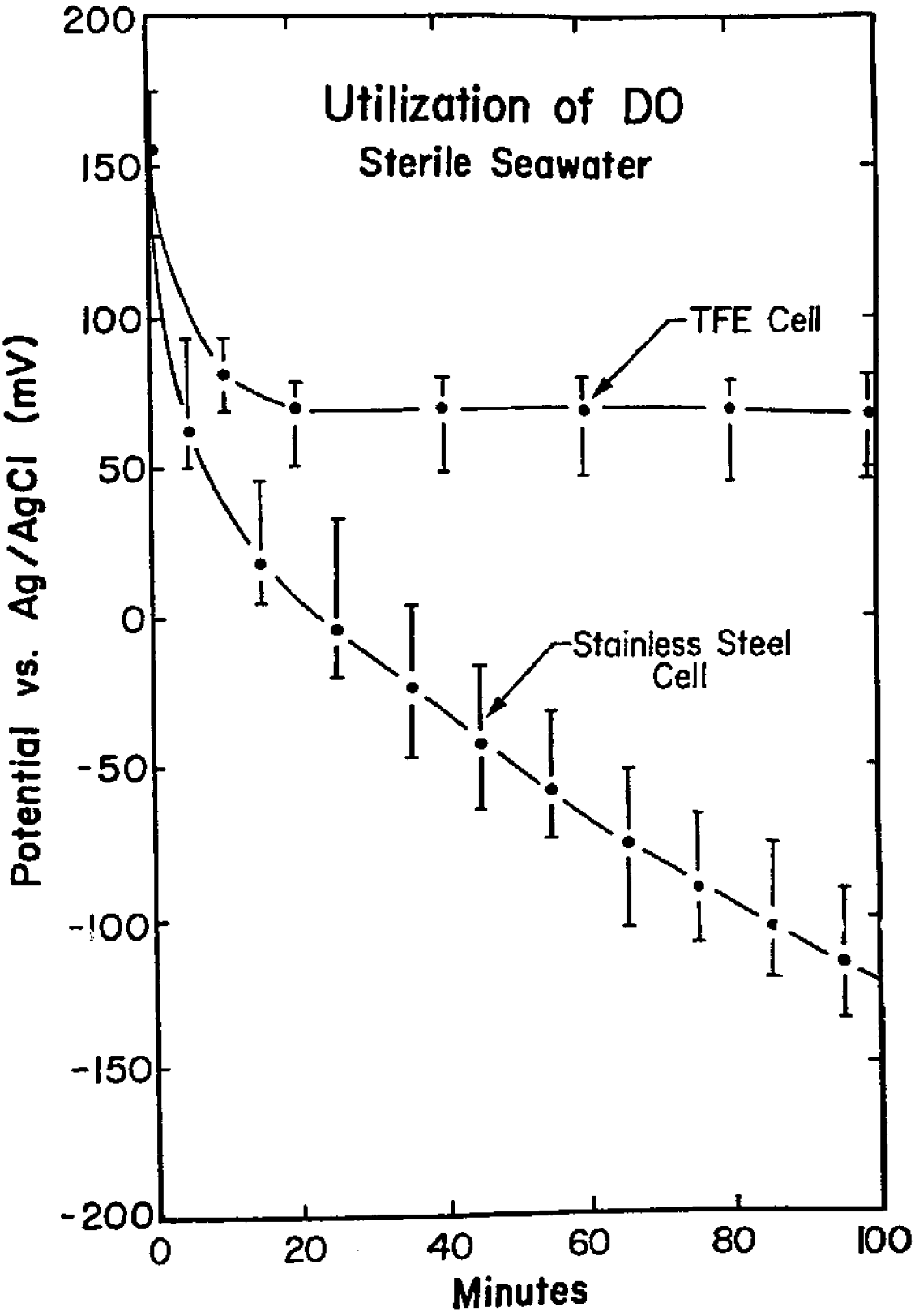

Figure 3 Utilization of dissolved oxygen in the TFE and stainless steel cells as monitored by the change in platinum electrode potential with time in sterile seawater.

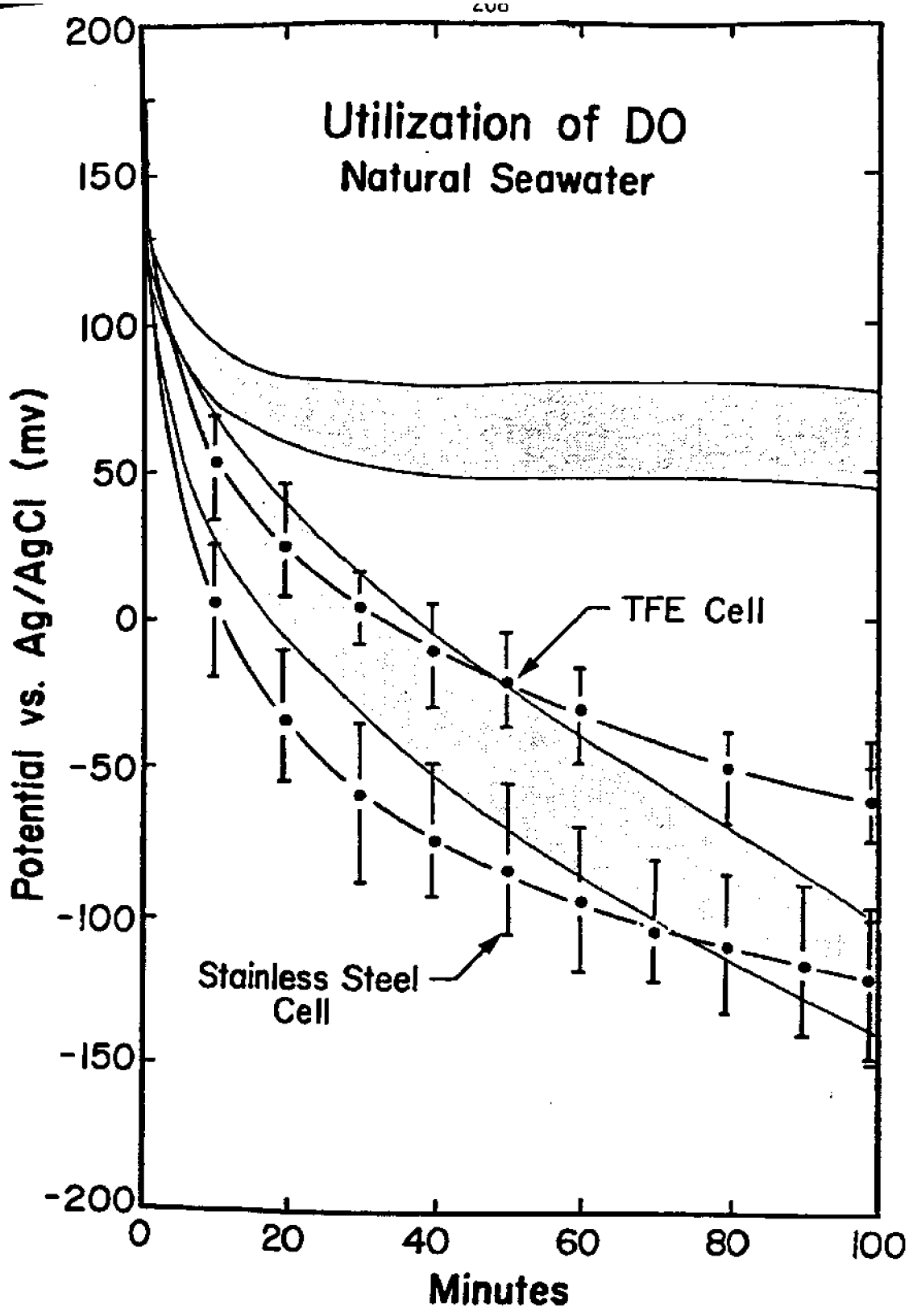

Figure 4 Utilization of dissolved oxygen in the TFE and stainless steel cells as monitored by the change in platinum electrode potential in natural seawater. The shaded bands show the data from Figure 3 for comparison.

V. ACCELERATED TESTING

PAPER NUMBER
71

CORROSION 83

The International Corrosion Forum Sponsored by the
National Association of Corrosion Engineers
Anaheim Convention Center, Anaheim, California
April 18-22, 1983

ACCELERATED LABORATORY TESTS FOR CREVICE CORROSION OF STAINLESS ALLOYS

Nikhil S. Nagaswami and Michael A. Streicher
Department of Chemical Engineering
University of Delaware
Newark, Delaware 19711

ABSTRACT

Two accelerated laboratory tests have been used to study the initiation of crevice corrosion on 12 stainless alloys. For these same alloys data on crevice corrosion from immersion tests in natural seawater are now available.

In the laboratory tests, specimens with rubber band-Teflon crevices were immersed in ferric chloride solutions to determine crevice corrosion temperatures. Temperature was also used as the criterion for evaluating the 12 alloys in an electrochemical test in synthetic seawater with Delrin multiple crevice devices. By means of a new instrument, a preselected, constant anodic potential was applied to the creviced specimen and the current monitored for a preselected time at each test temperature. The temperature at which the current exceeded a preset critical level (corresponding to initiation of crevice attack), was recorded as the crevice corrosion temperature.

The instrument permits the preselection of a number of experimental parameters (applied potential, current measuring time at each temperature, critical current level, starting temperature) and provides automatic control of test temperature, interval between temperatures and current measuring time at test temperatures.

Preliminary results obtained in the two laboratory tests are presented and compared with the data obtained in recent crevice corrosion immersion tests in natural seawater, and with each other.

INTRODUCTION

Laboratory investigations are being conducted on a range of 46 alloys used in the recent OTEC (1) and Navy (2) seawater immersion test programs at the Francis L. LaQue Center for Corrosion Technology at Wrightsville Beach, NC. Materials from these 46 alloys have been supplied for our program. In some cases, the actual panels used for the seawater tests were made available by R. M. Kain, Inco, and H. P. Hack, U. S. Naval Research and Development Laboratory, Bethesda, MD.

All OTEC and Navy tests were made on the same size panels with identical Delrin® multiple crevice devices. The tests were made concurrently in filtered, essentially quiescent seawater, at 30°C. The tests on the 13 alloys in the OTEC series were made on panels with mill finishes and for testing times of 30, 60 and, in some cases, 90 days, with two levels of torque, 25 in-lb and 75 in-lb. The Navy series included 36 wrought and 9 cast alloys. Twelve of the wrought alloys were also used in the OTEC tests. To "normalize" the surfaces, the panels were given a 120-grit finish, 50 mm in diameter, under the crevice devices. All tests were for 30 days and with a torque of 75 in-lb.

R. M. Kain did not rate or rank the alloys tested in the OTEC program. H. P. Hack classified the 45 alloys in the Navy series into four groups. However, he found that "Data variability in this study is large, therefore, a detailed ranking of materials is not possible." However, in order to compare the crevice corrosion results obtained on the 46 alloys in natural seawater with the measurements being made in our accelerated laboratory tests, a more detailed assessment of the data obtained in natural seawater was required (3).

Even though accelerated laboratory tests have been conducted on most of the alloys tested in the OTEC and Navy programs, results presented in this paper are limited to the 12 alloys common to both OTEC and Navy programs. Table 1 gives the chemical compositions of these alloys in addition to several others used in studying the effects of test parameters.

Several tests have been developed over the years to study crevice corrosion of stainless alloys. These include immersion tests in natural seawater under various conditions and tests in accelerated laboratory environments. Among the latter, the electrochemical techniques used to rate alloy resistance to localized attack include potentiodynamic tests (slow scan and rapid scan), potentiostatic tests (scratch tests and induction time studies), galvanostatic polarization tests, cyclic polarization or anodic hysteresis-loop techniques and pitting and crevice temperature

---

®Registered Trademark, E. I. du Pont de Nemours & Co., Inc., Wilmington, DE.

determinations at constant applied potentials.

In this first part of our investigation, two types of accelerated laboratory crevice tests were selected to study initiation of crevice corrosion:

i) The determination of crevice corrosion temperatures (C.C.T.) in 10% ferric chloride solutions.

ii) The determination of crevice corrosion temperatures (C.C.T.) in synthetic seawater under constant applied potentials.

Ferric Chloride Immersion Tests

The ferric chloride crevice test provides an intensification of several factors which are known to cause chloride crevice corrosion on stainless-type alloys (low pH of 1.6, high chloride ion concentrations, high redox potential of +0.60 V vs. S.C.E., large differences in concentrations of oxidants inside vs. outside the crevices). Increasing the temperature of the ferric chloride test solution may be viewed as another means for increasing the aggressiveness of this test and for increasing the rate of attack whenever crevice corrosion is initiated.

The temperature at which crevice corrosion is initiated in ferric chloride solutions has been used extensively as a criterion for measuring resistance to crevice attack, for comparing crevice corrosion resistance of a large number of alloys and to develop new alloys (4-10). However, considerable variability has been observed in data on crevice corrosion initiation in ferric chloride tests within each test procedure (11). Furthermore, there are considerable differences in the test procedures adopted by various investigators, including crevice design, ferric chloride solution and pH, test matrix and durations, inspection procedures, and surface finish.

Electrochemical Tests in Synthetic Seawater

Electrochemical measurements of critical crevice potentials have shown (12) that the range of values observed is so wide that they cannot be used to rank alloys. Problems have also been reported with the hysteresis method of B. E. Wilde (13). R. J. Brigham (14,15) has used measurements of critical pitting temperatures at constant applied potentials, CPT, to compare alloys. However, measuring the CPT with standard electrochemical instruments is a rather time consuming task. The development of a new instrument, the Santron CTD-400 potentiostat (made in Sweden), by S. Bernhardsson and co-workers (16) in recent years has greatly facilitated the determination of critical crevice and pitting temperatures of alloys in different solutions. Furthermore,

S. Bernhardsson and co-workers (17,18,19) have claimed good agreement between CPT data on a range of stainless alloys with extended in-service experience.

EXPERIMENTAL PROCEDURES

Specimens

All tests were conducted on flat specimens prepared from sheet stock or from seawater immersion test panels. The specimens were saw-cut to dimensions of approximately 5 x 2.5 cm (2 x 1 in), care being taken to avoid any sheared edges. Specimen thicknesses varied from 1.27 to 0.16 cm (1/2 to 1/16 in). The specimens were wet-ground to 120-grit SiC on all sides, care being taken to avoid sharp edges.

The specimens used in the electrochemical tests were drilled in the center (8 mm dia) to allow the attachment of the crevice assembly, and also near the top edge (1 mm dia) to permit threading the platinum wire support. Care was taken to deburr the edges and to smooth the inside surfaces of these holes. All specimens were scrubbed with detergent using a nylon bristle brush, degreased in acetone, dried and weighed prior to use.

Crevice Assemblies

Rubber band - Teflon crevice devices as per A.S.T.M. G 48 were used for the ferric chloride tests. All rubber bands were boiled in distilled water for 1 hr prior to use. Teflon surfaces in contact with the specimen were ground flat to 600-grit SiC.

Delrin multiple crevice washers (12 serrations per washer), with serrated faces carefully ground to 600-grit SiC, were used for the electrochemical tests. These were fastened using Hastelloy C-276 nuts, bolts (1/4 in dia - 20 threads per in) and washers. The Hastelloy bolts were insulated from the test specimens by means of teflon tape. Clearance was provided between the insulated bolt and alloy sample to avoid generating secondary crevices. Electrical insulation was checked before and after every test. A torque of 8.5 N.m (75 in-lb) was applied to the crevice assemblies just prior to starting each test using a calibrated torque wrench. Torque levels observed at the end of each test were recorded to determine the relaxation. The extent of relaxation in the torque has been seen to increase with maximum temperature reached in the test and measuring times at each temperature (Table 2). Detailed investigations of this problem are being conducted and relaxation effects are to date unresolved.

Solutions

All test solutions were prepared using distilled water. Solutions of 10% $FeCl_3 \cdot 6H_2O$ were prepared in accordance with A.S.T.M. G 48. For each test, 175 ml of ferric chloride solution (pH 1.35 - 1.6) was used. Synthetic seawater was prepared in accordance with A.S.T.M. D-1141-52 (Table 3), using synthetic sea salt purchased from the Lake Products Co., Inc., Baldwin, MO. Synthetic seawater solutions were stirred for 2 hrs to ensure complete dissolution of the salt. The solutions were then deaerated with high purity nitrogen for 90 min prior to each test, and for the duration of each test. Oxygen levels were thus maintained at a steady, low level (0.2 to 0.4 mg/L) over the entire range of temperatures encountered in the electrochemical tests.

Procedure for Ferric Chloride Immersion Tests

In the ferric chloride tests a total of 6 specimens of each alloy was tested. Two specimens were tested for 24 hrs each, and one specimen was tested for 48 hrs. The remaining 3 specimens were tested according to the following schedules at each temperature:

Specimen #	Test Times		
	Day 1	Day 2	Day 3
1	24 hrs*	+ 24 hrs*	+ 24 hrs*
2	----------	48 hrs*	+ 24 hrs*
3	----------	----------	72 hrs*

*Alloy specimen examined for crevice corrosion, then reinserted into solution for remainder of test time at temperature.

Following the 72 hr test time at a given temperature all unattacked specimens were removed, scrubbed clean and dried. Tests on attacked specimens were terminated. The solution temperature was then raised by 2°C over a 24 hr period. The unattacked crevice specimens were reassembled using fresh (boiled) rubber bands and reintroduced into the ferric chloride solution at the new test temperature. Solutions showing evidence of precipitates or discoloration at the end of a 72 hr run were discarded and freshly prepared solutions used for the next higher temperature.

All ferric chloride tests have been directed towards studying initiation of crevice corrosion by determining crevice corrosion temperatures. The lowest temperature at which crevice attack is

observed at any one of the six crevice sites on a specimen is recorded as the crevice corrosion temperature.

Procedure for Electrochemical Tests in Synthetic Seawater

The Santron CTD-400 potentiostat is used to determine the crevice corrosion temperatures under constant applied potentials for all the alloys tested. The instrument permits the preselection of a number of experimental parameters (Table 4) and provides automatic control of measuring temperature and measuring time. A preselected potential is applied to the alloy sample at the starting temperature of the test and the corrosion current is monitored for a preset 'measuring time' at this temperature. If the current does not exceed a preset critical level over the duration of the measuring time, the applied potential is switched off and the solution temperature is automatically stepped up by a 5°C increment.

When the new temperature is reached, the preselected potential is applied again and the current monitored for the same measuring time. This procedure is repeated until the current exceeds the preset critical current level for a 'minimum' time period (the 'propagation' or 'decision' time), whereupon the instrument terminates the test and indicates that the critical temperature has been reached. The present instrument does not provide control of the 'propagation' time required to indicate critical temperature. This time currently ranges from 5-15 sec. Since our present investigations are directed only to a study of initiation of crevice corrosion, this control is not essential to the present work.

On the basis of our experience with the Santron CTD-400 potentiostat some changes were proposed (Table 4) and have now been incorporated for us by the manufacturer in a new Santron CTD-400 potentiostat. The cell used in our electrochemical tests is represented schematically in Fig. 1.

In all Santron tests to date, a critical current level of 1000 μA (corresponding to critical current densities of 33 $\mu A/cm^2$ based on total specimen area or 1500 $\mu A/cm^2$ when based on effectiv crevice area) was used. This current level provided visual evidence of crevice attack under the serrated washers in the short decision time required by the instrument to indicate that the critical temperature had been reached. Either platinum gauze or a pair of high purity graphite rods were used as counter electrodes, with identical results.

Typical results are shown in Fig. 2 for Type 304 and in Figs. 3 and 4 for Hastelloy C-276. Tests on these two alloys were made in non-deaerated synthetic seawater with oxygen levels between 5 to 7 mg/l at 20°C. The current spike at each temperature corresponds to the reapplication of the preset applied

potential. This potential is removed during the rise in temperature and the specimen is allowed to return to its corrosion potential at that temperature.

The variable parameters involved in the electrochemical measurements are listed in Table 5. Tests are in progress to determine the effect of these parameters on the crevice corrosion temperature. Results of some of the tests conducted to study the effect of preset applied potentials and measuring times on the critical temperature determined are presented in Tables 6 and 7. In general, higher potentials and longer measuring times are seen to yield lower failure temperatures, though the extent of these effects is seen to depend on the alloy being tested.

RESULTS AND DISCUSSION

The results of the accelerated laboratory tests are presented for the 12 alloys common to both OTEC and Navy programs. All accelerated laboratory tests to date have been directed to the study of initiation of crevice corrosion on alloys with a 120-grit finish. The detailed analyses of the OTEC and Navy seawater immersion tests (3) clearly show that, especially for initiation, the surface finish has a major effect in cases of alloys in the medium range of resistance. This is also the group of alloys for which more than 30 days of testing are needed to define their ranking. The Navy tests which were made on 120-grit surfaces were all limited to 30 days. Therefore, at this point, the data on initiation from laboratory tests in ferric chloride and in synthetic seawater, can only be compared with the less distinct results of the 30-day, 3-panel Navy tests.

Data on crevice-corrosion initiation tests in ferric chloride are presented in Table 8. In each case, average temperatures are shown for six test specimens. The variation in observed crevice corrosion temperatures, $\pm 10°C$, is still relatively large. (The effect of test duration up to 72 hours is still unclear.) Both the total number of sites and the number of sides which showed attack (initiation parameters) in the 3-panel Navy tests are shown for comparison. The alloys are listed according to their Navy (initiation) ranking. In these 30-day tests the rankings based on sides and on sites are identical. However, when these rankings are compared with the results in the ferric chloride test, the agreement is best at the top of the list. The rest merely follow a general trend.

Further investigation of the ferric chloride test is necessary to study the effects of solution composition, pH and oxygen levels, test durations and surface finish. The present variability of $\pm 10°C$ is too large and does not permit a precise ranking of the alloys.

The results of the crevice corrosion initiation tests in synthetic seawater are presented in Table 9 along with the 30-day Navy initiation data. The fixed parameters for these electrochemical tests are listed in Table 10. A comparison of the results yields good agreement at the top of the list, while the rest follow a general trend.

In both cases, however, it is seen that 254 SMO is ranked high in the laboratory tests as compared to the Navy ranking. A further verification of its performance in long-time natural seawater tests would be useful.

The variability of $\pm$2.5°C observed in the synthetic seawater tests is very good when one considers that the minimum temperature step presently provided by the instrument is 5°C. These data have been found to be very reproducible for the entire range of alloys studied.

The best agreement is provided by a comparison of the crevice corrosion temperatures in the two laboratory tests (Table 11). For both test series, the potential on the test specimens was +0.60 V vs. S.C.E. The applied potential in the synthetic seawater was deliberately selected to be the same as the corrosion potential in the ferric chloride solution. The major differences between the tests are: the type of crevice devices (rubber band - Teflon crevices for the ferric chloride vs. Delrin serrated washers for the electrochemical test), the pH (1.6 for the ferric chloride solution vs. 7.6 for that of synthetic seawater), and oxygen level (6.0 mg/l in the ferric chloride solution vs. 0.3 mg/l for synthetic seawater). Nevertheless, the differences between the rankings are limited to variations within the four groups shown in Table 11.

The results obtained in the ferric chloride immersion tests and the electrochemical measurements in synthetic seawater are being used to define new test procedures for more reliable and reproducible results. The preliminary data indicate the limitations of the present ferric chloride test and illustrate the potential of the electrochemical test in synthetic seawater.

The results of the immersion tests in natural seawater provide a valuable database for comparison of laboratory tests. The detailed analysis of the crevice corrosion behavior of the 46 alloys in the immersion test program serves as a guide for defining further laboratory tests on initiation and growth of crevice corrosion and for interpretation of results.

ACKNOWLEDGMENT

We would like to acknowledge the support of the National Sea Grant Office under Contract Number NA 81 AA-D-00006, Sea Grant Program on Marine Corrosion, R. Kolf, Sea Grant Office Program Monitor, and S. C. Dexter, University of Delaware, Overall Program Director.

The authors also wish to acknowledge assistance with laboratory work by Alicia Canedo and Rick Sund, who prepared the specimens and carried out the many corrosion tests.

REFERENCES

1. Kain, R. M., Crevice Corrosion and Metal Ion Concentration Cell Corrosion Resistance of Candidate Materials for OTEC Heat Exchangers, Parts I and II, OTEC Report ANL/OTEC-BCM-022, May (1981).

2. Hack, H. P., Corrosion/82, NACE Meeting, Houston, Preprint No. 65, March (1982).

3. Streicher, M. A., Corrosion/83, NACE Meeting, Anaheim, Preprint No. 70, April (1982).

4. Streicher, M. A., Corrosion, Vol. 30, p. 77 (1974).

5. Streicher, M. A., J. Electrochem. Soc., Vol. 103, p. 375 (1956).

6. Streicher, M. A., Corrosion, Vol. 30, p. 115 (1974).

7. Lizlovs, E. A., Crevice Corrosion of Some High-Purity Ferritic Stainless Steels, ASTM STP 516, Philadelphia, p. 201 (1972).

8. Bond, A. P., Dundas, H. J., Ekerot, S., Semchyshen, M., Stainless Steels for Seawater Service, Stainless Steel '77, p. 197, Climax Molybdenum Co., (1978).

9. Streicher, M. A., Stainless Steels: Past, Present and Future, Stainless Steel '77, p. 1, Climax Molybdenum Co., (1978).

10. Brigham, R. J., Corrosion, Vol. 30, p. 396 (1974).

11. Brigham, R. J., Corrosion, Vol. 37, p. 608 (1981).

12. Lizlovs, E. A., J. Electrochem. Soc., Vol. 117, p. 1335 (1970).

13. Wilde, B. E., Corrosion, Vol. 28, p. 283 (1972).

14. Brigham, R. J., Tozer, E. W., Canadian Metallurgical Quarterly, Vol. 12, 2, p. 171 (1973).

15. Brigham, R. J., Tozer, E. W., Corrosion, Vol. 29, p. 33 (1973).

16. Bernhardsson, S., Mellström, R., Brox, B., Corrosion/80, NACE Meeting, Chicago, Preprint No. 85, March (1980).

17. Bernhardsson, S., Mellström, R., Stainless Steels for Seawater Service, Fifth International Congress on Marine Corrosion and Fouling, Barcelona, Spain, May (1980).

18. Bernhardsson, S., Mellström, R., Oredsson, J., Corrosion/81, NACE Meeting, Toronto, Preprint No. 124, April (1981).

19. Bernhardsson, S., Melström, R., Brox, B., Limiting Conditions with Regard to Pitting of Stainless Steels, Eighth International Congress on Metallic Corrosion, Mainz, Sept. (1981).

Table 1

Analyses of Wrought Stainless Alloys Used in Laboratory Tests

Alloy	Composition, Percent by Weight									
	Cr	Ni	Mo	Mn	C	Si	S	Other		
A.L. 29-4C	28.85	0.79	3.81	0.22	0.012	0.19	0.002	-	0.026 N	0.59 Ti
Monit (Uddeholm)	25.30	4.10	3.80	0.43	0.012	0.31	0.006	0.37 Cu	0.031 P	-
Crucible 6C-1	25.56	2.14	2.94	0.20	0.01	0.25	0.004	0.04 Al	0.016 N	0.51 Ti
Ferralium 255 (Cabot)	26.15	5.64	3.20	0.77	0.02	0.37	-	1.75 Cu	0.19 N	0.16 Co
Haynes 20 Mod (Cabot)	21.58	25.52	4.95	0.90	<0.01	0.49	-	<0.05 Cu	-	0.41 Co
A.L. 6X	20.35	24.64	6.45	1.39	0.018	0.41	0.001	-	0.022 P	-
254 SMO (Avesta)	20.00	17.90	6.10	0.49	0.013	0.41	0.008	0.78 Cu	0.023 P	0.203 N
904L (Uddeholm)	20.50	24.70	4.70	1.46	0.014	0.46	0.005	1.57 Cu	0.028 P	-
Jessop 700	20.70	25.20	4.45	1.65	0.013	0.42	0.008	0.24 Cu	0.28 Nb	-
Jessop 777	20.80	25.60	4.48	1.37	0.023	0.48	0.013	2.18 Cu	0.24 Nb	0.25 Co
Carpenter 329	26.98	4.22	1.39	0.28	0.052	0.39	0.014	0.09 Cu	-	-
Nitronic 50 (Armco)	21.08	13.70	2.28	4.81	0.045	0.47	0.012	-	0.025 P	0.26 N

Above 12 alloys common to both OTEC and Navy programs.

Table 1 (cont.)

Alloy	Composition, Percent by Weight							Other		
	Cr	Ni	Mo	Mn	C	Si	S			
Type 304	18.34	8.60	0.20	1.62	0.055	0.60	0.015	0.11 Cu	0.026 P	0.14 Co
A.L. 4X	20.15	24.38	4.44	1.45	0.014	0.57	0.001	1.5 Cu	0.019 P	-
Hastelloy G (Cabot)	22.22	46.84	5.78	1.52	0.007	0.43	-	1.85 Cu	2.07 Nb	1.27 Co*
Hastelloy G-3 (Cabot)	22.76	43.69	7.01	0.82	0.006	0.37	-	1.85 Cu	0.19 Nb	3.49 Co+
Hastelloy C-276 (Cabot)	15.51	54.72	15.49	0.46	0.003	0.04	-	0.11 Cu	3.82 W	1.89 Co
44LN (Uddeholm)	25.00	5.90	1.46	1.75	0.028	0.53	0.003	0.12 Cu	0.19 N	-
A.L. 29-4-2	29.50	2.20	3.95	0.10	0.002	0.10	0.010	-	0.01 P	0.011 N
Carpenter Exp. 58	20.67	14.73	4.92	5.41	0.073	0.52	0.005	0.14 Cu	0.014 P	0.25 N°

*0.28 W
+0.95 W
°0.07 Co

Table 2

Torque Relaxation of

Delrin Crevice Assembly*

Test Condition		Test Duration	Initial Torque	Final Torque
Environment	Temp. °C	(hr)	(in-lb)	(in-lb)
H_2O	30	1	75	70
		2	75	65
		4	75	45-50
H_2O	40	1	75	70
		2	75	60
H_2O	100	1	75	≤20
		1	100	35-40
		2	100	20-25
		1	150	60
H_2O	21	24	75	60
		48	75	50-65
		72	75	55-60
Air	21	18	100	70-80
		24	75	65-70

*Delrin multiple crevice assembly; 12 serrations per washer 0.6638 cm^2 effective crevice area. Hastelloy C-276 nuts, washers and bolt (1/4 in dia - 20 threads per in).

Table 3

Substitute Ocean Water

A.S.T.M. D-1141-52

(American Society Testing Material) Formula A

Table 1, Sec. 4

COMPOSITION

NaCl	58.490%
$MgCl_2 6H_2O$	26.460%
Na_2SO_4	9.750%
$CaCl_2$	2.765%
KCL	1.645%
$NaHCO_3$	0.477%
KBr	0.238%
H_3BO_3	0.071%
$SrCl_2 6H_2O$	0.095%
NaF	0.007%

Chlorinity -19.38 mg/L

Salinity ~35.01 mg/L

Supplied by Lake Products Co., Inc., Baldwin, MO.

Table 4

Santron CTD-400 Potentiostat

Range of Instrument Parameters

	PRESENT	PROPOSED
· Applied Potential	± 2000 mV	± 2000 mV
· Potential Application	Intermittent	Intermittent or Continuous
· Critical Current	± 2000 μA	± 2000 μA
· Measuring Time	0-3 hr	0-30 hr
· Temperature Step	5°C	5°C
· Propagation (Decision) Time	No Control (5-15 sec)	Preselection 0-30 hr
· Current Integration	-	Incorporated

Table 5

Variable Parameters in Santron Tests

A. Test Solution
- Solution Composition
- Oxygen Concentration
- pH
- Chlorinity, Salinity
- Flow rate, Stirring

B. Potentiostat Conditions
- Applied Potential
- Intermittent vs. Continuous Potential
- Critical Current Density
- Measuring Time
- Propagation (Decision) Time
- Temperature Step
- Heating Rate

C. Specimen Assembly
- Surface Finish - Alloy Sample, Crevice Device
- Crevice Assembly Design - Geometry, Dimensions, Material
- Crevice - Bold Area Ratio
- Crevice Tightness - Applied Torque, Pressure Relaxation

Table 6

fect of Applied Potential (mV vs S.C.E.) on Crevice Corrosion Temperature[a]

	600 mV	400 mV	
Jessop 777	30	37.5	*
Nitronic 50	40	45	*
Type 329	40	45	†
44 LN	40	50	†
904L (Uddeholm)	42.5	70	*
A.L. 4X	47.5	>90	†

† - 15 min. measuring time

* - Nitrogen sparging, 20 min. measuring time

[a] - Synthetic Seawater, Delrin Multiple Crevice Assembly 75 in-lb torque, 120 grit finish, 1000 μA critical current.

Table 7

Effect of Measuring Time on Crevice Corrosion Temperature[a]

	15 min.	60 min.
Haynes 20 Mod.	55	45
Ferralium 255	60	55
Monit	60	55
HAST G	60	45
254 SMO	70	60
HAST G-3	75	55
29-4-2	80	70

[a] Synthetic Seawater, Delrin Multiple Crevice Assembly 75 in-lb torque, 120 grit finish, 600 mV vs S.C.E. applied potential, 1000 μA critical current.

Table 8

Initiation of Crevice Corrosion in Ferric Chloride Tests and Immersion Tests in Seawater

(120-Grit Finish)

ALLOY	INITIATION MEASUREMENTS					
	Navy Tests[a]				Ferric Chloride Tests[b]	
	Sites	Rank	Sides	Rank	Failure Temperature °C*	Rank
A.L. 29-4C	0	1	0	1	>55	1
Monit (Uddeholm)	0	2	0	2	47	2
Crucible SC-1	1	3	1	3	45	4
Ferralium 255 (Cabot)	2	4	2	4	37	5
Haynes 20 Mod	6	5	2	5	28	8
A.L. 6X	11	6	4	6	37	6
254 SMO (Avesta)	18	7	5	7	46	3
904L (Uddeholm)	36	8	5	8	22	10
Jessop 700	47	9	5	9	31	7
Jessop 777	60	10	6	10	14	12
Carpenter 329	73	11	6	11	25	9
Nitronic 50	112	12	6	12	15	11

[a] Filtered seawater, 30°C, 30-day tests, 75 in-lb torque, multiple crevice assembly, 3 panels.

[b] 10% $FeCl_3 \cdot 6\ H_2O$ solution, rubber band-teflon crevices, up to 72 hours.

* Average of 6 specimens tested; variability ± 10°C.

Table 9

Initiation of Crevice Corrosion in Electrochemical Tests and Immersion Tests in Seawater

(120-Grit Finish)

ALLOY	INITIATION MEASUREMENTS					
	Navy Tests[a]				Santron Tests[b]	
	Sites	Rank	Sides	Rank	Failure Temperature °C*	Rank
A.L. 29-4C	0	1	0	1	90.0	1
Monit (Uddeholm)	0	2	0	2	67.5	2
Crucible SC-1	1	3	1	3	60.0	5
Ferralium 255 (Cabot)	2	4	2	4	60.0	4
Haynes 20 Mod	6	5	2	5	47.5	7
A.L. 6X	11	6	4	6	57.5	6
254 SMO (Avesta)	18	7	5	7	62.5	3
904L (Uddeholm)	36	8	5	8	42.5	9
Jessop 700	47	9	5	9	45.0	8
Jessop 777	60	10	6	10	30.0	12
Carpenter 329	73	11	6	11	40.0	11
Nitronic 50	112	12	6	12	40.0	10

[a] Filtered seawater, 30°C, 30-day tests, 3 panels, multiple crevice assembly: 20 serrations per side, 1.3716 cm^2 effective crevice area, 1:220 crevice-bold area ratio, 75 in-lb torque.

[b] Synthetic seawater, 600 mV vs. S.C.E. applied potential, 1000 μA critical current, 20 min. measuring time, multiple crevice assembly: 12 serrations per side, 0.6638 cm^2 effective crevice area, 1:40 crevice - bold area ratio, 75 in-lb torque.

* Average of at least 4 values, variability ±2.5°C.

Table 10

Fixed Parameters in Santron Tests

TEST SOLUTION	
• Solution:	Synthetic Seawater [A.S.T.M. D-1141-52 Formula A]
• Dissolved Oxygen:	0.2 to 0.4 mg/L
• pH:	7.6 to 7.9
• Chlorinity:	-19.38 mg/L
• Salinity:	-35.01 mg/L
Specimen Assembly	
• Surface Finish:	
Alloy Sample	120 grit SiC
Delrin Multiple Crevice	600 grit SiC
• Delrin Multiple Crevice:	12 serrations
• Crevice - Bold Area Ratio:	1:40
• Initial Applied Torque:	8.5 N.m (75 in-lb)
Potentiostat Conditions	
• Applied Potential:	600 mV vs. S.C.E.
• Critical Current Density on the Basis of:	
A. Total Specimen Area	33 $\mu A/cm^2$
B. Effective Crevice Area	1500 $\mu A/cm^2$
• Measuring Time:	20 min.
• Temperature Step:	5°C
• Constant Heating Rate:	

Table 11

Initiation of Crevice Corrosion in Ferric Chloride Tests and Electrochemical Tests in Synthetic Seawater

	SANTRON-[a] (120 Grit Finish)		FERRIC CHLORIDE-[b] (120 Grit Finish)	
	Crevice Corrosion Temperature °C*	Rank	Failure Temperature† °C	Rank
A.L. 29-4C	90.0	1	>55	1
Monit (Uddeholm)	67.5	2	47	2
254 SMO (Avesta)	62.5	3	46	3
Carpenter Exp 58	62.5	4	33	7
Ferralium 255 (Cabot)	60.0	5	37	5
Crucible SC-1	60.0	6	45	4
A.L. 6X	57.5	7	37	6
Haynes 20 Mod	47.5	8	28	9
Jessop 700	45.0	9	31	8
904L (Uddeholm)	42.5	10	22	11
Nitronic 50	40.0	11	15	12
Type 329	40.0	12	25	10
Jessop 777	30.0	13	14	13

[a] Synthetic seawater, 75 in-lb torque, 600 mV vs. S.C.E. applied potential, 1000 µA critical current, 20 min. measuring time.

* Average of at least 4 values, variability ±2.5°C.

[b] 10% $FeCl_3 \cdot 6H_2O$ solution, rubber band-teflon crevices.

† Average of 6 specimens tested, variability ±10°C.

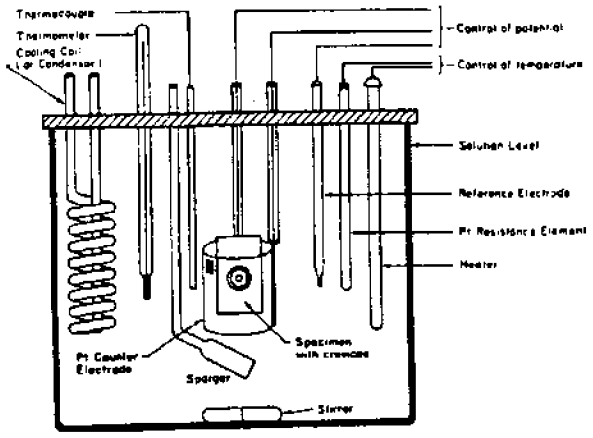

Fig. 1 Elevation of Crevice Corrosion Cell.

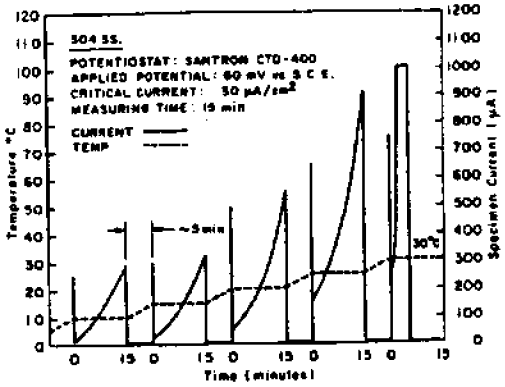

Fig. 2 Effect of Temperature on Crevice Corrosion of Type 304 Stainless Steel at Constant Potential in Synthetic Seawater.

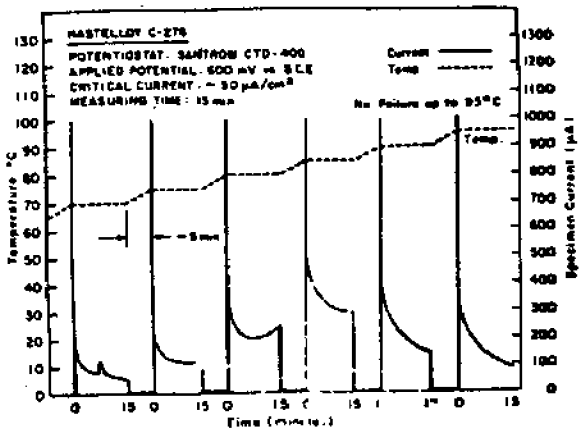

Fig. 3 Effect of Temperature on Crevice Corrosion of Hastelloy C-276 at Constant Potential (600 mV vs S.C.E.) in Synthetic Seawater: Measuring time - 15 min.

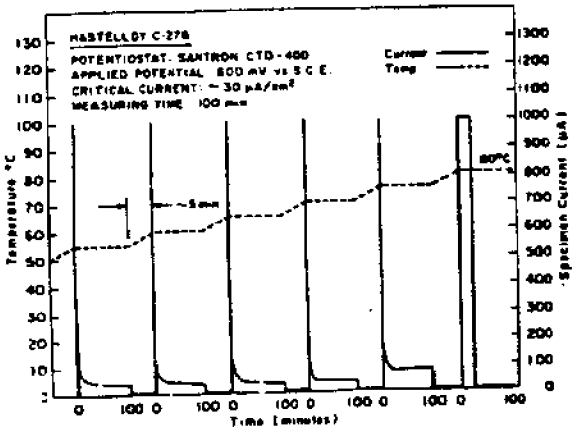

Fig. 4 Effect of Temperature on Crevice Corrosion of Hastelloy C-276 at Constant Potential (600 mV vs S.C.E.) in synthetic Seawater: Measuring time - 100 min.